THE BOVINE SPLICEOSOMAL U1 SMALL NUCLEAR RIBONUCLEOPROTEIN PARTICLE: A STUDY OF ITS AUTOANTIGENICITY AND BIOCHEMICAL PROPERTIES

A thesis presented in partial fulfilment of the requirements for the degree of Doctor of Philosophy in Biochemistry at Massey University, Palmerston North, New Zealand.

Andrew James Robertson
2006

Abstract

Despite individual autoimmune diseases being relatively rare, collectively these diseases afflict 8 % of the population according to the American Autoimmune Related Diseases Association. With over 75 % of those affected being women, autoimmune disease has been recognised, by the World Health Organisation and the US National Institutes of Health, as a major global women's health issue. One third of autoimmune sufferers have a rheumatological disorder, which commonly affect the joints, muscle, skin, salivary glands and kidneys. Antibodies against nuclear antigens are a serological hallmark of these diseases. Detection of these antibodies is used in the diagnosis and prognosis of the disease. The sensitivity and specificity of the test, of which the antigen is a key component, is pivotal to correct disease diagnosis and management.

The relationship between circulating autoantibodies and the target antigen is complex. Improving the effectiveness of a test to assist in diagnosis and prognosis comes from characterisation and understanding these complex relationships.

This thesis compares bovine spliceosomal U1 small nuclear ribonucleoprotein particle (U1 snRNP) complex with its human equivalent, and examines the validity of using this bovine derived autoantigen in the diagnosis of the human autoimmune diseases, systemic lupus erythematosus and mixed connective tissue disease.

Differences between bovine and human U1 snRNP composition were characterised using a combination of electrophoretic, immunoassay and mass spectrometry techniques. Although the U1C protein could not be identified in bovine U1 snRNP, all other specificities were present. U1A remained intact, whilst the U1 snRNP specific 68K protein was dephosphorylated and a large C-terminal domain was removed, such that 68K migrated as a 30-36 kDa cluster on SDS-PAGE. Bovine SmD proteins, present in U1 and non-U1 snRNPs,

were unaffected, whereas, SmB′/B was truncated to a 12 kDa peptide, which interestingly, was no longer reactive with anti-RNP sera in western blot.

The recognition of human SmB′/B protein by anti-RNP sera in western blot was further examined. A technique was developed to immunoaffinity purify tryptic digests of SmB′/B which could then be analysed by mass spectrometry. Interestingly, the human replication element protein (HREP) was tentatively identified, rather than SmB′/B as expected. It may be possible, therefore, that anti-RNP sera may be reacting with a protein other than SmB′/B.

To examine the contribution of the individual U1 snRNP proteins to anti-RNP and anti-Sm sera reactivities, a method was developed to dissociate bovine U1 snRNP and to purify the individual component antigens. It was demonstrated both empirically and through anecdotal feedback from a commercial diagnostic kit producer that patient sera respond better to purified Sm-free 68K than the recombinant 68K antigen.

The effect of commercial processing of bovine thymus, the source for U1 snRNP antigen, was determined. In this study, variables that may be controlled during processing, such as temperature, protease activity and pH, were investigated. Hydrolysis of the intact human 68K protein with the necrotic protease, cathepsin L, produced 38 and 25 kDa fragments, whereas exposure to ambient temperature and low pH produced 32 kDa peptide fragments similar to those observed in purified bovine 68K. It was therefore proposed that 68K protein may undergo autocatalytic hydrolysis during necrotic cell death.

Thorough characterisation of the bovine spliceosomal U1 snRNP proteins has not only validated their use as diagnostic reagents in autoimmune disease but also provided some insight into the inactivation of U1 snRNP function during early cell death.

Acknowledgements

I would like to thank the many people who have encouraged and assisted me during this study.

Special thanks are extended to my supervisors, Dr. Gillian Norris of the Institute of Molecular BioSciences, Massey University and Dr. Neil Cook, AroTec Diagnostics Limited, for their patient guidance and support.

I must also thank some people who have worked with me during the time spent on this thesis: Tim Catchpole, Rebecca Wymer, Erin Boshier and Amelia Knight at AroTec Diagnostics for keeping me sane. A particular mention should go to Greta Moraes of Industrial Research Limited for her empathy and encouragement. Thanks also to those in the Norris Lab at Massey University, particularly Dr. Santanu Deb Choudhury for his assistance with the operation of the MALDI mass spectrometer and Trevor Loo for his general helpfulness.

My gratitude also to family and friends, particularly my partner Liz Doolin without whose love, devotion and sacrifice I could not have completed this thesis. Also our gorgeous children, Gemma, Campbell and Matthew, whose cuddles, giggles and smiles make everything worth while.

Finally, many thanks to Technology New Zealand and Arotec Diagnostics Limited for their financial support.

.

Table of Contents

List of Figures

List of Tables

List of Abbreviations

2A2MP	2-amino-2-methylpropanol
2D	two dimensional
aDMA	asymmetrical dimethylarginine
ANA	anti-nuclear antibody
BCIP	5-bromo 4-chloro 3-indolylphosphate
BCR	B-cell receptor
BSA	bovine serum albumin
CD	cluster designation
CHAPS	3-(3-cholamidopropyldimethyl ammonio) propanesulfonic acid
CHT	ceramic hydroxyapatite
CIE	counterimmunoelectrophoresis
Da	dalton
DID	double immunodiffusion
DIG	digoxigenin
DNA	deoxyribonucleic acid
DTT	dithiothreitol
EDTA	ethylenediaminetetraacetic acid
EIA	enzyme-linked immunoassay
ELISA	enzyme linked immunosorbent assay
ENA	extractable nuclear antigen
FN	false-negative
FP	false-positive
HeLa	cervical carcinoma cell line (Helen Lane)
HEPES	N-(2-hydroxyethyl) piperazine N′(2-ethanesulfonic acid)
HPLC	high performance liquid chromatography
HREP	human replication element protein
HRP	horse radish peroxidase
HT	hydroxyapatite
IEF	isoelectric focussing
Ig	immunoglobulin

IIF	indirect immunofluorescence
IPG	immobilised pH gradient
kDa	kilodalton
m^7G	monomethylguanosine
MALDI-TOF	matrix assisted laser desorption ionisation time of flight
MCTD	mixed connective tissue disease
MFG-E8	milk fat globule epidermal growth factor–8
MHC	major histocompatibility complex
mRNA	messenger ribonucleic acid
NBT	nitrobenzamidine triazine
NMWCO	nominal molecular weight cut off
nt	nucleotides
O-GalNAc	O-linked β-N-acetylgalactosamine
O-GlcNAc	O-linked β-N-acetylglucosamine
PBS	phosphate buffered saline
PBST	phosphate buffered saline containing 0.02 % v/v Tween 20
pI	isoelectric point
PIE	polyadenylation inhibitory element
PMSF	phenylmethylsulfonyl fluoride
PP	protein phosphatase
r68K	recombinant 68K protein
RA	rheumatoid arthritis
RNA	ribonucleic acid
RNAse	RNA nuclease
RNP	ribonucleoprotein particle
RP-HPLC	reverse phase HPLC
RRM	RNA recognition motif
sDMA	symmetrical dimethylarginine
SDS	sodium dodecyl sulfate
SDS-PAGE	SDS-polyacrylamide gel electrophoresis
SF-A	U1 snRNP-free U1A
SLE	systemic lupus erythematosus
SmB^{trunc}	truncated SmB protein

SMN	survival of motor neuron complex
snRNA	small nuclear ribonucleic acid
snRNP	small nuclear ribonucleoprotein particle
SPE	SP-Sepharose column elution
TBE	tris borate EDTA
TCR	T-cell receptor
TEMED	N,N,N′,N′-tetramethylethylenediamine
TLR	toll-like receptor
TMG	trimethylguanosine
Topo I	DNA topoisomerase I
Triton x100	4-(1,1,3,3-tetramethylbutyl)phenyl-polyethylene glycol
Tween-20	polyethylene glycol sorbitan monolaurate
UV	ultra violet
v/v	volume/volume
w/v	weight/volume

Abbreviations for amino acids

Amino acid	Three-letter abbreviation	One-letter symbol
alanine	ala	A
arginine	arg	R
asparagine	asn	N
aspartic acid	asp	D
cysteine	cys	C
glutamine	gln	Q
glutamic acid	glu	E
glycine	gly	G
histidine	his	H
isoleucine	iso	I
leucine	leu	L
lysine	lys	K
methionine	met	M
phenylalanine	phe	F
proline	pro	P
serine	ser	S
threonine	thr	T
tryptophan	trp	W
tyrosine	tyr	Y
valine	val	V

Chapter One

General Introduction

Autoimmunity can be defined as immune recognition and reaction against an individual's own tissues. In simple terms, ***autoimmune disease*** results from the breakdown of the individual's self-tolerance mechanisms leading to uncontrolled, pathogenic self-reaction. Exactly how and why this happens remains largely unanswered.

1.1 Self-Tolerance

The adaptive immune system is central to maintaining health by destroying or removing potentially harmful agents. Receptors expressed on the surface of antibody producing B-cells (BCR) and cytokine producing T-cells (TCR) are collectively so diverse that they can recognise almost any molecule or antigen. By various means, these BCR and TCR are capable of targeting the antigen for destruction or clearance from the body. Naturally this recognition will include antigens which are expressed within an individual's own tissues (autoantigens). At the turn of the nineteenth century Ehrlich coined the term "horror autotoxicus" to describe the recognition of self-tissues by the immune system, and he observed that mechanisms must be in place to prevent this autoreactivity. He realised that regulation or stopping autoantibody production was the key to self-tolerance (Dighiero and Rose, 1999).

Gradually over the next century key research by Lederberg (Lederberg, 1959), Bretscher (Bretscher and Cohn, 1970) and Lafferty (Lafferty and Ronald, 1993) revealed some of the likely tolerance strategies. However, it has been the use of transgenic and knock-out systems in the last few decades that has helped to fine tune our knowledge of tolerogenesis, in mice at least (Amagai *et al.*, 2000; Stoll and Gavalchin, 2000).

Nature it seems is not content with one mechanism of tolerance. Four major processes have evolved to prevent autoreactive B- and T-lymphocytes from responding to their "cognate" autoantigens: clonal deletion; clonal abortion; anergy; suppression. The method adopted depends on a number of factors including the maturity of the lymphocyte, the nature and concentration of the autoantigen, tissue distribution and co-expression with the major

histocompatibility complex (MHC) molecules. Most is known about T-cell tolerance with the mechanisms of B-cell tolerance remaining sketchy.

1.1.1 T-cell tolerance

Precursor thymic lymphocytes (T-cells) undergo what is known as central tolerance. Figure 1.1 is a schematic representation of how thymic central tolerance is thought to occur. Precursor T-cells express both cluster designation cell surface markers CD4 and CD8, which later define whether they become helper T-cells ($CD4^+$) or cytotoxic T-cells ($CD8^+$). In the thymus cortex, T-cells encounter thymic epithelial cells which express MHC class I and class II molecules. T-cells which engage with either MHC class II or MHC class I molecules through their TCR and CD marker are positively selected for survival. Non-interacting cells, however, undergo apoptosis or programmed cell death. This positive selection is also known as MHC class restriction and ensures that T-cells only recognise cognate antigen presented with MHC.

Dendritic cells are specialised antigen presenting cells found mostly in the lymph tissues, thymus and spleen. The role of the dendritic cell is critical to central tolerance. Surface MHC molecules of dendritic cells display or present peptide fragments of self-proteins. Precursor T-cells, expressing TCR for self-protein, encounter and interact with cells presenting their cognate peptide, thus initiating apoptosis. Self or autoreactive T-cells are removed from the T-cell repertoire by clonal deletion, whilst non-self T-cells survive to enter the mature pool by negative selection (Goodnow *et al.*, 2005).

Less than 3 % of the precursor T-cells entering the thymus make it to the mature T-cell pool. A proportion of these will be autoreactive cells that have escaped deletion either through poor MHC-autoantigen presentation or lack of exposure to the cognate autoantigen. Therefore, alternative mechanisms must be in place to preserve immune tolerance. Collectively, these mechanisms are

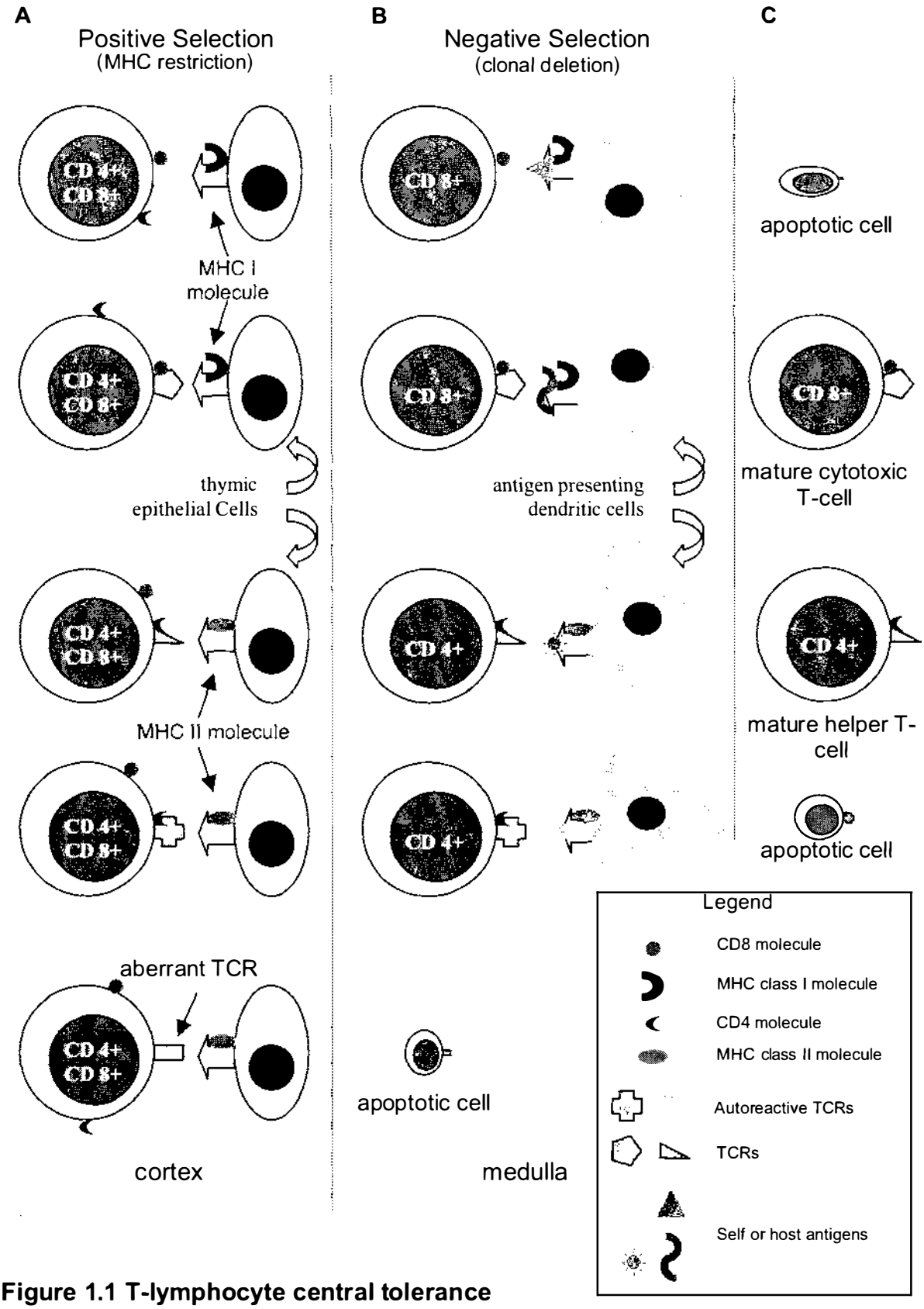

Figure 1.1 T-lymphocyte central tolerance
A, In the cortex, T-cells engaging with MHC class molecules are selected for survival. Cells which do not engage with MHC undergo apoptosis. **B**, T-cells in medulla encounter dendritic cells presenting self-antigens with MHC. Engagement with these cells results in apoptosis. **C**, self-tolerant mature T-cells survive due to negative selection.

referred to as peripheral tolerance and they occur in a number of ways:

- tolerance by ignorance – T-cells do not encounter their cognate autoantigen;
- clonal anergy - despite recognising their cognate autoantigen, T-cells are rendered useless or anergic by the lack of co-stimulatory signals;
- T-cell suppression – activated autoreactive cells can be anergised by the release of inhibitory cytokines from suppressor T-cells (Maloy and Powrie, 2001).

Inadequate management of any of these tolerance mechanisms is likely to result in autoimmunity or perhaps even autoimmune disease.

1.1.2 B-cell tolerance

The notion that B-cell tolerance is a result of T-cell tolerogenesis no longer holds true. High affinity immunoglobulin (Ig) production cannot occur without the necessary T-cell help. However, B-cells are now recognised as being far more than antibody factories (Mitchison and Wedderburn, 2000). It is clear that they play an essential role in many aspects of immune system reactivity in both health and disease (Lipsky, 2001). The immune system has evolved many strategies to achieve and maintain B-cell self-tolerance.

The specifics of positive and negative selection of B-cells during tolerogenesis are still unknown. While it is clear that stromal cells in the bone marrow assist in the positive selection of cells with productive rearrangments of Ig genes, the co-factors and receptors involved have not yet been elucidated. Negative selection occurs throughout all developmental stages either in the bone marrow or in germinal centres in the secondary lymphoid tissues (spleen or lymph nodes). Clonal abortion occurs when immature B-cells expressing autoreactive surface IgM molecules encounter their cognate autoantigen in the bone marrow. The surface IgM is sequestered and further differentiation is arrested. Those autoreactive cells that migrate from the bone marrow to the secondary lymphoid tissues are exposed to soluble monomeric antigens. If the antigens are present above a critical concentration, the cells become anergised through down-

regulation of surface IgM. These cells are unable to receive T-cell help and hence cannot proliferate, produce antibodies, or participate in B-cell functionality. Anergy can be reversed, however, if the cells are stimulated with cytokine interleukin-4.

Cells that do survive are induced by a combination of follicular dendritic cells and T-cell help to undergo the B-cell unique process of somatic hypermutation. The variable region of the Ig gene is mutated in order to increase the BCR avidity for the cognate antigen. Even at this stage the B-cell is tested by antigen presenting follicular dendritic cells to ensure that defective or autoreactive Igs have not been produced by the mutational machinery.

In fact, B-cells are scrutinised throughout their development and their survival is dependent on BCR-antigen interaction coupled with co-stimulatory events such as:

- signaling thresholds mediated by the cell surface markers CD19 (Inaoki *et al.*, 1997) and CD22 (O'Keefe *et al.*, 1999);
- stimulation by cytokines secreted from T-cells or follicular dendritic cells;
- interaction with other factors such as B-cell activation factor (Mackay and Mackay, 2002).

Despite the checks and balances, a small population of B-cells escape this scrutiny. These cells appear early in development and express the T-cell specific cell surface marker CD5 (Casali and Notkins, 1989). Igs from these cells are natural autoantibodies.

1.2 Natural Autoimmunity

A substantial proportion of circulating Igs are natural autoantibodies (Shoenfeld *et al.*, 1982; Satoh *et al.*, 1983). These antibodies are derived from minimally-mutated germline genes. They are characteristically multireactive, restricted to a number of non-critical epitopes, have low affinities and are non-pathogenic. The $CD5^+$ B-cells do not undergo affinity maturation (Coutinho *et al.*, 1995), although iso-type switching does occur, as evidenced by the circulation of IgM,

IgA and a normal distribution of IgG subclasses 1-4 (Algiman *et al.*, 1992). The repertoire of autoantibodies is selected early in B-cell development and their pattern of reactivity is conserved throughout an individual's life. Autoreactivity is controlled by anti-idiotype (anti-variable region) IgM (Kazatchkine, 1994). Therefore, under normal conditions the idiotype/anti-idiotype network helps to determine the pattern of autoreactivity.

The physiological need for natural autoantibodies is not entirely clear. They have been reported to be involved with clearance of autoantigens from tissues after apoptotic events (perhaps in conjunction with C1q complement), various regulatory functions (Kazatchkine, 1994) and promotion of tissue repair (Asakura *et al.*, 1998). Natural autoreactive T-cells are present in healthy individuals, and like natural autoreactive Igs, auto T-cells play a role in maintenance of self-tolerance and tissue repair (Schwartz and Cohen, 2000).

Clearly, autoimmunity is a normal physiological phenomenon. Therefore, what changes to turn it into a pathogenic condition? Does natural autoimmunity provide any clues about the emergence of autoimmune disease or are these immune system events quite independent?

1.3 Pathogenic Autoimmunity

Before trying to answer these questions, some attempt should be made to explain the events leading to the break in tolerance and the production of pathogenic autoreactive B- and T-lymphocytes. A number of theories exist to explain the mounting of a pathogenic autoimmune response, some of which are discussed below (Nakamura and Nakamura, 1992).

1.3.1 Apoptosis

Apoptosis plays a pivotal role in central tolerance by destroying or deleting autoreactive clones and providing a source of self-antigens for tolerising T-cells (Mahoney and Rosen, 2005). Defects in the pathways initiating apoptotic death and the recognition and clearance of apoptotic cells by phagocytes (dendritic cells or macrophages) can result in poor tolerance induction (Lauber *et al.*,

2004). Failure of tolerance may later lead to the development of autoimmune disease. Irregularities in the expression of Fas or FasL apoptotic markers, for example, are known to lead to insufficient clonal deletion allowing autoreactive B- and T-lymphocytes to escape death, a phenomenon which occurs in Canale-Smith syndrome (Drappa *et al.*, 1996) and also in mice with defective Fas (Watanabe-Fukunaga *et al.*, 1992). More recently, it has been observed that poor expression of another proapoptotic protein, *Bim*, impairs apoptosis of autoreactive lymphocytes (Hughes *et al.*, 2006).

There are multiple pathways for the recognition and clearance of apoptotic cells by phagocytes. As with apoptosis induction, impairment of these pathways reduces the potency of tolerogenesis. An example of this involves the recognition of apoptotic cells by phagocytes via bridging molecules. One such molecule, the milk fat globule epidermal growth factor-8 (MFG-E8), binds to apoptotic cells and appears to mediate not only the binding of the target cell to phagocytes but also its subsequent internalisation (phagocytosis). Experiments with MFG-E8 knockout mice have demonstrated the reduced ability to phagocytose apoptotic cells despite other phagocytic functions operating normally. Moreover, these knockout mice also develop autoimmune lupus-like traits (Hanayama *et al.*, 2004).

1.3.2 Aberrant antigen modifications

Specific self-antigens that contain unusual post-translational modificatons, for example, the enzymic conversion of arginines to citrulline (van Venrooij and Pruijn, 2000), arginine methylation (Brahms *et al.*, 2000), proteolytic cleavage (Casciola-Rosen *et al.*, 1999) or even glycosylation may act as antigens without apparently breaking tolerance (Utz *et al.*, 2000; Doyle and Mamula, 2001). Whether these modified antigens are the causative agents of specific diseases remains to be elucidated.

1.3.3 Antigen cross-reactivity

Molecular mimicry, cross-reactivity of autoantigen epitopes with unrelated viral or microbial proteins, has been touted as a likely ætiologic event in many

autoimmune diseases (Horsfall, 1992; Benoist and Mathis, 2001). This mimicry can occur in a number of ways:

- B-cells can be stimulated to produce antibodies in a T-cell independent manner by microbial (lipopolysaccharide) or viral (Epstein Barr) "superantigens" (Klinman and Steinberg, 1987). If an autoreactive B-cell is stimulated in this way autoantibody production will result, although in the absence of T-cell help these antibodies will have low affinity;

- Antigen mimicry can also elicit T-cell activation and subsequent B-cell stimulation. High concentrations of microbial antigens bearing cross-reactive cryptic self-epitopes can prime T-cells via professional antigen presenting cells. The primed T-cells will then recognise low abundance autoantigens expressed on tissue cells without the need for co-stimulation;

- Microbial antigens bearing autoreactive B-cell epitopes can break tolerance and elicit T-cell help by presenting microbial foreign epitopes to T-cells.

Conversely, self-antigens can recruit the innate immune system into activating the adaptive system (B- and T-cells) by being recognised as microbial or viral antigens. Activation is thought to occur via toll-like receptors (TLRs) that identify invading organisms by pathogen-associated molecular patterns rather than by a specific epitope (Ozinsky e*t al.*, 2000). Autoreactive B-cells have been stimulated by the nucleic acid-containing chromatin-IgG immune complex through the engagement of both BCR and TLR9 on the B-cell. The presence of deoxyribonucleic acid (DNA) has been shown to be essential for cell activation, whereas, other types of immune complex have not elicited proliferation responses (Leadbetter e*t al.*, 2002). Double-stranded (ds) and single stranded (ss) regions of the ribonucleic acid (RNA) can mimic RNA virus structure. This pathogen-associated pattern is found in the RNA associated with the spliceosomal small nuclear ribonucleoprotein particles (snRNP), and it can induce inflammatory cytokine, type-I interferon, production through interaction with TLR3, 7 and/or 8. A potential role of snRNA as an adjuvant increasing the immunogenicity of snRNP proteins during the initiation of an autoimmune

response is inferred (Kelly *et al.*, 2006). These proposed mechanisms of TLR mediated stimulation of the immune system may explain the dominance of nucleic acid binding proteins as autoantigens in systemic autoimmune diseases.

1.3.4 Idiotypic induction

The high affinity of most autoantibodies can only arise through somatic mutation and the continual presentation of antigens by follicular dendritic cells. This phenomenon, along with the co-existence of autoantibodies to different epitopes on the same molecule, would indicate an autoantigen driven response rather than a response due to a foreign mimic (Miller *et al.*, 1990). But how is the necessary T-cell help acquired? One likely mechanism is idiotypic induction (Tomer *et al.*, 1993), illustrated schematically in Figure 1.2. Natural autoantibodies interact with an autoantigen to form a complex that is then captured by an autoreactive B-cell. The natural idiotype is presented and a T-cell recognising the idiotype gives the B-cell consent to produce autoantibody. This is the likely mechanism for pathogenic anti-DNA autoantibody production in systemic lupus erythematosus (Shlomchik *et al.*, 1987) and is consistent with the dysregulation of the anti-idiotype network and the C1q (complement) deficiency (Pickering and Walport, 2000).

1.3.5 Genetics

There are a number of substantial reviews covering the genetic influence in autoimmune disease susceptibility (Harley *et al.*, 1998). It is irrefutable that certain human leucocyte antigen haplotypes are related to the onset of certain autoimmune diseases. Non-MHC genetics and the influence of epigenetic interactions are also implicated (Wandstrat and Wakeland, 2001). A general female bias towards autoimmune disease, with women making up 90 % of the sufferers of some conditions, demonstrates an influence of male and female genetics (Stewart, 1998; Whitacre, 2001). Sex hormones affect the immune system, oestrogens enhance the immune response, whereas, androgens and progesterone are immuno-suppressive. The levels of oestrogen in synovial joint fluid is elevated in both female and male sufferers of rheumatoid arthritis (Cutolo *et al.*, 2004).

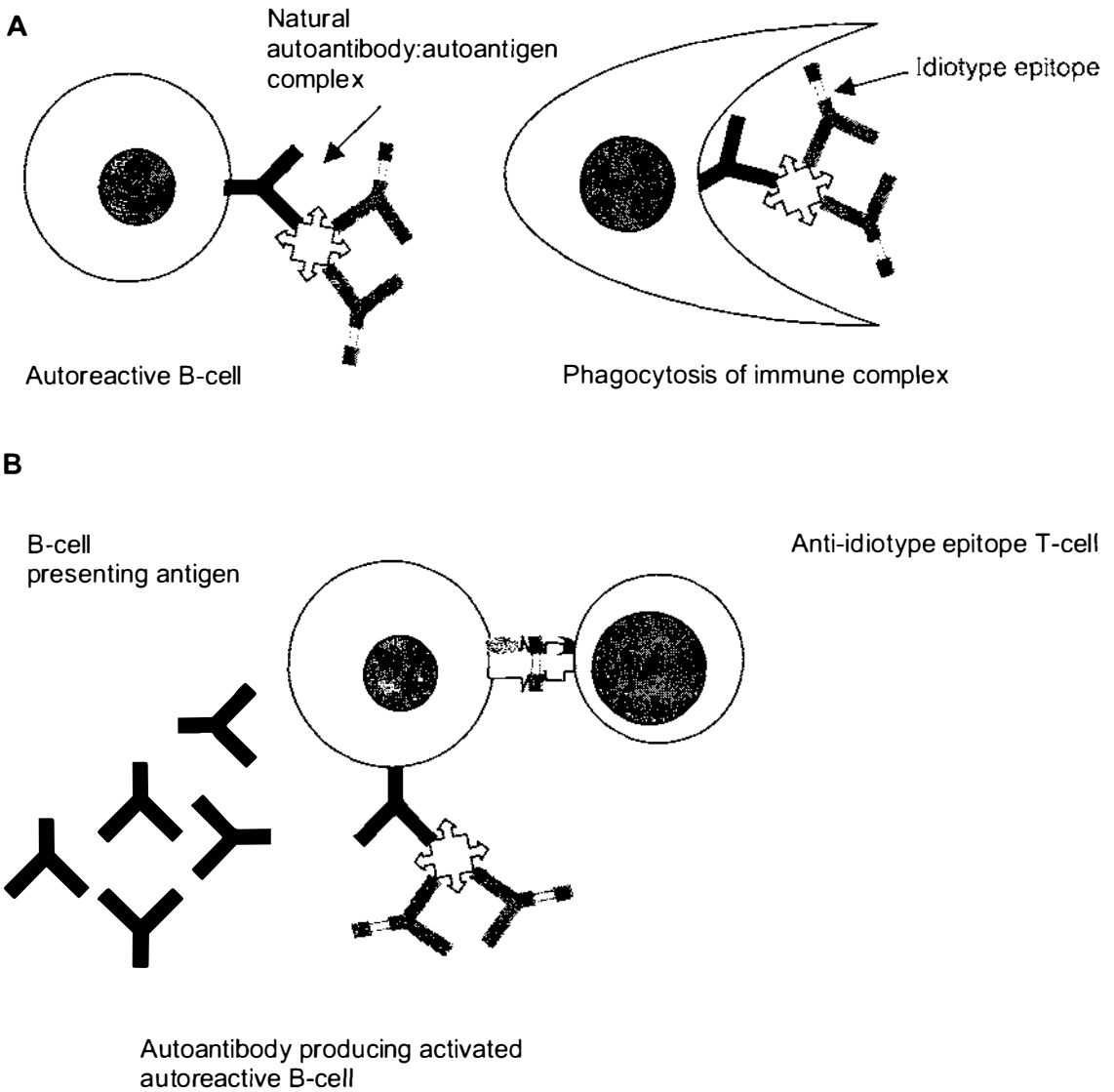

Figure 1.2 Idiotype induction mechanism of activating autoreactive B-cells

A, autoreactive B-cells engage and phagocytose an immune complex of autoantigen and natural autoantibody. **B**, the B-cell acts as an antigen-presenting cell and displays a natural autoantibody idiotype peptide with MHC class II molecule. This cell encounters an anti-idiotype T-cell that results in activation of the B-cell and autoantibody production.

Gender differences other than sex hormones may contribute equally to autoimmune disease. One such difference relates to the X-chromosome inactivation. This creates two cell groups each carrying genes expressed from

different parental X-chromosomes. Potentially tolerogenesis could occur for one set of X-chromosome gene products but not the other, allowing some self-reactive lymphocytes to survive (Stewart, 1998).

The breaking of immune tolerance by the mechanisms described so far do not amount to autoimmune disease. A number of conditions have to coincide to overcome tolerance and mount a pathogenic autoimmune response (Sompayrac, 1999):

- Firstly, the MHC molecules (under genetic influence) present self-antigens to TCR in such a way that the cells are not negatively selected;
- Secondly, the population of T- and B-cells must express sufficient cognate autoreactive receptors. This repertoire of autoreactive cells is transient and, therefore, is different between individuals at any one time, even in identical twins;
- Thirdly, a sustained stimulation and co-stimulation environment must exist. Inflammation sites provide this environment because at such a site, there is an accumulation of immune cells, the release of stimulatory cytokines co-incident with exposure to potential autoantigens. In fact, it has been shown that the onset of autoimmune disease often occurs after an infection (Wraith *et al.*, 2003).

No definitive answer exists to explain pathogenic autoimmunity. It is clear that resulting pathologies are as varied as the possible explanations for pathogenesis.

1.4 Disease Pathology

Autoimmune disease pathologies range from organ-specific, where the T-cell and B-cell target epitopes are apparent and the damage caused is a direct consequence of this (Levinson, 1994), to systemic, where the relationship between epitope and inflicted damage is not obvious (Leff *et al.*, 1992). Systemic pathologies, also referred to as rheumatological autoimmune diseases, will be the focus of further discussions in this thesis.

Systemic lupus erythematosus (SLE) is the archetypal multi-system disease. It is characterised by clinical features including erythematous or red skin rashes, photosensitivity, joint inflammation or arthritis, lung membrane (pleuritis) and heart membrane (pericarditis) inflammation, kidney damage, depression or psychosis and haemolytic anemia (Condemi, 1992). The consensus of opinion is that SLE is a B-cell or autoantibody mediated pathology (Mitchison and Wedderburn, 2000; Lipsky, 2001). Hyperactive B-cells produce large quantities of autoantibodies, the majority of these targeting nuclear components. These antibodies form immune complexes that are deposited systemically in affected tissues where they elicit a hypersensitivity type III inflammatory response.

SLE is one of a group of overlapping systemic syndromes sharing a number of immunological and clinical features (Hay, 1995). These disorders include:

- systemic sclerosis – typified by skin pitting and subsequent thickening of the skin, which also becomes smooth and waxy. These symptoms are often preceded by Raynaud's phenomenon which is the restriction of blood supply to the tips of fingers and toes;
- Sjögren's syndrome – dry eyes, dry mouth and recurrent salivary gland pain. Often a secondary disease in association with SLE or rheumatoid arthritis (RA). Over 90 % of sufferers are female;
- rheumatoid arthritis – joint swelling, joint erosive damage, joint deformity and appearance of subcutaneous nodules;
- dermatomyositis and polymyositis – characterised by skeletal muscle weakness, and in the case of dermatomyositis, a subtle skin lesion often only appearing on the eyelids and knuckles, and muscle vascular damage.

In 1972, Sharp described another systemic disease in a number of patients who presented with symptoms of SLE, myositis and systemic sclerosis (Mukerji and Hardin, 1993). This is known as Sharp syndrome or more commonly mixed connective tissue disease (MCTD). The multifactorial nature of systemic disease means that there is considerable overlap of clinical presentation. Symptom-based evaluation alone is difficult (Hay, 1995) and often leads to misdiagnosis (Anon, 1992). The status of MCTD as a discrete syndrome has

been heavily debated (Lazaro e*t al.*, 1989; Piirainen and Kurki, 1990; Smolen and Steiner, 1998), and defining the serological features of this and other systemic diseases will help to settle the debate, leading to correct diagnosis and appropriate treatment of the disorder.

The serological hallmark of systemic autoimmune diseases is the presence of circulating autoantibodies termed anti-nuclear antibodies (ANA) that are specific for normally inaccessible cellular antigens known as extractable nuclear antigens (ENA) (Sturgess, 1992). The link between specificity and the clinical symptoms, despite the lack of pathology and epitope link, is perhaps the most remarkable attribute of systemic diseases, an attribute that has been successfully exploited in disease diagnosis (Smeenk, 2000).

Immunochemical and molecular characterisation of the ANA and ENA specificities have shown that autoantigens are highly conserved molecules present in all cell types and in many species (Tan e*t al.*, 1988). It appears that the specificity of response is not the result of a specific ætiologic stimulus but rather to the context, location and duration of the stimulus (Nagaraju e*t al.*, 2000). Whatever the mechanism, it is clear that systemic diseases can be distinguished on the basis of their individual ANA/ENA profiles, providing ideal diagnostic markers (Table 1.1). Increasing knowledge about ENAs, their clinical association and prognostic impact, is fuelling the demand for their detection (Smolen e*t al.*, 1997). Some antigens are highly disease specific while others appear in several systemic diseases. The complex nature of some ENAs makes their characterisation with conventional diagnostic tests difficult. These antigens consist of multiple proteins associated with a RNA entity and are termed ribonucleoprotein particles (RNPs). RNPs harbour a multitude of ANA epitopes and the correlation of epitope with clinical observation may provide useful data regarding disease diagnosis, prognosis or even new therapeutic approaches. This can only be achieved through detailed analysis of the complex antigens and the use of improved immunodiagnostic approaches.

Table 1.1 Disease association of the most common extractable nuclear antigen specificities

Eponym	Antigen(s)	Function	Disease Association
"native" DNA	Double-strand DNA		SLE (40 %)
U1-RNP	68K, A and C proteins complexed with small nuclear U1-RNA	Pre-mRNA splicing	SLE (32 %), MCTD (>95 %,), (> 90 % high anti-68K), RA, SS
SS-A (Ro) 60	60 kD protein complexed with Y1-Y5 RNAs	?	SjS (60 %), SLE (35 %), SCLE (70 %), NL
SS-A (Ro) 52	52 kD protein complexed with Y1-Y5 RNAs	?	As for SS-A 60, PM (20 %), CREST
SS-B/La	48 kD protein complexed with RNA pol III transcripts Y1-Y5 RNAs	RNA pol III transcription termination factor	SjS (40-80 %), SLE (15 %) NL
Jo-1	Histidyl tRNA synthetase	tRNA aminoacylation	Polymyositis PM (25-45 %)
CENP-B	80 kD centromere protein	Cell division	CREST (70-80 %)
Scl-70	70 kD degradation product of DNA topoisomerase I	mRNA, rRNA transcription	Diffuse SS (35-70 %)
SmB,B':SmD	Smith antigens common to U1, U2, U4 and U5 RNAs	Pre-mRNA splicing	SLE (30 %)
Ribosomal P	P0 (38 kD), P1 (19 kD) and P2 (17 kD) of 60S ribosome subunit	protein assembly	SLE (13-36 %), SLE psychosis (70 %)

SLE- systemic lupus erythematosus; MCTD- mixed connective tissue disease; RA- rheumatoid arthritis; SjS- Sjögren's syndrome; SCLE- subcutaneous lupus erythematosus; NL- neonatal lupus; SS- systemic sclerosis; CREST- calcinosis, Raynaud's phenomenon, oesophogyl dysfunction, sclerodactyly and telangiectasiae. (Nakamura and Nakamura, 1992; Guma and Krakauer, 1994; Rutjes *et al*., 1997; Greenwood *et al*., 2002)

Chapter Two

Literature Review

2.1 The Spliceosome

Autoantibodies reacting with small nuclear ribonucleoproteins (snRNPs) from patients with SLE and MCTD have contributed significantly to the understanding of events surrounding pre-messenger RNA splicing (Lerner and Steitz, 1979).

Splicing of nascent pre-messenger RNA to remove *introns* (non-coding) and anneal *exons* (coding), a pivotal step in mRNA synthesis, is faithfully achieved by the spliceosome. In its entirety, the spliceosome consists of a complex of five snRNPs designated U1, U2, U4, U5 and U6, and more than 300 splicing/RNA processing associated proteins (Rappsilber *et al.*, 2002). U1 RNP acts as a homing device and initiates the sequential assembly of the spliceosome around the nascent messenger RNA (mRNA) through binding to the 5′ splice site. Once assembled, the spliceosome undergoes rearrangements in order to create an active site. The ensuing phospho-transesterification reactions occur in two stages, the excision of an intron, followed by ligation of the exons on either side of it (Figure 2.1).

Spliceosomal snRNPs consist of highly structured non-coding uridine-rich RNAs, named U1, U2, U4, U5 and U6, which are expressed from over 40 genes (Eddy, 1999). These snRNAs, with the exception of U6, are monomethylated guanosine (m^7G) 5′ capped RNA polymerase II transcripts ranging in size from 117 (U5) to 189 (U2) nucleotides. They are adorned with a number of proteins. Some are common to U1-U5 RNPs, such as the seven core Sm proteins (B′/B, D1, D2, D3, E, F and G), whereas other proteins are snRNP specific. U6 snRNP is different from the other particles in that it is a product of RNA polymerase III transcription and the assembled particle does not contain the Sm common core proteins.

Not only do snRNAs provide a framework for protein attachment, but they also have a vital role in splicing site recognition and may actually be the catalyst for the transesterification reactions (Yean *et al.*, 2000; Sontheimer, 2001).

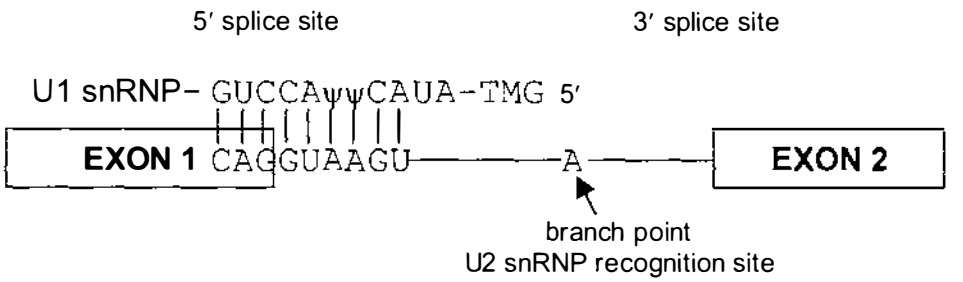

Step 1: Spliceosome assembly and 5′ intron cleavage

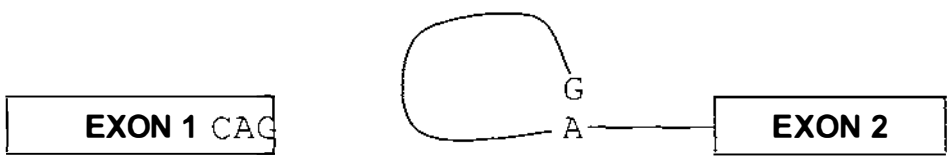

Step 2: Intron excision and exon annealing

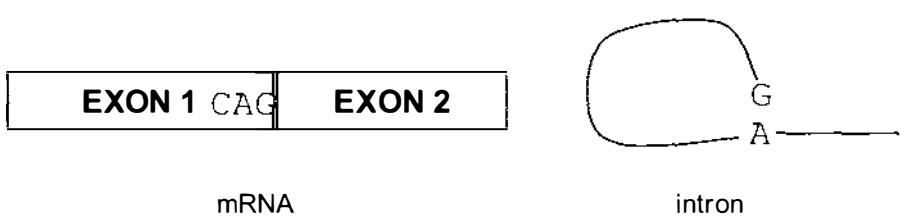

Figure 2.1 Pre-mRNA splicing reaction

The steps involved in spliceosome-catalysed excision of the introns of pre-mRNA and ligation of the exons to create the mRNA. The U1 snRNA 5′ recognition site docks with 5′ exon and initiates spliceosome assembly. U1 snRNA sequence includes a number of pseudouridine (ψ) nucleotides.

2.1.1 Biogenesis of the uridine-rich small nuclear ribonucleoprotein particles (snRNPs)

The assembly of the snRNPs is a multi-step process taking place in both the nucleus and cytoplasm (Will and Lührmann, 2001) and is schematically represented in Figure 2.2. Sm proteins encounter the methylosome, the first of two large multimeric protein complexes involved in snRNP biogenesis, in the cytoplasm (Friesen *et al.*, 2002). The methylsome has a 20 Svedburg unit sedimentation coefficient (20S) and consists of a phosphoprotein (PICln) which regulates Sm protein association with the methylosome (Freisen *et al.*, 2001), a

tryptophan-aspartic acid (WD) repeat protein (MEP50) which facilitates Sm/methylosome interactions (Freisen *et al.*, 2002), and a methyltransferase (JBP1) which symmetrically dimethylates specific arginine residues in SmD1, D3 and B′/B. Symmetrical dimethylated arginines (sDMA) enhance the binding affinity of Sm proteins for the second multimeric protein conglomerate involved in snRNP biogenesis, the survival of motor neuron (SMN) complex (Massenet *et al.*, 2002; Gubitz *et al.*, 2004). This complex is the assembly point for snRNP and consists of an oligomeric SMN protein, plus a group of proteins named gemins. The SMN protein acts as a chaperone to the Sm proteins by preventing them from making inappropriate associations with each other and their cognate snRNA (MacKenzie and Gendron, 2001). This interaction between Sm and SMN is essential for snRNP biogenesis. In the fatal disorder spinal muscular atrophy, a point mutation in the SMN 1 gene results in poor Sm binding to the SMN complex leading to impaired snRNP biogenesis (Selenko *et al.*, 2001).

Export of the RNA components of snRNPs from the nucleus to the cytoplasm is mediated through the binding of cap binding proteins to the m^7G RNA cap (Izaurralde *et al.*, 1995), followed by interaction with the nuclear export receptor *Exportin 1* (Hamm and Mattaj, 1990). Once in the cytoplasm, snRNA binds to the SMN complex in an RNA sequence-dependent manner (Yong *et al.*, 2004). Attachment of a seven-membered Sm protein ring to the highly conserved Sm binding nucleotide sequence of the snRNA is orchestrated by the SMN complex. Association of the RNP specific proteins with the snRNA is then permitted (Nelissen *et al.*, 1994). This is followed by the hypermethylation of m^7G at the 5′ end of the RNA, to trimethylguanosine (TMG) (Mattaj, 1986). Re-entry of the newly assembled snRNP is mediated through an *Importin* receptor which recognises the complete Sm core structure and the TMG cap of the U snRNA (Fischer *et al.*, 1993). Figure 2.3 schematically represents fully assembled U1 snRNP.

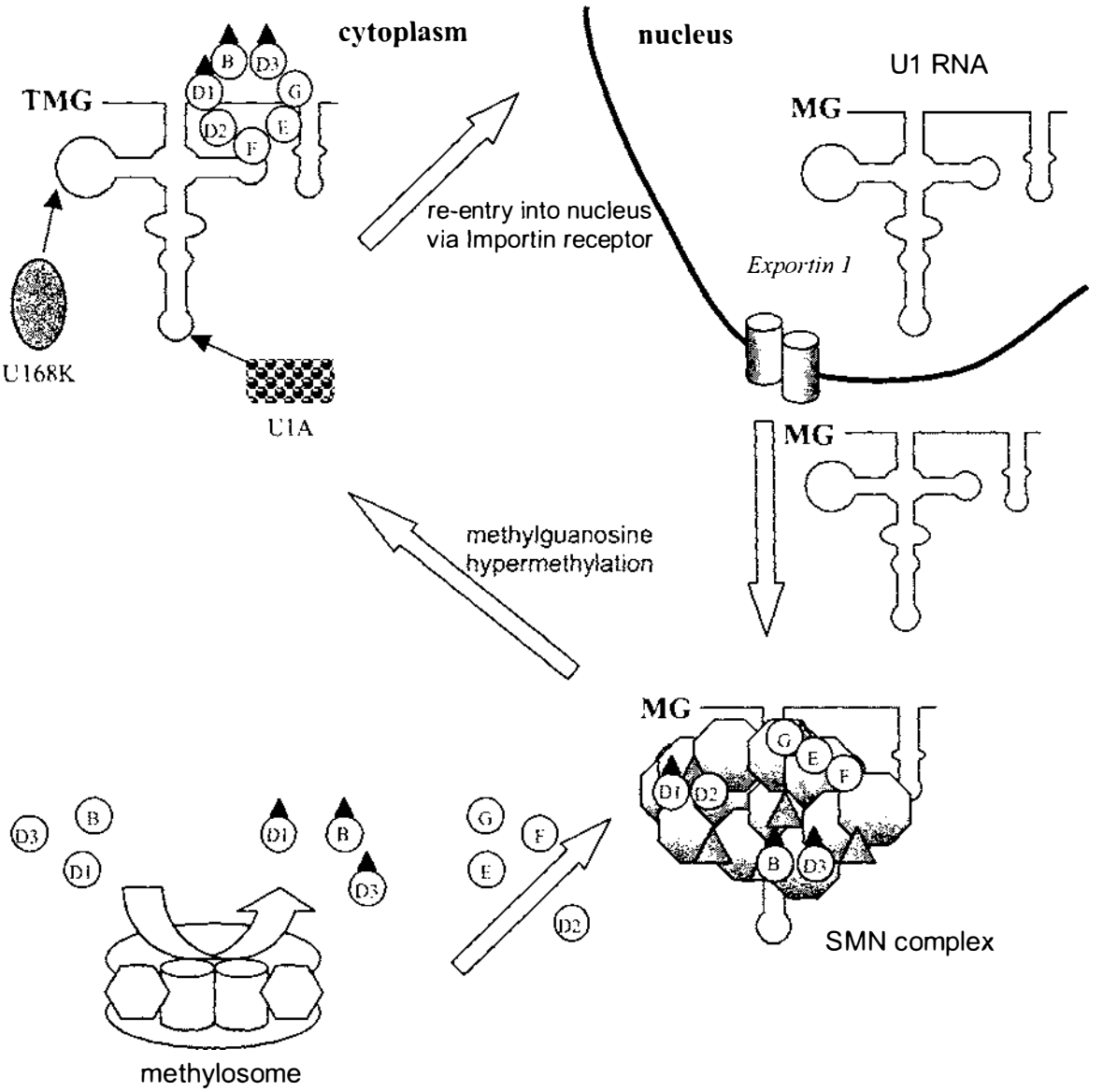

Figure 2.2 U1 snRNP biogenesis

Sm proteins encounter the methylosome in the cytoplasm and specific arginines on SmD1, D3 and B become dimethylated. Sm proteins then interact with the survival of motor neuron (SMN) complex where they rendezvous with U1 snRNA. Sm core assembles and attaches to U1 snRNA which becomes hypermethylated before re-entering the nucleus.
▲ represents symmetrical dimethyl arginines (sDMA); **MG**- methylguanosine; **TMG**-trimethylguanosine.

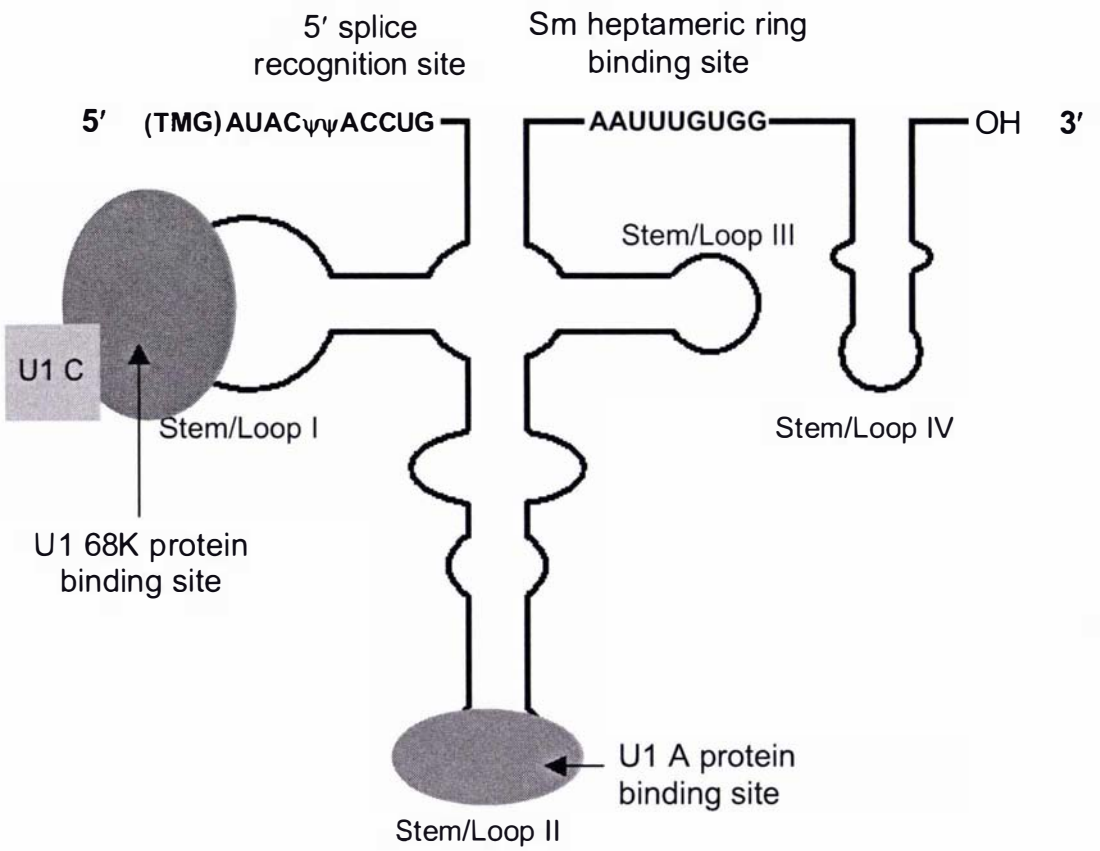

Figure 2.3 U1 snRNP structure and composition

Secondary stem/loop structure of U1 RNA highlighting the Sm ring binding site and the 5′ splice recognition site which anchors the spliceosome at the splicing region. The shaded ovals represent the U1 specific protein (U1 68K and U1A) RNA binding sites. The U1 specific C protein (shaded square), interacts directly with U1 68K protein rather than the RNA. The 5′ end of the U1 RNA is capped with a trimethylguanosine (TMG).

2.2 Sm Proteins

The Sm proteins, B′/B (29,28 kDa), D1 (16 kDa), D2 (16.5 kDa), D3 (18 kDa), E (12 kDa), F (11 kDa) and G (9 kDa), form a distinct family characterised by an Sm domain (Lehmeier *et al.*, 1990). SmB′/B protein results from alternative splicing of a single gene whereby the 11 C-terminal residues are replaced by two leucine residues (Chu and Elkon, 1991) (Figure 2.4). The SmB′ alternative splice product occurs only in humans and its functional significance is not known.

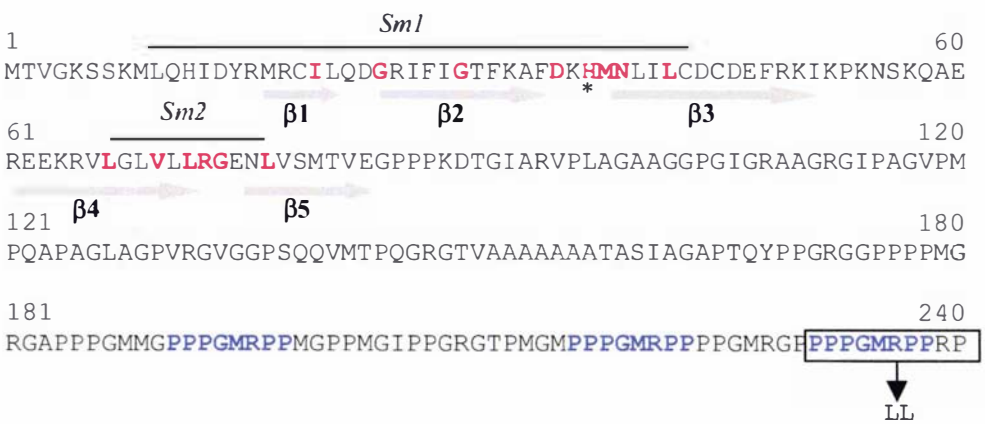

Figure 2.4 SmB′/B primary sequence

The alternative splice product of SmB′ has the 11 C terminal residues replaced by two leucine residues. Sm motif residues conserved in Sm and Sm-like proteins are red and the 5 β-strands are annotated with shaded arrows. The Loop 3 RNA contact is marked *. The blue residues indicate the proposed cross-reactive immunodominant epitopes.

The phylogenetic distribution of Sm proteins is testament to their importance in RNP assembly and RNA metabolism (Salgado-Garrido *et al.*, 1999). Sm and Sm-like proteins are expressed in all eukaryotes from yeast to human, in archae (SmAP) (Mura *et al.*, 2003) and eubacteria (Hfq) (Moller *et al.*, 2002).

All proteins containing Sm domains consist of two conserved Sm motifs, Sm1 and Sm2. These are separated by a linker of variable length and are involved in Sm protein-protein interactions (Hermann *et al.*, 1993; Cooper *et al.*, 1995). Sm proteins can form stable, RNA-free multimers (D1•D2, B′/B•D3, E•F•G) (Raker *et al.*, 1996). The three dimensional structures of the heterodimers

D1•D2 and B′/B•D3 have been solved and reveal almost structurally identical Sm domains made up of antiparallel β-sheet (Kambach *et al.*, 1999). Such a striking similarity in structure is shared by the SMN protein and, therefore, is likely to be due to a specific function such as Sm:RNA interactions and/or SMN oligomerisation (Selenko *et al.*, 2001). Sm heteromers are held together primarily by hydrogen bonding between the β4 and β5 strands at the Sm-Sm interface (Figure 2.5). The Sm core uses this structural motif to form a closed heptameric ring around the conserved uridine-rich Sm binding site of the U snRNA (Urlaub *et al.*, 2001). Using photo-crosslinking, Urlaub demonstrated that the Sm site RNA-Sm protein interaction occurred with Sm proteins B and G. The site specific interaction with SmG was to the first uridine in the U4 Sm site (AAUUUUUGA), and with SmB to the third uridine in the same site. Contacts between RNA and amino acid occur within loop 3 (between β2 and β3 strands) of both SmG and SmB. This general arrangement of the Sm core and its interactions is supported by cryoelectron microscopy (Stark *et al.*, 2001).

The arrangement and spatial proximity of the U1 snRNP proteins fosters interactions between U1 68K protein and SmD2 or SmB′/B, and between C protein and SmB′/B (Nelissen *et al.*, 1994). Interactions with assembled core proteins may mediate the binding of the U1 specific proteins to the U1 snRNP.

2.3 U1 snRNP Specific Proteins

The U1 specific proteins U1 68K (52 kDa), U1A (31 kDa) and U1C (17.5 kDa) make up the remainder of the 12S U1 snRNP complex. Both U1 68K and U1A are directly associated with the snRNA. These interactions are mediated through their RNA recognition motifs (RRM) which contain the highly conserved short motifs RNP1 and RNP2. U1C does not have a RRM but rather interacts with U1 68K protein and possibly SmB′/B through a zinc finger (CC-HH) type domain (Nelissen *et al.*, 1991; Nagai *et al.*, 2001).

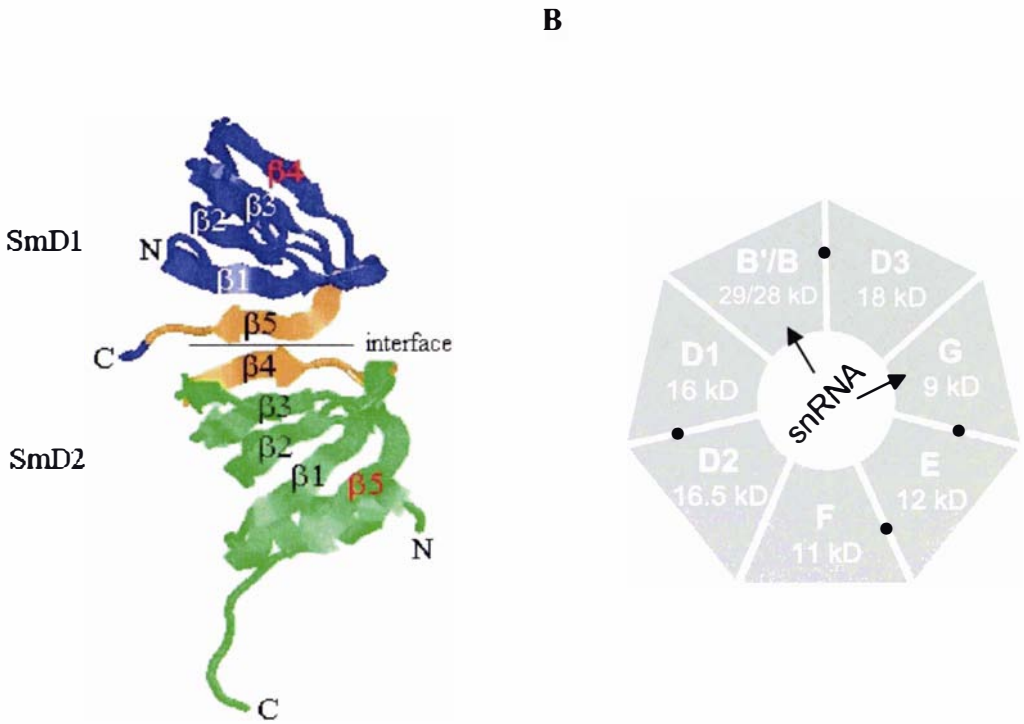

Figure 2.5 Sm core assembly

A: Sm domain anti-parallel β sheet structure. To clearly display the dimer interface between SmD1 β5 and SmD2 β4 (coloured orange) only the SmD1 core domain (residues 9-72) is shown. Strands β4 and β5 of SmD1 and D2 (labelled red) are thought to form similar interactions with adjacent Sm protomers to form a heptameric ring core complex. RasMol was used to display the Sm structure, which was adapted from Kambach *et al.* (1999).

B: Proposed heptameric 'doughnut' ring with the U snRNA in the hole. The arrows illustrate the interaction between SmB and SmG with RNA.

2.3.1 U1 68K protein

Despite its name, U1 68K has a molecular mass of 52 kDa. Regions of high acidic sidechain content in its 437 residue sequence cause U1 68K to migrate aberrantly at 68 kDa on SDS-polyacrylamide gel electrophoresis (SDS-PAGE). U1 68K is highly heterogeneous, consisting of at least thirteen distinct isoforms with pIs ranging from pH 6.7-8.6 (Elkon and Jankowski, 1985; Woppmann *et al.*, 1990). Varying degrees of phosphorylation and glycosylation (Chen and Agris, 1992) contribute to the microheterogeneity.

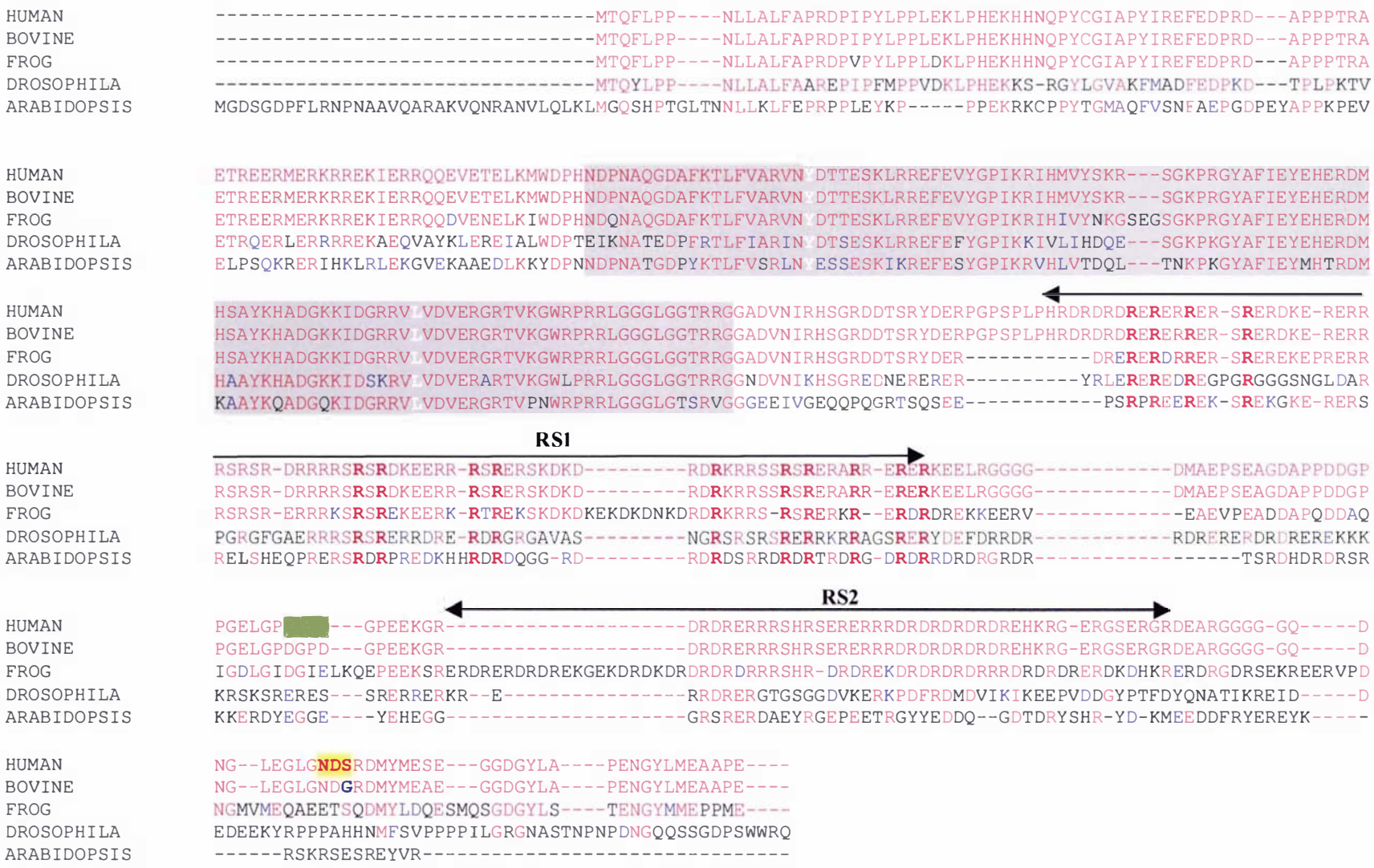

Figure 2.6 U1 68K protein sequence alignment The RNA binding domain is highlighted in gray with residues interacting directly with the U1 snRNA shown in white. The SR protein domains are annotated RS1 and RS2. The caspase 3 cleavage site (DGPD-G) is highlighted green in the human sequence. The potential N-linked glycosylation site is highlighted in yellow.

U1 68K associates with U1 snRNA stem/loop I (Figure 2.3) in an RNA-specific manner and requires eight nucleotides between 28 and 37 in the RNA loop I region for successful binding (Surowy *et al.*, 1989). The precise location of this interaction has been elucidated using a protein cross-linking approach (Urlaub *et al.*, 2000), which showed that Tyr^{112} and Leu^{175} of the RNA binding domain were associated with Guanosine 28 and Uridine 30 of stem/loop I (respectively). This interaction is highly conserved across all species.

The U1 68K protein is necessary for stable and faithful recognition of the pre-mRNA 5′ splice site, with the serine/arginine (SR) repeat splicing factor protein ASF/SF2 acting to assist U1 68K in this role. Interaction between these proteins is mediated through the first of two arginine rich regions (RS1) in U1 68K, comprising residues (248-270) (Figure 2.6). This region of primary structure is punctuated with short SR repeats which classifies U1 68K as a member of a SR protein sub-family (Cao and Garcia-Blanco, 1998). Exactly how ASF/SF2 and U1 68K RS1 interact is not clear. Their association is enhanced by phosphorylation of the serines in RS1, which promotes spliceosome assembly at the 5′ splice site, a reaction that is carried out by a specific SR Protein Kinase 1. However, splicing cannot occur without dephosphorylation of either the ASF/SF2 splicing factor (Cao *et al.*, 1997) or U1 68K (Tazi *et al.*, 1993). Therefore, phosphatase activity is critical for the disruption of the U1 snRNP/splicing factor interaction and the replacement of U1 snRNP with U6 snRNP at the 5′ splice site.

Lectin and chemical composition analysis of U1 68K imply the presence of an N-linked glycan, although the exact nature of the glycosylation has never been determined. One potential N-glycosylation site (Asn^{408}-Asp-Ser) exists in the human primary sequence, although it does not appear in other known U1 68K sequences. A more common modification in nuclear proteins is O-linked glycosylation with β-N-acetylglucosamine (O-GlcNAc) (Comer and Hart, 2000). The interplay between O-GlcNAc and O-phosphorylation of the same or adjacent residues has been shown to control a number of important regulatory activities including transcription and translation (Wells *et al.*, 2001; Wells *et al.*,

2002a). The role of O-GlcNAc, if any, in the regulation of U1 68K function has never been addressed.

One of the earliest events in apoptosis is the proteolytic cleavage of U1 68K to release a 40 kDa fragment (Casciola-Rosen *et al.*, 1994). Caspase 3 (or apopain) is proposed to mediate U1 68K cleavage at the site $DGPD^{341P1}$-$G^{342P1'}$ which falls between the RS1 and RS2 domains (Casciola-Rosen *et al.*, 1996). Intriguingly, this cleavage site sequence is not conserved among species. The susceptibility of U1 68K to metal-catalysed oxidative cleavage has been previously observed (Casciola-Rosen *et al.*, 1997), and although the precise fragmentation has not been ascertained, it seems to be associated with the aspartic acid-rich regions of the protein. Both apoptotic cleavage and oxidative fragmentation have been implicated in the development of U1 68K as an autoantigen. In fact, these modified forms of the autoantigen may be associated with particular clinical features of rheumatalogical disease (Greidinger *et al.*, 2000).

2.3.2 U1A protein

The 31 kDa U1A protein contains two RNA recognition motifs, although only the N-terminal motif (residues 9-88) is essential for U1A RNA binding (Figure 2.7). The interaction of the RNA binding domain with its cognate RNA has been elucidated from the structure of the U1A and U1 snRNA loop II complex (Oubridge *et al.*, 1994; Rupert *et al.*, 2003). This model has been used to predict how other proteins may bind RNA through RRMs (Nagai *et al.*, 1995).

The spliceosome can function normally in the absence of U1A, implying that this U1 snRNP specific protein is not essential to the splicing reaction (Will *et al.*, 1996). However, U1A may play a role in the communication between the 5′ and 3′ ends of the pre-mRNA splice region, linking splicing and mRNA processing reactions (Cooke and Alwine, 2002). For example, U1A has been shown to stabilise the interaction between the cleavage and polyadenylation specificity factor and 3′ mRNA, thus improving polyadenylation efficiency (Lutz, *et al.*, 1996).

Interestingly, free U1A regulates its own expression by inhibiting polyadenylation (Boelens *et al.*, 1993). A single U1A protein binds to a 3′ untranslated region of its own mRNA, known as the polyadenylation inhibitory element (PIE). A second U1A protein binds to the first to form a homodimer which then cooperatively binds to the PIE with high affinity. The $(U1A)_2$-PIE RNA complex specifically inhibits the poly (A) polymerase, preventing further mRNA processing (Klein-Gunnewiek *et al.*, 2000). By sequentially substituting residues in U1A using site directed mutagenesis, the homodimerisation, RNA cooperative binding and polyadenylation inhibition activities could be dissected showing that an 18 residue (98-115) domain was responsible for autoregulatory activity (Guan *et al.*, 2003).

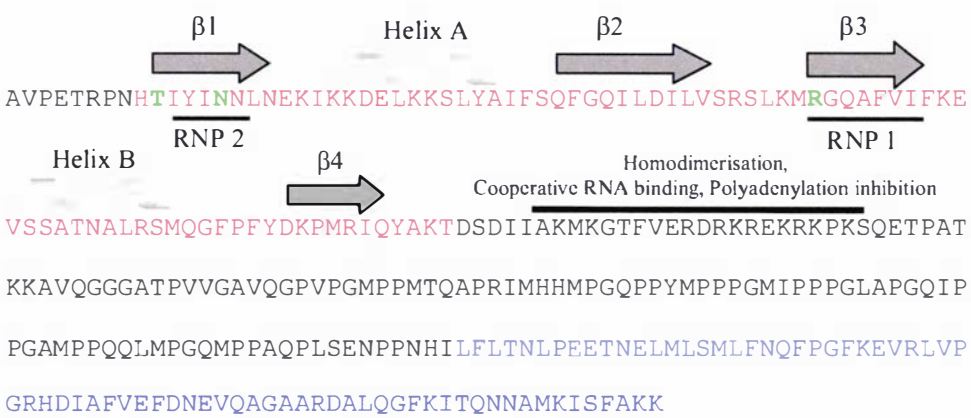

Figure 2.7 U1A primary sequence
The location of the N-terminal RNA binding domain is shown in red and the C-terminal domain is shown in blue. The topology of the U1 snRNA binding N-terminal domain is illustrated. Residues critical for RNA binding are highlighted in green. The autoregulatory domain is annotated.

2.3.3 U1C protein

The 17.5 kDa U1C protein requires the presence of both the Sm core and 68K proteins for incorporation into the U1 snRNP assembly. Unlike other snRNP proteins it lacks an RNA binding domain and, therefore, interacts with the 68K protein rather than directly associating with the U1 snRNA (Nelissen *et al.*, 1991; Nagai *et al.*, 2001). This protein:protein interaction is facilitated via a N-

terminal CC-HH zinc finger motif (Figure 2.8) which co-ordinates a single zinc atom (Muto *et al.*, 2004). Functionally, the U1C protein promotes and stabilises the formation of the early spliceosomal complexes through the terminal 60 amino acids which contain the zinc finger motif (Klein-Gunnewick *et al.*, 1995).

The remaining two thirds of U1C protein is dominated by repetition of proline, glycine and methionine residues (24 %, 9.5 % and 14 % respectively). The pro-gly-met motif mediates 5′ and 3′ intron splice site bridging through interaction with the protein, FBP21 (Bedford *et al.*, 1998). FBP21 in turn associates with the other pro-gly-met rich proteins SmB′/B and the branchpoint binding protein. FBP21 contains a WW type domain which is a short 38 amino acid fold with two conserved tryptophan residues spaced 20 residues apart in the consensus sequence. Although this domain interacts specifically with proline rich sequences, there is no apparent interaction between the pro-gly-met rich sequences of the U1A protein and FBP21.

```
  1 MPKFYCDYCDTYLTHDSPSVRKTHCSGRKHKENVKDYYQKWMEEQAQSLIDKTTAAFQQG
 61 KIPPTPFSAPPPAGAMIPPPPSLPGPPRPGMMPAPHMGGPPMMPMMGPPPPGMMPVGPAP
121 GMRPPMGGHMPMMPGPPMMRPPARPMMVPTRPGMTRPDR
```

Figure 2.8 Primary sequence of U1C protein
The zinc finger domain is highlighted in red and the key zinc co-ordinating residues in green. The C-terminal proline residues (magenta) make up 24 % of the amino acid composition. The main cross-reactive autoepitope is underlined.

2.4 snRNP Diagnostic Significance

The discovery of antibodies specific for snRNP associated proteins has been pivotal not only to the understanding of the spliceosome and its role in mRNA splicing (Balczon, 1993; Kamachi *et al.*, 2002), but also in defining the diagnostic and prognostic significance of snRNP autoantigen specificities.

The prevalence and specificity of autoantibodies to snRNP components can be used to differentiate between specific systemic autoimmune diseases. Anti-snRNP specificity predominates in MCTD and SLE (Tan *et al.*, 1988), with some

incidence in RA (Nishikai *et al.*, 1984) and systemic sclerosis (Ihn *et al.*, 1999). In general, but not absolutely, this specificity is associated either with U1 snRNP specific antigens (MCTD) or with U1-U5 common Sm core proteins (SLE). However, the ability to discriminate these reactivities has as much to do with the choice of diagnostic method as the antigen source.

2.4.1 Diagnostic methods

There are a large number of techniques available to qualitatively and quantitatively determine antinuclear antibodies. These assays vary in sensitivity, complexity and applicability to a clinical diagnostic laboratory (Kavanaugh, 2001; Phan *et al.*, 2002; Orton *et al.*, 2004).

2.4.1.1 Indirect immunofluorescence (IIF)

Screening ANA sera by indirect immunofluorescence (IIF) was first used in 1957 (Holborow *et al.*, 1957; Friou *et al.*, 1958). Diluted patient serum is incubated with human epithelial Hep-2 cells fixed on a glass slide. The cells are washed and then incubated with an anti-human IgG antibody conjugated with the fluorophore fluorescein. Serum is considered ANA positive if a discernible fluorescent staining pattern can be observed. Common nuclear staining patterns include homogeneous, nuclear rim, speckled and nucleolar patterns, all of which are disease associated. The speckled pattern is associated mostly with anti-RNP and anti-Sm antibodies in MCTD and SLE, and the interpretation of such patterns is highly dependent on the experience of the analyst. An interlaboratory study of IIF-ANA result interpretation demonstrated a coefficient of variance ranging from 36 % - 51 % (Tan *et al.*, 1997). This level of inaccuracy is compounded by up to 5 % SLE patients presenting with IIF-ANA negative serology (Maddison *et al.*, 1981). Despite these limitations, IIF is still used as the ANA screening method of choice in many clinical laboratories (Blomberg *et al.*, 2000; Smeenk, 2000).

2.4.1.2 Double immunodiffusion (DID)

The double immunodiffusion (DID) or Ouchterlony test relies on immuno-precipitation of the nuclear antigen by its cognate antibody (Bunn and Kveder, 1993). A crude nuclear antigen in the centre of an agarose plate diffuses

towards patient and control sera placed in the surrounding wells. After an incubation time of 18-48 hours a precipitin line should appear where the diffused antigen and antibody meet. Patient sera specificity can be determined through interpretation of the precipitin lines that form between the patient sera and the adjacent control wells. The method is subjective and requires well-trained and experienced operators for correct interpretation.

2.4.1.3 Counterimmunoelectrophoresis (CIE)

Counterimmunoelectrophoresis (CIE) is also dependent on immuno-precipitation. Rather than relying on passive diffusion, antigen and test sera are forced together by applying an electric field within the agarose. The precipitins that form are clearer and sharper than in DID, making interpretation easier. This method was first used to determine ANA by Kurata and Tan (1976) and has since been adapted for the characterisation of systemic autoimmune sera (Meilof e*t al.*, 1990; Parodi e*t al.*, 1998), and the discrimination of anti-RNP and anti-Sm sera (Bunn e*t al.*, 1982). However, the ability of CIE to reliably detect anti-Sm specificity is disputed (Molden e*t al.*, 1985; Navarro and Palau, 1991).

Not all autoantigen specificities are amenable to testing by CIE as the technique favours those antigens carrying a negative charge. For example, the scleroderma antigen, Scl-70, is poorly detected using this technique (Phan e*t al.*, 2002). Like DID, the sensitivity is dependent on the antibodies being able to form precipitins. As many as 19 % primary Sjögren's syndrome sera fail to be detected using DID or CIE (Beer e*t al.*, 1996).

2.4.1.4 Enzyme linked immunosorbent assay (ELISA)

ELISA was first introduced in 1972 for the quantification of antibodies (Engvall and Perlmann, 1972). The method relies on immobilised antigen on a solid phase reacting with autoantibodies in the patients' sera. The reactants are quantified spectrophotometrically from colour formation catalysed by enzyme (peroxidase or phosphatase) conjugated to anti-human IgG antibodies. This method has become the most widely used technique in clinical immunology

laboratories due to its sensitivity, high throughput format, quantitative results and the ability to automate many of the steps involved.

ELISA methods have been used extensively to characterise autoimmune sera (Buyon *et al.*, 1993; Dorner *et al.*, 1994; Jaskowski *et al.*, 1995; Halse *et al.*, 2000; Pourmand *et al.*, 2000), and the clinical value of the method has been established (Froelich *et al.*, 1990; Grigolo *et al.*, 1995; Benito-Garcia *et al.*, 2004). Over twenty companies have now commercialised ELISA kits as aids for systemic autoimmune disease diagnosis. Consistency and accuracy between the available kits is paramount when using them as reliable diagnostic tools. Studies evaluating the performance of commercial kits and ANA detection methods have highlighted the lack of standardisation and the need to reduce method variability through external quality assessment programs (Smolen *et al.*, 1997; Bizzaro *et al.*, 1998; Tan *et al.*, 1999).

ELISA methods used to detect anti-Scl-70, anti-Jo-1, anti-dsDNA and anti-Sm antibodies are consistently of low sensitivity. Two factors contribute to sensitivity and specificity, antigen quality and purity, and assay development. Antigen characteristics are governed by the source of the antigen. The difference afforded by native *vs.* recombinant antigen remains contentious. Native antigens have the advantage of authentic tertiary/quaternary structure and post-translational modifications (Venables *et al.*, 1983; Utz *et al.*, 2000), whereas, recombinant technology offers the ability to isolate large quantities of low abundance proteins that may or may not have exactly the same fold as the native protein (Schmitt and Papisch, 2002). Tan *et al.* (1999) found no significant variation in assay sensitivity and specificity between native and recombinant antigen. It is apparent, however, that superior sensitivity is observed with native Scl-70, SmD and SSA/Ro60 antigens (Wagatsuma *et al.*, 1993; Meheus *et al.*, 1999; Bizarro *et al.*, 2000), which relates to the optimal presentation of the native autoantigen.

Numerous variables can affect the development of an ELISA method. Plate type, antigen characteristics, coating conditions, blocking conditions, sera

diluent, wash buffer, and detection conjugate and substrate are common factors that require optimisation to achieve the desired assay sensitivity and specificity (Tijssen, 1993). Non-specific interactions have a direct impact on assay specificity, and strategies to reduce noise such as the addition of normal serum and changing buffer composition are well-documented (Kato *et al.*, 1980; Hogg and Davidson, 1982). There is a trade off, however, between improved specificity and improved sensitivity. Unacceptable levels of false positive or false negative detection are the outcome of the failure to reach an adequate compromise.

Multi-autoantigen complexes, such as snRNP, present a problem for the ELISA testing format as this method will detect snRNP only as a single antigen. Differentiating between patient sera with either anti-U1 RNP protein or anti-Sm protein specificities is important in the diagnosis of MCTD and SLE respectively. Some discrimination can be achieved using ELISA by measuring patient sera reactivity against both whole U1 snRNP (often termed RNP/Sm) and Sm. By expressing the optical density readings as a ratio RNP/Sm:Sm, a quotient (Q) is obtained which crudely differentiates sera containing anti-RNP, anti-Sm and both anti-RNP and Sm (Tsay *et al.*, 1987). The need for this approach can be circumvented by either using purified recombinant U1 snRNP constituent proteins (Gaubitz *et al.*, 2002) or by first separating the U1 snRNP proteins by electrophoresis.

2.4.1.5 Western (immuno) blotting

Western blotting is the process of electrophoretically transferring and immobilising proteins, separated by SDS-PAGE, onto a solid membrane support (Towbin *et al.*, 1979). Antigens can then be detected on the solid phase membrane in much the same way as in ELISA methods, allowing differentiation of immune responses to multiple antigens in ribonucleoprotein complexes (Guldner *et al.*, 1983; Meyer *et al.*, 1989; Buyon *et al.*, 1993; Dorner *et al.*, 1994; Bridges *et al.*, 1997; Bizzaro *et al.*, 1998).

Despite being a powerful immunodiagnostic tool, there are a number of caveats associated with the use of immunoblotting. Antibody recognition that is dependent on antigen conformation can be masked because of antigen denaturation during SDS-PAGE (Manoussakis *et al.*, 1993). The best example of this phenomenon is with SSA-60 antigen where some sera contain antibodies exclusive to conformation-dependent epitopes and are hence not detected by immunoblotting techniques (Boire *et al.*, 1991). In some cases antigens immobilised on the membrane surface can be re-natured by altering the conditions sufficiently to permit re-folding. Applying this process to SSA-60 antigen has been of limited success (Zampieri *et al.*, 2000).

Interpretation of immunoblots can be difficult, again limiting the effectiveness of the technique (Bizzaro *et al.*, 2000). Conventionally the antigen source is a crude HeLa (immortalised cervical cancer) cell or nuclear extract (Verheijen *et al.*, 1993). The complexity of this antigen mix, coupled with the often complex autoantibody specificities, introduces the possibility of incorrect autoantigen designation due to the presence of co-migrating reactivity or cross-reactivity (Yago *et al.*, 1999).

Caveats aside, immunoblotting is considered superior to other immuno-diagnostic procedures for the detection of U1 snRNP and SS-B/La antigens (Bizarro *et al.*, 2000). Despite the superiority of immunoblotting, and other membrane-based immunoassays in some instances (Ermens *et al.*, 1997; Lopez-Longo *et al.*, 2002), these techniques cannot compete with the high throughput and quantifiable format of ELISA.

2.4.1.6 Multiplex bead arrays

Development of an assay format capable of quantifying multiple analytes (multiplexing) in a single tube may challenge ELISA's dominance as a diagnostic tool (Vignali, 2000). Multiplex bead arrays consist of uniquely coded fluorescent beads coated with antigen. A mixture of beads is incubated with the patient sample, and binding of antibody to the antigen bead is detected using a fluorescently labelled anti-human Ig. The coded beads and associated antibody

conjugate are then analysed by dual laser flow cytometry (Luminex Corp., USA). Although performance data is currently limited, published studies show the multiplexing approach has a high concordance (99-100 %) with routine tests (Rouquette *et al.*, 2003; Gilburd *et al.*, 2004; Martins *et al.*, 2004).

2.4.2 Diagnostic serology for MCTD and SLE

The autoimmune response in MCTD is predominantly IgG mediated (Vlachoyiannopoulos *et al.*, 1996). Antibodies to U1 snRNP specific antigens are found in over 90 % MCTD patient sera. A high ANA titre and speckled pattern in immunofluorescence is characteristic of MCTD, and elevated anti-U1 68K antibody titre is particularly concordant with this disease (van Venrooij and Sillekens, 1989; Smolen and Steiner, 1998). Sera from MCTD patients almost exclusively immunoprecipitate U1 snRNP, although very occasionally U2 snRNP is also precipitated (Pettersson *et al.*, 1986; Combe *et al.*, 1989). Autoantibody interactions specific to heterogenous nuclear RNP A2 (Hassfeld *et al.*, 1995), heat shock protein hsp73 (Appelboom *et al.*, 1995) and some U1A epitopes (Barakat *et al.*, 1991) have been reported but none have gained diagnostic traction.

SLE is more complex in its serological presentation because of the multiple nuclear antigens that can be targeted (McMurdy *et al.*, 1992; Kotzin, 1996). Autoantibodies to the Sm component of snRNPs occur in 20-30 % SLE patients and are highly concurrent with the disease (Sturgess, 1992). Sera containing these autoantibodies are characterised by reactivity to Sm in one of the diagnostic procedures outlined above and by immunoprecipitation of U1-U6 snRNPs. Differentiation between SLE and MCTD on the basis of anti-U1 snRNP serology is therefore not clear, with up to 30 % SLE patients reacting exclusively with U1 snRNP components (Smolen and Steiner, 1998). A recent comprehensive study concluded that anti-Sm antibody testing should only be used to support SLE diagnosis, and that although the presence of anti-RNP antibodies strongly supported MCTD diagnosis, they could not be used to confirm SLE (Benito-Garcia *et al.*, 2004).

The exclusive association between anti-Sm specificity and SLE diagnosis has been studied intensely. Anti-SmB′/B antibodies are present in all Sm positive sera in conjunction with a combination of anti-SmD1 (80 %), SmD2 (17 %) and SmD3 (22 %) (McClain *et al.*, 2002). The exclusivity of SmB′/B protein as a SLE autoantigen is unclear, because, immunoblot assays, using whole nuclear extract as the antigen source, consistently detect SmB′/B reactivity in MCTD sera (Habets *et al.*, 1985a; Pettersson *et al.*, 1986; de Rooij *et al.*, 1988; Combe *et al.*, 1989; Ghirardello *et al.*, 1996). Reactivity with SmB′/B appears to be the rule rather than the exception for U1 snRNP sera. A longitudinal study carried out using immunoblotting, implicated U1 68K and B′/B as the predominant immunogens in the U1 snRNP complex (Greidinger and Hoffman, 2001). Despite the apparent prevalence of antibodies to the common core SmB′/B protein, anti-RNP sera consistently only immunoprecipitate U1 snRNP.

In contrast to the immunoblotting data, ELISA does not support the association of SmB′/B with MCTD. Takeda *et al.* (1989) electroeluted RNP antigens from SDS-PAGE separated U1 snRNP, and used the separated polypeptides in an ELISA format. This essentially mimics the immunoblot method and shows that anti-SmB′/B antibodies are present in MCTD sera. However, when chromatographically purified native or recombinant U1 snRNP polypeptides are used as the antigen source in ELISA or immunoblot anti-SmB′/B antibodies are not detected in MCTD patient sera (Williams *et al.*, 1988; Hines *et al.*, 1991). Characterisically good anti-SmB′/B responses are obtained for SLE sera.

This disparity between the detection of SmB′/B in MCTD patient sera by immunoblotting and ELISA has not been discussed in the literature. It is likely that the origin and purity of the antigen, autoantibody cross-reactivities and the selection of patient cohorts are the key sources of difference.

2.5 Autoantibody Fine Specificity

Determining fine specificity of autoantibodies using epitope mapping techniques has been criticised as providing "answers without questions" (Venables, 1993). Epitope mapping studies are useful, however, for explaining the often complex U1 snRNP reactivities.

2.5.1 SmD and SmB′/B autoepitopes

Eight antigenic regions of SmB′/B have been identified using SLE patient sera (James and Harley, 1992). The immunodominant autoepitope is undoubtedly within the proline rich C-terminus (Elkon *et al.*, 1990; Rokeach *et al.*,1990; de Keyser *et al.*, 1992), with the majority of Sm positive sera reactive towards the PPPGMRPP octapeptide repeat (Figure 2.9) (Williams *et al.*, 1990; Rokeach and Hoch, 1992a; James *et al.*, 1995a). Only 91 % of Sm positive sera interact with full length recombinant SmB′ protein compared to 96 % that interact with the 27 SmB′ C-terminal residues alone that contain two proline repeats (Hines *et al.*, 1991). Anti-RNP sera occasionally react with the SmB′ C-terminal region. The sequence similarities in high proline regions within U1A (^{165}PPPGMIPP) and U1C (^{93}PAPGMRPP) are the most likely source of this cross-reactivity (Habets *et al.*, 1990; Williams *et al.*, 1990; Guldner, 1992).

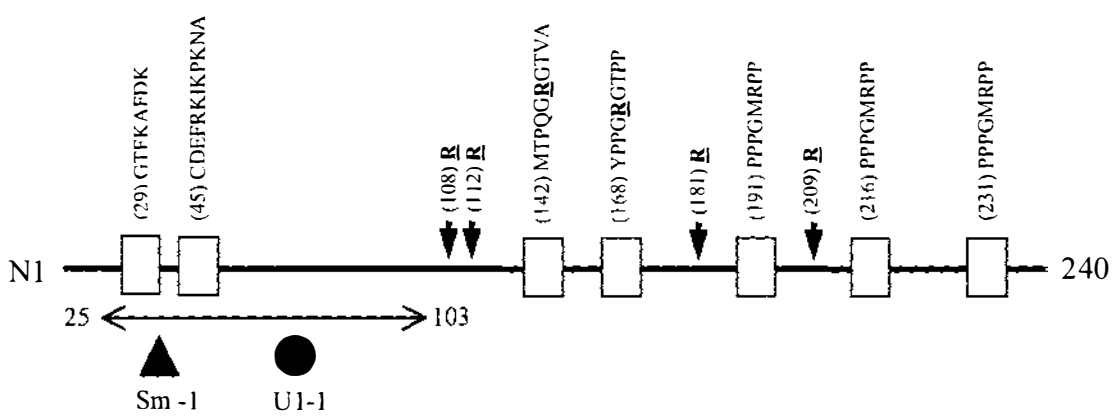

Figure 2.9 SmB′ epitopes

Positions of the cross-reactive sDMA are shown by **R**. The solid triangle and circle within peptide $B^{25\text{-}103}$ represent the proposed snRNP common ($B^{Sm\text{-}1}$) and U1 snRNP specific ($B^{U1\text{-}1}$) epitopes respectively. (James and Harley, 1992; Ohosone *et al.*, 1992 and Brahms *et al.*, 2001).

Linear N-terminal autoepitopes in SmB′/B are targeted less frequently. Conformation-dependant antibodies are not detected using this experimental approach and so the existence of discontinuous epitopes cannot be discounted. James and Harley (1992) identified two autoepitopes within the Sm motif, ^{29}GTFKAFDK and ^{45}CDEFRKIKPKNA. A separate study proposed the presence of two epitopes, Sm-1 and U1-1 within residues 25-103 (Ohosone *et al.*, 1992). Autoantibodies recognising the Sm-1 epitope are able to immunoprecipitate U1-U6 snRNPs, whereas, the U1-1 epitope is a region accessible only within U1 snRNP. As described above, MCTD sera immunoprecipitate U1 snRNP despite reacting with the U1-U6 common SmB′/B on immunoblot. The existence of U1 snRNP-specific SmB′/B epitopes is a possible interpretation of this phenomenon.

Despite their apparent lack of sequence homology, SLE Sm positive sera recognise cross-reactive regions within SmB′/B, SmD1 and SmD3 (Habets *et al.,* 1985b), a phenomenon shared with the MRL *lpr/lpr* lupus mouse derived monoclonal antibody mAb Y12 (Lerner *et al.*, 1980). The likely autoepitopes have been mapped to SmB′/B $^{115\text{-}231}$, SmD1 $^{95\text{-}116}$ and SmD3 $^{104\text{-}124}$ using a series of synthetic overlapping peptides (Barakat *et al.*, 1990; James and Harley, 1992; Hirakata *et al.*, 1993; Riemekasten *et al.*, 1998). Despite recognising synthetic peptides in ELISA, and native human SmB′/B and SmD in western blot, mAb Y12 did not recognise the full recombinant equivalents of these proteins in western blots (Hirakata *et al.*, 1993).

MRL *lpr/lpr* monoclonals have proved useful in defining other SmD1 autoepitopes (James *et al.*, 1994a). The SmD1-specific monoclonal, KSm 2, identified an epitope in the C-terminal SmD1$^{82\text{-}90}$. This finding corroborated the mapping studies of Rokeach *et al.* (1992b) and confirmed SmD1 82-119 as the immunodominant region for SLE sera recognition.

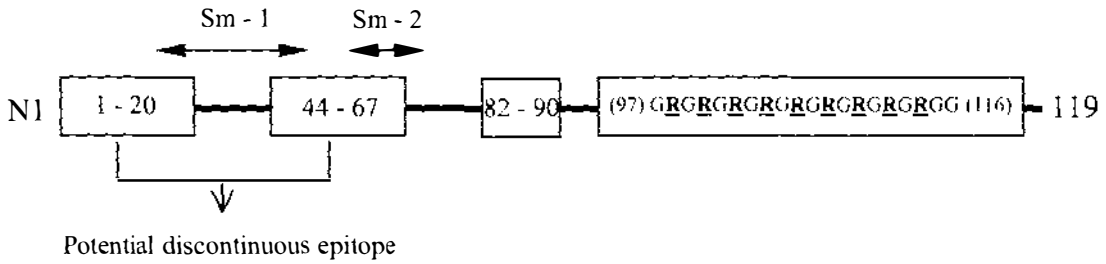

Figure 2.10 SmD1 proposed epitopes

The sDMA (**R**) rich C-terminal sequence $D1^{(97\text{-}116)}$ is shown and is the site of anti-SmB′/B cross-reactivity and the mAb Y12 epitope. The Sm protein specific Sm 1 and 2 motifs are marked. A discontinuous epitope is thought to reside within the Sm motifs. (Barakat *et al.*, 1990; James *et al.*, 1994a and Brahms *et al.*, 2000).

Brahms *et al.* (2000) performed limited proteolysis of the native SmD1 and SmD3 proteins to isolate mAb Y12 epitopes. Mass spectrometry and Edman sequencing identified the major epitope as nine and four sDMA in SmD1 and SmD3 C-termini respectively (Figure 2.10). This recognition is highly specific. When sDMAs are substituted with the more common asymmetrical DMAs (aDMA), suitable epitopes are not produced (Figure 2.11). In addition, a single sDMA, $SmD3^{112}$, has been identified as a specific target for some anti-Sm autoantibodies (Mahler *et al.*, 2004).

SmB′/B contains six sDMA (108, 112, 147, 172, 181 and 209) all within a G/A-R-G consensus sequence (Brahms *et al.*, 2001). This motif appears to be the consensus substrate for a type II protein arginine methyltransferase, PRMT5, which forms part of the methylosome described earlier (Section 2.1.1).

The role of such specific post-translational modifications may be central not only to the pathogenesis of autoimmune disease, but also to the motor neuron disease spinal muscular atrophy (Lefebvre *et al.*, 1997; Brahms *et al.*, 2001).

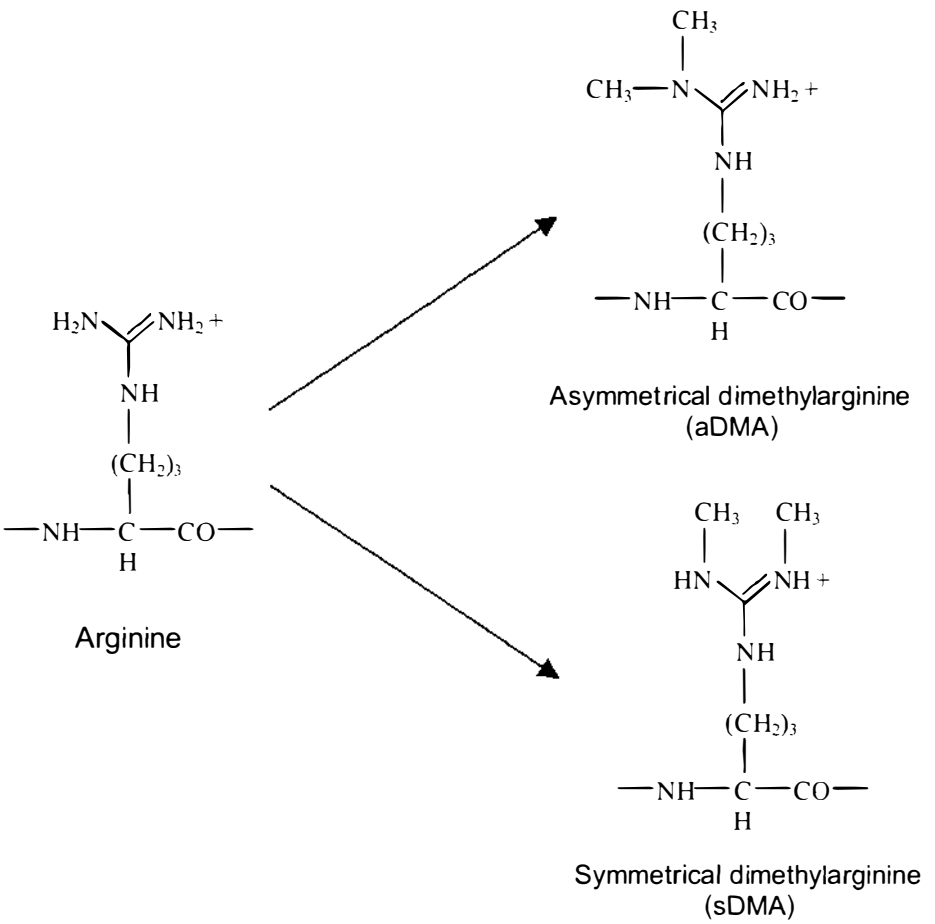

Figure 2.11 Arginine methylation

Mature B-cell response to Sm antigens cannot occur without help from T-cell immunity. Anti-Sm T-cell epitopes are highly restricted in SLE patients (Talken *et al.*, 2001). They are encoded within Sm motif 1 and Sm motif 2 of SmB′/B and SmD, but also have a third SmB′/B epitope $B^{(136\text{-}153)}$. Interestingly, this third epitope contains a sDMA consensus GRG motif, although the T-cell response to sDMA has not yet been determined.

2.5.2 U1 68K autoepitopes

U1 snRNP specific 68K antigen is the major autoantigen for MCTD diagnosis. This protein, however, is also reactive to SLE patient autoantibodies. Epitope mapping of the 68K antigen has failed to identify immunodominant regions to differentiate between a MCTD and a SLE response. The autoepitopes are

clustered in five main regions (Figure 2.12): a N-terminal region (11-73); a RNA binding domain (92-202); two RS1 regions, residues 231-260 and 264-296; one RS2 region, residues 355-377 (Netter *et al.*, 1990; Netter *et al.*, 1991; James *et al.*, 1994b; Pelsue and Agris, 1994).

Using a series of synthetic peptides, James *et al.* (1994b) were able to map a number of linear epitopes to the RNA binding domain. This approach resulted in a major conformational epitope being missed. It was later shown that valine 125 within the tight Helix A and β2 structure (Figure 2.6) was critical in maintaining a significant conformational epitope (Welin-Henriksson *et al.*, 1999). The presence of this epitope was confirmed using phage display technology and recombinant human anti-68K autoantibodies (Degen *et al.*, 2000a). The use of this technology revealed a further epitope. Some recombinant anti-68K antibodies unable to recognise intact U1 68K in a western blot, reacted strongly with the 40K apoptotic fragment. While the nature of this neoepitope is not known, a number of changes accompany apoptosis including proteolysis, phosphorylation and dephosphorylation events (Degen *et al.*, 2000b). The generation of such a neoepitope upon apoptosis is thought to drive the U1 snRNP autoimmune response (Greidinger *et al.*, 2000).

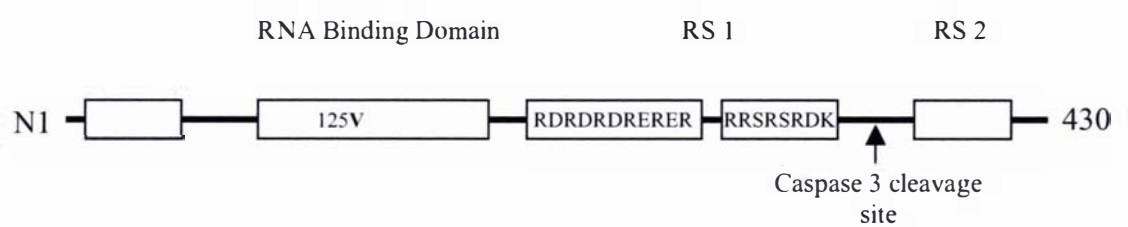

Figure 2.12 U1 68K main autoepitopes

Valine 125 is critical for a major conformational epitope within the RNA binding domain. Charged epitopes representative of those found within the RS1 domain are shown. The apoptotic cleavage site is also marked. Apoptosis apparently reveals an immunodominant neoepitope. (Pelsue *et al.*, 1993; James *et al.*, 1994b; Welin-Henriksson *et al.*, 1999 and Greidinger *et al.*, 2000).

The highly charged serine/arginine (SR) and arginine/aspartic acid (RD) repeats of the RS1 and RS2 domains of U1 68K are also antigenic (Pelsue *et al.*, 1993; James *et al.*, 1994b). These epitopes, however, are not solely sequence dependent but also display a structural component as determined by circular dichroism (Pelsue and Agris, 1994).

2.5.3 U1A autoepitopes

Patients with autoantibodies to U1A fall into two groups, those which interact with multiple U1A epitopes, and a group whose interaction is restricted to two major U1A epitopes (James and Harley, 1996). One of the restricted epitopes (A3) is found within the β2 - β3 strands of the RNA binding domain (^{44}LVSRSLKMRGQAF), while the other epitope (A6) is located within the dimerisation domain (^{103}ERDRKREKRKPKS) (Figure 2.7).

The A3 autoepitope is interesting for two reasons. Firstly, rabbits immunised with the synthetic peptide corresponding to this sequence not only develop an SLE-like syndrome, but the immune response spreads to include other U1A specific peptides commonly identified by human disease sera. Surprisingly the response is not only restricted to U1A. Antibodies to U1 68K, U1C, SmD1 and SmB′/B are also detected (McClain *et al.*, 2004). Secondly, the A3 peptide has been identified as a highly specific MCTD autoepitope with 95 % U1A positive sera recognising this peptide, as opposed to only 19 % of U1A positive SLE sera (Barakat *et al.*, 1991). In contrast, immunisation with the A6 peptide raises a solely anti-A6 response.

U1A displays two cross-reactive epitopes described as epitope 1 (165-185) and epitope 2 (232–256) by Habets *et al.* (1989). The proline rich epitope 1 shows three patterns: U1A specific; U1A and SmB′/B specific; U1A, SmB′/B and U1C specific (Guldner, 1992). This epitope contains the peptide ^{165}PPPGMIPP, which is proposed to be cross-reactive with SmB′/B and U1C. Epitope 2 is located in the C-terminal RNA binding domain of U1A which shares almost 90 % sequence similarity with the U2 snRNP specific protein B′′. Autoantibodies that cross-react with U1A and U2B′′ are found in up to 50 % of anti (U1/U2)

RNP sera (Habets *et al.*, 1989). Neither epitope 1 nor epitope 2 is immunodominant, with only 30 % and 24 % recognition by U1A positive sera respectively (Habets *et al.*, 1990).

2.5.4 U1C autoepitopes

Relatively few studies have covered epitope mapping of the U1C protein. Epitope clusters are either U1C specific or cross-reactive with other snRNP components (James and Harley, 1995b). The U1C specific autoantibodies target both N-terminal and C-terminal domains (Figure 2.13). Surprisingly, the main structural element of U1C, a CC-HH zinc finger, which is responsible for its ability to interact with snRNP, is not a major epitope. Recombinant human monoclonal autoantibodies identified the sequence between residues 30-63 as a major U1C specific epitope (Hoet *et al.*, 1999), a finding corroborated by James and Harley (1995b).

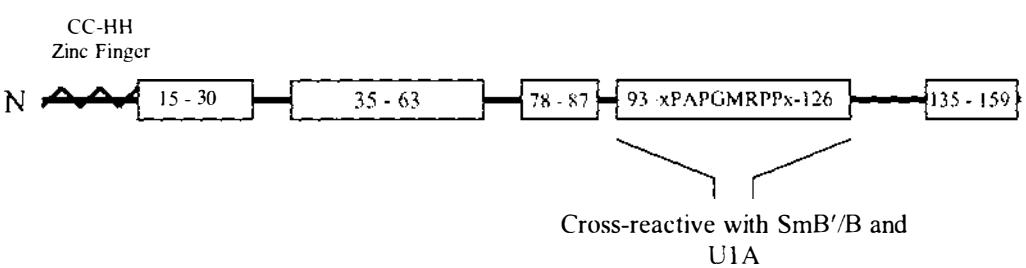

Figure 2.13 U1C autoepitope clusters

The cross-reactive U1C epitopes cluster in the C-terminal proline rich region between residues 98-126. James and Harley (1995b) showed that all sera with reactivity to this region, in particular the PAPGMRPPMG sequence, are Sm positive. Antibodies purified by immunoaffinity chromatography from the poly-proline sequence are able to immunoprecipitate U1-U6 snRNPs. The poly-proline repeats (PPPGMRPP) in SmB′/B are responsible for this cross-reactivity.

2.6 Research Aims and Strategy

Although human-derived autoantigens are desirable reagents for diagnosing autoimmune disease, the high degree of sequence conservation between human and other mammalian species means that many commercial diagnostic kits use U1 snRNP antigen sourced from either bovine or rabbit thymus (Collins *et al.*, 1989). The time taken between animal slaughter, thymus excision and freezing, however, is sufficient for the tissue to undergo some necrotic and/or apoptotic changes. The onset of these changes can degrade or otherwise modify proteins and nucleic acids. Consequently, bovine thymus U1 snRNP does not share the characteristic polypeptide pattern associated with human U1 snRNP purified from HeLa cells. In fact, attempts to characterise this modified pattern have failed to completely identify all the autoantigenic polypeptides (Takano *et al.*, 1981; White *et al.*, 1981; Duran *et al.*, 1984). In addition, the existence of three distinct SmD proteins was not established until 1990 (Lehmeier *et al.*, 1990) and the identity of these proteins in bovine-derived U1 snRNP has not yet been determined.

The first aim of this project is to characterise U1 snRNP protein antigens purified from bovine thymus and to investigate the effect of their modification on autoantibody recognition and diagnostic performance.

The ability to discriminate between SLE and MCTD, and monitor disease progress in both conditions is of clinical and scientific importance (Gaubitz *et al.*, 2002). The specificity of antibody-antigen interactions with anti-RNP patient sera is very complex. Intact U1 snRNP as a diagnostic substrate in IIF-ANA or ELISA, although useful, can produce ambiguous results. While improved differentiation has been achieved by using individual polypeptide antigens, most of the work has been done using commercially available recombinant antigens. There have been no comparative studies with native polypeptide antigens.

The second objective of this project is to establish conditions for the dissociation of bovine U1 snRNP and purification of the RNP constituent polypeptides. This

will enable the purified native antigens to be compared to the recombinant equivalents both biochemically and immunologically.

Modification of U1 snRNP proteins during necrosis and/or apoptosis has been implicated in the generation of the initial antigens that break tolerance and drive the autoimmune response. Truncation of bovine U1 68K produces a distinctive and stable cleavage pattern, the cause of which is largely unknown. Determining how truncated 68K is formed during calf thymus processing may provide links towards understanding the initiation of the anti-RNP autoimmune response.

The third objective is to examine whether U1 snRNP-specific protein modification is a direct consequence of calf thymus gland processing and whether the necrotic proteolytic pathway has any influence on the cleavage pattern of 68K.

Disparity between autoimmune sera reactivity with SmB′/B in western blot and ELISA has not been satisfactorily resolved. The issue is complicated by the number of cross-reactions between RNP component proteins. Determining the cause of this disparity may influence the diagnostic discrimination of MCTD and SLE connective tissue diseases.

A fourth objective of this study is to determine the nature of the disparate U1 snRNP SmB′/B reactivity in western blot of human U1 snRNP.

Chapter Three

General Materials and Methods

3.1 Materials

Calf thymus glands were purchased frozen from either Taylor Preston Limited, Wellington or New Zealand Dairy Meats, Auckland, and were stored at –20 °C until use.

Immortalised human cervical cancer (HeLa-S3) cell pellets were purchased from the Computer Cell Company, Mons, Belgium. These were stored at –80 °C until use.

Chromatography resins and columns were purchased from Amersham Bio-sciences, Uppsala, Sweden unless otherwise stated.

Antibody conjugates were products of Jackson ImmunoResearch Laboratories Inc., West Grove, USA.

All chemicals were analytical grade and were obtained from Ajax Finechem unless otherwise stated.

3.2 Methods

3.2.1 Preparation of bovine thymus extracts

Extracts were prepared from bovine calf thymus using a method modified from Northway and Tan (1972). All buffers and solutions were pre-equilibrated to 2-8 °C and contained 0.1 mM PMSF and 0.2 M DTT. Briefly, the tissue was homogenised in two volumes of homogenisation buffer (20 mM Tris-HCl pH 7.5, 30 mM KCl, 5 mM $MgCl_2$) in a Model 24CB10 Waring blender on high speed for two minutes. The homogenate was strained through a layer of cheesecloth, after which the filtrate was centrifuged for 15 minutes at 4 600 x g, 4 °C in a Sorval RC3B centrifuge to remove insoluble material. The supernatant was retained and the pellet was washed with one volume of homogenisation buffer containing 0.25 M sucrose and 0.3 % w/v Triton x100. After centrifuging under the same conditions as described above, the supernatants were pooled, filtered and adjusted to pH 7.5. The pellet was discarded.

3.2.2 Partial purification of U1 snRNP

An anti-U1 snRNP immunoaffinity matrix was prepared as follows. Essentially, IgGs were isolated from either an anti-RNP positive patient sera using protein G-Sepharose affinity matrix (Harlow and Lane, 1988). The purified IgGs were coupled to cyanogen bromide activated Sepharose 4B according to a procedure described by Takano *et al.* (1981) to form affinity matrices that were then equilibrated in 20 mM Tris-HCl pH 7.5, 0.4 M NaCl, 3.5 mM $MgCl_2$. Bovine thymus extract was applied through a column containing the anti-U1 snRNP affinity matrix. After washing to remove any non-bound material, U1 snRNP was eluted using 20 mM Tris-HCl pH 6.5, 3.5 M $MgCl_2$ (Gaither and Harley, 1985; Yoshida and Reichlin, 1990). This is hereafter referred to as an anti-RNP immunoaffinity elution.

3.2.3 Human cell nuclear extract

Nuclei were prepared from HeLa (human cervical carcinoma) cells according to the protocol of Verheijen *et al.* (1993). Essentially a frozen cell pellet (25 $x10^9$ cells) was thawed, cells were resuspended in hypotonic buffer (20 mM Tris-HCl pH 7.5, 20 mM KCl, 1.5 mM $MgCl_2$) and 0.1 volumes of 10 % v/v Tween 20 were added. The cells were disrupted with 7 strokes at 800 rpm (RW20 stirrer, IKA) of a teflon-in-glass Potter homogeniser (Wheaton, USA). Nuclei were pelleted by centrifugation (1500 g, 10 minutes, 4 °C) and then washed with hypotonic buffer and pelleted again. Nuclear antigens were extracted by suspending the nuclei in extraction buffer (20 mM Tris-HCl pH 7.8, 3 mM $MgCl_2$, 20 mM KCl, 0.4 M NaCl, 15 % v/v glycerol, 0.75 mM EDTA, 0.5 mM PMSF, 0.2 mM DTT) and rotating end-over-end for 1 hour at 2-8 °C (Hoch, 1990; Kramer, 1990). Extracted nuclei were centrifuged at 40 000 g for 40 minutes at 2-8 °C. The salt extractable nuclear antigens were recovered in the supernatant and frozen at –80 °C until required.

3.2.4 Purification of HeLa cell U1 snRNP

Human U1 snRNP was purified from HeLa nuclear extract using conventional chromatography following the method of Kramer (1990) with minor modifications. In brief, HeLa nuclear extract was diluted 1:4 with buffer A (20

mM Tris-HCl pH 7.9, 6.25 % v/v glycerol, 3.4 mM $MgCl_2$, 0.5 mM PMSF, 0.2 mM DTT) and applied to a DEAE Sepharose fast flow (HiTrap) equilibrated in buffer B (20 mM Tris-HCl pH 7.9, 10 % v/v glycerol, 0.1 M KCl, 3 mM $MgCl_2$, 0.5 mM PMSF, 0.2 mM DTT). The bound snRNP was eluted in one step with 0.5 M KCl in buffer B. The elution was diluted 3:7 with buffer A containing 24.2 % v/v glycerol before loading onto Heparin Sepharose pre-equilibrated with buffer B containing 0.15 M KCl. The bound material was again eluted with 0.5 M KCl in buffer B.

The heparin elution was diluted 1:4 with 62.5 mM Tris-HCl pH 7.9, 22.5 % v/v glycerol, 3.4 mM $MgCl_2$ then applied to a Source 30 Q packed column equilibrated with buffer C (50 mM Tris-HCl pH 7.5, 10 % v/v glycerol, 0.1 M KCl, 3 mM $MgCl_2$, 0.2 mM DTT, 0.1 mM PMSF). The bound protein was eluted with a linear gradient of 0 – 100 % 1 M KCl in buffer C. The fractions containing U1 snRNP were pooled and applied to a ceramic hydroxyapatite (CHT) (Bio-Rad Laboratories, Hercules, USA) column equilibrated in 5 mM phosphate pH 7.4, 0.1 M KCl, 10 % v/v glycerol, 1.5 mM $MgCl_2$, 0.2 mM DTT, 0.1 mM PMSF. Bound U1 snRNP was eluted over 15 column volumes with a linear gradient, 0 – 80 % 500 mM phosphate in the equilibration buffer. Fractions containing U1 snRNP were pooled, concentrated using Vivaspin™ 10 kDa nominal molecular weight cut-off (NMWCO) centrifugal concentrators (Vivascience, Hannover, Germany) and frozen at –80 °C for later use.

3.2.5 Enzyme linked immunosorbent assay (ELISA)

Antigen was diluted to either 0.5 or 1.0 $\mu g.mL^{-1}$ in 20 mM Tris-HCl pH 7.5, 0.15 M NaCl, 0.02 % w/v sodium azide. Microtitre polystyrene (96 well) plates (Nunc Maxisorb™, Denmark) were coated with 100 µL antigen and incubated over-night at 2-8 °C. Excess antigen was tapped out, and 200 µL blocking solution (1 % w/v bovine serum albumin (BSA), in phosphate buffered saline (PBS) containing 0.02 % v/v Tween 20) was added to the wells and incubated for 2 hours. Patient or control sera were diluted 1/100 in dilution buffer containing 1 % w/v casein, 1 % w/v BSA, 10 mM phosphate, 0.5 M NaCl and 0.1 % v/v Tween 20. After tapping out the blocking solution, 100 µL diluted sera were added to the wells in duplicate and incubated for 1 hour at ambient temperature.

The wells were then washed three times with wash buffer containing 10 mM phosphate pH 7.4, 0.5 M NaCl and 0.1% v/v Tween 20. Horseradish peroxidase (HRP)-conjugated goat anti-human IgG was diluted 1:30 000 in dilution buffer and 100 μL was added to each well. The plate was incubated for a further hour before tapping out the contents and washing as described above. Antigen-specific reaction was visualised by adding 150 μL substrate (125 $\mu g.mL^{-1}$ trimethylbenzamidine, 0.1 M acetate pH 5.5, 0.03 % v/v hydrogen peroxide). After ten minutes incubation at ambient temperature, the reaction was stopped by adding 50 μL 2 M sulfuric acid. The absorbance was determined at 450 nm with a microplate reader (Bio-Rad Model 550, Hercules, USA).

3.2.6 Determination of protein concentration

A protein assay kit (Bio-Rad Laboratories, Hercules, USA) based on the dye binding method of Bradford (1976), was used to measure total protein concentration. The protocol adapted for microtitre plates was performed according to the manufacturer's instructions. BSA was used as the standard protein.

3.2.7 Absorbance spectra

Scanning spectra were performed between 260 nm and 340 nm using an Ultrospec 2000 spectrophotometer (Amersham BioSciences, Chalfont, UK). A 260:280nm absorbance ratio was determined as a measure of nucleic acid content (see Appendix).

3.2.8 Immunoprecipitation

Protein A-agarose beads (Bio-Rad Laboratories, Hercules, USA) were equilibrated in PBST (10 mM phosphate pH 7.2, 0.15 M NaCl, 0.02 % v/v Tween 20, 0.05 % w/v azide). Antibody (5 μL) was mixed for 2 hours at ambient temperature with 10 μL equilibrated beads suspended in 25 μL PBST. The beads were washed with PBST and non-bound material was removed by centrifuging at 13 000 rpm for 30 seconds. The affinity beads were resuspended in 25 μL PBST and incubated with 25 μL of either HeLa cell or bovine thymus nuclear extract for 2 hours at ambient temperature. The beads

were washed 3 times with PBST as described above. For analysis of immunoprecipitated RNA, the bound material was eluted in 100 μL 0.5 % w/v sodium dodecylsulfate (SDS) at 65 °C. The RNA was extracted with 100 μL triazol™ (Invitrogen, Carlsbad, USA) /chloroform (1:1). The aqueous layer was removed and the RNA was recovered by ice cold ethanol precipitation with 1 μL mussel glycogen (10 $mg.mL^{-1}$) (Sigma Chemical Co., St Louis, USA) as a carrier.

For immunoprecipitation of proteins, antibodies were first covalently bound to the protein-A beads using the protocol described in Harlow and Lane (1988). Briefly, the antibody-coupled beads were resuspended in 200 μL 0.2 M borate pH 9.0. Approximately 1 mg dimethylpimelimidate (Sigma Chemical Co., St Louis, USA) was added to give 20 mM final concentration. The mixture was incubated for 30 minutes at ambient temperature before washing and resuspending the affinity beads in 0.2 M ethanolamine pH 8.2. The beads were washed three times in PBST and mock eluted with 100 μL elution buffer (0.1 M glycine-HCl pH 2.2). The beads were re-equilibrated in PBST and then incubated with nuclear extract as described above. After washing to remove non-bound material, bound protein was eluted with 25 μL elution buffer. The recovered eluate was immediately neutralised by adding 2.5 μL 1 M Tris-HCl pH 8.0.

3.2.9 SDS-polyacrylamide electrophoresis

Discontinuous denaturing SDS-PAGE was used for the separation and analysis of proteins (Laemmli, 1970). A SE250 mini vertical electrophoresis assembly (Hoefer Inc., San Francisco, USA) was used unless otherwise stated. The acrylamide:N,N′-methylenebisacrylamide (bisacrylamide) ratio was 29:1. In general, a 13.5 % acrylamide separating gel containing 0.375 M Tris-HCl pH 8.8, 0.1 % w/v SDS was overlaid with a 4 % acrylamide stacking gel containing 0.125 M Tris-HCl pH 6.8, 0.1 % w/v SDS. Gels were polymerised by the addition of 0.1 % v/v N,N,N′,N′-tetramethylethylenediamine (TEMED) and 0.5 % v/v of a 10 % w/v ammonium persulfate solution.

Protein samples were prepared for electrophoresis by adding 10 μL 0.2 M DTT and 10 μL electrophoresis sample buffer (0.25 M Tris-HCl pH 6.8, 50 % v/v glycerol, 5 % w/v SDS, 0.001 % w/v bromophenol blue) to 30 μL sample prior to heating at 100 °C for 90 seconds. Gels were electrophoresed at 30 mA constant current with electrode buffer consisting of 25 mM Tris HCl pH 8.2, 0.2 M glycine, 0.2 % w/v SDS. The gels were run until the bromophenol blue tracking dye was within 0.5 cm from the bottom of the separating gel. Molecular weight markers (Invitrogen, Carlsbad, USA) were used to calibrate protein size.

Proteins were visualised by immersing the gel in Coomassie R250 stain (0.6 % w/v Coomassie brilliant blue R250 dissolved in 50 % v/v methanol, 5 % v/v glacial acetic acid) for 30 minutes. The gel was destained with 30 % v/v methanol, 5 % v/v acetic acid until the gel background was clear. Alternatively, for increased sensitivity, silver stain was used to visualise the proteins (Blomberg *et al.*, 1995).

3.2.10 Immunoblotting

Proteins were transferred from SDS-PAGE onto nitrocellulose (Protran BA85, Schleicher & Schuell, Dassel, Germany) using semi-dry electro-transfer (Towbin *et al.*, 1979). If required, nitrocellulose-bound proteins were visualised using Ponceau S reversible protein stain (0.1 % w/v Ponceau S dissolved in 5 % acetic acid) before blocking the membrane in 1 % w/v BSA in PBST for 1 hour at ambient temperature. Membranes were gently rocked overnight at ambient temperature in primary antibody (patient sera) diluted 1/200 in 1 % w/v casein in PBST. They were then washed 3 times in PBST before probing with goat anti-human IgG alkaline phosphatase conjugate (Jackson ImmunoResearch Laboratories Inc., West Grove, USA) diluted 1/6000 in 1 % w/v casein in PBST for 1 hour at ambient temperature. Membranes were washed as previously and then antigen-specific interaction was visualised with alkaline phosphatase substrate (22 mM nitrobenzamidine triazine (NBT), 23 mM 5-bromo 4-chloro 3-indolyl phosphate (BCIP) dissolved in 70 % v/v dimethylsulphoxide) diluted 1/100 in 50 mM Tris-HCl pH 9.5, 100 mM NaCl, 5 mM $MgCl_2$. The reaction was stopped by washing with water.

3.2.11 Immunoblot strips

Test antigen was treated with SDS-PAGE sample buffer including DTT and 120 μL was applied to the entire width of a 4 % acrylamide stacking gel over-laid on a 13.5 % acrylamide resolving gel. The sample was separated by SDS-PAGE and electro-transferred onto nitrocellulose membrane. After blocking in 1 % w/v BSA in PBST for 1 hour, the membrane was washed briefly with distilled water and then air-dried. Lines were ruled along the top and bottom edges of the nitrocellulose before cutting into 3 mm width vertical strips. Antigen strips were numbered before placing in a 24 lane incubation tray (Hoefer Instruments, USA). The strips were immunoprobed as described in section 3.2.8.

3.2.12 Antibody elution from immunoblot

Immunoblotted antigens were used to affinity purify specific antibodies. Antigen was prepared for SDS-PAGE and loaded along the entire width of the stacking gel and separated by SDS-PAGE before electro-transfer as described for immunoblot strips. The location of the desired antigen was visualised using Ponceau S stain and its position was marked. After blocking the membrane, the antigen strip was cut out and then probed with antibody as usual. The strip was washed 5 times with PBST before eluting bound antibodies with first 400 μL, followed by 350 μL, 0.1 M glycine-HCl pH 2.2. The eluted antibody was neutralised by adding 100 μL 1 M Tris-HCl pH 8.0.

Eluted antibodies were concentrated to approximately 50 μL using Vivaspin 10 kDa NMWCO 0.5 mL concentrators.

3.2.13 Isoelectric focussing (IEF) on immobilised pH gradient

Sample (5 – 50 μg) was desalted by buffer exchange into rehydration buffer consisting of 8 M urea, 2.5 % w/v CHAPS, 10 mM DTT and 0.001 % w/v bromophenol blue. Ampholytes pH 3-10 (Bio-Rad Laboratories, Hercules, USA) or pH 6-11 (Amersham BioSciences, Uppsala, Sweden) were added to the sample at a concentration of 2 % v/v. The 7 cm IPG strips pH 3-10 or pH 6-11 were assembled in a Zoom® IPG runner™ cassette (Invitrogen, Carlsbad, USA) and 155 μL sample was added to each IPG strip. The cassette was sealed and left for at least 16 hours to fully rehydrate the strips. The IPG cassette was

assembled with the electrode according to the manufacturer's instructions. The strips were focussed by ramping the voltage as follows: 200 V for 20 minutes, 450 V for 15 minutes, 750 V for 15 minutes and 1000 V for 60 minutes. The strips were removed from the cassette and either prepared for the second dimension immediately or frozen at –80 °C for later use.

3.2.14 Second dimension SDS-PAGE

Gel lanes or IPG strips were placed in 15 mL conical centifuge tubes to which 5 mL SDS equilibration buffer (2 % w/v SDS, 10 % v/v glycerol, 0.001 % w/v bromophenol blue, 50 mM Tris-HCl pH 6.8) was added. Complete reduction of the proteins was achieved by adding DTT (23 mg) to a final 30 mM concentration and incubating the strip at 55 °C for 15 minutes. The equilibration solution was removed and the replaced with 5 mL equilibration solution containing 100 mM iodoacetamide (Serva, Germany). The strip was incubated with gentle rocking for a further 15 minutes at room temperature.

A 1 mm thick 13.5 % acrylamide separating gel overlaid with a 4 % acrylamide stacking gel was used for the second dimension. The equilibrated and alkylated IPG or gel strip was inserted between the gel plates and gently manoeuvred to the stacking gel surface. The strip was sealed in place with 1 % w/v agarose in SDS-PAGE electrode buffer. The gel was electrophoresed as described in section 3.2.7 followed by Coomassie staining, silver staining or immunoblotting to visualise the proteins.

3.2.15 RNA extraction

RNA was extracted from samples containing U snRNPs by adding an equal volume triazol/chloroform (1:1) and mixing for 5 seconds. The mixture was centrifuged (Biofuge *pico*, Heraeus, Germany) at 16 000 x g for 2 minutes and the top aqueous layer was pipetted into a fresh microcentrifuge tube. The solution was made to 0.1 $mg.mL^{-1}$ with mussel glycogen. RNA and glycogen carrier were precipitated with 2.5 volumes ice cold ethanol and pelleted by centrifugation (16 000 x g, 2 minutes). The pellet was washed with ice cold 70 % v/v ethanol and the recovered pellet was stored at –80 °C until use.

3.2.16 RNA gel electrophoresis

A continuous 10 % acrylamide gel containing 7 M urea, 89 mM Tris, 89 mM boric acid, 2 mM EDTA pH 8.9 was prepared using a 19:1 acrylamide:N,N′-methylenebisacrylamide (bisacrylamide) solution. Polymerisation was catalysed with 0.1 % v/v TEMED and 0.5 % v/v of a 10 % w/v ammonium persulfate stock. The gel was pre-run at 10 mA for 15 minutes with 89 mM Tris, 89 mM boric acid, 2 mM EDTA pH 8.9 (TBE) electrode buffer.

RNA samples were resuspended in 5 μL sample buffer (8 M urea, 0.01 % w/v xylene cyanol, 0.001 % w/v bromophenol blue) and heated to 70 °C for 10 minutes and placed on ice before loading 1-5 μL into gel lanes. The gel was electrophoresed at 250 V constant voltage until the bromophenol blue dye was 0.5 cm from the bottom of the gel. Nucleic acid was visualised by staining with 0.05 $\mu g.mL^{-1}$ ethidium bromide for 15 minutes. The gel was washed 3 times 5 minutes with water to remove excess ethidium bromide. The gel was visualised immediately under ultraviolet transillumination.

3.2.17 In-gel digestion

Proteolytic digestion of Coomassie stained gel pieces was performed according to the methods published by Jeno *et al.* (1995) and Wilm and Mann (1996) with slight modifications. Coomassie stained gel pieces were carefully excised and placed in a clean microfuge tube. The pieces were homogenised with the blunt end of a plastic innoculation loop. Gel pieces were incubated with several changes of 100 μL 50 % v/v acetonitrile in 50 mM ammonium hydrogen carbonate until the pieces were completely destained. Gel trapped protein was reduced in 100 μL 30 mM DTT for 1 hour at 55 °C. The protein was then alkylated by first removing excess fluid and adding 100 μL 75 mM iodoacetamide (Serva, Germany) and incubating for 30 minutes at room temperature in the dark. To remove the DTT and iodoacetamide, the gel pieces were subjected to 3 cycles of dehydration in 100 μL of 50 % v/v acetonitrile and reswelling in the same volume of 50 mM ammonium hydrogen carbonate. A steady stream of nitrogen was used to partially dry the gel pieces. Trypsin (0.5 μg in 18 μL 25 mM ammonium hydrogen carbonate) was added to the dried gel

pieces and incubated for 6 hours at 37 °C to digest the protein. Tryptic peptides were recovered by adding 20 μL 50 % v/v acetonitrile, 2.5 % v/v formic acid in ultrapure water to the gel pieces and vortexing for 10 minutes. Peptide eluate was removed to a sterile microfuge tube and the process was repeated once more. A final extraction was carried out with 10 μL 100 % v/v acetonitrile and the eluates were combined. The peptides were reduced to approximately 5 μL in a Savant Speed Vac™ and stored at –80 °C until use.

3.2.18 MALDI-TOF mass spectrometry of tryptic digested peptides

Tryptic peptides were analysed using matrix-assisted laser desorption/ionisation time-of-flight (MALDI-TOF) mass spectrometry with a Micromass® MaldiMicro™ (Waters Inc., Milford, USA). Sample was prepared using an adaptation of the fast evaporation method proposed by Vorm *et al*. (1994).

Pure nitrocellulose and matrix, 3,5 dimethoxy 4 hydroxycinnamic acid (Sigma Chemical Co., St Louis, USA) were dissolved in 50 μL acetone plus 50 μL isopropanol to give a final concentration of 5 $mg.mL^{-1}$ nitrocellulose and 20 mg/mL peptide matrix. Solubilised matrix (0.5 μL) was pipetted rapidly onto the stainless steel target plate and allowed to dry. Peptide sample (0.5 μL) was applied to the dried matrix. Where necessary, another 0.5 μL peptide mixture was overlaid on the first with drying in between applications. The dried sample was washed with 10 μL ice cold 10 % v/v formic acid followed by 10 μL ultrapure water to remove excess salts and matrix contaminants. The peptide targets were dried at ambient temperature before analysis. Bovine angiotensin (Sigma Chemical Co., St Louis, USA) was used as a reference peptide or 'lock mass' and was prepared as above.

Mass spectrometric analysis was carried out in reflectron mode with a 2 470 V pulse voltage and 15 000 V source voltage. Peptide peaks were deconvoluted using MassLynx program v. 4.0.

Chapter Four

Characterisation of Bovine U1 snRNP

4.1 Introduction

4.1.1 Identification of bovine thymus U1 snRNP associated proteins

Antigenic equivalence of human U1 snRNP and bovine U1 snRNP has been confirmed by the use of purified bovine U1 snRNP in many commercially available anti-nuclear antibody diagnostic tests (Boak *et al.*, 1984; James *et al.*, 2000). Despite its acceptance as an aid in connective tissue disease diagnosis, bovine U1 snRNP is poorly characterised. Defining the composition of bovine tissue extracted U1 snRNP is hindered by its altered appearance in SDS-PAGE compared to the protein profile of the human equivalent. SDS-PAGE analysis of both bovine (Takano *et al.*, 1981; Duran *et al.*, 1984) and rabbit (White *et al.*, 1981; White *et al.*, 1982) thymus extracts consistently shows the presence of proteins at 68 kDa, 30-38 kDa (cluster), 29 kDa (doublet) and 13-16 kDa. Whilst it is likely that these proteins correspond to those identified in the extensively studied human cell extracted U1 snRNP, they have neither been positively identified nor characterised.

It is an emerging view that the sequence and structural characteristics of autoantigenic proteins are not the sole autoepitope determinants (Wu *et al.*, 2001). Numerous examples now exist of autoantibodies specific to post-translational modifications (Doyle and Mamula, 2001). These modifications may occur as a result of a spontaneous chemical process or as a product of a physiological enzymic process (Cloos and Christgau, 2004). Aberrantly modified protein, or impairment of the mechanisms designed to correct or remove modifications, may result in breaking self-tolerance, and hence lead to autoimmune disease.

The U1 snRNP proteins contain a number of notable post-translational modifications resulting from both spontaneous and physiological activities. The Sm proteins D1, D3 and B contain several sDMA residues which constitute one of the immunodominant epitopes. In addition, it has been postulated that the spontaneous conversion of aspartate residues to isoaspartate in SmD1 may act as an immunologic stimulus in SLE (Mamula *et al.*, 1999). The existence of

isoaspartyl residues in SmD1, however, has not been categorically demonstrated.

The 68K protein component of U1 snRNP is known to be phosphorylated and may also be glycosylated (Chen and Agris, 1992). Using two dimensional (2D) electrophoresis, Woppmann *et al*. (1990) determined the extent of heterogeneity of this protein in both human and mouse U1 snRNP. At least thirteen variants of the 68K protein were observed in both species. Phosphorylation of the 68K protein was examined using a combination of ^{32}P labelling, tryptic digestion and separation of the tryptic peptides from individual 68K protein variants on thin layer cellulose-coated plates. Phosphorylation alone did not account for the many variants observed. There are no accounts in the literature of the phosphorylation or glycosylation patterns of bovine U1 snRNP.

Several nuclear autoantigens, including the U1 snRNP associated 68K antigen, undergo cysteinyl aspartate specific protease- or caspase-dependent cleavage during apoptosis (Casciola-Rosen *et al*., 1994; Casciola-Rosen *et al*., 1996). This and other apoptotic modifications profoundly influence autoantigenicity (Utz *et al*., 2000). In the case of 68K, there is a single C-terminal caspase 3 specific cleavage site that produces a 40 kDa fragment. It is postulated that this apoptotic modification reveals a neoepitope which consequently becomes a superior diagnostic marker compared to the intact antigen (Greidinger *et al*., 2002; Greidinger *et al*., 2004; Hof *et al.,* 2005).

The first goal of this study was to characterise bovine U1 snRNP and non-U1 snRNP purified from calf thymus tissue. The study identified the constituent proteins of bovine U1 snRNP and the presence of Sm proteins associated with non-U1 snRNP. The type of modification, if any, carried by some of these proteins was determined, using affinity purified antibodies, 2D-gel electrophoresis and mass spectrometry. Bovine U1 snRNP antigenicity was compared to its human HeLa extracted equivalent using both immunoblotting and ELISA techniques. Of particular interest was the affect of the apparent 68K truncation on other post-translational modifications within the protein. These were investigated by examining the phosphorylation and glycosylation status of 68K

using phosphorus and glycan detection methods. Determining how spliceosomal antigens are modified during events such as apoptotic or necrotic cell death may provide clues to understanding how immune tolerance is broken, and potentially provide platforms for specific autoimmune therapies (Monneaux *et al.*, 2003).

4.2 Experimental Procedures

Purified bovine U1 snRNP (catalogue #: ATR01) and non-U1 snRNP (catalogue #: ATS02) were kindly provided by AroTec Diagnostics Limited, Wellington, NZ.

4.2.1 Preparation of samples for isoelectric focussing (IEF)

RNA was removed from purified U1 snRNP to avoid interference with the first dimension IEF. To achieve this, U1 snRNP was denatured in the presence of 7 M urea, 10 mM DTT and 1 % w/v triton x100 before adding TRIzol®/chloroform 1:1. After removing the top phase, the precipitated protein at the interface between phases was harvested and washed with ten volumes of ice cold acetone to remove residual chloroform. The protein pellet was resuspended in the required volume of 8 M urea, 2 % w/v CHAPS, 10 mM DTT and 2 % v/v ampholyte.

4.2.2 Protein dephosphorylation

Bovine U1 snRNP was buffer exchanged into 0.1 M Tris-HCl pH 9.5, 0.15 M NaCl, 5 mM $MgCl_2$ and then treated with 0.4 % (w/w U1 snRNP) porcine mucosal alkaline phosphatase (Sigma Chemical Co., St Louis, USA) for 1 hour at 37 °C. Alternatively, RNA was first removed from the U1 snRNP sample using the method described in the section above, and the protein was resuspended in 8 M urea. Prior to dephosphorylating the protein with alkaline phosphatase, the urea concentration was diluted to 1 M.

4.2.3 Determination of protein bound phosphate

The phosphate content of proteins was determined by hydrolysing seryl and threonyl bound phosphates and quantifying the phosphate groups released using the malachite green and phosphomolybdenate colorimetric detection method described by Ekman and Jager (1993). Briefly, protein was acetone precipitated, dried and then alkali hydrolysed by resuspending in 200 μL 1 M NaOH. The sample was heated at 100 °C for 15 minutes before interrupting the hydrolysis with the addition of 100 μL 4.7 M HCl. Phosphate detection reagent was freshly prepared by mixing 1 volume 10 % w/v ammonium molybdenate in

4 M HCl with 3 volumes 0.2 % w/v malachite green (Sigma Chemical Co., St Louis, USA). After the addition of 100 μL phosphate reagent to the hydrolysed protein the absorbance was measured at 595 nm. Phosphate standards ranging from 3 – 50 μM were treated in an identical way to the samples.

All glassware and plasticware containers were treated with 6 M HCl, then rinsed in ultrapure water and dried to reduce interference from exogenous inorganic phosphate.

4.3 Results

4.3.1 Bovine U1 snRNP composition

A comparison of bovine thymus purified U1 snRNP with the same complex purified from human cell nuclei using SDS-PAGE and western blotting, highlighted significant differences in their respective compositions (Figure 4.1). The classical U1 68K, A, B′/B, C and D subunit structure associated with human U1 snRNP was not present in bovine U1 snRNP. Bovine U1 snRNP proteins cover a broad range of molecular weights, as shown in Figure 4.2, with the corresponding weights for the HeLa U1 snRNP components listed in Table 4.1. Clustering of polypeptides around 30 kDa, in addition to the presence of a 14 kDa molecular weight species, has been described previously in both rabbit and bovine thymus extracts (Takano *et al.*, 1981; White *et al.*, 1982).

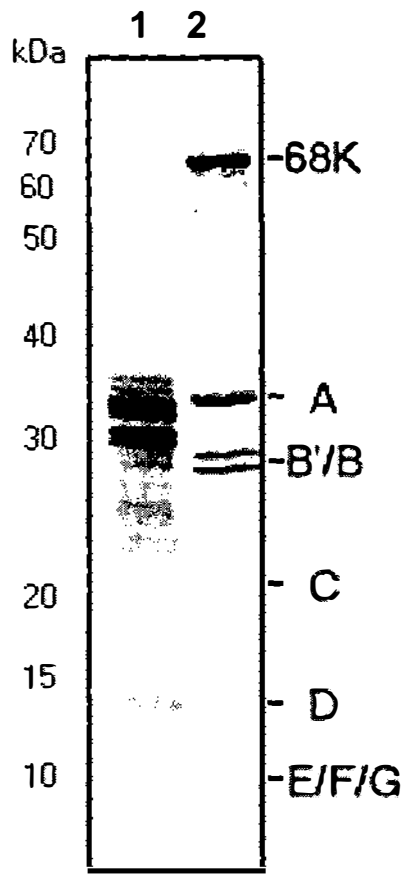

Figure 4.1 Comparison of human and bovine thymus U1 snRNP

U1 snRNP purified from bovine thymus (Lane 1) and human HeLa cells (Lane 2) were compared by analysis on SDS-PAGE and western blotting. Protein antigen components were visualised by immunoprobing with RNP and Sm +ve sera diluted 1/300. The positions of the well-characterised human U1 snRNP subunits (68K, A, B′/B, C, D and E/F/G) are annotated.

Table 4.1 Observed molecular weights of the human U1 snRNP component proteins

U1 snRNP component	68K	A	B′	B	C	D3	D2	D1	E	F	G
MW (kDa)	69.6	34.3	29.3	28.2	20.4	14.1	13.4	13.4	11.0	10.6	9.6

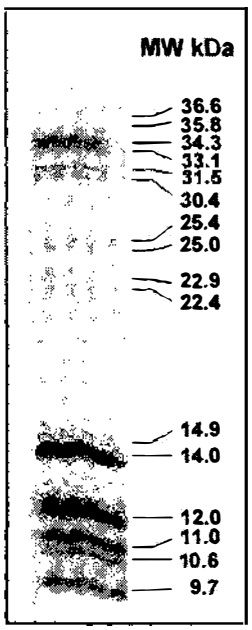

Figure 4.2 Molecular weight profile of bovine thymus U1 snRNP

Purified bovine U1 snRNP was analysed by SDS-PAGE and Coomassie stained to visualise the proteins. A molecular weight ladder was used to calculate the molecular weights of the observed bands.

By immunoprobing first with an anti-RNP specific patient sera and then re-probing with an anti-Sm sera, the distribution and possible identity of the various polypeptides was assessed. The bovine polypeptides could be crudely separated into RNP specific proteins, 25 kDa and above, and Sm core proteins, 14 kDa and below. The small molecular weight group included bands that could be related to their human equivalents, SmD, SmE, SmF and SmG. However,

bands comparable to human 68K, U1A, U1C and SmB proteins were less obvious in purified bovine U1 snRNP.

4.3.2 Identification of protein components in bovine U1 snRNP

To identify the component antigens of purified bovine U1 snRNP, antigen specific autoantibodies were immunoaffinity purified from patient sera using antigen immobilised onto nitrocellulose strips. Recombinant 68K, U1A and U1C proteins (Diarect, Fribourg, Germany) were used as the antigen sources to purify their respective antibodies. Immobilised human-derived SmD and SmB′/B were used as the antigen source for purifying Sm specific antibodies. Affinity purified autoantibodies were tested on human U1 snRNP immunoblots in order to characterise their specificities and to confirm that there were no significant cross-reactivities with other antigens. Results from the selected affinity purified antibodies are shown in Figure 4.3. Immunoaffinity purified autoantibodies with no significant cross-reactivity with other U1 snRNP antigens were then used to confirm the antigen composition of purified bovine U1 snRNP (Figure 4.4).

The 68K protein appears as a truncated polypeptide cluster ranging from 30 – 36 kDa in bovine thymus U1 snRNP, with the U1A protein migrating amongst the 68K polypeptide cluster on SDS-PAGE. In contrast to 68K, U1A is not truncated and has the same molecular weight (34 kDa) as the human U1 snRNP equivalent. The remaining RNP specific protein, U1C, is not identified within the bovine RNP preparation using affinity purified anti-U1C.

The identification of Sm proteins using this technique demonstrated only that SmD was present. SmB was not detected either with the anti-SmD antibodies which cross-react with epitopes on SmB, or with anti-SmB antibodies affinity purified from anti-RNP sera which do not cross-react with SmD.

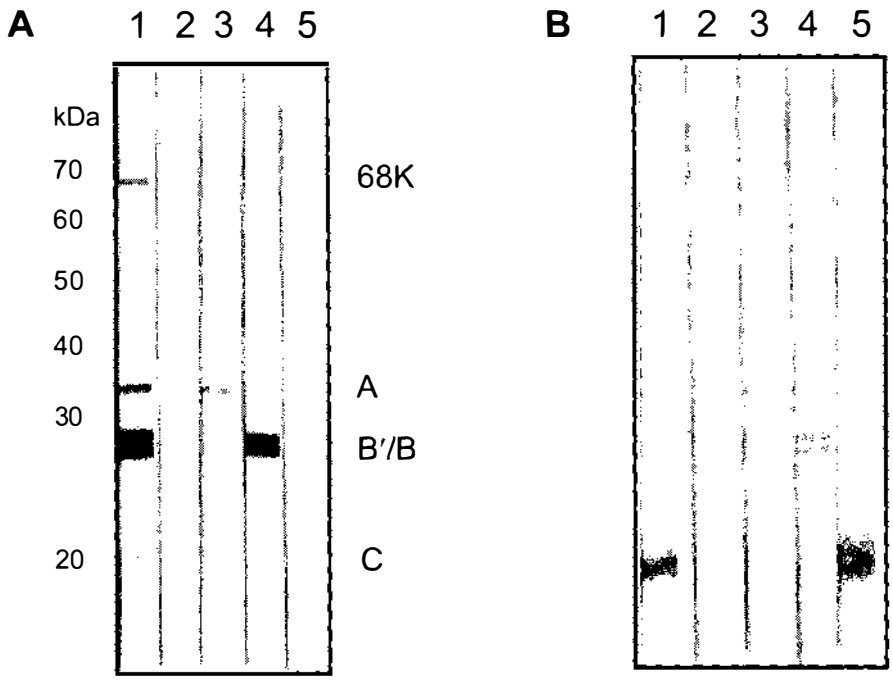

Figure 4.3 Cross-reactivity testing of purified autoantibodies

Human U1 snRNP was western blotted onto nitrocellulose, which was then cut into strips. Individual strips were immunoprobed with either patient sera or affinity purified antibodies. **A:** antibodies affinity purified from anti-RNP sera R10. **B:** antibodies affinity purified from anti-RNP sera R15. Strips: 1, whole sera specificity; 2, immunoaffinity purified anti-68K; 3, anti-U1A; 4, anti-SmB′/B; 5, anti-U1C.

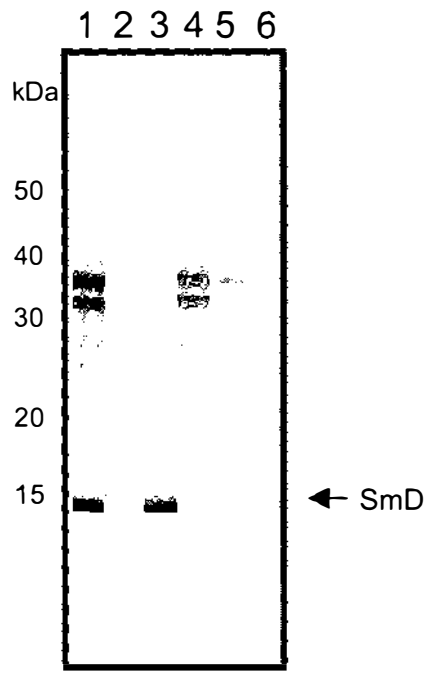

Figure 4.4 Identity of bovine U1 snRNP antigens

Bovine U1 snRNP was western blotted onto nitrocellulose which was then cut into strips. The individual strips were then probed with affinity purified antibodies. Strips: 1, anti-RNP/Sm patient sera; 2, anti-U1C; 3, anti-SmD; 4, anti-68K; 5, anti-U1A; 6, anti-B′/B.

4.3.3 Confirming the presence of SmB

Characteristic of most U snRNPs is the formation of a closed ring structure around the snRNA by the Sm proteins (Zieve and Khusial, 2003). Given that other members of the closed circle, such as SmD, are present, it is surprising that SmB cannot be identified in bovine U1 snRNP. To determine whether the same is true of non-U1 snRNP, Superdex S-200HR size exclusion chromatography was used to further purify the non-U1 snRNP, and the fractions analysed by SDS-PAGE, western blot and RNA electrophoresis (Figure 4.5).

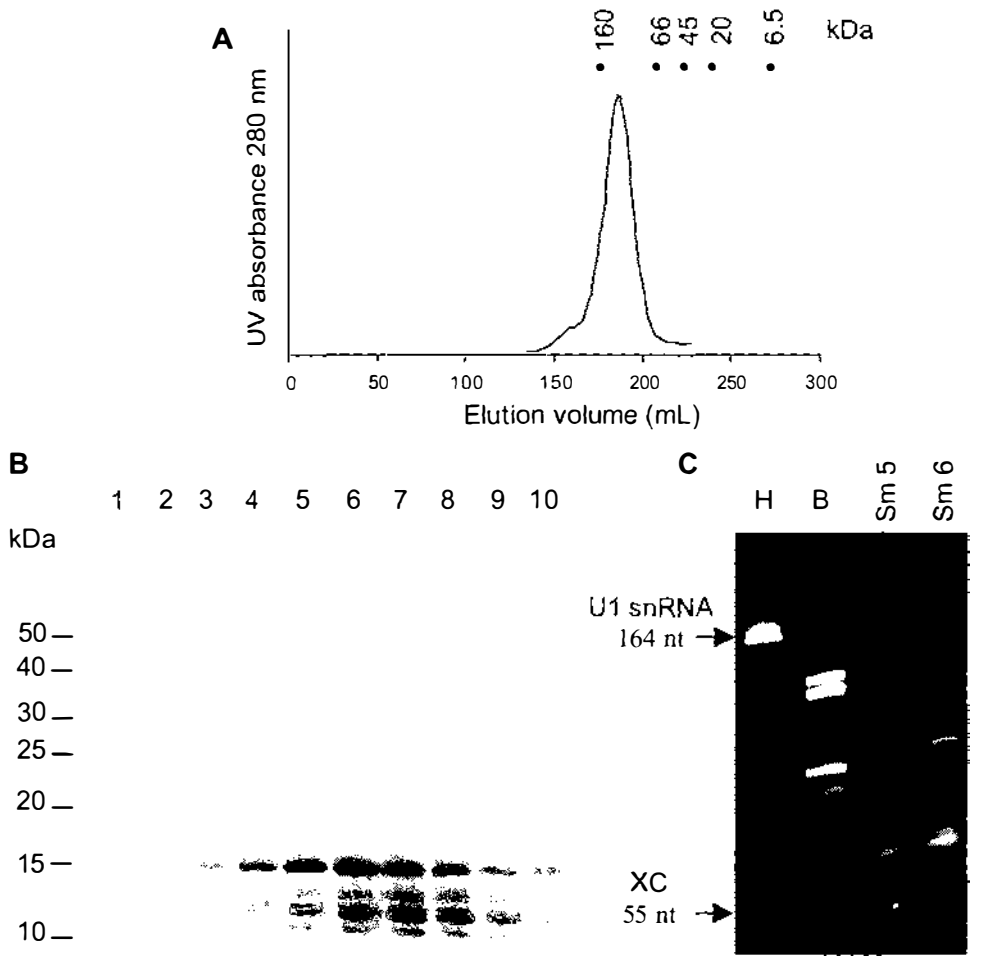

Figure 4.5 Separation of non-U1 snRNP

Non-U1 snRNP was separated on Superdex S200HR. **A**: UV absorbance trace of the Sm protein elution showing the elution volume of molecular weight standards. **B**: Coomassie stained SDS-PAGE. Lanes 1-10 are the 5 mL fractions collected between 150 and 200 mL elution volume. **C**: Ethidium bromide stained RNA separated by 10 % (T) polyacrylamide TBE-urea gel. H, HeLa cell extracted human U1 RNA; B, U1 RNA extracted from purified bovine U1 snRNP; Sm 5, RNA extracted from Lane 5 fraction; Sm 6, RNA extracted from Lane 6 fraction. The position of the 164 nt U1 snRNA and the xylene cyanol (XC) marker dye (55 nt) are annotated.

The Sm proteins eluted as a complex that corresponded to approximately 125 kDa by size exclusion chromatography and RNA extracted from these peak fractions implied that the Sm proteins form part of a non-U1 snRNP complex. The absence of U1 snRNA was confirmed by RNA electrophoresis, although there was non-U1 RNA clearly associated with the Sm proteins that was smaller than the 164 nt human cell derived U1 snRNA.

The non-U1 snRNP was used to test the specificities of a variety of anti-Sm patient sera in the absence of U1 snRNP specific protein, giving a higher signal to noise ratio for these antigens (Figure 4.6).

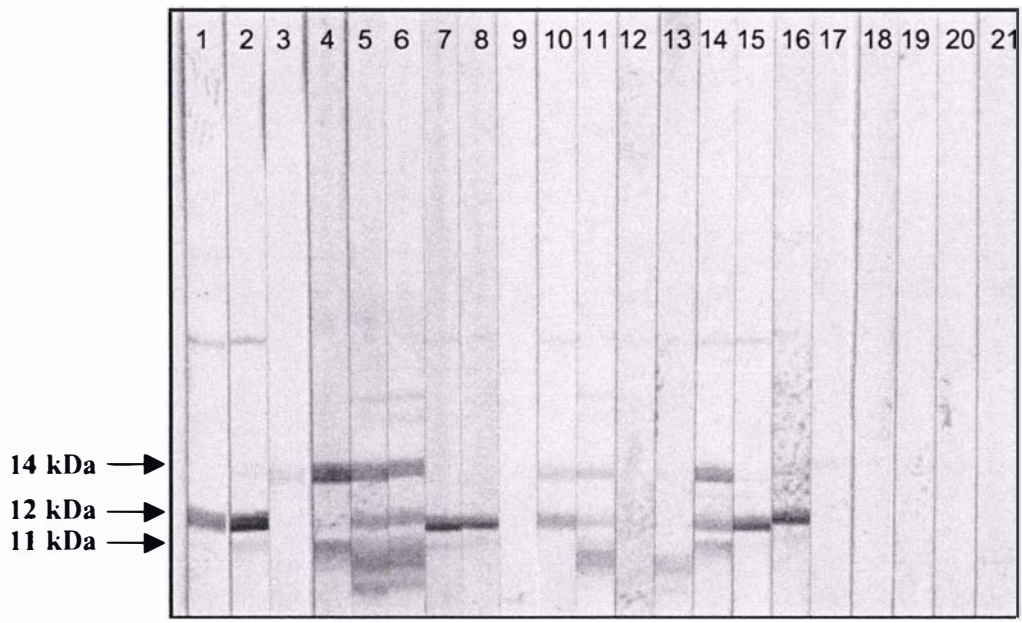

Figure 4.6 Specificities of anti-Sm and anti-RNP autoimmune sera using bovine non-U1 snRNP antigen

Non-U1 snRNP antigen (Sm) was western blotted onto nitrocellulose which was then cut into strips. Individual strips were immunoprobed with a range of anti-Sm and anti-RNP autoimmune patient sera. Strips 1-17 are classed as Sm +ve and 18-21 as RNP + ve.

Interestingly, many of the sera tested reacted with a 12 kDa protein as well as the 14 kDa SmD protein. To determine the identity of the 12 kDa protein, the relevant band was excised from a Coomassie stained SDS-PAGE gel and prepared for analysis by peptide mapping as described in section 3.2.15. The mass spectrum of tryptic peptides produced is shown in Figure 4.7.

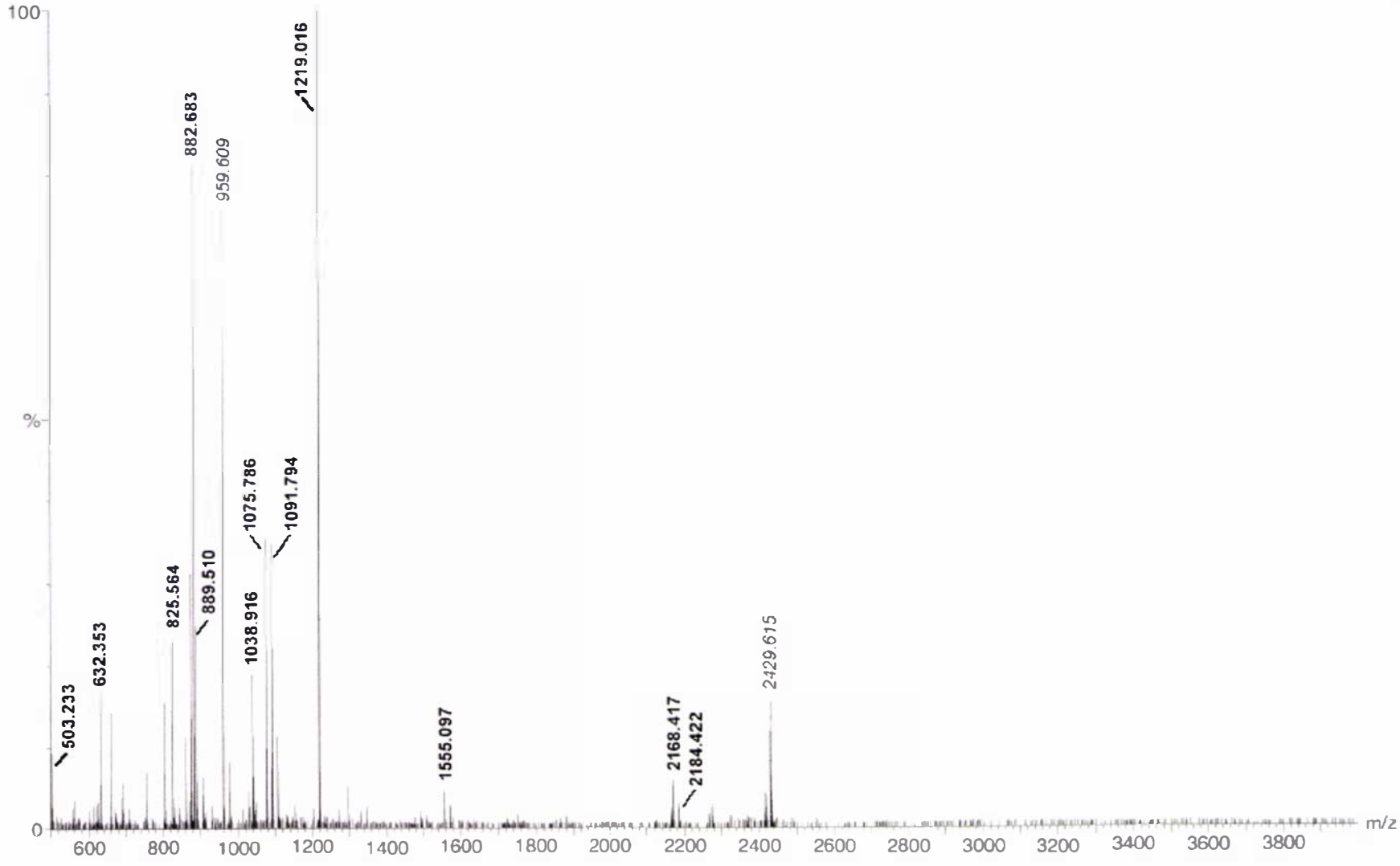

Figure 4.7 Mass spectrum of the bovine SmB tryptic peptides

Masses in bold were matched to SmB. Masses in italics represent the largest peaks not matched to SmB.

The associated peptide masses and matched sequence identities to human SmB are tabulated and annotated in Figure 4.8.

1 MTVGKSSK*ML QHIDYRMRCI LQDGRIFIGT*
*FKAFDKHMNL ILCDCDEFR*K IKPK*NSKQAE*
61 *REEKRVLGLV LLRGENLVSM TVEGPPPKDT*
*GIAR*VPLAGA AGGPGIGRAA GRGIPAGVPM
121 PQAPAGLAGP VRGVGGPSQQ VMTPQGRGTV
AAAAAAATAS IAGAPTQYPP GRGGPPPPMG
181 RGAPPPGMMG PPPGMRPPMG PPMGIPPGRG
TPMGMPPPGM RPPPPGMRGP PPPGMRPPRP
241

Peptide	Observed mass	Expected mass	δ	Sequence
9 - 16	1075.786	1075.5353	0.25	MLQHIDYR
17 - 25	1091.794	1091.5448	0.25	MRCILQDGR
26 - 32	825.564	825.4869	0.08	IFIGTFK
33 - 49	2184.422	2183.9670	0.05	AFDKHMNLILCDCDEFR
55 - 64	1219.016	1218.6073	0.41	NSKQAEREEK
58 - 64	889.510	889.4374	0.07	QAEREEK
65 - 73	1038.916	1038.7146	0.20	RVLGLVLLR
66 - 73	882.683	882.6135	0.07	VLGLVLLR
74 - 88	1555.097	1554.7832	0.31	GENLVSMTVEGPPPK
74 - 94	2168.417	2168.1015	0.32	GENLVSMTVEGPPPKDTGIAR
89 - 94	632.353	632.3362	0.02	DTGIAR

Figure 4.8 Human SmB′ primary sequence

The primary sequence of human SmB′ was taken from Swiss Prot Accession number P14678. Sequence highlighted in red italics shows the sequence covered by tryptic peptides mapped by mass spectrometry. Mass data was matched using Mascot (Matrix Science) (Perkins *et al.*, 1999).

Possible matched peptide sequences are clustered in the N-terminal region of the SmB protein. Coverage of this region is complete with the exception of peptide 1-8 and a small peptide 49-55. No peptides were obtained from the

protein beyond residue 94. Observed masses of all the identified peptides were within 0.4 Da of their expected values. Even with a 0.2 Da tolerance, the probability of the peptides belonging to SmB is still highly significant.

The SmB (1-94) fragment has a calculated mass of 11 kDa (SwissProt MW calculator) compared to the observed 12 kDa by SDS-PAGE. Such a small disparity in molecular weight may reflect anomalous migration of the peptide on SDS-PAGE, or more likely, that the truncation of SmB occurs between residue 94 and the following tryptic cleavage site at residue 108.

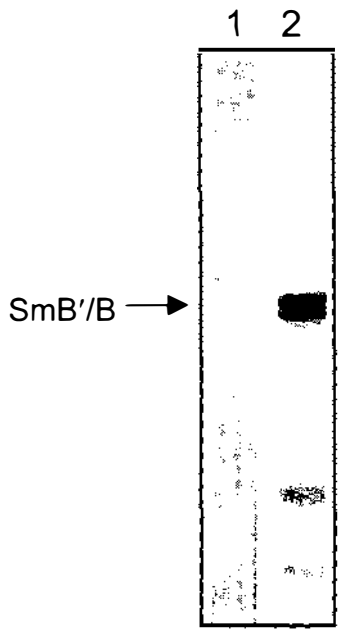

Figure 4.9 Antibody confirmation of bovine SmB identity

Human Sm was western blotted onto nitrocellulose and strips were probed with 1; putative SmB monospecific serum and 2; standard anti-Sm sera.

To confirm the identity of the 12 kDa truncation product as SmB, both intact human SmB′/B and the putative 12 kDa fragment were immunoprobed with anti-Sm patient sera. Confirming identity solely on the basis of sera reactivity is, however, not definitive because of the possible cross-reactivity between SmD and SmB epitopes. It had been observed that anti-RNP sera often react with what appears to be intact human SmB′/B on western blot. These sera, however, were unreactive with the 12 kDa truncated product and were therefore

not used for identity confirmation. One patient serum (Figure 4.6 Strip 1) reacts only with the 12 kDa fragment and does not react with other U1 snRNP component proteins. This serum was incubated with western blot nitrocellulose strips of human derived SmB′/B to confirm the specificity of the serum. Figure 4.9 shows the monospecific serum reacting weakly with human SmB′/B compared to a much stronger reaction elicited with a standard anti-Sm serum.

4.3.4 Comparative immunoreactivity of bovine and human U1 snRNP

To determine whether the modified composition of bovine U1 snRNP affects its immunoreactivity, purified bovine U1 snRNP and human U1 snRNP were compared by ELISA against a cohort of patient sera. Figure 4.10 shows a correlation plot of human against bovine U1 snRNP reactivities in ELISA. The coefficient of determination (r^2) for the data is 0.96, demonstrating a high degree of correlation between the ability of the two snRNP preparations to detect anti-RNP positive sera. Antibody reactivity to bovine U1 snRNP is marginally higher compared to the human equivalent, probably reflecting differences in the purity of the two preparations.

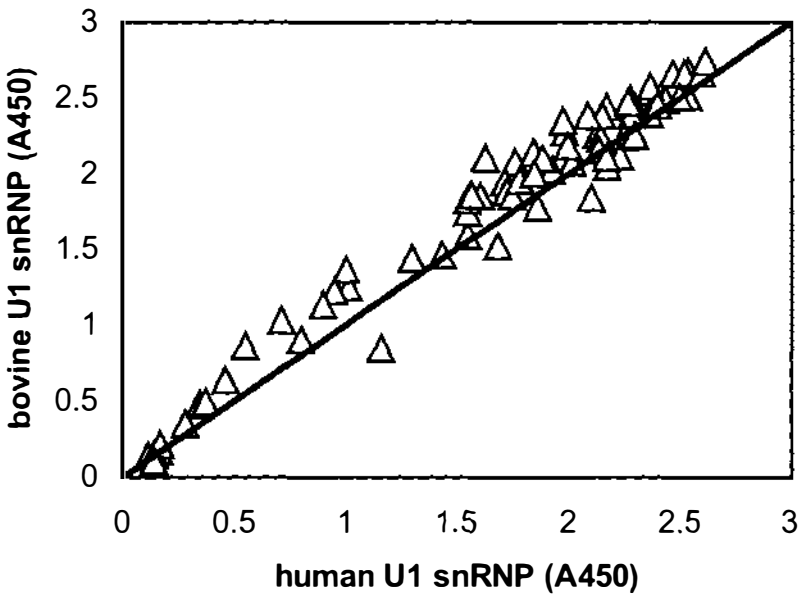

Figure 4.10 Comparison of the ELISA performance of U1 snRNP purified from bovine and human material using a patient sera cohort (n=56)

The diagonal line represents the ideal correlation. △ represent the reactivity of human and bovine U1 snRNP with one patient serum. Data points below the line respond greater to human U1 snRNP whereas points above the line respond better to the bovine preparation.

4.3.5 U1 snRNP heterogeneity

Proteins can be post-translationally modified in numerous ways, either enzymically (glycosylation, phosphorylation, methylation, proteolysis) or chemically (oxidation, deamidation, glycation) (Cloos and Christgau, 2004). Proteins are initially homogeneous translation products of a mRNA blueprint but rapidly become a heterogeneous mixture of protein isoforms.

2D-gel electrophoresis has been used effectively to examine heterogeneity within human U1 snRNP protein components (Woppmann *et al.*, 1990). The same technique was used in this study on purified bovine U1 snRNP proteins. Due to the potential interference from RNA in the first dimension IEF, snRNP proteins were separated from RNA by TRIzol®/chloroform extraction before IEF. The second dimension gel was either stained with Coomassie R250 or western blotted.

Approximately ten isoforms of bovine 68K protein can be seen with pIs that range from pH 8.1 to 9.9 (Figure 4.11). Interestingly, the isoforms group into five clusters with the dominant cluster around pH 9.5. The lower molecular weight 68K truncated polypeptides have fewer isoforms.

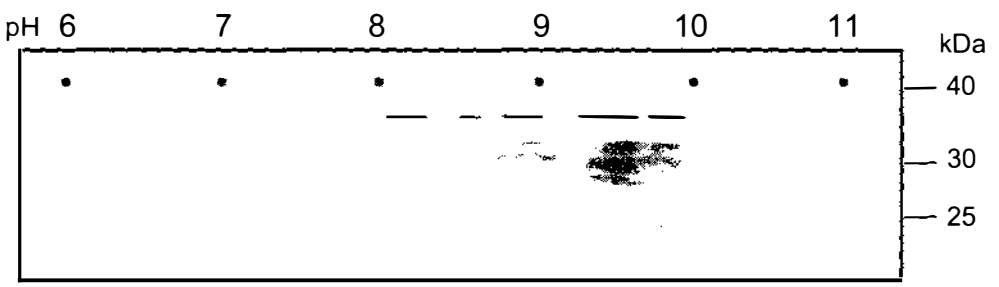

Figure 4.11 2D-gel electrophoresis of bovine U1 snRNP

2D gel western blotted and probed with a standard anti-RNP serum. The lines mark the positions of the five isoform clusters.

Human 68K protein is known to be phosphorylated, which contributes to the heterogeneity as observed by 2D-gel electrophoresis (Woppmann *et al.*, 1990). Attempts were made to remove bound phosphates from bovine U1 snRNP in order to observe the effect of phosphorylation on the distribution of the 68K

isoforms and other RNP components. The activity of the alkaline phosphatase was confirmed using a *p*-nitrophenol phosphate substrate, before it was incubated with the 68K protein and the other RNP components. Despite confirming that the enzyme was active, it appeared to have no effect on the isoform pattern of bovine 68K as observed by 2D-gel electrophoresis.

4.3.6 Phosphate content of the bovine 68K protein

The phosphate content of 68K was determined in triplicate for 25, 50, 75 and 100 μg protein using the phosphomolybdenate colorimetric method (Figure 4.12). The linear regression analysis calculated the phosphate amount per unit 68K as 7.831 pmoles/μg 68K. Using 32 kDa as the average molecular mass of bovine 68K, 1 μg was calculated as 31.25 pmols protein. Therefore, the phosphate content of 68K was determined as 0.25 mol phosphate/mol protein. The phosphate content was again determined after incubating 68K with alkaline phosphatase to remove any covalently linked phosphates from the protein, but no significant decrease in phosphate concentration was observed.

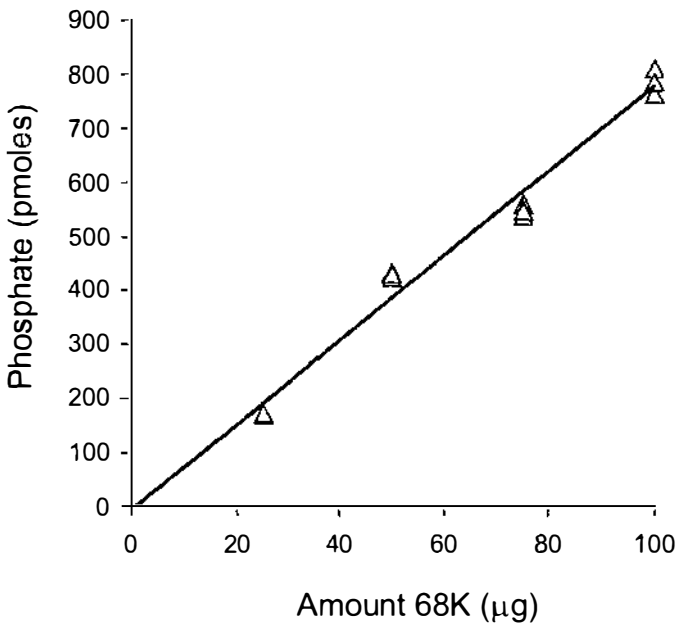

Figure 4.12 Protein-bound phosphate content in bovine 68K

Protein-bound phosphate content of bovine 68K was determined using the phosphomolybdenate colorimetric method. Linear regression analysis produced the equation $y = 7.831(x) - 6.55$, $R^2=9.83$.

4.3.7 Bovine U1 snRNP protein glycosylation

Intact 68K protein from rabbit thymus is reported to be glycosylated (Chen and Agris, 1992), however, it is unknown whether the events leading to the truncation of 68K have an effect on its glycosylation pattern. To examine the glycosylation of bovine 68K, purified 68K protein was western blotted onto nitrocellulose and the carbohydrate groups were detected using a glycan detection kit (Roche Diagnostics, Auckland, New Zealand) (Figure 4.13). Glycosylation of the truncated bovine 68K protein was confirmed, with a detection limit between 0.2 and 0.09 μg.

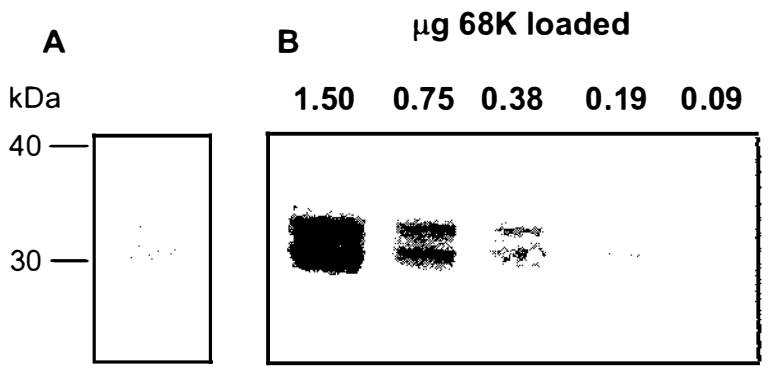

Figure 4.13 Glycan detection in bovine 68K

Amounts ranging from 1.5 to 0.09 μg 68K were western blotted onto nitrocellulose and glycans were detected by periodate oxidation, followed by reaction with DIG-3-O-succinyl-ε-aminocaproic acid hydrazide and anti-digoxigenin (DIG) alkaline phosphatase conjugated antibody according to the manufacturer's instructions. **A**, ponceau stained 68K prior to glycan detection; **B**, glycan detection in 68K.

To determine whether glycosylation has an influence on the isoform distribution of 68K, 2D-gel electrophoresis was performed and glycosylation of the isoforms was investigated as described above (Figure 4.14). The major cluster of 68K at pI 9.5 appears to be the only glycosylated isoform. Either the glycan content of the lower pI isoforms falls below the limit of detection or glycosylation may not contribute to the isoform distribution of bovine 68K.

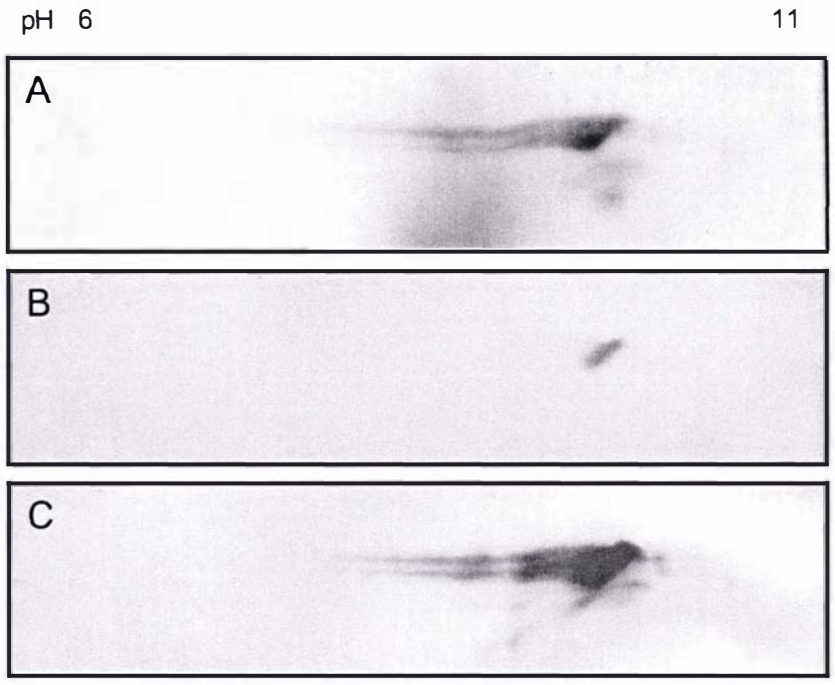

Figure 4.14 Detection of bovine 68K glycosylated isoforms by 2D-gel electrophoresis

68K (25 μg) was separated using 2D electrophoresis using a pH 6-11 IEF first dimension. The three panels show: **A,** Coomassie stained 68K; **B,** glycan detection in western blotted 68K 2D gel; **C,** standard western blot immunoprobing with anti-RNP serum.

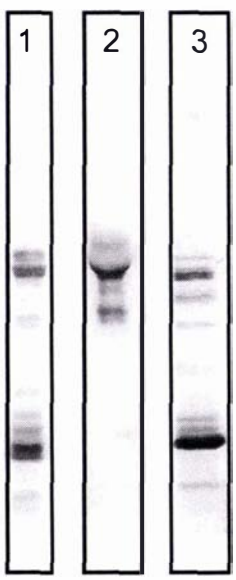

Figure 4.15 Glycan detection in U1 snRNP components

U1A, bovine and human snRNP were separated on SDS-PAGE and western blotted onto nitrocellulose. Glycans were detected on nitrocellulose strips using the DIG method. Lanes: **1**, bovine U1 snRNP; **2**, bovine U1A; **3**, human U1 snRNP.

Other U1 snRNP component proteins were tested to determine whether glycosylation was restricted to 68K. Bovine U1A, bovine and human U1 snRNP were analysed by western blotting with glycan detection carried out on the nitrocellulose (Figure 4.15). Glycans were detected not only on bovine U1A, as described by Chen and Agris (1992), but also on bovine and human SmD proteins. The periodation protocol in the glycan detection kit can be modified to selectively oxidise N-acetyl neuraminic acid (sialic acid) which can then be detected using the DIG method. This method when applied to western blotted bovine 68K, showed that no sialic acid was present in the glycan.

Unlike the consensus amino acid sequence Asn-X-Ser/Thr for N-linked glycosylation, there are no obvious consensus sequences identifying potential O-glycosylation sites. A number of neural network algorithms are available to predict O-linked sites on the basis of structural features and primary sequence (Gupta *et al.*, 1999a). 68K sequence was examined using three neural networks: NetOGlyc (Hansen *et al.*, 1998) which predicts mucin type O-linked N-acetylgalactosamine; DictOGlyc (Gupta *et al.*, 1999a) which determines possible O-linked α-N-acetylglucosamine; YinOYang (Gupta and Brunak, 2002) which predicts O-linked β-N-acetylglucosamine (O-GlcNAc) sites. No mucin type O-glycosylation sites were predicted in 68K using NetOGlyc. One probable O-linked α-N-acetylglucosamine modification was identified at Ser226 using DictOGlyc. Table 4.2 shows the results for O-GlcNAc modification of 68K and of other RNP component proteins using the YinOYang prediction server. YinOYang is able to predict both O-GlcNAc and O-phosphorylation sites and identifies possible reciprocal O-GlcNAc/O-phosphate sites.

The three serine residues (226, 259 and 266) predicted to be glycosylated are located within the RS domain of 68K. By digesting 68K with chymotrypsin (section 6.2.2) a large C-terminal peptide containing the RS domain is produced. Bovine 68K was hydrolysed with chymotrypsin, separated by SDS-PAGE and western blotted onto nitrocellulose. Potential glycosylation within the RS1 domain was again examined using the DIG glycan detection method. The RS1 peptide was visualised with Ponceau S reversible stain to confirm its

transfer to nitrocellulose, but no glycan was detected within the peptide domain (Figure 4.16).

Table 4.2 Potential O-GlcNAc modifications and O-GlcNAc/O-phosphate reciprocal sites

Residue		O-GlcNAc	Potential	Threshold (1)	Threshold (2)	NetPhos Potential	YinOYang
68K							
58	T	++	0.5097	0.3552	0.4291	0.574	Y
259	S	+	0.3887	0.3602	0.4359	0.996	Y
266	S	+	0.3561	0.3498	0.4219	0.998	Y
U1A							
66	S	++	0.6057	0.4619	0.5730	0.714	Y
218	S	++	0.5092	0.4125	0.5064	-	-
293	T	+	0.5131	0.4344	0.5359	-	-
SmB							
2	T	++	0.4466	0.3583	0.4334	-	-
90	T	+	0.4018	0.3689	0.4476	-	-
149	T	+	0.4542	0.4054	0.4968	0.671	Y
158	T	+	0.4861	0.4316	0.5321	-	-
160	S	+	0.4668	0.4218	0.5189	-	-
SmD1							
35	S	+	0.4674	0.4401	0.5436	-	-
SmD2							
26	T	+	0.4492	0.3720	0.3984	-	-
80	S	++	0.3990	0.3323	0.3984	0.997	Y

Predicted O-GlcNAc modification sites within 68K, U1A, SmB, SmD1 and SmD2 using YinOYang prediction neural network (www.cbu.dk/services/YinOYang). The SmD3 sequence was entered but did not return any positive results. Potential O-GlcNAc sites are compared to the potential for phosphorylation of the same residue. Coincidence of the two modifications indicates a possible reciprocal O-GlcNAc/O-phosphate interplay or "YinYang". S-serine, T-threonine.

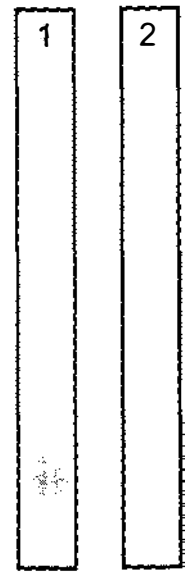

Figure 4.16 Glycan detection in the bovine 68K RS domain

68K was digested with chymotrypsin to yield the RS1 domain. It was western blotted onto nitrocellulose and either stained with Ponceau S for peptide content (Lane 1) or subjected to DIG glycan detection (Lane 2).

4.4 Discussion and Future Work

The performance or predictive value of an immunodiagnostic test, relates directly to whether the autoantigen used in the test is the closest possible match to the actual autoantigen. It is important, therefore, that the autoantigen should be well characterised to ensure that all likely autoepitopes are represented. Detection of circulating antibodies to U1 snRNP is the basis for the diagnosis of MCTD and SLE. The objective of this section of work was to characterise U1 snRNP derived from bovine thymus and to examine some of the differences between bovine thymus and human derived U1 snRNP. Frozen thymus was used in this study as this is the most common source of material for the commercial purification of nuclear autoantigens. There would be some merit in using fresh thymus in order to characterise changes in U1 snRNP composition, however, the use of fresh thymus would not be practical on a commercial scale.

4.4.1 RNP components are not all accounted for in bovine U1 snRNP

Bovine U1 snRNP derived from thymus retains structural similarity to its human equivalent. It consists of the U1 RNA moeity with a number of snRNP specific and common Sm core proteins attached. Immunochemical examination of constituent proteins in bovine U1 snRNP showed that the cluster of polypeptides, with molecular weights of approximately 30 kDa, were truncated forms of the 68K protein, an observation consistent with previous research (White *et al*., 1982; Duran *et al.,* 1984). The human 68K protein is particularly sensitive to proteolysis, containing two specific cleavage sites for caspase-3 and granzyme B, to produce 40 kDa and 60 kDa proteins respectively (Casciola-Rosen *et al*., 1996; Hof *et al*., 2005) (Figure 4.17). These two truncated proteins are thought to be the autoantigenic targets involved in the onset of autoimmune disease (Greidinger *et al*., 2002). Production of the 68K peptide cluster observed in bovine U1 snRNP must, however, involve proteases other than, or in addition to, caspase-3. Research into the progression of primary and secondary necrosis did not detect specific 68K cleavage fragments, but instead indicated there was a gradual loss of detectable antigen (Wu *et al*., 2001). The source of the cleavage fragments observed in bovine RNP is not

known and will be discussed further in chapter six. Nevertheless these fragments are relatively stable and are observed in all preparations of bovine U1 snRNP.

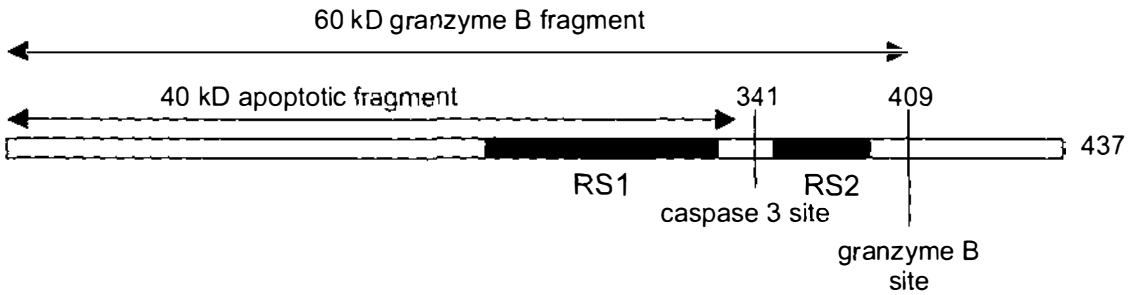

Figure 4.17 Proteolytic cleavage sites on human 68K

The actual molecular weight of the human 68K antigen, as calculated from its primary amino acid sequence, is 52 kDa. The caspase-3 cleavage fragment has a 40.4 kDa calculated weight and this correlates with its 40 kDa migration on SDS-PAGE. The granzyme B cleavage fragment has a 49 kDa calculated weight and an observed 60 kDa migration on SDS-PAGE. The molecular weight discrepency indicates that the C-terminal RS2 domain is largely responsible for the aberrant migration of the 68K antigen. Assuming that the truncated 68K peptide cluster is a result of C-terminal cleavage, the 30 kDa observed molecular weight on SDS-PAGE is likely to be a true representation of the cluster size.

U1A is unaffected by proteolysis suggesting that this protein lacks protease sensitive sites or is shielded from proteolytic attack by its conformation and RNA binding. A 1:1 stoichiometric relationship is thought to exist between U1A and the 68K protein (Hochleitner *et al*, 2005). Intriguingly, bovine U1 snRNP appears to have a greater ratio of 68K to U1A. As apoptotic events apparently do not affect U1A (Hof *et al.*, 2005), losses of U1A from bovine U1 snRNP must occur either through dissociation from the complex or through non-caspase dependent proteolysis.

Methods used to identify the presence of the RNP specific protein U1C in the bovine snRNP complex, were unsuccessful. However, the loss of U1C did not

appear to have adverse effects on the correlation of autoantigenicity between U1C (+) human U1 snRNP and U1C (-) bovine U1 snRNP. As patient sera with monospecific anti-U1C antibodies are extremely rare, the absence of U1C will not have a significant impact on diagnostic validity when bovine U1 snRNP is used as the antigen.

The RNA component of snRNPs has recently been shown to act as an adjuvant in stimulating the immune system and may therefore play a vital role in the autoimmune response (Greidinger *et al.*, 2006; Kelly *et al.*, 2006). U1 snRNA extracted from purified bovine U1 snRNP is truncated and is smaller than the intact human U1 snRNP purified from HeLa cells. The cleavage of U1 snRNA is known, however, to occur as a consequence of apoptosis (Degen *et al.*, 2000b). Caspase-3 activated nuclease cleaves between pseudouridine nucleotides 6 and 7 at the 5′ end of U1 snRNA, removing the TMG cap and destroying the 5′ recognition site (Figure 4.18). This prevents U1 snRNP from docking with the pre-mRNA and initiating spliceosome assembly.

Bovine U1 snRNA is at least 30-40 nt less than the human RNA. Clearly this cannot be a result of apoptotic loss of the six 5′ nucleotides. Cell death by necrosis will undoubtedly release a number of ribonucleases. Although proteins bound to the complex protect most of the U1 RNA from degradation, the 5′ region and the 3′ stem/loop IV structure are potentially exposed to nucleases. Cleavage of the 3′ terminal 28 nucleotides could account for the reduction of bovine U1 snRNA size compared to human. Such cleavage could be analysed using primers specific for regions within U1, such as the 3′ stem/loop IV. U1 snRNA is also a common target for autoantibodies with some specific reactivity towards the TMG 5 ′ cap structure (Okano and Medsger, 1992). Therefore, anti-TMG antibodies could be used to determine whether TMG is cleaved in the bovine U snRNAs.

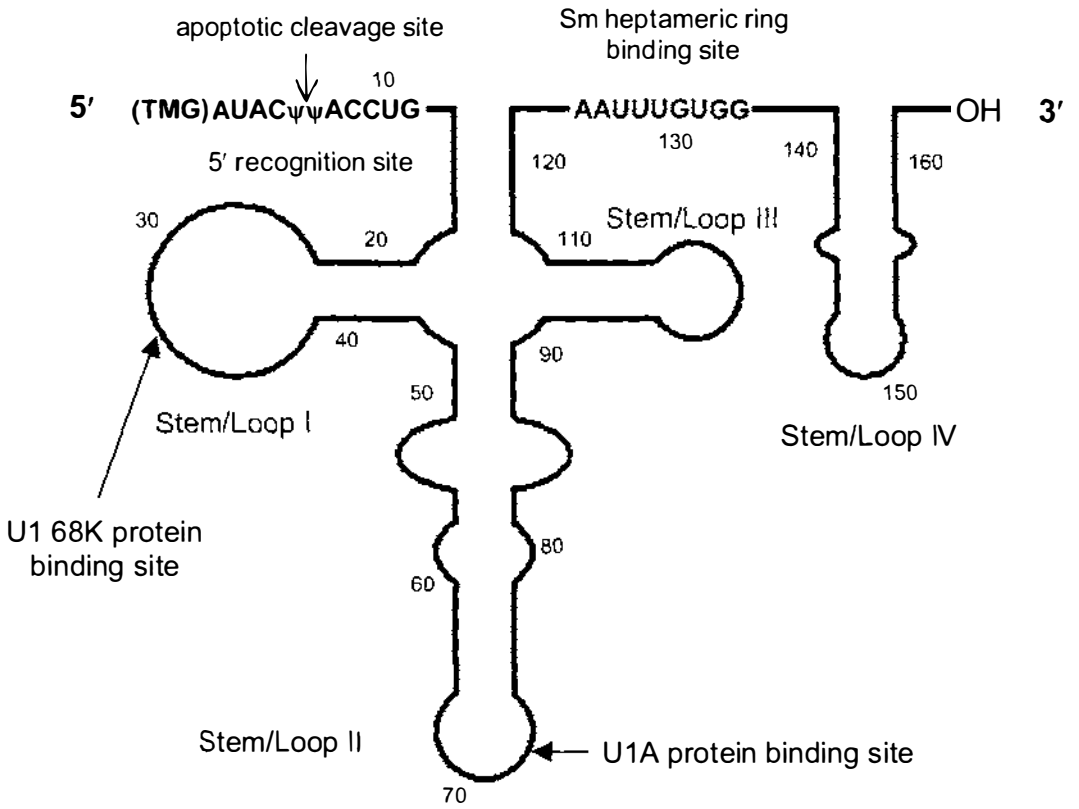

Figure 4.18 Apoptotic cleavage site in U1 snRNA

Stem/Loop structure of 164 nucleotide U1 snRNA with 68K and U1A binding sites annotated. The apoptotic cleavage site of the 5′ splice recognition sequence is also shown.

Non-U1 snRNA was shown to be associated with the Sm proteins purified by immunoaffinity chromatography. Using anti-Sm immunoaffinity columns it is possible that the snRNAs U2 (189 nt), U4 (144 nt), U5 (117 nt) and U6 (106 nt) could co-elute. In fact, purified Sm proteins were shown to be associated in a complex with RNA by size exclusion chromatography. Purified non-U1 snRNP consisted only of the Sm core proteins having a molecular weight of 84 kDa as calculated from SDS-PAGE. Although other proteins are associated with spliceosomal U snRNA, using high ionic strength during processing results in the dissociation of these proteins from the complex (Lührmann *et al.*, 1990). RNA, co-purifying with the Sm proteins must contribute at least 41 kDa or 150 nt to the complex. The actual RNA contribution appears less than calculated as

the extracted RNA ranges between 100-130 nt. However, size exclusion is not an absolute measure of molecular weight and is affected by the dynamic radius and shape of a molecule. These factors could account for the deviation between the observed and calculated weights of the non-U1 snRNP.

4.4.2 Sm truncation reveals a useful epitope

Experiments on caspase mediated cell death suggest that SmB is not sensitive to proteolysis (Hof *et al.*, 2005). It was surprising, therefore, to find no trace of intact SmB in bovine U1 snRNP. SmB was instead identified as a truncated 12 kDa peptide by a combination of mass spectrometry of peptides derived from in-gel tryptic digestion and the use of a patient serum which reacted solely with the 12 kDa peptide. Eleven out of 24 tryptic peptides submitted for MASCOT analysis were matched to SmB, and the remainder, including a number of significant mass peaks, could not be accounted for. This lack of match may be due to contaminant peptides, incomplete removal of Coomassie stain prior to trypsinolysis or post-translational modifications. The truncation of SmB is the first indication that SmB may be protease sensitive. While SmB's resilience to caspase cleavage during apoptosis has been studied, the influence of primary or secondary necrotic events on SmB has not been reported.

Migration of truncated SmB on SDS-PAGE is consistent with a cleavage site between residues 103 and 109. Truncated SmB (SmB^{trunc}) consists of the N-terminal domain including the RNA and Sm protein binding motifs (Figure 4.19). By removing the immunodominant and cross-reactive PPPGMRPP sequence, as well as the sDMA sequences, SmB specific epitopes could be examined.

A combination of low affinity and the lower relative concentration of the SmB N-terminal epitope is the most likely reason for the poor binding of monospecific anti-SmB^{trunc} antibodies to intact human SmB′/B. Conformation dependent epitopes have been reported in the Sm motif domain, which may explain the poor antibody affinity in immunoblotting. Reactivity in ELISA was also low despite the tendency of this test to maintain antigen conformation.

```
1                                                            60
MTVGKSSKMLQHIDYRMRCILQDGR***IFIGTFKAFDKHMNLILCDCDEFRKIKPKNSKQAE***

61                                                           120
***REEKRVLGLVLLRGENLVSMTVEGPPPKDTGIARVPLAGAAG***GPGIGRAAGRGIPAGVPM

121                                                          180
PQAPAGLAGPVRGVGGPSQQVMTPQGRGTVAAAAAAATASIAGAPTQYPPGRGGPPPPMG

181                                                          240
RGAPPPGMMGPPPGMRPPMGPPMGIPPGRGTPMGMPPPGMRPPPPGMRGPPPPGMRPPRP
```

Figure 4.19 SmB primary sequence

The sequence is annotated to show the epitope region (bold italics) proposed to be recognised by RNP +ve and SmD -ve patient sera. The arrows mark the region between which the proteolytic event causing the truncation is thought to occur.

Most anti-RNP sera from MCTD sufferers are only able to immunoprecipitate U1 snRNP. These sera often react on western blot with SmB′/B, which is common to most U snRNPs, and therefore might be expected to immunoprecipitate all U snRNPs. A number of explanations have been proposed to reconcile this finding. Perhaps the most plausible, described by Ohosone *et al.* (1992), suggests that SmB contains epitopes accessible only on native U1 snRNP. This conclusion was drawn through experiments with two β-galactosidase fusion proteins, one containing SmB residues 25-103 and the other encoding residues 191-205. Both regions contain epitopes which are specific for U1 snRNP; that is, antibodies immunoaffinity purified from the expressed fusion proteins, that only immunoprecipitate U1 snRNP. SmB 191-205 contains the immunodominant epitope PPPGMRPP which is shared with U1A. It is therefore implied that the U1 snRNP specificity of this epitope is due to recognition of U1A. Interestingly, antibodies immunoaffinity purified from SmB 25-103 using anti-Sm sera were able to immunoprecipitate all U snRNPs, suggesting that this region also contains a Sm-specific epitope. It is therefore likely that the U1 snRNP specific epitopes are otherwise masked by RNA or proteins and are hence inaccessible in the other SmB bearing U snRNPs.

The truncated SmB identified in this study covers the N-terminal epitopes within residues 25-103 discussed by Ohosone *et al.* (1992) (Figure 4.19). Most, but not all, anti-Sm sera react well with SmB^{trunc} in agreement with Ohosone's findings. However, despite reacting with intact human SmB′/B, none of the anti-RNP sera tested recognised the truncated SmB, and hence the proposed U1 snRNP specific epitope, in western blot. In addition, none of the anti-RNP sera tested in western blot showed SmB/U1A cross-reactivity. Of course this does not rule out the presence of antibodies reactive to the immunodominant PPPGMRPP epitope or the fact that anti-RNP sera may genuinely react with other SmB epitopes. It does, however, add to the number of inconsistent findings related to SmB recognition by anti-RNP sera. Recognition of SmB in western blotted HeLa cell nuclear extracts by anti-RNP sera (see supplement 1) has not been replicated with either recombinant SmB (Hines *et al.*, 1991) or SmB purified to homogeneity by high performance liquid chromatography (Williams *et al.*, 1988). All studies use different patient sera, and therefore, sera selection could be a possible source of disparity. Furthermore, the use of a crude nuclear extract as the antigen source for western blotting leads to a potential misinterpretation or incorrect assignment of antibody specificity.

Preliminary experiments using immunoaffinity purification of tryptic peptides of the in-gel digested SmB′/B region of HeLa U1 snRNP suggested that anti-RNP autoantibodies may be reacting with a human replication element protein (HREP). These results are presented and discussed in Chapter seven. HREP has a similar molecular weight to SmB and also has an alternatively spliced product with a slightly lower weight. It belongs to the WD-type protein family which are known to facilitate protein:protein and protein:nucleic acid interactions (Neer *et al.*, 1994).

Further work is required to validate these preliminary results, but the findings to date provide some very controversial data.

4.4.3 Post-translational modifications and heterogeneity of 68K

Phosphorylation has a well-established role in pre-mRNA splicing events (Misteli and Spector, 1997). The interaction of 68K with splicing factor ASF/SF2 and binding of U1 snRNP with 5′ recognition site is dependent on correct 68K phosphorylation. Thirteen isoforms of human 68K were identified by 2D-gel electrophoresis with pIs ranging from pH 6.8 – 8.7 (Woppmann *et al.*, 1990). All variants were phosphorylated, although phosphorylation alone could not account for the range of pIs. In contrast, bovine thymus 68K is phosphorylated at only 0.24 mol phosphate per mol 68K. This lack of phosphorylation is reflected not only in the low number of charged variants but also in the dominance of variants with high pIs observed using 2D-gel electrophoresis. The phosphate content of the 68K protein can be reduced by removal of phosphorylated domains such as RS2 during its truncation or through dephosphorylation by phosphatases (Xiao and Manley, 1997). Dephosphorylation by protein phosphatases I (PP1) and 2A (PP2A) is critical for splicing catalysis and spliceosome disassembly (Mermoud *et al.*, 1994). An additional serine/threonine phosphatase (protein phosphatase 2Cγ) is required early in spliceosome assembly and remains associated with the spliceosome (Murray *et al.*, 1999).

Cell death induced proteolysis and dephosphorylation is known to occur in another nuclear autoantigen, La/SSB (Rutjes *et al.*, 1999). This protein is involved in RNA polymerase III transcript termination, release and reinitiation, a process that is mediated through a dephosphorylation/phosphorylation cycle (Maraia *et al.*, 1994). Dephosphorylation appears to involve PP2A-like phosphatase activity, which together with protein cleavage is moderated by caspase-3 activation (Santoro *et al.*, 1998). A similar scenario could occur in the case of 68K whereby proteolysis and dephosphorylation work in tandem to prevent splicing activity.

Phosphorylation is critical to the autoantigenicity of some antigens with only the phosphorylated forms of RNA polymerase I and polymerase II being recognised by autoantibodies from SLE patients (Stetler and Jacob, 1984; Satoh *et al.*,

1994). However, as with La/SSB, dephosphorylation of 68K does not adversely affect its autoantigenicity. In fact, dephosphorylation may be responsible for the neoepitope created during apoptosis which results in greater recognition by MCTD autoimmune sera than the non-apoptotic 68K (Greidinger *et al.*, 2002).

Further work is necessary to characterise the fate of 68K phosphorylation during apoptosis. Cultured cells labelled with ^{32}P could be used to monitor the affects of apoptosis induction upon radiolabelled 68K. In addition, a number of sophisticated mass spectrometric techniques could be used for phosphorylation analysis (Garcia *et al.*, 2005). This work would benefit from the use of phosphatase inhibitors such as sodium vanadate, pyrophosphate and sodium fluoride to determine more accurately the position and fate of the phosphorylation.

Glycosylation of bovine 68K has been demonstrated in this study and confirms previous findings (Chen and Agris, 1992), although neither the glycosylation type nor glycan structure have been determined. Work by Chen and Agris implied the presence of an N-linked glycan. The 68K primary structure only contains one Asn-X-Ser/Thr consensus sequence at the C-terminus which would be cleaved from the truncated 68K during cell death. This consensus sequence, required for N-linked glycosylation, is unlikely to be present in bovine 68K. Other possible glycosylations in 68K might be O-linked GalNAc or GlcNAc, with the latter being the most probable in a nuclear protein (Comer and Hart, 2000). More unusual would be O-mannosylation or C-glycosylation which *are* not usually found in nuclear proteins.

A tool, such as YinOYang, for predicting O-GlcNAc content of a protein is not infallible, so neither the presence nor absence of predicted glycosylation confirms or precludes O-GlcNAc existence. For example, the nuclear pore protein Nup155 contains 26 predicted O-GlcNAc sites, however, analysis of O-GlcNAc using the β-elimination followed by Michael addition with DTT (BEMAD method) (Wells *et al.*, 2002b), confirmed only one O-GlcNAc at a serine residue, which was not predicted by YinOYang.

O-GlcNAc is an abundant modification that is essential for many cellular functions. All O-GlcNAc modified proteins are also phosphorylated and in several cases the O-GlcNAc and O-phosphate occur at the same or adjacent hydroxyls of serine or threonine (Comer and Hart, 2001; Wells *et al.*, 2001). This so-called "yin-yang" modification serves to regulate protein function in *a* variety of processes. The identification of three possible "yin-yang" type sites within 68K imply a possible role in the control of the spliceosome cycle, a role that has not previously been reported. Predicted glycosylation sites fall within the RS domain, however, glycans were not detected within the 68K C-terminal chymotryptic peptide. Either the amount of peptide was insufficient for O-GlcNAc detection or the majority of carbohydrate is located in non-RS domain sites.

A number of methods now exist to determine O-GlcNAc content and position through modification and enrichment of O-GlcNAc peptides with subsequent characterisation by mass spectrometry (Haynes and Aebersold, 2000; Whelan and Hart, 2003; Khidelkel *et al.*, 2004). A method which could be applied to determining 68K O-GlcNAc sites is the BEMAD approach whereby the protein undergoes in-gel digestion with trypsin and then O-GlcNAc or phosphate is removed by β-elimination in mild alkali (Wells *et al.*, 2002b). DTT is then used as a nucleophile to react with the α,β-unsaturated carbonyl group formed by β-elimination (Figure 4.20). DTT labelled peptides can be enriched using thiol affinity chromatography and the peptides can be detected using mass spectrometry. A mass shift of 66.8 Da is expected with the loss of O-GlcNAc (203.0) and addition of DTT (136.2).

Future work to determine O-GlcNAc content of the bovine 68K protein should include the use of the O-GlcNAc-beta-N-acetylglucosamidase inhibitor, PUGNAc, to prevent removal of the O-GlcNAc during the purification process.

Confirmation of glycosylation of U1A and Sm proteins will help to establish an hypothesis for the role of O-GlcNAc in the control of U1 snRNP assembly and the interaction of component proteins with other spliceosome constituents.

However, carbohydrates other than O-GlcNAc may be involved in pre-mRNA splicing. Both galectin-1 and -3 (N-acetylgalactosamine and N-acetyl-lactosamine binding lectins) have been shown to be necessary for snRNP biogenesis and pre-mRNA splicing (Dagher *et al.*, 1995; Park *et al.*, 2001). The carbohydrate binding proteins interact directly with the SMN protein complex via Gemin4, but it is not clear whether the Sm core proteins interact with the galectins during snRNP assembly.

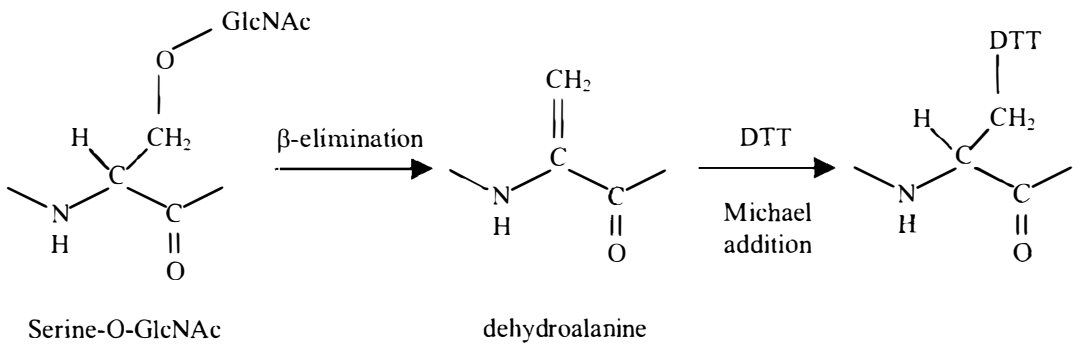

Figure 4.20 O-GlcNAc detection by β-elimination and Michael addition with DTT (BEMAD)

Chapter Five

Purification and Characterisation of Sm-Free U1 68K Antigen

5.1 Introduction

U1 snRNP complex is established as a reagent in the diagnosis of rheumatological diseases such as MCTD and SLE (Bizzarro *et al.*, 1998; Benito-Garcia *et al.*, 2004). However, the use of such a complex antigen in ELISA means that some of its diagnostic and prognostic value is lost. There would be a diagnostic advantage therefore in being able to detect and discriminate between autoantibody responses to the individual constituent proteins of U1 snRNP. For example, high titres of circulating anti-U1 68K protein antibodies correlates highly to an MCTD diagnosis, with 90 % prevalence of Raynaud's phenomenon and increased risk of fatal pulmonary hypertension (Smolen and Steiner, 1998).

There are a number of advantages to producing recombinant autoantigens for use as diagnostic reagents (Schmitt and Papisch, 2002). Using this technology it is possible to obtain authentic sequence and high expression levels, and to introduce tags that aid in purification. However, the inability to faithfully reproduce post-translational modifications or incorrect structural conformation of some recombinant proteins can significantly reduce the efficacy of the antigen (Brahms *et al.*, 2000; Burlinghame, 2005). Recombinant human 68K (r68K) antigen is commercially available and has been used successfully to measure anti-RNP antibodies specific for 68K protein in ELISA format (Nyman *et al.*, 1990; Seelig *et al.*, 1991; Gaubitz *et al.*, 2002). According to the literature, r68K is truncated to contain only the main autoepitopes. Expression of the full-length protein in high yield has proven difficult due to the presence of inhibitory elements within the protein sequence (Northemann *et al.*, 1995). It was noted in a recent study that some anti-RNP sera could only be detected using purified U1 snRNP antigen rather than recombinant proteins (Luyckx *et al.*, 2005).

Native bovine U1 68K antigen shares at least 98 % sequence identity with the human equivalent. It is relatively abundant in calf thymus tissue and is truncated due to proteolysis. It is well reported that U1 68K is a primary target for modification in apoptosis and necrosis with the potential creation of neo-epitopes (Casciola-Rosen *et al.*, 1994; Degen *et al.*, 2000a; Wu *et al.*, 2001;

Greidinger *et al.*, 2004). The availability of a native purified 68K antigen would provide a useful and perhaps superior alternative to using recombinant antigen in autoimmune disease diagnosis.

Isolation of individual RNP protein components requires disruption of the RNA:protein complex for which a variety of approaches have been used. Methods such as preparative electrophoresis (Takeda *et al.*, 1989), high performance liquid chromatography (Williams *et al.*, 1988), RNAse T1 hydrolysis (Achsel *et al.*, 1999) and controlled pH and temperature (Bach *et al.*, 1990; Sumpter *et al.*, 1992) have demonstrated some success with both HeLa cell and rabbit thymus U1 snRNP. However, none of these approaches is amenable to the scale of production necessary to supply commercial antigens to diagnostic kit producers.

Disruption of the RNP complex has reportedly been induced using high concentrations of $MgCl_2$ (Satoh *et al.*, 1997) which incidentally is used to disrupt autoantibody:antigen interaction in immunoaffinity purification. This approach will be evaluated therefore as a strategy for purifying viable quantities of RNP specific proteins in the absence of the common Sm antigens. The diagnostic performance of the purified antigens will be compared to the recombinant equivalent.

5.2 Experimental Procedures

5.2.1 Isolation of Sm-free U1 68K protein

Anti-RNP immunoaffinity elutions were applied to a ceramic hydroxyapatite type I (CHT) column equilibrated in 5 mM phosphate pH 7.4 followed by washing the media with 5 mM phosphate containing 5 M urea. Bound protein was eluted first with 80 mM phosphate pH 7.4, 5 M urea and then with 0.5 M phosphate pH 7.4, 5 M urea buffer. The first elution was adjusted to 7 M urea, 10 mM DTT and filtered through a glass fibre filter (Machery-Nagel, Germany) before being applied to a SP-Sepharose FF column equilibrated in 20 mM Tris-HCl pH 7.5, 0.1 M KCl, 6 M urea, 10 mM DTT. Column elution was performed firstly with 20 mM Tris-HCl pH 7.5, 0.25 M KCl, 6 M urea, 10 mM DTT followed by the same buffer containing 1 M KCl. Further fractionation was achieved by size exclusion chromatography of the first SP-Sepharose elution on a Superdex 200HR column equilibrated in 20 mM HEPES pH 7.5, 0.4 M NaCl, 4 M urea.

Purification was carried out at 2 – 8 °C and all stages were analysed for protein concentration by the Bradford dye-binding assay, UV absorbance spectrum, SDS-PAGE and western blot.

5.2.2 Determining the influence of urea on bovine U1 snRNP dissociation

Hydroxyapatite (HT) Biogel (Bio-Rad Laboratories, Hercules, USA) was equilibrated with 5 mM phosphate buffer pH 7.4. Biogel slurry (1 mL) was pipetted into 20 microfuge tubes and the Biogel was pelleted by centrifugation. The pellet was resuspended in 1 mL anti-RNP immunoaffinity elution and mixed for 30 minutes at 2 - 8 °C. After centrifugation, the supernatant was removed and the Biogel resuspended once more with immunoaffinity elution. HT in individual tubes was then washed 3 times with equilibration buffer containing 18 increments of urea (0 – 7 M), before eluting bound protein with 0.25 M phosphate buffer pH 7.4 containing the same urea concentration used in the final wash buffer.

Elutions were buffer exchanged into SP-Sepharose equilibration buffer containing 20 mM Tris-HCl pH 7.5, 10 mM $MgCl_2$, 80 mM KCl and the appropriate urea concentration. HT elutions were applied to pre-equilibrated SP-Sepharose Hi-Trap columns (1 mL) (Amersham Biosciences, Uppsala, Sweden) and the non-bound material was collected. Bound protein was eluted with 20 mM Tris-HCl pH 7.5, 10 mM $MgCl_2$, 1 M KCl containing the appropriate urea concentration. Protein concentrations of SP-Sepharose non-bound and elutions were measured by Bradford dye-binding assay.

5.2.3 RNAse digestion of U1 snRNP

Purified bovine U1 snRNP/Sm (6 mg) was incubated with approximately 700 Units of T1 RNAse (Worthington Biochemicals, USA) for 1 hour at 37 °C. The sample was diluted 1:4 with cold 20 mM Tris-HCl pH 7.5 and placed on ice for 15 minutes before being applied to a SP-Sepharose FF Hi-Trap 1 mL column equilibrated in 20 mM Tris-HCl pH 7.5, 80 mM KCl. After washing with equilibration buffer the protein was eluted with 20 mM Tris-HCl pH 7.5, 1 M KCl.

5.3 Results

5.3.1 Dissociation of bovine U1 snRNP

High Mg^{2+} concentrations are known to destabilise and disrupt the human U1 snRNP complex (Satoh *et al.*, 1996; Satoh *et al.*, 1997). It is reasonable to assume that bovine U1 snRNP is therefore dissociated using the same conditions. An anti-RNP immunoaffinity column elution, containing 3.5 M $MgCl_2$, was used to establish whether the high Mg^{2+} concentration facilitated the disruption of the U1 snRNP complex and the separation of the component proteins from snRNA. It was found that the majority of the protein from the anti-RNP immunoaffinity elution bound to a CHT column despite the high ionic strength (Figure 5.1). Increasing phosphate concentrations were used to try and elute RNP specific proteins from CHT. Unfortunately, no separation was achieved between RNA and RNP constituent proteins as demonstrated by a 260:280 nm ratio of 1.98, which indicates high nucleic acid content in the CHT elutions.

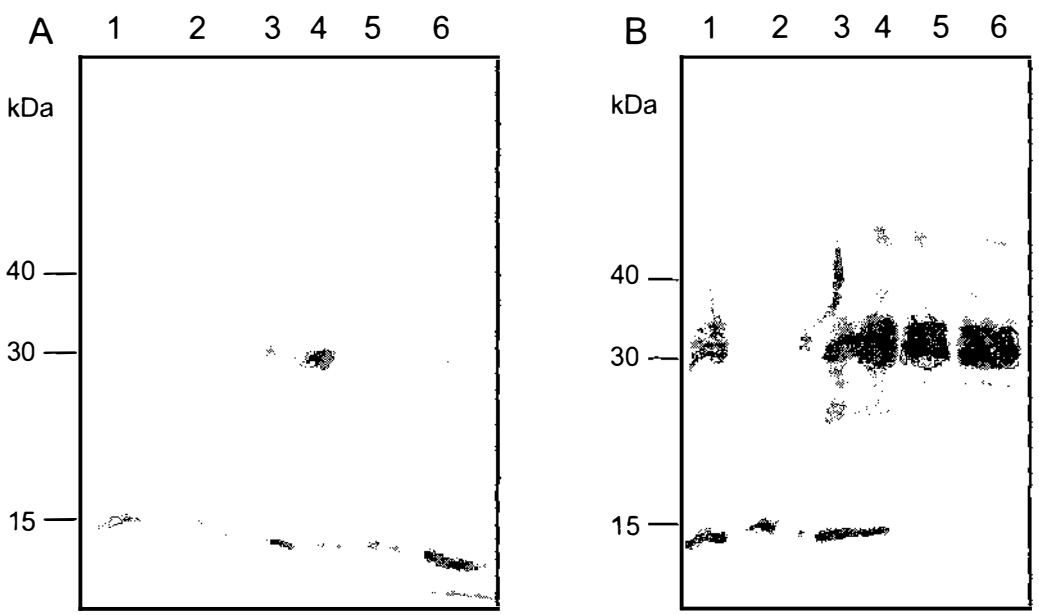

Figure 5.1 Purification of U1 snRNP on ceramic hydroxyapatite (CHT)

RNP eluted from an anti-RNP matrix in 3.5 M $MgCl_2$ was applied to a CHT column and eluted with increasing amounts of phosphate (P). All fractions and elutions were analysed by SDS-PAGE and proteins were visualised by **A:** Coomassie stain and **B:** Western blot immunoprobed with anti-Sm (+) patient serum. Lanes: 1, anti-RNP elution; 2, CHT non-bound; 3, 5 mM P wash; 4, 100 mM P; 5, 200 mM P and 6, 500 mM P.

Intact U1 snRNP binds strongly to Q-Sepharose FF. To determine whether the RNP eluted from CHT existed as a complex or as a mixture of independent components, the sample was applied to Q-Sepharose FF and eluted with a stepwise increase in salt concentration (Figure 5.2). Although U1 snRNP was eluted from a Q-Sepharose FF column, a small amount appeared not to have bound to the column.

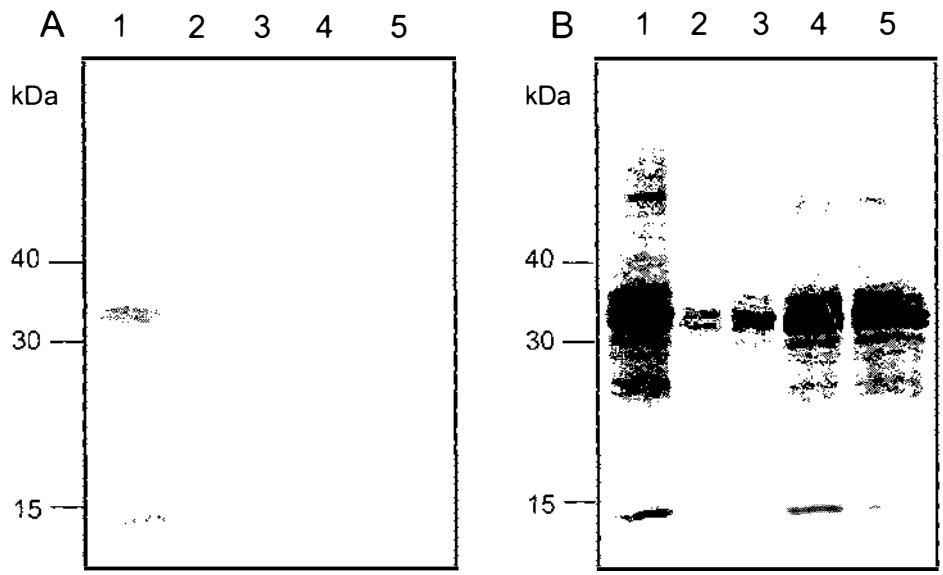

Figure 5.2 Purification of U1 snRNP CHT elution on Q-Sepharose FF

CHT 100 mM phosphate elution was applied to a Q-Sepharose column equilibrated in 20 mM Tris-HCl pH 7.5, 80 mM KCl. Fractions were eluted with increasing KCl concentrations. The elutions were analysed by SDS-PAGE. Proteins were visualised by **A:** Coomassie stain and **B:** Western blotting and immunoprobing with an anti-Sm(+) patient serum. Lanes: 1, CHT elution; 2, Q-Sepharose non-bound; 3, 0.25 M KCl; 4, 0.4 M KCl; 5, 1 M KCl.

An alternative strategy was trialled to elute RNP bound to CHT with the aim of obtaining individual RNP components. By adding urea (5 M) to the CHT elution buffers, the RNP was maintained in a denaturing environment. Even under these conditions, nucleic acid and protein still co-eluted from the CHT column (Figure 5.3). When this elution was applied to Q-Sepharose FF column equilibrated in denaturing buffer, however, the majority of the RNP component proteins appeared in the non-bound fraction (Figure 5.4). This indicates dissociation of protein from RNA, confirmed by the 260:280 nm ratio of 0.706. Still no separation of individual RNP constituent proteins was achieved using this approach.

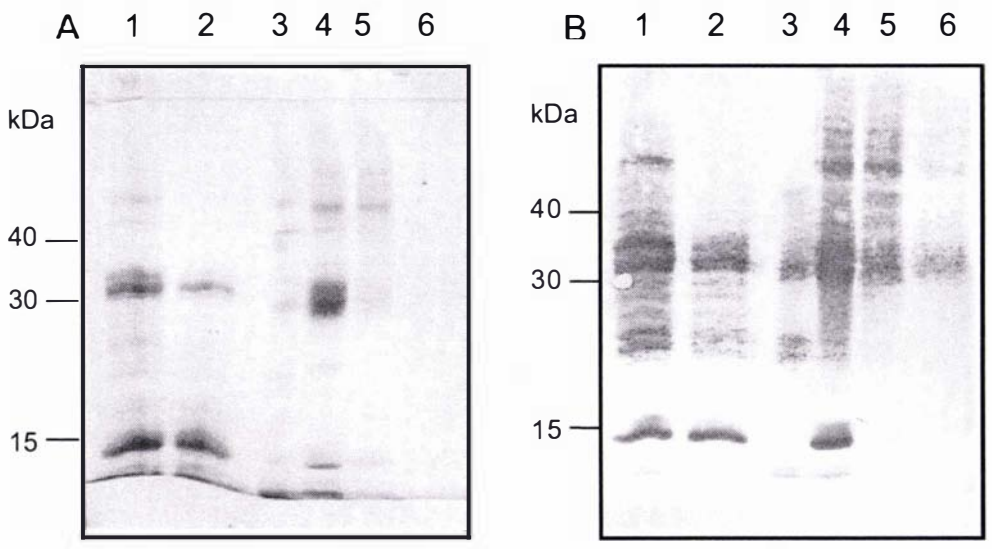

Figure 5.3 Effect of urea on the purification of U1 snRNP on CHT

RNP eluted from an anti-RNP matrix in 3.5 M $MgCl_2$ was applied to a CHT column and eluted in 5 M urea containing increasing amounts of phosphate (P). All fractions and elutions were analysed by SDS-PAGE and proteins were visualised by **A:** Coomassie stain and **B**: Western blot immunoprobed with anti-Sm (+) patient serum. Lanes: 1, anti-RNP elution; 2, CHT non-bound; 3, 5 mM P wash; 4, 100 mM P; 5, 200 mM P and 6, 500 mM P.

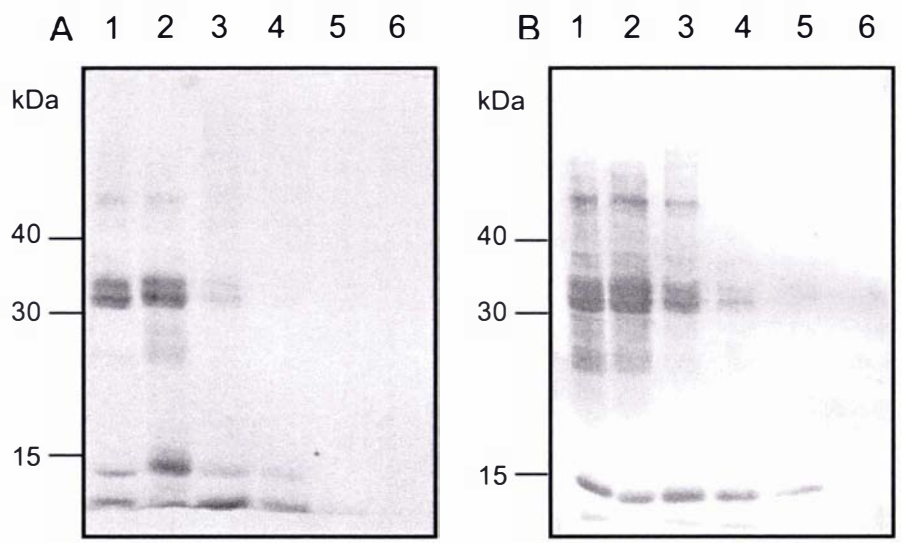

Figure 5.4 Effect of urea on the purification of CHT elution on Q-Sepharose

CHT 100 mM phosphate, 5 M urea elution was applied to Q-Sepharose column equilibrated in 20 mM Tris-HCl pH 7.5, 80 mM KCl, 5 M urea. Fractions were eluted with increasing KCl concentrations. The elutions were analysed by SDS-PAGE. Proteins were visualised by **A:** Coomassie stain and **B:** Western blotting and immunoprobing with an anti-Sm(+) patient serum. Lanes: 1, CHT elution; 2, Q-Sepharose non-bound; 3, 0.15 M KCl; 4, 0.25 M KCl; 5, 0.4 M KCl; 6, 1 M KCl.

A third strategy, for the separation of individual U1 snRNP component proteins, takes advantage of protein pI. Table 5.1 documents the range of pIs attributed to RNP proteins. Since the majority are basic proteins, with the exception of SmF subunit, it is reasonable to assume that they would bind to a cation exchange matrix like SP-Sepharose under neutral buffering conditions.

Table 5.1 RNP pIs taken from SwissProt

68K	A	C	B	D1	D2	D3	E	F	G
6.7-8.6	10.0	10.4	10.7	10.5	10.2	9.8	10.3	3.3	8.8

CHT elution in high urea concentration was applied to a SP-Sepharose column equilibrated in 20 mM Tris-HCl pH 7.5, 80 mM KCl, 5 M urea and eluted with increasing salt concentration. Nucleic acid content of the SP-Sepharose FF fractions was monitored by UV absorbance (Figure 5.5). The nucleic acid component of U1 snRNP appears in the non-bound fraction of the SP-Sepharose matrix, whereas the elution apparently contains protein only.

Using this strategy, partial separation of RNP specific protein from Sm common components was also achieved (Figure 5.6). Interestingly, the 68K protein co-purifies in the first elution (SPE1, Lane 3) with a 14 kDa protein. Despite sharing a similar molecular weight to SmD proteins, the 14 kDa protein reacts poorly with the Sm sera used to immunoprobe the western blot. In contrast, the same sera reacts strongly with the "Sm" protein eluted at higher ionic strengths (SPE2, Lanes 4 and 5).

A combination of high Mg^{2+} and urea concentrations, and chromatographic separation on a CHT column followed by a SP-Sepharose column, have been effective in dissociating and partially separating the constituent proteins of bovine U1 snRNP.

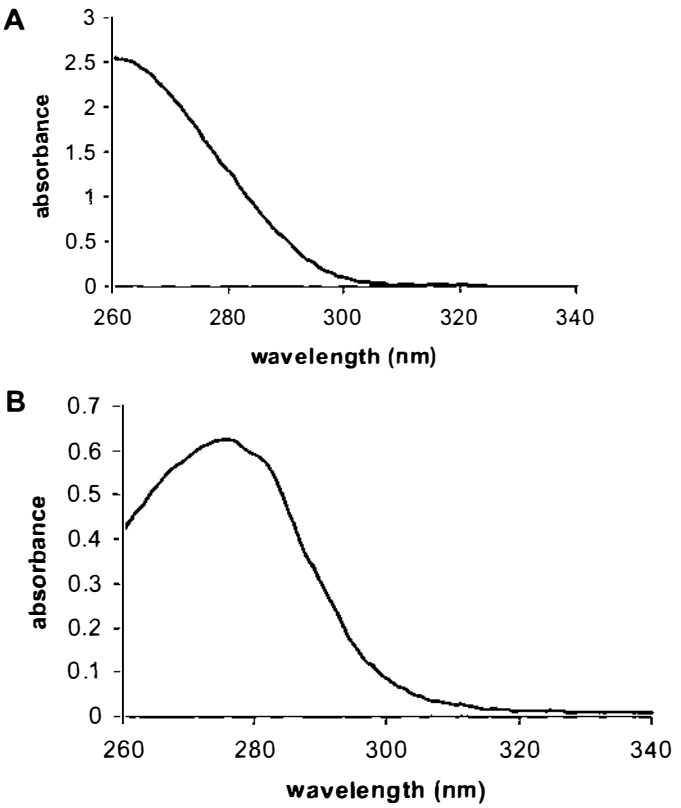

Figure 5.5 UV absorbance spectra of dissociated RNP on SP-Sepharose

Absorbance spectra were measured from 260 – 340 nm using the appropriate buffer as reference. **A.** spectrum of SP-Sepharose non-bound and **B.** SP-Sepharose 0.25 M KCl elution (SPE1).

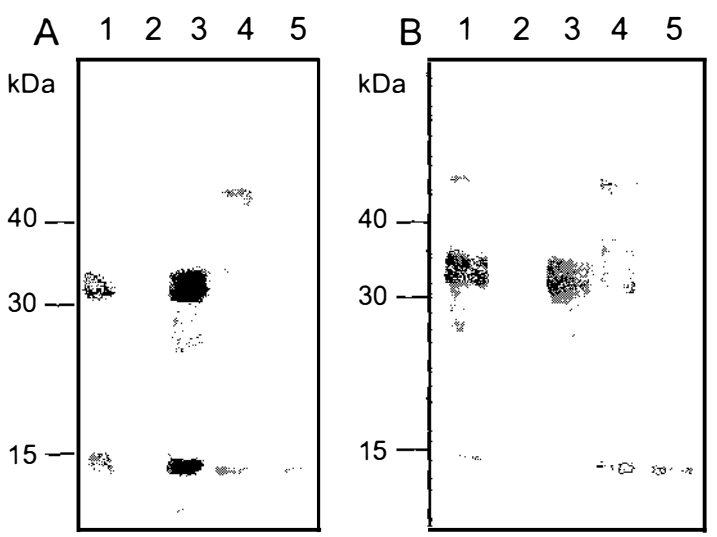

Figure 5.6 Separation of RNP proteins on SP-Sepharose

CHT 100 mM phosphate, 5 M urea elution was applied to a SP-Sepharose column equilibrated in 20 mM Tris pH 7.5, 6 M urea, 80 mM KCl and eluted step wise with increasing KCl concentrations. All fractions were analysed by SDS-PAGE. Proteins were visualised by **A.** Coomassie stain and **B.** Western blot immunoprobed with anti-Sm (+) human patient serum. Lanes: 1, SP-Sepharose load sample; 2, SP-Sepharose non-bound; 3, 0.25 M KCl; 4, 0.4 M KCl; 5, 1 M KCl.

5.3.2 U1A separation by serendipity

Determination of anti-68K antibody levels is a specific measure for MCTD. It is essential, therefore, that the 68K antigen used as a diagnostic antigen is highly purified and free of the less specific U1A. Unfortunately, bovine U1 snRNP U1A protein has a similar molecular weight to truncated 68K. A U1A specific sera was used to test for U1A in the purified 68K in SPE1 (Figure 5.7).

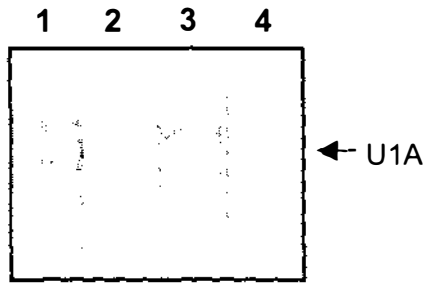

Figure 5.7 Loss of U1A from U1 snRNP as a consequence of dissociation

Intact bovine U1 snRNP (Lanes 1 and 2) and SPE1 fraction from the dissociation of U1 snRNP (Lanes 3 and 4) were Western blotted onto nitrocellulose and their reactivity with anti-RNP sera was tested. Lanes 1 and 3 were immunoprobed with a patient sera with both anti-68K and U1A specificities; Lanes 2 and 4 were immunoprobed with anti-68K (-)/anti-U1A (+) patient sera.

The 68K SPE1 fraction contains no detectable U1A by Western blotting, which implies that U1A has somehow been removed during the purification process. Testing each stage of the purification process revealed that most of the U1A protein appeared in the CHT non-bound fraction. This fraction was buffer exchanged into 20 mM Tris-HCl pH 7.5, 80 mM KCl, 10 mM $MgCl_2$ by diafiltration using regenerated cellulose ultrafiltration membrane with 30 K NMWCO mounted in a Sartocon slice assembly (Sartorius, Gottingen, Germany). The U1A containing fraction was then loaded onto a Q-Sepharose FF (20 mL packed bed) column, equilibrated in diafiltration buffer. The column was washed, and then eluted in one step with diafiltration buffer containing 0.5 M KCl (Figure 5.8). U1A is present in both non-bound and eluted fractions. The relative nucleic acid content of each fraction, however, is distinctly different. Non-bound U1A has a 260:280 ratio of 0.908, whereas, the Q-Sepharose elution has a 260:280 ratio of 2.046.

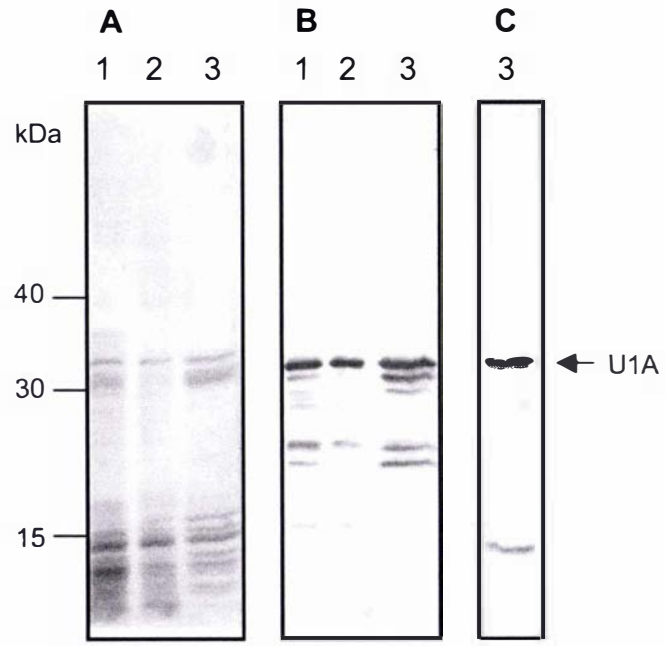

Figure 5.8 Separation of U1A populations on Q-Sepharose

Anti-RNP immunoaffinity elution containing 3.5 M $MgCl_2$ was fractionated on CHT. U1A-containing CHT non-bound was buffer exchanged and loaded onto a Q-Sepharose FF column. The column was eluted with equilibration buffer containing 0.5 M KCl. The fractions were analysed on SDS-PAGE and proteins were detected by **A**: Coomassie stain; **B**: Western blot and immunoprobed with anti-RNP (+) patient serum and **C**: Western blot and immunoprobed with anti-Sm (+) serum. Lanes: 1, CHT non-bound; 2, Q-Sepharose non-bound; 3, Q-Sepharose elution.

Protein eluted from the Q-Sepharose column was concentrated using a 30 kDa cut-off Vivaspin centrifugal ultrafiltration device and fractionated further by size exclusion chromatography on Sephacryl S200 equilibrated in tris buffered saline. Fractions were analysed by SDS-PAGE and western blot (Figure 5.9). U1A elutes between 0.37 and 0.44 of a column volume which corresponds to a molecular weight of 180 – 100 kDa according to a calibration performed using IgG, BSA, ovalbumin and chymotrypsinogen protein standards.

Fractions represented by Lanes 2-7 all contain nucleic acid as determined by UV absorbance spectra. Peaks of U1A and Sm reactivity with patient sera co-elute in nucleic acid containing fractions. However, peak U1A and Sm do not coincide with each other indicating that these proteins may not be part of the same complex and represent different populations. The other proteins observed

in Figure 5.9A are clearly not immunoreactive with the patient sera and are therefore impurities.

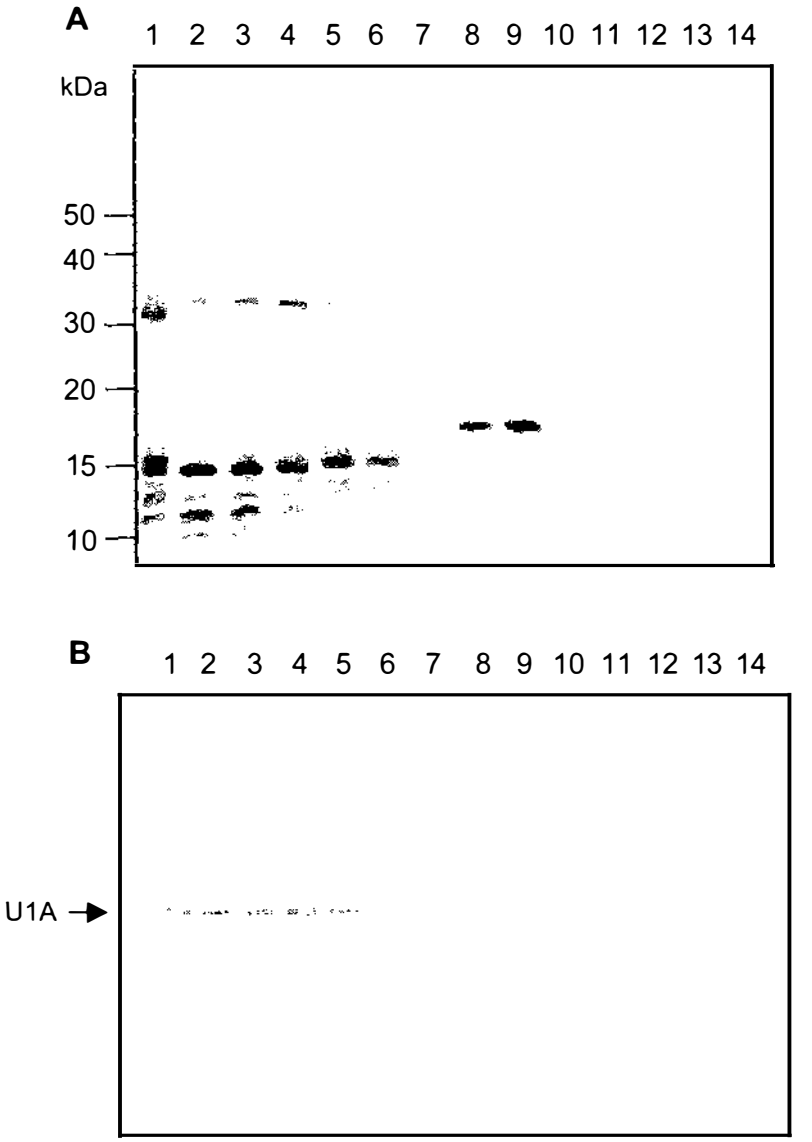

Figure 5.9 Separation of U1A on Sephacryl S200

Q-Sepharose elution containing U1A was concentrated and loaded onto an Sephacryl S200 size exclusion column and separated in Tris buffered saline pH 7.4. The fractions were analysed on SDS-PAGE. Proteins were visualised by **A**: Coomassie staining and **B**: Western blotting and immunoprobing with anti-Sm (+) patient serum. Lanes: 1, Q-Sepharose elution; 2-14, fractions collected from Sephacryl S200 column.

Bovine U1A protein was successfully removed from the U1 snRNP specific 68K protein by CHT chromatography. Two forms of U1A were isolated, one associated with an RNA moiety and the other RNA-free, which did not bind to an anion exchange matrix.

5.3.3 Removal of Sm proteins from U1 68K in SPE1

Complete removal of Sm protein is imperative for the use of 68K as a diagnostic reagent. Sm contamination in SPE1 was removed by size exclusion chromatography on Superdex 200. Fractions containing 68K were analysed by ELISA for anti-Sm reactivity in addition to SDS-PAGE and western blotting (Figure 5.10).

Fractions containing 68K free of Sm contamination eluted between 160 and 180 ml. These fractions were pooled and used to determine the diagnostic performance of the Sm-free 68K antigen.

The overall yield of 68K from an anti-RNP immunoaffinity elution is presented in Table 5.2. 68K was isolated to >90 % purity, in commercially viable quantities, using a combination of denaturing chromatographic techniques. CHT effected the removal of U1A, SP-Sepharose removed U1 snRNA and some SmD protein, and size exclusion chromatography separated 68K from the remaining Sm contaminants.

Table 5.2 Purification yields of Sm-free 68K protein

Purification Step	Total Protein		
	Concentration (mg/ml)	Amount (mg)	% recovery
Anti-RNP affinity elution	0.451	360.6	100
CHT Elution 1	1.025	73.8	20.5
SP Elution 1	0.561	32.0	8.9
Superdex 68K pool	0.400	8.2	2.3

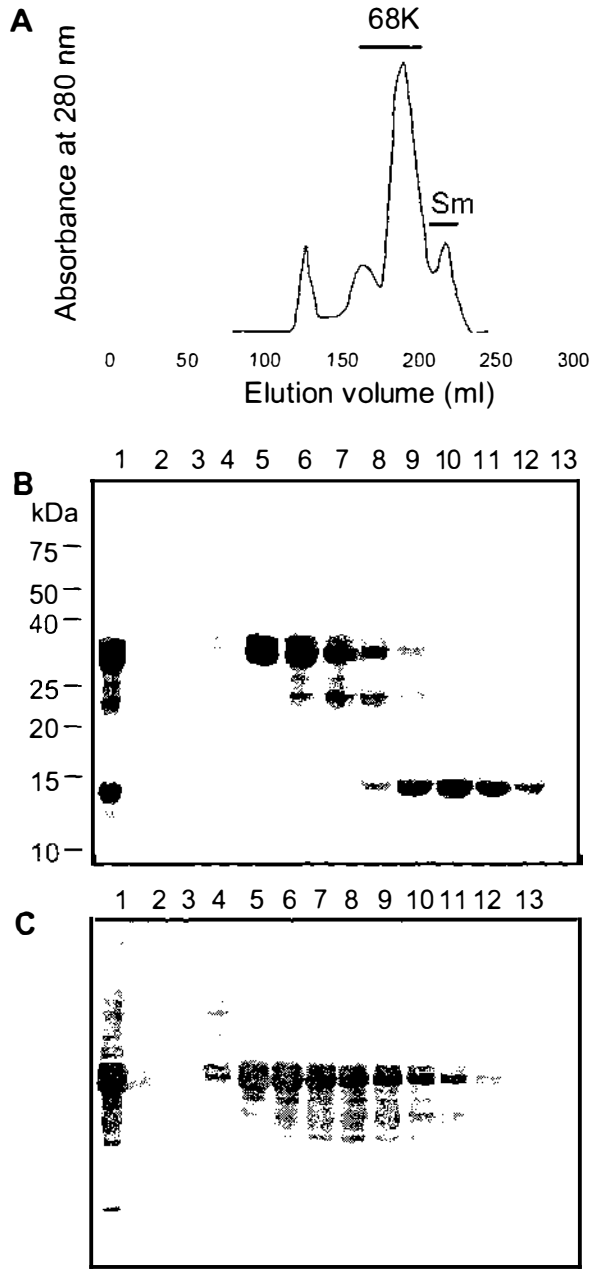

Figure 5.10 Separation of 68K from Sm by size exclusion chromatography

SP-Sepharose 0.25 M KCl elution was concentrated to approximately 5 ml and applied to a Superdex 200HR column equilibrated in 20 mM HEPES pH 7.5, 0.4 M NaCl, 4 M urea. The elution was monitored at 280 nm and 5 ml fractions were collected from 80 ml – 240 ml. **A**: 280 nm absorbance trace. The relative positions of 68K and Sm proteins are annotated as determined by: **B**: SDS-PAGE and Coomassie stain of column fractions; **C**: Western blot and immunoprobing with anti-Sm (+) patient serum. Lanes: 1, Superdex load sample; 2-13 fractions collected.

5.3.4 Separation of Sm proteins

Differences in recognition of the Sm-like proteins found in SPE1 and SPE2 may be due to the specificity of the patient sera used for immunoprobing (see section 5.3.1). Nitrocellulose strips of western blotted SPE1 and SPE2 were prepared and immunoprobed with a variety of Sm positive and RNP positive patient sera (Figure 5.11). Anti-Sm positive sera consistently recognised the Sm-like proteins in both SPE1 and SPE2 although the response was often greater with SPE2. Some anti-RNP positive sera have a low specificity for the Sm-like proteins in both SPE1 (Strip 7) and SPE2 (Strip 19).

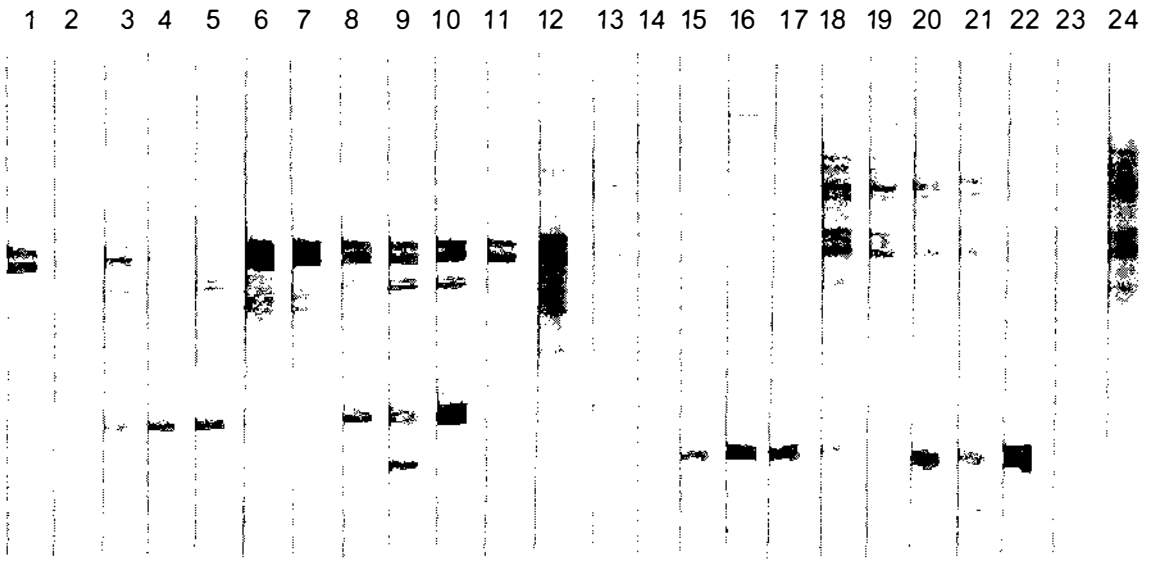

Figure 5.11 Reactivity of Sm-like proteins separated on SP-Sepharose

SPE1 and SPE2 were western blotted onto nitrocellulose and cut into strips corresponding to 1-12 and 13-24, respectively. Each set of strips were immunoprobed with the same array of patient sera ie. Strip 1 has the same sera as Strip 13 and so on. Sera used to immunoprobe Strips 1,2,7,11,12,13,14,19,23 and 24 are considered anti-RNP (+) and anti-Sm (-).

How these Sm-like proteins compared to Sm antigen was quantified by ELISA. First both SPE1 and SPE2 Sm proteins were purified by separating on a Superdex 200HR size exclusion chromatography column to remove the majority of the anti-RNP reacting proteins. The three antigens, Sm, SPE1 Sm and SPE2 Sm were coated on to Maxisorb (Nunc) microtitre plates at 0.1 μg per well overnight at 2-8 °C. An array of anti-Sm positive and anti-Sm positive patient sera were tested for their specificity to the three antigens. SPE1 and Sm (Panel

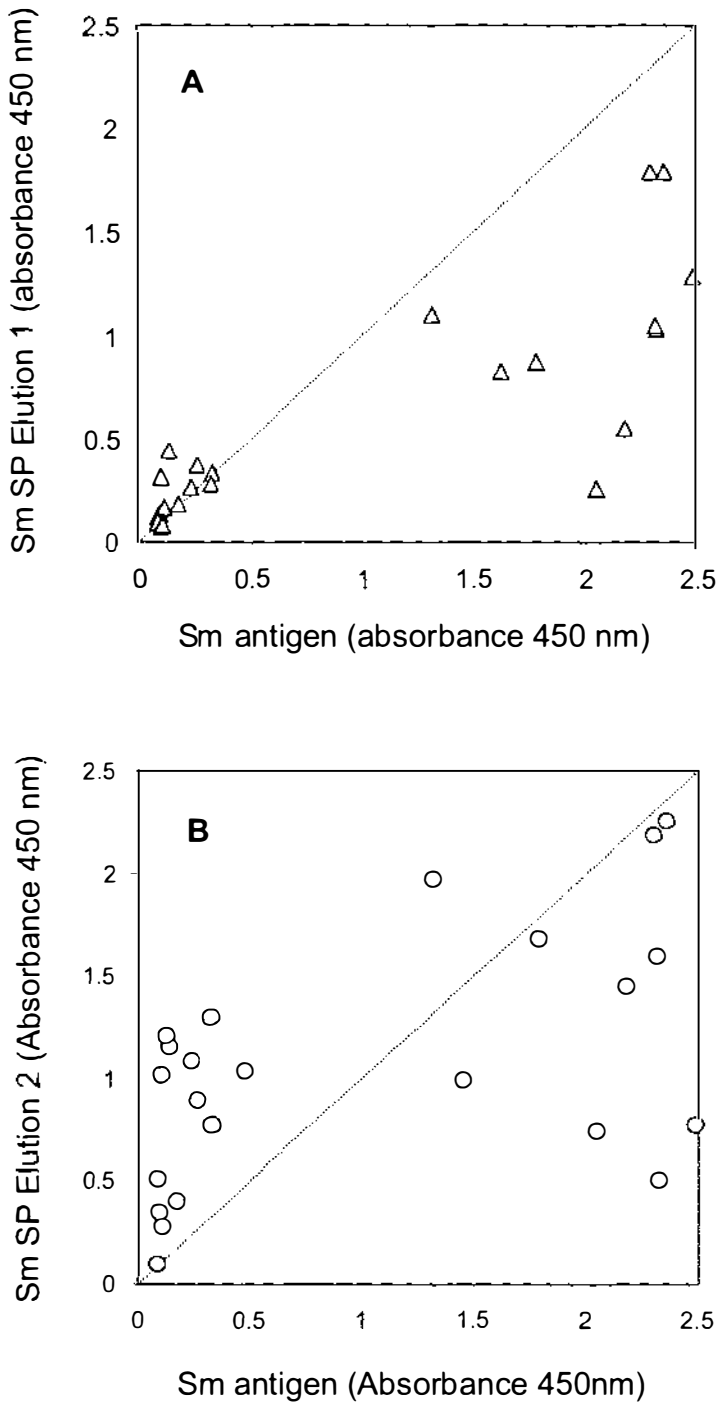

Figure 5.12 Correlation of patient sera cohort (n=26) reactivity with Sm antigen and the Sm-like proteins isolated from SPE1 and SPE2

Reactivities of purified Sm antigen (AroTec ATS02), SPE1 Sm and SPE2 Sm to a cohort of patient sera containing anti-RNP and/or anti-Sm antibodies were compared by ELISA. **A.** Sm vs. SPE1 Sm correlation; **B.** Sm vs. SPE2 Sm correlation. The dashed line corresponds to the ideal correlation.

A) and SPE2 and Sm (Panel B) correlated poorly in their response to patient sera (Figure 5.12), with the SPE2 Sm antigen correlating particularly poorly with the anti-RNP positive/anti-Sm negative sera indicating that it may still be contaminated with U1 snRNP specific proteins.

5.3.5 Identification of Sm proteins in SPE1 and SPE2

Coomassie stained bands of Sm-like proteins in SPE1, separated on Superdex 200HR (Figure 5.10B Lane 10), and SPE2 (Figure 5.6A Lane 4) were excised and subjected to in-gel digestion with trypsin. Masses of the resultant peptides were obtained by MALDI-TOF mass spectrometry and then analysed using MASCOT.

The Sm protein in the SPE1 Superdex fraction was identified as a mixture of SmD2 and SmD3 (Figure 5.13), while SPE2 contains SmD1 (Figure 5.14). Despite not all mass peaks being identified, sufficient peptide matches were obtained to confirm identity. Peptide coverage for each protein was greater than 30 %, and as expected, regions known to be post-translationally modified, such as the symmetrical dimethylated arginine (gly-arg-gly) sequences, were not matched.

SP-Sepharose chromatography, under denaturing conditions, facilitated the separation of SmD1 from SmD2 and SmD3 common core snRNP proteins. These proteins responded differently to anti-Sm patient sera in both western blot and ELISA immunoassays.

A

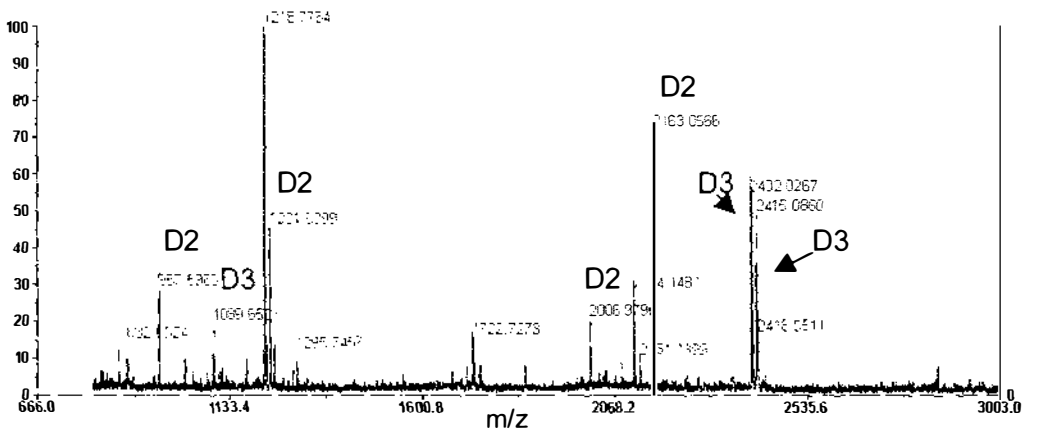

B

MSLLNKPKSEMTPEELQK**REEEEFNTGPLSVLTQSVKNNTQVLINCR**NNKKLLGRVKAFD
RHCNMVLENVKEMWTEVPKSGKGKKKSKPVNKDRYISKMFLR**GDSVIVVLR**NPLIAGK

Peptide	Observed	δ	Sequence
19 - 37	2163.0566	-0.0361	REEEEFNTGPLSVTQSVK
20 - 37	2006.9796	-0.0120	EEEEFNTGPLSVTQSVK
38 - 47	1231.6399	0.0187	NNTQVLINCR
103 - 111	957.5963	0.0236	GDSVIVVLR

C

MSIGVPIK**VLHEAEGHIVTCETNTGEVYR**GK**LIEAEDNMNCQMSNITVTYR**DGRVAQLEQ
VYIRGSKIR**FLILPDMLK**NAPMLKSMKNKNQGSGAGRGKAAILKAQVAARGRGRGMGRGNIFQ
KRR

Peptide	Observed	δ	Sequence
9 - 29	2414.0909	-0.0495	VLHEAEGHIVTCETNTGEVYR
32 - 51	2402.0267	-0.0517	LIEAEDNMNCQMSNITVTYR
70 - 78	1089.6501	0.0125	FLILPDMLK

Figure 5.13 Confirmation of Sm protein identities in SPE1

Coomassie stained Sm bands were excised from SDS-PAGE gel of SPE1 and subjected to trypsinolysis. **A**: Mass spectrum of peptides with Sm identities annotated.

B: peptide coverage and peak identities for SmD2. **C**: peptide coverage and peak identities for SmD3.

A

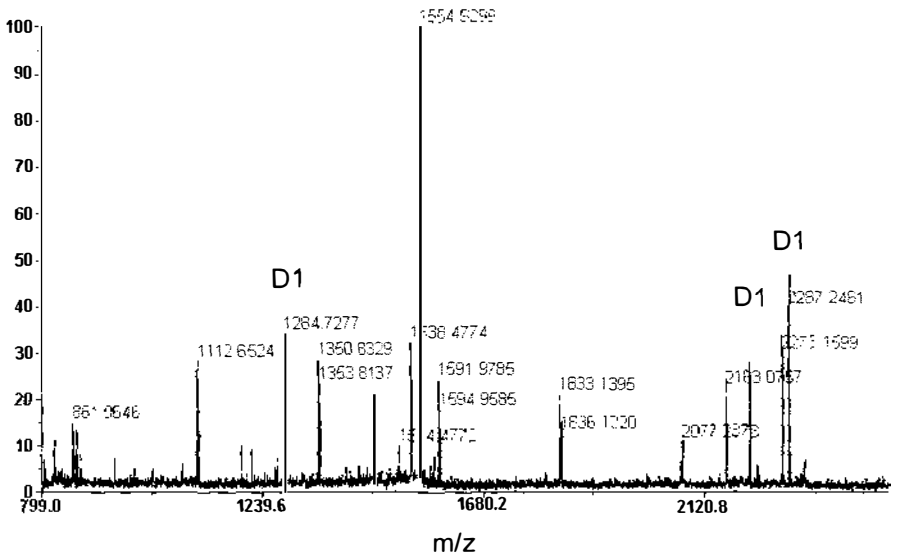

B

MKLVRFLMKLSHETVTIELK**NGTQVHGTITGVDVSMNTHLK**AVKMTLKNR**EPVQLETLSI**
RGNNIR**YFILPDSLPLDTLLVDVEPK**VKSKKREAVAGRGRGRGRGRGRGRGRGRGGPRR

Peptide	Observed mass	δ	Sequence
21 - 41	2209.1030	0.0001	NGTQVHGTITGVDVSMNTHLK
51 - 61	1284.7277	0.0119	EPVQLETLSIR
67 - 86	2287.2461	-0.0010	YFILPDSLPLDTLLVDVEPK

Figure 5.14 Confirmation of Sm protein identity in SPE2

Coomassie stained Sm bands were excised from SDS-PAGE gel of SPE2 and subjected to trypsinolysis. **A**: Mass spectrum of peptides with Sm identities annotated. **B**: peptide coverage and peak identities for SmD1.

5.3.6 The influence of urea concentration on U1 snRNP dissociation

CHT chromatography of the anti-RNP immunoaffinity 3.5 M $MgCl_2$ elution and subsequent elution with 80 mM phosphate buffer containing 5 M urea is effective in almost completely dissociating the U1 snRNP complex into its constituent proteins. To examine the effect of the denaturant urea on the

stability of the U1 snRNP complex more closely, batch wise elution from hydroxyapatite (HT) was carried out in urea concentrations ranging from 0 – 7 M with 18 increments. Each elution was then buffer exchanged into 20 mM Tris-HCl pH 7.5, 0.08 M KCl containing the same urea concentration as used to elute the protein from HT. The dissociation of U1 snRNP was then determined by measuring the amount of protein eluted from SP-Sepharose with 20 mM Tris-HCl pH 7.5, 0.5 M KCl containing the relevant urea concentrations.

The protein in each SP-Sepharose elution was assumed to be dissociated from U1 snRNA. The dissociated protein concentrations were thus plotted against urea concentration to obtain a curve similar to that observed for the determination of protein conformational stability (Figure 5.15) (Pace e*t al.*, 1990; Gupta and Ahmad, 1999b). Curves were analysed using the same strategies as those used for protein stability measurements.

Assuming an equilibrium exists between undissociated and dissociated U1 snRNP, this equilibrium can be expressed as a constant K using equation 5.1.

$$\text{Equilibrium constant (K)} = (y_u - y)/(y - y_d) \qquad \textbf{5.1}$$

Where y = measured parameter i.e. total protein at a given urea concentration; y_u = amount of undissociated U1 snRNP; y_d = amount of dissociated U1 snRNP.

Values for undissociated and dissociated U1 snRNP were calculated by extrapolating the pre-transition (y_u) and post-transition (y_d) regions of the curve (Figure 5.15). K was then calculated for a given urea concentration within the transition region and related to Gibb's free energy change using equation 5.2.

$$\Delta G = -RT \ln K \qquad \textbf{5.2}$$

Where ΔG = change in Gibb's free energy; R = gas constant (1.987 cal/degree/mol); T = temperature (Kelvin) i.e. 0 °C = 273.2 K; K = Equilibrium constant calculated using equation 5.1.

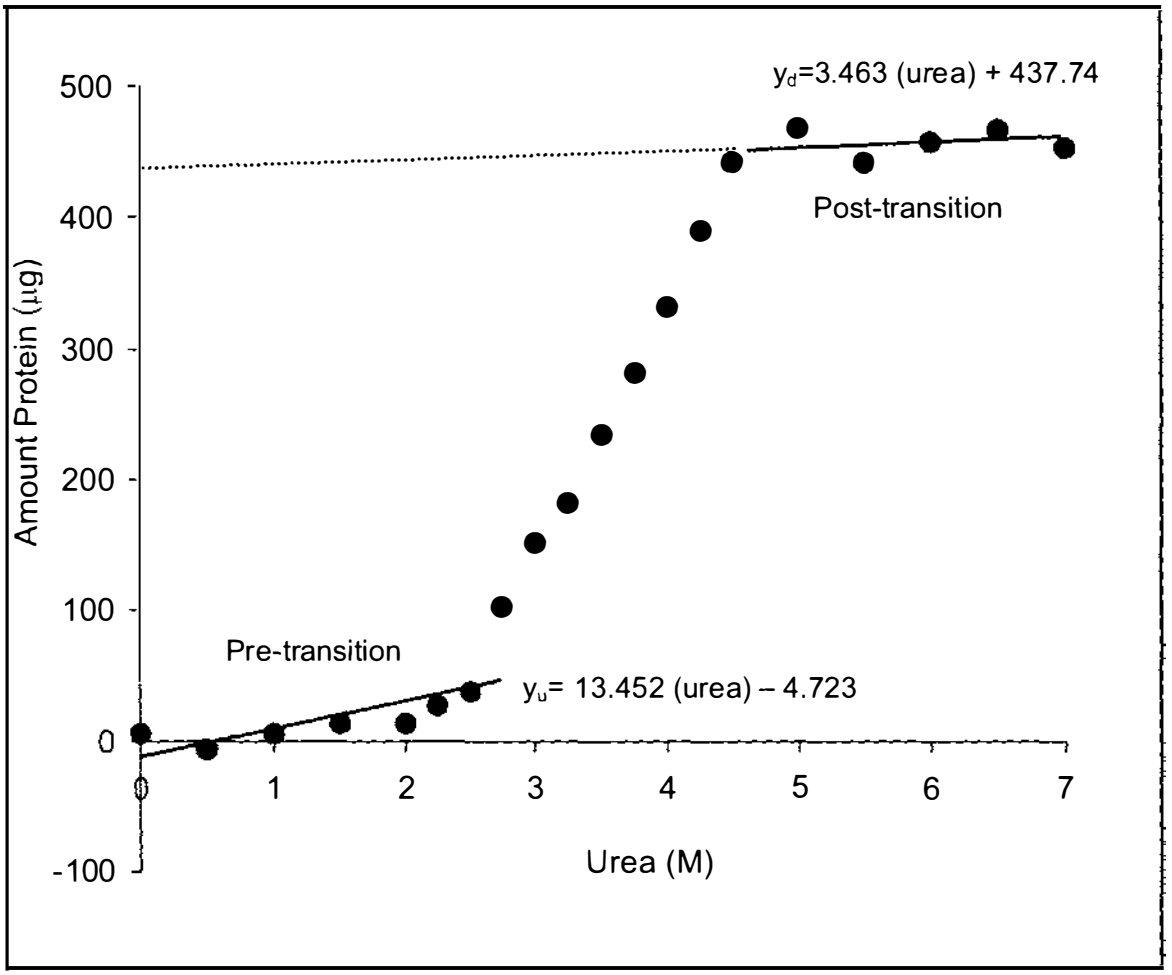

Figure 5.15 Urea induced dissociation curve for bovine U1 snRNP

Anti-RNP immunoaffinity elution containing 3.5 M $MgCl_2$ was applied batch-wise to HT and then the RNP eluted with 0.25 M phosphate buffer containing increments of urea from 0-7 M. The elutions were buffer exchanged into 20 mM Tris-HCl pH 7.5, 80 mM KCl containing the same urea concentration and applied to a SP-Sepharose column. After elution with buffer containing 0.5 M KCl and increments of urea, protein content was determined and the amount plotted against urea concentration. Linear regression is applied to the pre-transition and post-transition regions of the curve to calculate y_u (undissociated) and y_d (dissociated) values, respectively. The closed circles represent the mean of three replicate experiments.

The results are displayed in Table 5.3.

ΔG was plotted against urea concentration to estimate the stability of U1 snRNP as an anti-RNP affinity elution in the absence of urea, ΔG (H_2O) (Figure 5.16).

Table 5.3 Analysis of transition region from the U1 snRNP urea dissociation curve

Urea (M)	Y	K	Δ G (cal/mol)
2.75	102.352	0.203	884.095
3.00	151.175	0.389	523.673
3.25	182.131	0.536	345.595
3.50	233.720	0.885	67.5550
3.75	280.857	1.384	-180.373
4.00	331.859	2.361	-476.756
4.25	389.475	5.351	-930.506

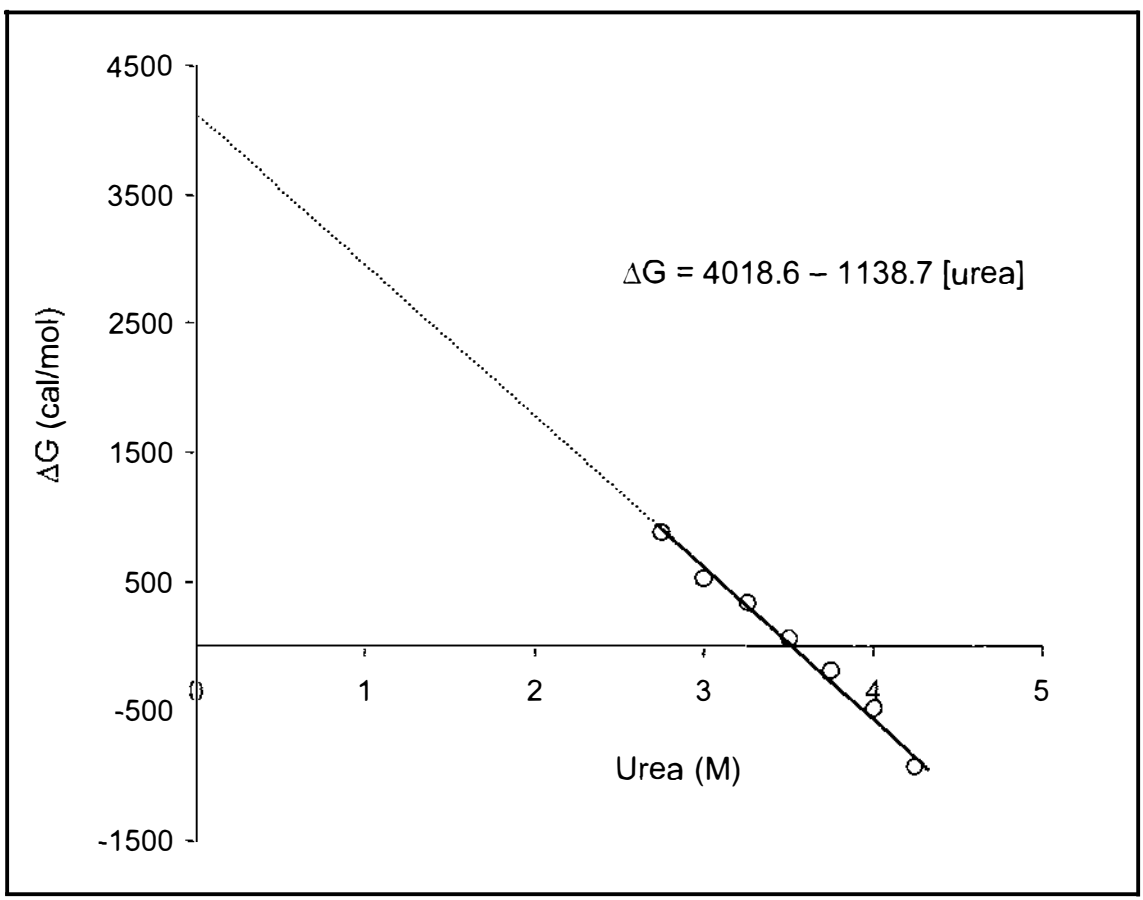

Figure 5.16 Relationship between ΔG and U1 snRNP dissociation as a function of urea concentration

The open circles show the observed ΔG calculated using equation 5.2 and presented in Table 5.3. The dotted line shows the linear extrapolation from the data for which the linear regression equation is displayed.

Assuming that the relationship between ΔG and urea concentration remains linear, ΔG can be extrapolated to 0 M urea by linear regression using equation 5.3.

$$\Delta G = \Delta G\ (H_2O) - m\ [urea] \qquad \textbf{5.3}$$

Where ΔG = change in Gibb's free energy; $\Delta G(H_2O)$ = Gibb's free energy in the absence of denaturant; m = linear regression gradient (ΔG/[urea]); [urea] = urea concentration.

According to Figure 5.16, the estimated $\Delta G(H_2O)$ is 4.019 kcal/mol and m is 1.139 kcal/mol/M. The concentration of urea giving half dissociation of anti-RNP affinity elution $[urea]_{1/2}$ is calculated by $\Delta G(H_2O)/m$, therefore, $[urea]_{1/2}$ is 3.5 M.

5.3.7 The influence of $MgCl_2$ concentration on U1 snRNP dissociation

To determine the influence of high $MgCl_2$ concentration on the dissociation of U1 snRNP, an anti-RNP immunoaffinity elution was dialysed into 20 mM Tris-HCl pH 7.5, 0.4 M KCl, 10 mM $MgCl_2$. Experiments described in the section above were then repeated using the dialysed, low $MgCl_2$ concentration, U1 snRNP as the sample. Briefly, dialysed U1 snRNP was mixed batch-wise with HT equilibrated in the dialysis buffer, and eluted with a series of 0.25 M phosphate buffers containing urea increments. The elutions were buffer exchanged and then applied to a SP-Sepharose column. Eluted protein amount was determined and plotted against urea concentration (Figure 5.17).

The $MgCl_2$ concentration of the sample applied to HT has a significant influence on the ability of urea to dissociate the U1 snRNP complex. Very little dissociation of the U1 snRNP was achieved using an immunoaffinity elution dialysed into a low $MgCl_2$ concentration buffer. Elution of HT and SP-Sepharose column with buffer containing 7 M urea only gave 30 % of the expected snRNP protein concentration. Ideally, dissociation curves should be used only if the dissociation is complete. This data was not processed further.

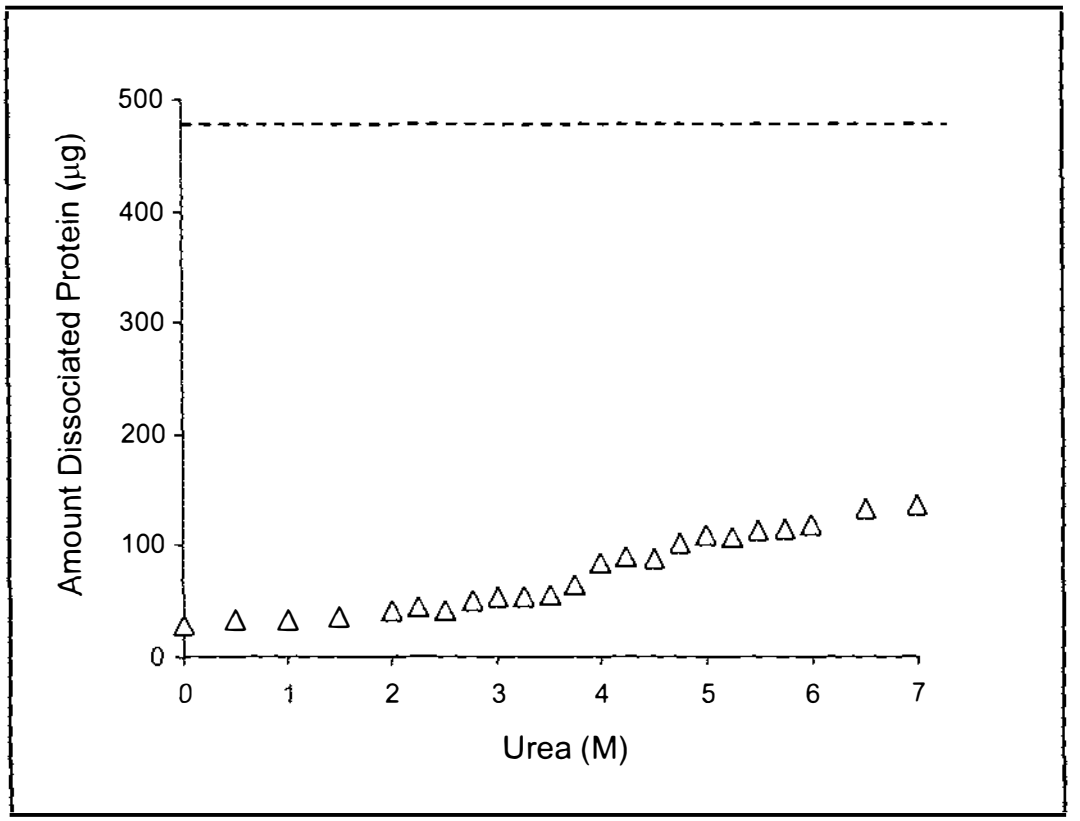

Figure 5.17 Influence of urea concentration on Q-Sepharose purified U1 snRNP

U1 snRNP was dialysed into low $MgCl_2$ containing buffer, applied to CHT and eluted with 0.25 M phosphate buffer containing incremental urea concentration. After buffer exchange into 20 mM Tris-HCl pH 7.5, 80 mM KCl containing various urea concentrations, the samples were applied to SP-Sepharose. The eluted protein was determined and plotted against urea concentration. The open triangles represent the mean of three experimental replicates. The dotted line represents the protein concentration expected for dissociated U1 snRNP.

Bovine U1 snRNP was not dissociated into its constituent proteins and nucleic acid soley with high urea concentration. Dissociation occurred in two stages, high $MgCl_2$ was required to destabilise the U1 snRNP complex, and then urea was able to effect dissociation. When bovine U1 snRNP was first destabilised in buffer containing 3.5 M $MgCl_2$ at 2-8 °C, 3.5 M urea was calculated as the amount required to half dissociate U1 snRNP.

5.3.8 Effect of removing denaturant from purified bovine 68K protein

Urea is clearly necessary to promote dissociation of the U1 snRNP complex and to facilitate the purification of the 68K protein. However, it is possible that

the major conformational epitope within 68K may be affected by the presence of any denaturant (Welin-Henriksson *et al.*, 1999). Native conformation is more likely to be adopted in a non-denaturing buffer. The effect of buffer exchanging 68K protein into buffers containing decreasing urea concentrations was examined (Figure 5.18).

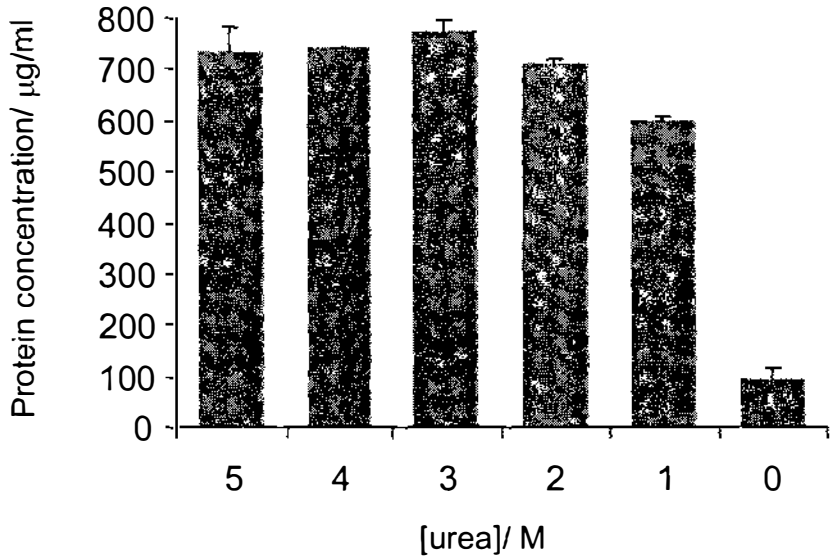

Figure 5.18 The effect of removing urea from purified bovine 68K

Purified 68K formulated in 20 mM HEPES pH 7.5, 0.4 M NaCl, 6 M urea was dialysed against the same buffer containing decreasing urea concentrations for 20 hours. The bar chart represents the protein concentration measured after dialysis against the urea concentration. The experiment was performed in duplicate and the standard error is shown.

There is a significant drop in 68K concentration when it is dialysed into a buffer containing no urea. The native structure of 68K was not restored simply by removing the denaturant, urea.

5.3.9 The use of RNAse to dissociate U1 snRNP

Human U1 snRNP has been successfully dissociated using ribonuclease digestion (Achsel *et al.*, 1999). This strategy was trialled as a method to dissociate bovine U1 snRNP instead of using a denaturant such as urea. The aim was to produce 68K antigen in its native form. Ribonuclease T1 was added to purified U1 snRNP and incubated at 37 °C for 1 hour. The RNP component proteins bound to the SP-Sepharose, but when eluted they still contained high

levels of nucleic acid as determined by UV absorbance (Figure 5.19). The A260:A280 ratio is 1.52 which is consistent with nucleic acid being present, although the ratio was lower than that for U1 snRNP prior to ribonuclease treatment.

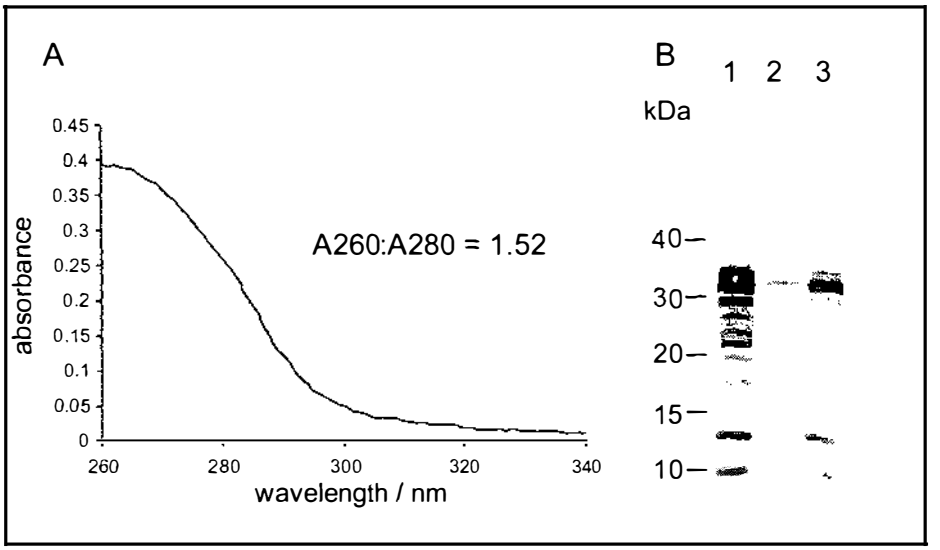

Figure 5.19 Ribonuclease induced U1 snRNP dissociation

Bovine U1 snRNP was incubated with 700 units of Ribonuclease T1 for 1 hour at 37 °C before being applied to a SP-Sepharose column. Bound material was eluted with 20 mM Tris-HCl pH 7.5, 1 M KCl. **A**: Absorbance spectrum of the eluted material. **B**: Western blot analysis on SDS-PAGE of SP-Sepharose fractions probed with anti-Sm (+) patient serum. Lanes: 1, ribonuclease treated U1 snRNP; 2, SP-Sepharose non-bound; 3, SP-Sepharose elution.

The SP-Sepharose elution was concentrated and applied to a Superdex 200HR size exclusion column. SDS-PAGE analysis showed that there was no separation of the 68K and Sm components. Therefore, this approach to dissociating bovine U1 snRNP was therefore abandoned without further investigation.

5.3.10 Purified bovine 68K versus recombinant 68K (r68K) in ELISA

To compete as a commercial reagent for diagnosis of autoimmune diseases, purified bovine 68K must compare favourably with recombinant antigens that are currently available. Microplate ELISA is the most common format used in diagnostic testing. To determine the optimal antigen concentration to coat

ELISA plates for antigen comparisons, purified 68K was titrated against bovine U1 snRNP using standard anti-RNP and anti-Sm sera (Figure 5.20).

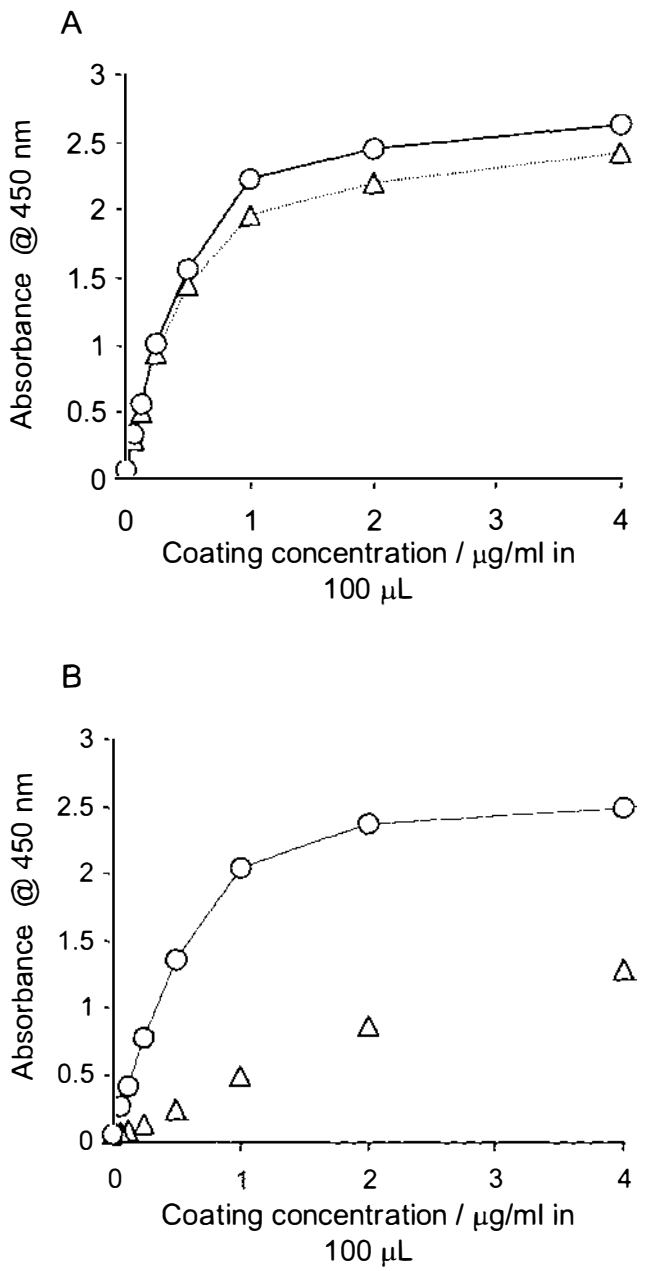

Figure 5.20 Optimal purified 68K coating concentration in ELISA

Bovine U1 snRNP (open circles) and purified 68K (open triangles) were titrated by serially diluting into microtitre plates. Each titration was incubated with either **A**: standard anti-RNP (+) serum diluted 1:100; or **B**: standard anti-Sm (+) serum diluted 1:100.

The 68K antigen titrated well with anti-RNP sera and produced the optimal response difference with anti-Sm sera at 0.1 μg per well coating. This coating amount was used for all subsequent experiments.

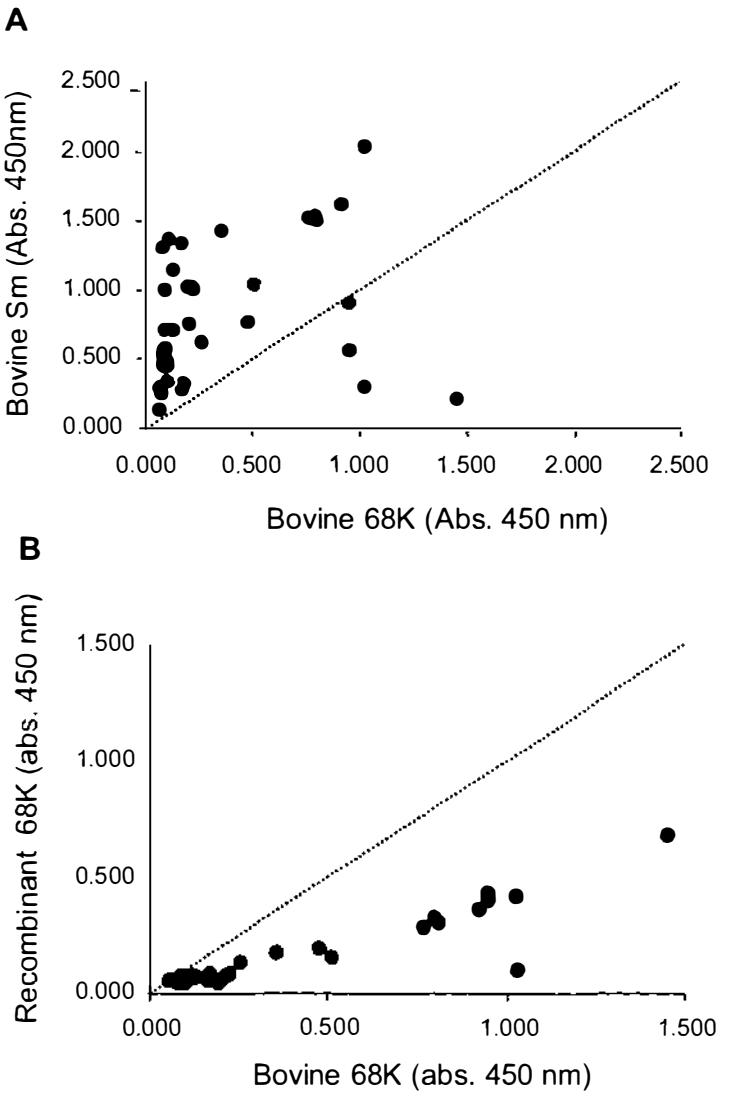

Figure 5.21 Reactivity of anti-Sm sera with bovine and recombinant 68K

Purified bovine 68K, r68K and bovine Sm antigens were coated onto ELISA plates at equal concentrations then probed with a cohort of anti-Sm (+) patient sera (n=39). **A**: Purified 68K correlated with bovine Sm. **B**: Purified 68K correlated with r68K. The dashed line represents a perfect correlation between data.

A cohort of anti-RNP and anti-Sm patient sera were then tested by ELISA for reactivity with bovine U1 snRNP, bovine Sm, recombinant U1A, recombinant 68K, recombinant U1C and purified bovine 68K. Correlation of Sm against the 68K protein was obtained by plotting their respective reactivity data. Figure 5.21

presents two graphs: one correlates the responses of bovine 68K with Sm antigen to verify the removal of Sm from the purified 68K, and the other illustrates how bovine 68K and the r68K respond to anti-Sm sera.

In general, anti-Sm sera reacted poorly with purified bovine 68K antigen indicating that the purified 68K antigen was substantially Sm-free (Figure 5.21A). However, anti-Sm sera are often polyspecific, that is, in addition to anti-Sm antibodies they may contain autoantibodies to multiple antigens including U1 snRNP constituent proteins. Some of the anti-Sm sera tested were reactive with 68K antigen. Responses of these polyspecific anti-Sm positive patient sera with bovine 68K and r68K correlated well, although, the autoantibody recognition of the recombinant antigen is generally lower than the purified antigen (Figure 5.21B).

Reactivities of purified bovine 68K and r68K were compared by screening with 48 anti-RNP patient sera (Figure 5.22). Responses to bovine 68K and r68K correlated very well, although, the sera responded better to bovine 68K as indicated by the response variation from the dashed line. There was an almost perfect agreement of the bovine U1 snRNP and the purified 68K protein with sera responding to 68K antigen, however, it is clear that some anti-RNP sera may be reacting strongly to other U1 snRNP components.

The responses of 68K and recombinant U1A and U1C antigens to anti-RNP sera were correlated (Figure 5.23). There was some correlation in the responses of some anti-RNP sera to U1A and 68K. However, no clear relationship between 68K and U1C response was established.

In summary, 68K was successfully purified from anti-RNP immunoaffinity elutions. The purification process was dependent on both high $MgCl_2$ and urea concentration for effective depletion of U1A, SmD and U1 snRNA. Purified 68K was demonstrated to be free from contaminating U1A and SmD proteins by western blot and ELISA immunoassay. The purified antigen was superior to r68K in its responses to both anti-Sm and anti-RNP patient sera.

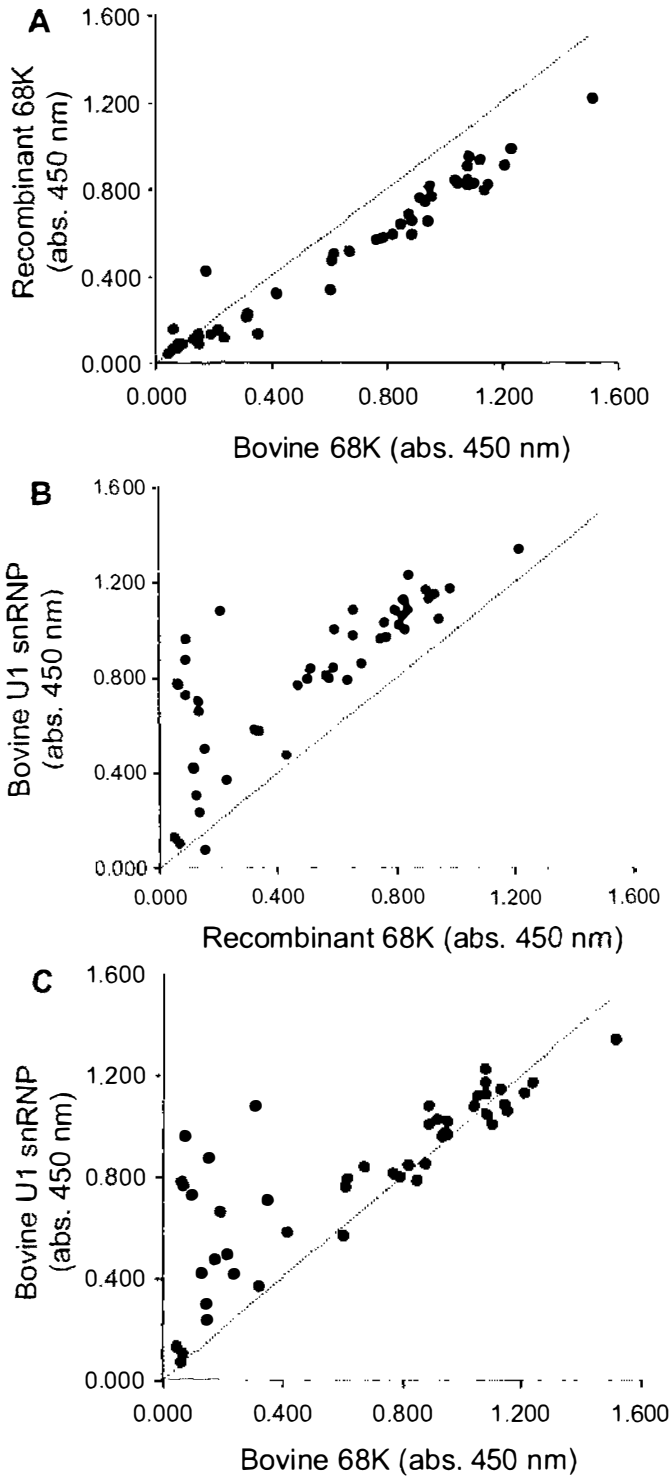

Figure 5.22 Reactivity of anti-RNP sera with bovine and recombinant 68K

Purified bovine 68K, U1 snRNP and r68K were coated onto ELISA plates at equal concentration and probed with a cohort of anti-RNP patient sera (n=48). **A**: Purified 68K correlated with r68K. **B**: r68K correlated with intact bovine U1 snRNP. **C**: Purified 68K correlated with bovine U1 snRNP. The dashed line represents a perfect correlation between data.

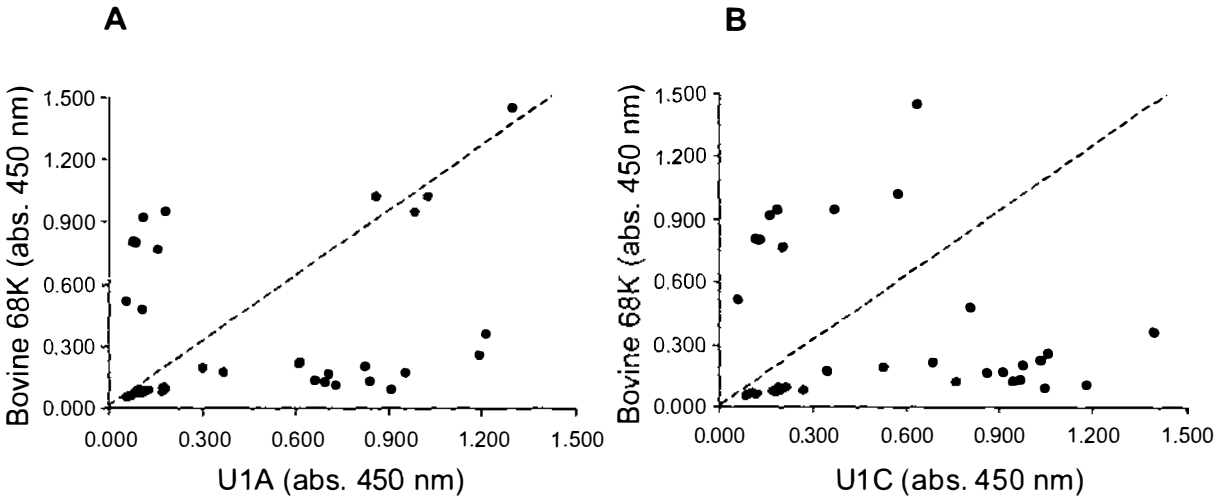

Figure 5.23 Relationship between purified 68K and the U1A/U1C snRNP components

Purified bovine 68K and recombinant U1A and U1C were coated onto ELISA plates at equal concentration and probed with a cohort of anti-RNP patient sera (n=48). **A**: Purified 68K correlated with recombinant U1A. **B**: Purified 68K correlated with recombinant U1C.

5.4 Discussion and Future Work

Bovine U1 snRNP constituent proteins were successfully dissociated from U1 snRNA and the individual proteins were purified as illustrated in Figure 5.24. Purified 68K protein was shown to contain no SmD protein, and was used to determine the titre of anti-68K antibodies in patient sera.

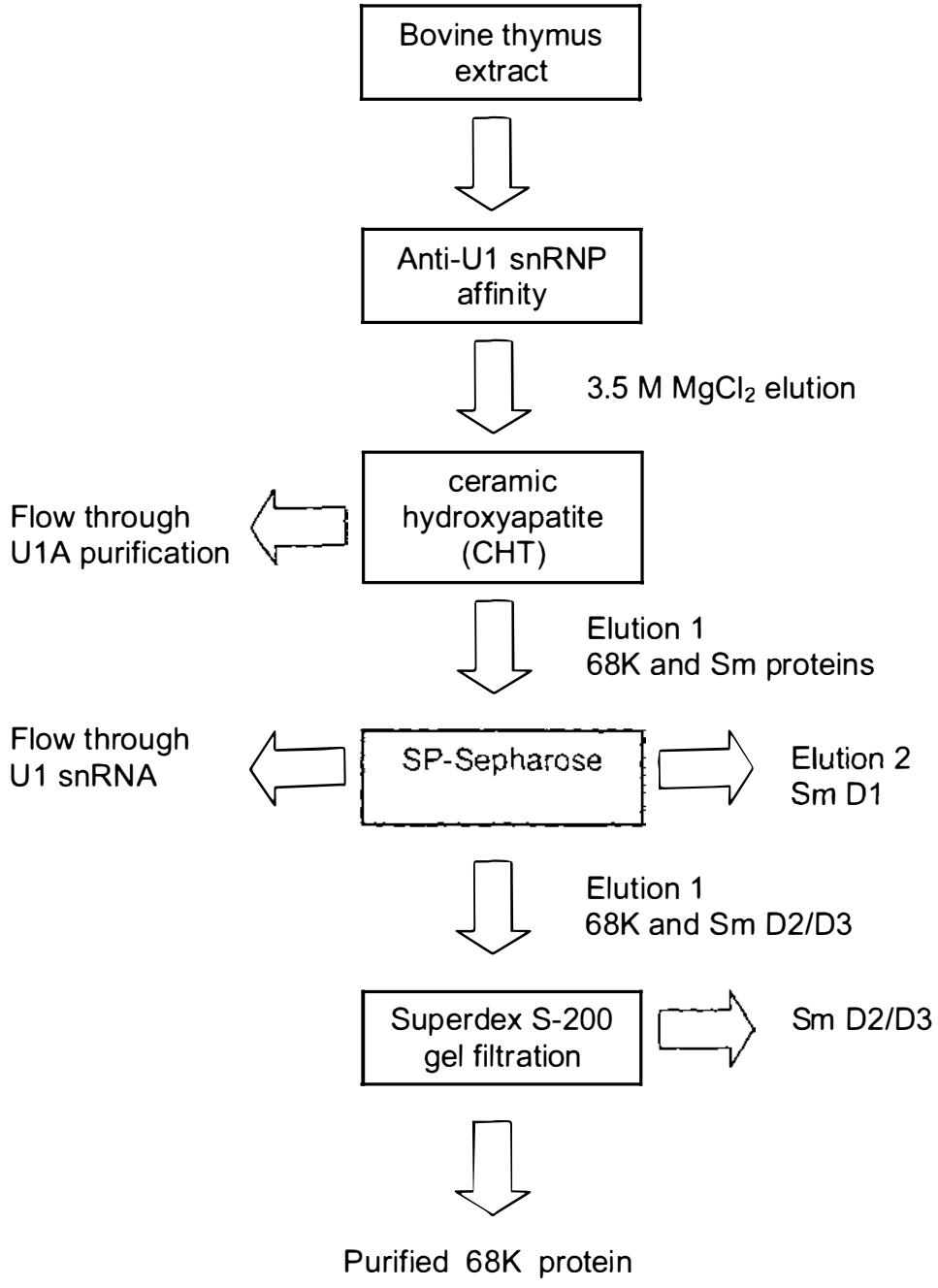

Figure 5.24 Flow diagram for the purification of bovine 68K protein

5.4.1 CHT facilitates U1 snRNP dissociation

Ceramic hydroxyapatite was proven to be an effective media for separating and purifying components of U1 snRNP. The unique ability of the media to bind protein in high ionic strength buffer facilitated the destabilisation of U1 snRNP and its subsequent dissociation in 5 M urea.

The capacity of CHT to bind U1 snRNP under these conditions is surprising. CHT works by mixed mode absorption, that is, it contains both anion and cation exchange modalities. Both high ionic concentrations and as little as 3 mM $MgCl_2$ have been used to elute proteins bound to CHT (Gorbunoff, 1984a; Borsi *et al.*, 1986). In general, basic proteins are more likely to elute with low levels of $MgCl_2$, whereas, acidic proteins can withstand high levels such as 3.5 M $MgCl_2$ (Gorbunoff and Timasheff, 1984b). Given that all U1 snRNP component proteins are highly basic, with the exception of SmF, an alternative binding mechanism probably accounts for U1 snRNP binding. CHT is used routinely to purify nucleic acids because they are able to bind to the matrix under a variety of conditions (Bernardi, 1971; Martinson, 1973). It is conceivable that U1 snRNP binds to CHT under high ionic strength by virtue of the ribonucleic acid, implying that U1 snRNP is intact in 3.5 M $MgCl_2$ during application to CHT. This theory is complicated by the inability of U1A, and a putative SmD protein, to bind to CHT under high $MgCl_2$ concentration.

5.4.2 U1A binding with U1 snRNP is disrupted in 3.5 M $MgCl_2$

Both U1A and 68K are reported to have very high affinities for the U1 snRNA moeity, with an equilibrium dissociation constant (K_D) $\approx 10^{-9}$ M (Bach *et al.*, 1990; Lutz-Freyermuth *et al.*, 1990). Despite the high affinity, Bach *et al.* (1990) depleted U1A from U1 snRNP using anion exchange chromatography at a temperature of 37 °C leaving 68K and Sm proteins still attached to the RNA. This result is consistent with the observations in this study in the presence of 3.5 M $MgCl_2$.

U1A interaction with U1 snRNA through a RNA recognition motif (RRM) has been used as a model for high affinity protein:RNA interactions and is well

characterised. RNA binding is thought to occur via an induced fit mechanism which relies on the inherent flexibility of the U1A RRM (Williamson, 2000; Showalter and Hall, 2003). The N-terminal RRM domain and the U1 snRNA hairpin II structure are shown in Figure 5.25. Association and stabilisation of U1A with the U1 snRNA hairpin II structure occurs in two independent steps. Electrostatic interactions favour U1A association, and hydrogen bonding or stacking interactions are important for complex stability (Katsamba *et al.*, 2001). More recently, specific electrostatic interactions were shown to play a role in U1A: RNA complex stability (Law *et al.*, 2006). Disruption of electrostatic interaction and hydrogen bonding by $MgCl_2$ may be responsible for the specific dissociation of U1A.

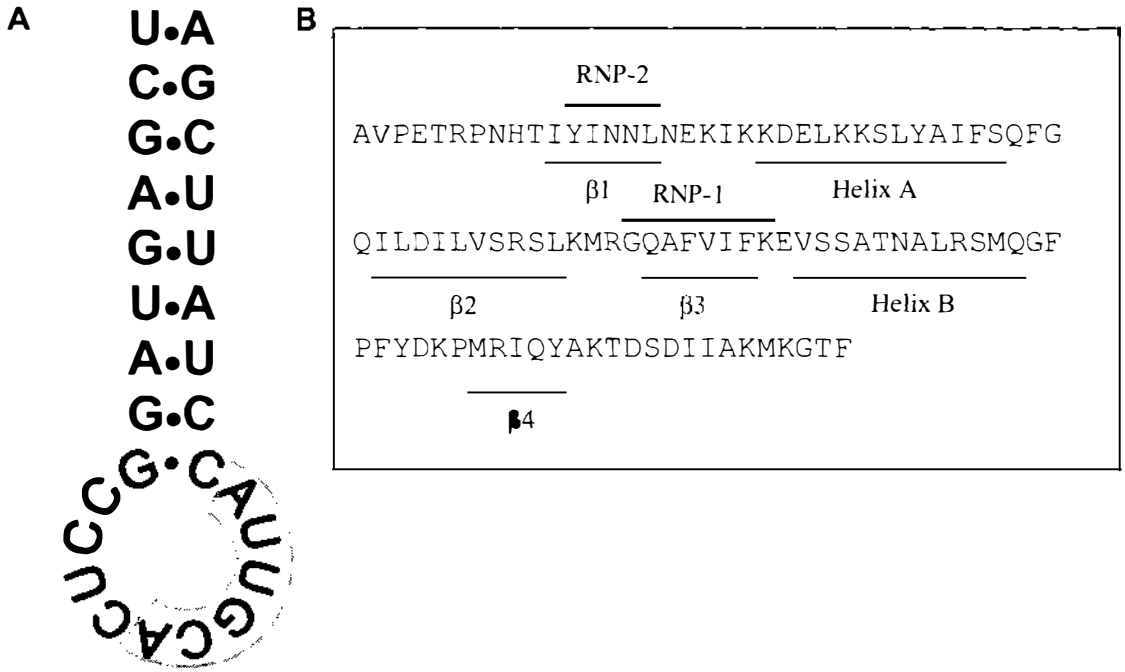

Figure 5.25 U1 snRNA hairpin II interaction with U1A

U1A interacts with the U1 snRNA hairpin II structure via its N-terminal RNA recognition motif (Adapted from Law *et al.*, 2006). **A**: U1 snRNA hairpin II structure. Nucleotides interacting with U1A are boxed. **B**: N-terminus of U1A 1-101. Structural features and RNA recognition sequences are underlined and overlined respectively.

Disrupting the secondary structure of the hairpin II, with high $MgCl_2$ concentration for example, may result in dissociation of U1A. Retention of the hairpin II structure is critical for U1A binding affinity. Two forms of U1 snRNA (U1a and U1b) are found in mouse and have slightly different hairpin II structures.

Consequently their affinities for U1A are significantly different (Bach *et al.*, 1990).

Bovine U1A in the CHT non-bound appears to exist in two populations, one associated with RNA and the other RNA-free. Attempts were made to determine the type of RNA that U1A was associated with, and although the results were not conclusive, it seemed likely that U1A was associated with U1 snRNA. It is not clear whether U1A and U1 snRNA are actually associated in the 3.5 M $MgCl_2$ buffer or whether they become associated upon buffer exchange into low ionic strength buffer. This could be clarified by separating the CHT non-bound components using size exclusion chromatography with buffer containing 3.5 M $MgCl_2$.

Sm protein that appeared in the CHT non-bound fraction is also associated with a U1-like RNA. This Sm protein is not necessarily associated on the same RNA moiety as U1A. Size exclusion experiments demonstrated that peak quantities of U1A and Sm did not co-elute and, therefore, these protein/RNA complexes may exist in distinct populations.

According to estimates by O'Connor *et al.* (1997), as much as 3 % of the total cellular U1A protein is present as U1 snRNP-free U1A (SF-A). SF-A forms part of a complex with a number of proteins which are involved in splicing and polyadenylation reactions (Lutz *et al.*, 1996; Lutz *et al.*, 1998; Liang and Lutz, 2006). U1A that is non-RNA associated may belong in this category and is worthy of further investigation. A range of proteins were found in the CHT non-bound fraction, so western blotting with antibodies specific to SF-A complex proteins would clarify whether U1A protein has simply dissociated from U1 snRNP or is a legitimate part of the SF-A complex.

The amounts of 68K and U1A proteins in bovine U1 snRNP deviate from the expected 1:1 stoichiometry (Hochleitner *et al.*, 2005). A greater amount of 68K than U1A was recovered during the dissociation of U1 snRNP. Modification of the U1 snRNP constituent proteins during cell death contributes to the disparity

in stoichiometry as evidenced by the absence of U1C. There have been no reports of cell death, by either apoptosis or necrosis, affecting the integrity of U1A, and hence disturbing U1 snRNP stoichiometry.

5.4.3 Bovine U1 snRNP is destabilised by the loss of U1A

Fractionation of U1A from U1 snRNP during CHT chromatography in high $MgCl_2$ concentration may contribute to the destabilisation of the remaining U1 snRNP complex. Elution of U1 snRNP from CHT in the presence of 5 M urea was sufficient to dissociate the complex. However, when dialysed into low ionic strength buffer and applied to CHT, U1 snRNP obtained by anti-RNP immunoaffinity chromatography did not dissociate, resulting in no loss of U1A from the complex. Adding urea to the CHT elution buffers in this case was also not sufficient to dissociate the U1 snRNP complex.

It is proposed that high $MgCl_2$ destabilises the U1 snRNP complex (Satoh e*t al.*, 1994), resulting in the dissociation of U1A protein from the complex with the concomitant reduction in the affinities of the 68K and Sm proteins for U1 snRNA. As a consequence, the Gibb's free energy, a measure of structural stability of the complex, is reduced. This simply means that a relatively small amount of denaturant (urea) is required to completely dissociate the complex allowing isolation of the individual proteins. In the absence of high $MgCl_2$ concentration, the snRNP complex is highly stable, as only partial dissociation can be achieved, even at 7 M urea. It is possible that other dissociants such as guanadinium hydrochloride could be used in conjunction with CHT. However, the extremely high ionic strength of this denaturant is not compatible with the ion exchange method used to establish dissociation.

The use of more sophisticated methods such as circular dichroism may be able to establish whether structural or conformational changes have occurred in U1 snRNP due to high $MgCl_2$. The impact of U1A depletion on U1 snRNP conformation could be assessed in a similar way. An alternative approach would be to deplete U1 snRNP of U1A using CHT and elute the complex in non-denaturing buffer. U1A-free U1 snRNP could be reapplied to CHT, eluted with

buffers containing urea, and the degree of dissociation determined by SP-Sepharose chromatography.

No distinction is made between dissociation (of protein or RNA) or denaturation in the dissociation experiments conducted in this study. The values calculated for Gibb's free energy are approximations and may be an over-simplification of U1 snRNP complex dissociation. Gibb's free energy is usually determined for a single protein through denaturation experiments. Unfortunately no examples of its use in the measurement of complex dissociation were found in the literature.

5.4.4 Non-denaturing U1 snRNP dissociation

Achsel *et al.* (1999) used ribonuclease T1 to dissociate the human U4.U5.U6 tri-snRNP particle and investigate LSm proteins on U6. Ribonuclease digestion of bovine U1 snRNP was attempted as a non-denaturing approach to dissociate and purify individual U1 snRNP proteins. Ribonuclease T1 hydrolyses after guanosine nucleotides of single stranded RNA and successfully digests U1 snRNA sufficiently to allow the snRNP proteins to bind to SP-Sepharose media. It is clear that not all the nucleic acid was hydrolysed because it was protected by the associated proteins. Rather than dissociating the complex, the proteins were 'cut out' of U1 snRNA. Furthermore, the protein/nucleic acid mixtures could not be separated, either by salt gradient elution from SP-Sepharose media or by size exclusion chromatography.

Sumpter *et al.* (1992) used a different non-denaturing dissociating method with buffers containing monovalent cations at pH 5.5 and an anion exchange matrix. This method was used to successfully dissociate human U1 snRNP, but did not achieve dissociation of the bovine U1 snRNP complex (unreported results, this study). Specifically, the recovery of RNA-free proteins was low and there was a tendency for the 68K protein to precipitate. Despite the apparent elegance of this method, it was not used to isolate bovine 68K.

5.4.5 68K may oligomerise by coiled-coil interaction

The lack of human 68K protein recovery was noted by Sumpter *et al.* (1992) and, in fact, parallels attempts in this study to exchange denatured bovine 68K into non-denaturing buffer. There is no explanation offered in the literature for the observed 68K aggregation. Examination of 68K primary structure shows regions of mixed-charge (glu-arg) repeats. Interestingly, this mixed charge repeat potentially contains the heptad repeat common to coiled-coil structures (Figure 5.26). The 68K sequence was entered into MATCHER, an algorithm for determining paired coil or coiled-coil structures. Indeed, two regions aligned to coiled-coil heptad repeats and are annotated in Figure 5.27.

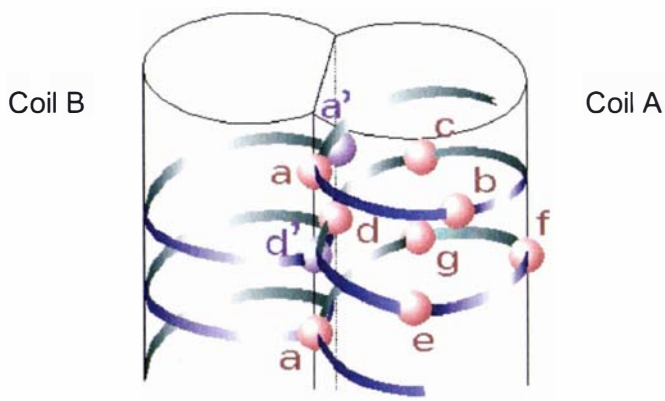

Figure 5.26 Paired coil structure of 68K

This image was taken from the MATCHER site (http://cis.poly.edu/~jps/coilcoil.html). It illustrates the heptad repeat which forms the coil (a,b,c,d,e,f,g) where each letter represents an amino acid. Coil A intercalates with coil B, which can be a coil from: within the same protein; another molecule of the same protein; a different protein, to form a paired coil structure.

68K participates in a number of protein-protein interactions during the course of mRNA splicing (Cao and Garcia-Blanco, 1998). It can be speculated that the splicing factor ASF/SF2, which also contains glu-arg repeat regions, interacts with the 68K RS1 region through a paired-coil mechanism. A similar mechanism may be responsible for linking U1 snRNP and U2 snRNP via the U2 auxiliary factors 1 (35 kDa) and 2 (65 kDa), which both contain glu-arg repeat regions (Boukis, 2004). Indeed, coiled-coil mediated protein-protein interactions occur in other nuclear proteins (Kataoka *et al.*, 1995).

Another property of glu-arg proteins is their propensity to form a speckled pattern in the nucleus when overexpressed, which can be observed by immuno-fluoresence microscopy (Yanagisawa *et al.*, 2000). This nuclear speckle pattern is often observed in ANA screening of anti-RNP patient sera by indirect immunofluoresence on immortalised Hep-2 cells. The speckles are thought to represent deposits of stored snRNP (Zieve and Khusial, 2003).

```
  1 MTQFLPPNLLALFAPRDPIPYLPPLEKLPHEKHHNQPYCGIAPYIREFEDPRDAPPPTRA
 61 ETREERMERKRREKIERRQQEVETELKMWDPHNDPNAQGDAFKTLFVARVNYDTTESKLR
121 REFEVYGPIKRIHMVYSKRSGKPRGYAFIEYEHERDMHSAYKHADGKKIDGRRVLVDVER
181 GRTVKGWRPRRLGGGLGGTRRGGADVNIRHSGRDDTSRYDERPGPSPLPHRDRDRDRERE
241 RRERSRERD ERERRRSRSRDRRRRSRSRD EERRRSRERSKD DRDRKRRSSRSRERAR
301 RERER EELRGGGGDMAEPSEAGDAPPDDGPPGELGPDGPDGPEEKGRDRDRERRRSHRS
361 ERERRRDRDRDRDRDREHKRGERGSERGRDEARGGGGGQDNGLEGLGNDSRDMYMESEGG
421 DGYLAPENGYLMEAAPE
```

Figure 5.27 Putative coiled-coil regions in 68K

The two putative coiled-coil regions are highlighted in red and the RNA binding region is boxed.

It is thus possible that these coiled-coil motifs may be responsible for self-association of 68K protein in the absence of U1 snRNA. The proximity of the N-terminal coiled-coil to the RNA binding domain could prevent interaction with either the C-terminal coil of the same protein or other proteins. When RNA is removed, oligomerisation, and hence precipitation, of 68K would be possible. Reconstitution or reassociation of 68K with U1 snRNA by buffer exchanging 68K and U1 snRNA together into non-denaturing buffer, may prevent 68K precipitation.

5.4.6 Differential reactivity of fractionated SmD proteins

Sm proteins dissociated from U1 snRNP have been fractionated on SP-Sepharose by virtue of their high pIs. The Sm proteins co-eluting with 68K were

identified as SmD2 and SmD3, whereas, the immunodominant SmD1 elutes at higher ionic strength. Each Sm protein is rich in the basic residues and, therefore, trypsinolysis will yield many small peptides and possible missed cleavages. This is reflected in the low tryptic peptide identification for all three Sm proteins by mass spectrometry. In addition, SmD1 and SmD3 contain several sDMA modifications. Tryptic peptides containing such modifications would not be identified using the conventional peptide finger-printing algorithms.

Reactivities of anti-Sm patient sera with purified SmD subunits correlate poorly with intact Sm antigen. Anti-Sm sera contain a range of Sm specificities with the majority SmD1 positive, approximately 17 % SmD2, and 22 % SmD3 (McClain *et al.*, 2002). The lack of correlation between intact Sm and purified Sm could be explained by these differences in specificity. Combining the purified SmD2, SmD3 and SmD1 fractions and then re-testing against intact Sm would help to clarify the discrepancies. The SmD1 preparation appears to contain non-Sm components which are probably snRNP specific proteins. These contaminants should be removed before any recombination experiment is carried out.

It is also possible that the anti-Sm sera contain antibodies specific for conformational epitopes. Sub-sets of autoantibodies specifically recognise RNA-bound 68K protein (Murakami *et al.*, 2002). RNA bound Sm proteins may similarly present epitopes that are either a combination of Sm and U snRNA, or a conformation of Sm protein adopted with bound RNA. These epitopes are abolished during the purification of the SmD proteins under denaturing conditions.

5.4.7 Purified Sm-free 68K is superior to the recombinant antigen

Sm-free 68K was purified in four steps from calf thymus extract in commercially viable quantities. Neither the apparent urea-induced loss of 68K structural conformation, nor the lack of RS2 C-terminal domain, had any impact on the detection of anti-68K patient sera in western blot and/or ELISA immunoassays. A very good correlation between the reactivities of anti-RNP sera with purified

68K and intact U1 snRNP was obtained. Any deviation from this correlation reflected anti-RNP sera responses to other antigens, in addition to 68K, within the U1 snRNP complex. Responses of anti-RNP sera to r68K and purified bovine 68K agreed extremely well. In general, the response to purified 68K was greater than for r68K. This may be due to correct post-translational modifications and/or authentic sequence, neither of which can be attributed to the recombinant antigen. Skewed responses, however, could also be due to incorrect determination of protein concentration.

Interestingly, the difference in the responses of anti-Sm sera to recombinant and purified 68K was greater than observed for anti-RNP sera. This difference is too great for protein concentration alone to be the major contributing factor. It is known that r68K protein lacks the RS1 domain which has been engineered out because it acts as an inhibitory element (Northemann *et al.*, 1995). Claims that RS1 does not contain autoepitopes is refuted by epitope mapping studies (Pelsue *et al.*, 1993; James e*t al.*, 1994b). It can be speculated that the reduced response of r68K in ELISA may be due to anti-RS1 domain autoantibodies. More specifically, the dominance of anti-RS1 autoantibodies associated with anti-Sm sera could be an additional marker for SLE diagnosis. Further work is required to confirm this association.

This study aimed to improve and add-value to the use of U1 snRNP in the diagnosis of MCTD and SLE by separating and characterising the performance of individual U1 snRNP components. Bovine U1 snRNP was destabilised with 3.5 M $MgCl_2$ and subsequently dissociated with high urea concentrations. This facilitated the purification of 68K to homogeneity. Purified bovine 68K was superior to r68K in its response to both anti-RNP and anti-Sm patient sera by ELISA.

Chapter Six

Truncation of Bovine U1 68K

6.1 Introduction

The protein composition of bovine U1 snRNP purified from calf thymus has been shown to be different from human U1 snRNP isolated from HeLa cells (Chapter 4). The U1C protein is missing from bovine U1 snRNP and both the SmB and 68K proteins are truncated. Truncation of the 68K antigen does not appear to affect its performance as a diagnostic reagent in the detection of anti-68K antibodies in SLE and MCTD patient sera. The susceptibility of the 68K protein to modification by either caspase-3 hydrolysis or metal-induced oxidative cleavage has been characterised (Casciola-Rosen *et al.*, 1997; Degen *et al.*, 2000a). Particular attention has been given to how nuclear autoantigens are modified during either apoptotic or necrotic cell death (Rosen and Casciola-Rosen, 1999; Wu *et al.*, 2001).

Apoptotic cells are cleared by macrophage phagocytosis and do not elicit an inflammatory or immune response (Savill and Fadok, 2000). However, if apoptotic cells are not cleared efficiently, or there is a defect in the phagocytic mechanism, cells can undergo secondary necrosis. Necrosis involves protease-mediated modifications that are independent of caspase and in some cases results in specific fragmentation patterns of nuclear antigens (Casiano *et al.*, 1998). Poly(ADP-ribose) polymerase and DNA topoisomerase I (topo I), for example, are reported to have distinct apoptotic and necrotic fragmentation (Wu *et al.*, 2001). Cells undergoing necrosis are able to elicit an inflammatory response. Exposure of a neoepitope, created as a result of antigen modification, to a proinflammatory environment could potentially trigger an autoimmune response against that antigen (Bondanza *et al.*, 2004).

Primary necrosis occurs as a result of injury, trauma or death, whereas, secondary necrosis follows apoptotic events (Leist and Nicotera, 1997), and the proteolytic pathways followed during the two forms of necrosis are indistinguishable (Wu *et al.*, 2001). The main necrotic proteases are the lysosomal cathepsins B, C, H and L (Turk *et al.*, 2000). While cathepsin L is important in a number of cellular functions (Turk *et al.*, 2001), it has been specifically implicated in CD4 T-cell selection (Nakagawa, 1998), epidermal and

hair follicle homoestasis (Roth, 2000) and angiogenesis (Felbor *et al.*, 2000). More recently, a role for cathepsin L in the degradation of the nuclear autoantigen topo I from 100 kDa to 70 kDa and 45 kDa necrotic fragments has been described (Pacheco *et al.*, 2005). The role of cathepsin L in generating other necrosis specific fragments from different nuclear antigens has not been fully determined.

Truncation of 68K in bovine U1 snRNP produces a distinctive and stable cleavage pattern, the cause of which is largely unknown. Previous work in this study established some of the post-translational modifications of 68K and developed a protocol for the purification of 68K for its use in diagnostic procedures. The experiments presented in this chapter build on this work by exploring how the 68K antigen is truncated, and investigate whether this is a direct consequence of calf thymus gland processing. The structural domain cleaved from bovine 68K is identified and the consequence of loosing this domain on diagnostic performance is established. The effects of the time used to thaw frozen calf thymus, prior to processing, on both the U1 snRNP purification and the 68K antigen truncation pattern is also determined. In addition, the necrotic protease, cathepsin L, is purified and its effects on intact 68K in human HeLa isolated U1 snRNP is investigated.

6.2 Experimental Procedures

6.2.1 Preparation of thymus acetone powders

Frozen calf thymus, or thymus which had been thawed at 2-8 °C for either 4 or 20 hours, was diced and then homogenised with two volumes of ice cold acetone at high speed for two minutes in a 24CB10 Waring blender. The homogenate was centrifuged and the supernatant was discarded. The pellet was homogenised with a further two volumes of cold acetone and centrifuged as above. The pellet was drained to remove excess acetone and then ground into a powder.

Antigens were extracted from the acetone powder as described in section 3.2.1, except that a handblender (Braun, Germany) was used to homogenise the powder with homogenisation buffer. Bovine U1 snRNP was isolated using an anti-RNP immunoaffinity matrix.

6.2.2 Chymotryptic digestion of 68K

Bovine purified 68K or recombinant 68K (r68K) was diluted to 1 M urea final concentration with 20 mM Tris-HCl pH 7.5, 0.2 M NaCl. Approximately 6 μg purified 68K or r68K in 30 μL final volume was incubated with chymotrypsin (Sigma Chemical Co., St Louis, USA) for three hours at 37 °C. The reaction was stopped by the addition of 10 μL SDS-PAGE sample buffer and 10 μL 0.2 M DTT, and incubated at 100 °C for 90 s. Samples were analysed by SDS-PAGE and Western blotting.

6.2.3 Purification of bovine kidney cathepsin L

Cathepsin L was purified from bovine kidney according to the method described by Sentandreu *et al.* (2004) with some modifications. Briefly, bovine kidney was homogenised in buffer containing 10 mM phosphate pH 7.4, 1 mM EDTA, 0.25 M sucrose. Whole cells, nuclei and cellular debris were removed by centrifugation at 4 000 x g for 15 minutes. The supernatant was centifuged at 20 000 x g for 20 minutes and the lysosome containing pellet was resuspended in 30 mM phosphate pH 5.8, 0.1 % w/v Triton x100. After homogenising the pellet with four strokes of a Potter homogeniser (Wheaton, USA), the

homogenate was frozen at –80 °C. To prepare the lysosomal-rich extract, the homogenate was thawed, homogenised again, and centrifuged at 40 000 x g for 90 minutes. Soluble lysosomal extract (supernatant) was further fractionated by ammonium sulfate precipitation. Protein precipitated between 30-70 % salt saturation was collected and resuspended in 5 ml 20 mM Bis-Tris-HCl pH 6.0 containing 0.2 M NaCl, 1 mM DTT, 1 mM EDTA. Cathepsin L was subjected to Sephacryl S200 size exclusion chromatography followed by SP-Sepharose chromatography in 20 mM citrate pH 4.8, 1 mM EDTA, 0.5 mM DTT. Cathepsin L was eluted from SP-Sepharose using a linear gradient from 0 – 0.5 M NaCl made up in the same buffer. Cathepsin L activity was detected using a synthetic substrate derivative of *para*-nitroanilide, benzoyl-phe-arg-pNA (Bachem, Switzerland), and gelatin zymography.

6.2.4 Cathepsin L digestion of U1 68K

Human U1 snRNP was purified from HeLa cells as described in Chapter 3 and buffer exchanged by diafiltration into either 20 mM HEPES-NaOH pH 7.5, 0.2 M NaCl, 0.5 mM DTT, 10 % v/v glycerol or 20 mM Bis-Tris-HCl pH 6.0, 0.2 M NaCl, 0.5 mM DTT, 10 % v/v glycerol. Twenty-four μg U1 snRNP (pH 7.5 or pH 6.0) was incubated with cathepsin L for 1 hour at 37 °C. The reaction was stopped by the 1:4 addition of SDS-PAGE buffer containing 0.2 M DTT followed by heating at 100 °C for 90 s. Protease inhibitors (0.5 mM PMSF, 1 mM EDTA, 10 μM leupeptin, 1 mM iodoacetamide) were added to the control samples to exclude possible endogenous proteases. Samples were analysed by SDS-PAGE and western blotting.

6.3 Results

6.3.1 Effect of thymus thawing time on U1 snRNP composition

Calf thymus used for acetone extraction was still partially frozen after 4 hours and was completely thawed after 20 hours at 2-8 °C. Bovine U1 snRNP composition remained very stable over the 4 hour thawing period and only a small molecular weight shift was observed after 20 hours (Figure 6.1).

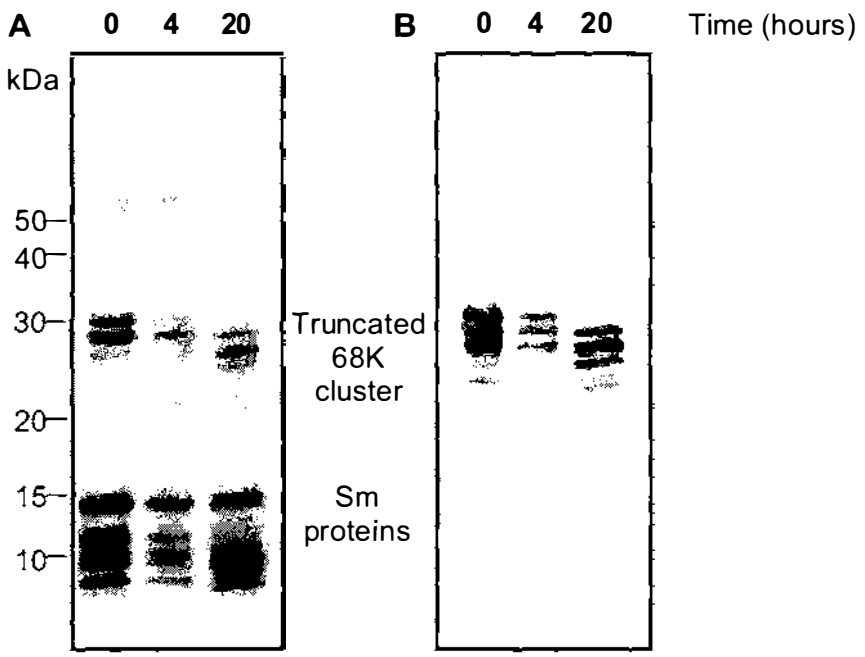

Figure 6.1 Effect of thymus thawing time on bovine U1 snRNP

Frozen bovine thymus was thawed at 2-8 °C for 0, 4 and 20 hours before preparing an acetone powder. The powders were extracted and U1 snRNP was purified by anti-RNP immunoaffinity chromatography. Purified U1 snRNP was analysed on SDS-PAGE **A**: Coomassie stain; **B**: Western blot immunoprobed with anti-RNP patient serum.

Sm proteins were purified from thymus acetone powders using an anti-Sm immunoaffinity column. Thawing time did not influence the appearance or reactivity of the Sm proteins (Figure 6.2).

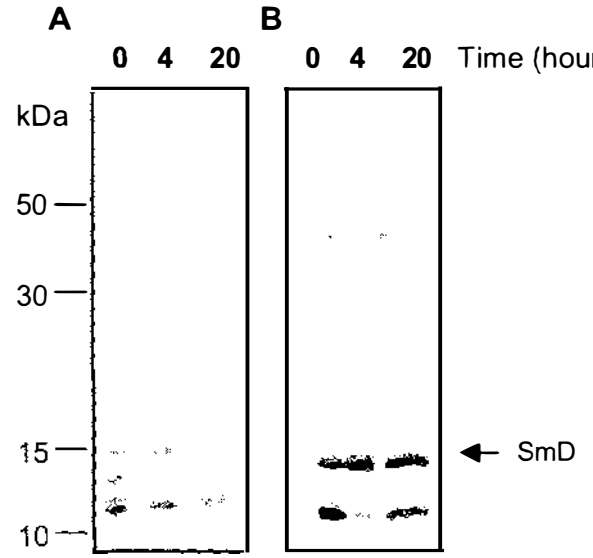

Figure 6.2 Effect of thawing time on SmD purification

Acetone powders prepared from frozen bovine thymus thawed for 0, 4 and 20 hours were extracted and passed through anti-RNP and anti-Sm immunoaffinity columns. The anti-Sm affinity elutions were analysed on SDS-PAGE. **A:** Coomassie stain; **B:** Western blot immunoprobed with anti-Sm serum.

6.3.2 Chymotryptic digestion of bovine 68K

It is not clear whether bovine 68K antigen is truncated N-terminally, C-terminally or both in necrotic cells. A simple approach to determining C-terminal cleavage is to examine the polypeptide fragments produced by chymotrypsin digestion. Chymotrypsin cleaves on the C-terminal side of tryptophan, tyrosine or phenylalanine residues. Digestion of full-length 68K produces a characteristic 22 kDa polypeptide fragment encompassing most of the C-terminal region (Woppmann *et al.*, 1993) (Figure 6.3). Various amounts of chymotrypsin were trialed to digest 68K and to determine the amount required to produce a stable 68K fragmentation pattern (Figure 6.4). Incubating 68K with 0.03 μg chymotrypsin for 3 hours at 37 °C produced a cluster of fragments ranging from 13.7 kDa to 12.4 kDa. These fragments were not detected by western blot immunoprobed with anti-RNP sera, suggesting that the immunoreactivity of 68K is abolished by chymotryptic digestion.

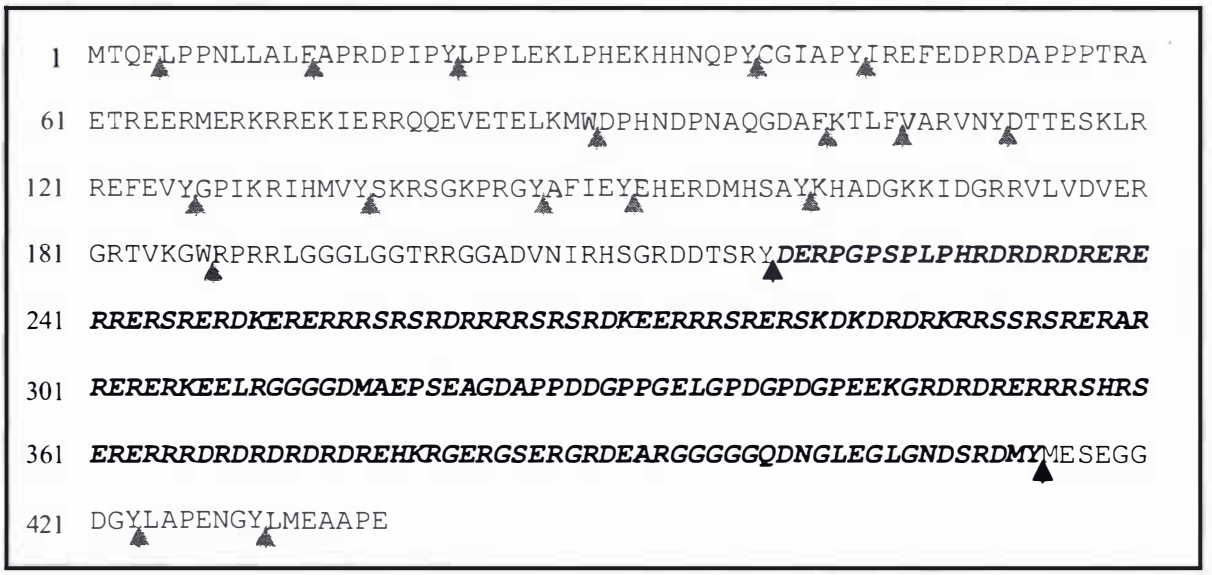

Figure 6.3 Chymotryptic cleavage of 68K

Amino acid sequence of 68K showing the 22 kDa proteolytic fragment of chymotrypsin in bold italic.The gray arrows indicate the predicted cleavage sites of chymotrypsin and the black arrows mark the cleavage sites of the 22 kDa RS domain fragment.

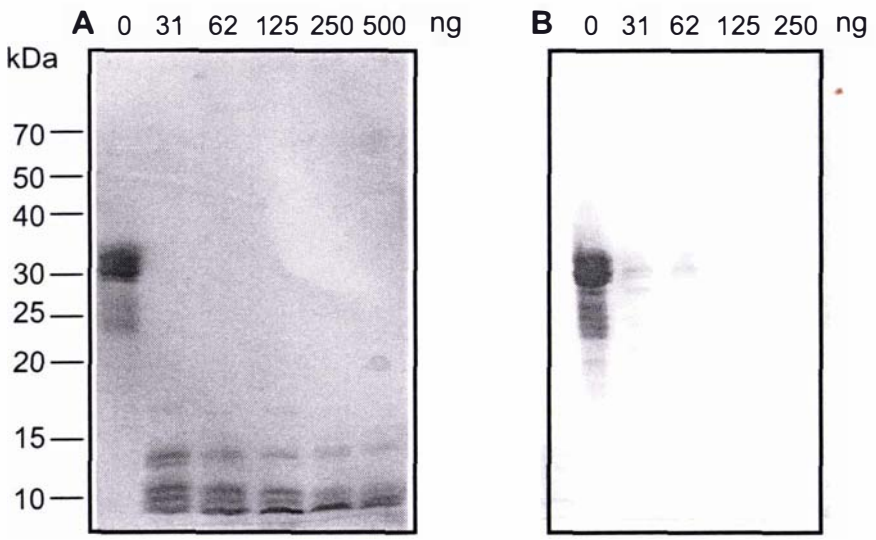

Figure 6.4 Digestion of 68K with increasing amounts of chymotrypsin

Bovine 68K protein was digested with 30 – 500 ng chymotrypsin for 3 hours at 37 °C. The digests were analysed on SDS-PAGE. **A**: Coomassie stain; **B**: Western blot immunoprobed with anti-RNP patient serum.

Using 0.03 μg of chymotrypsin, the optimum amount established in the previous experiment, a time course of the 68K protein digestion was carried out to determine the incubation time required to achieve a stable partial digestion (Figure 6.5). Digestion for 2-3 hours produced a stable 13 kDa 68K fragment.

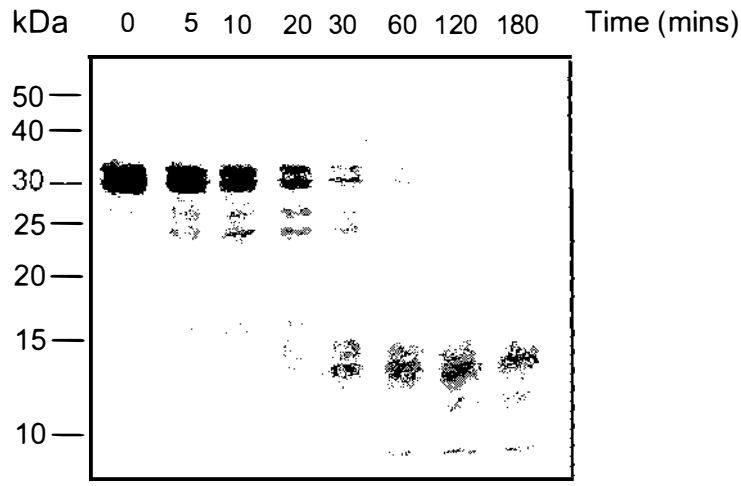

Figure 6.5 Time course of 68K digestion with chymotrypsin

Bovine 68K was digested with 0.03 μg chymotrypsin for different times at 37 °C. The digests were analysed by SDS-PAGE with Coomassie staining.

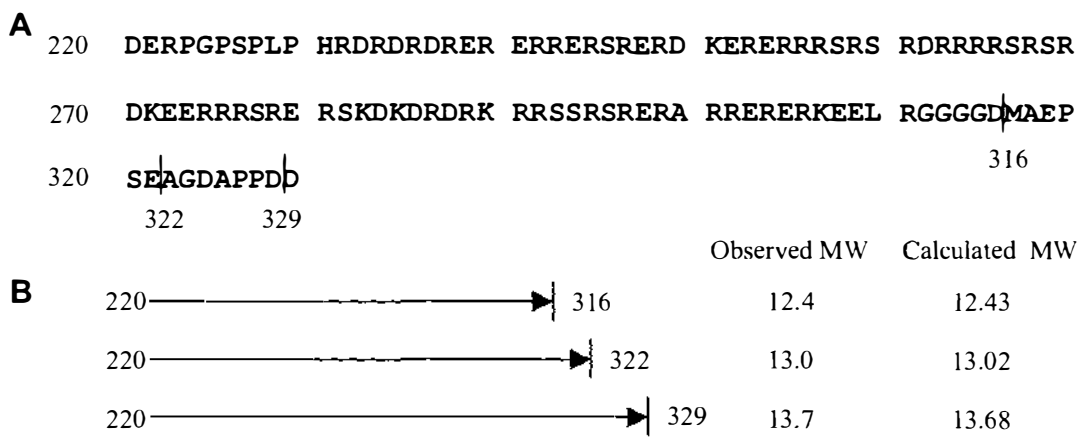

Figure 6.6 Potential truncation sites of bovine 68K

A: Partial sequence of the major 68K chymotryptic peptide with possible cleavage sites annotated. **B:** The arrows indicate the proposed chymotryptic peptides with their observed weights compared to weights calculated using SwissProt MW calculator (www.expasy.org).

Assuming the migration of the 68K chymotryptic peptides on SDS-PAGE reflects their true molecular weight, estimates of the cleavage sites within the C-terminal region can be calculated (Figure 6.6).

6.3.3 Mass spectrometry of 68K

The truncation of the C-terminus of the 68K protein has been investigated by chymotryptic digestion, however, cleavage of the N-terminus could equally contribute to the modification of the 68K antigen molecular weight. The 68K protein was electrophoresed and pieces of Coomassie stained gel were excised and prepared for MALDI mass spectrometry as described in Chapter 3 (Figure 6.7). Initial analysis of the detected peptides using MASCOT showed that most of the major peptides, except the 1739.99 peak, could be matched to 68K. The peptide masses were re-analysed to allow for possible N-terminal blockage by acetylation and the observed tryptic peptides are presented in Table 6.1. The calculated coverage of the full-length sequence is 25 % with a match score of 145. No peptides beyond residue 231 were detected (Figure 6.8).

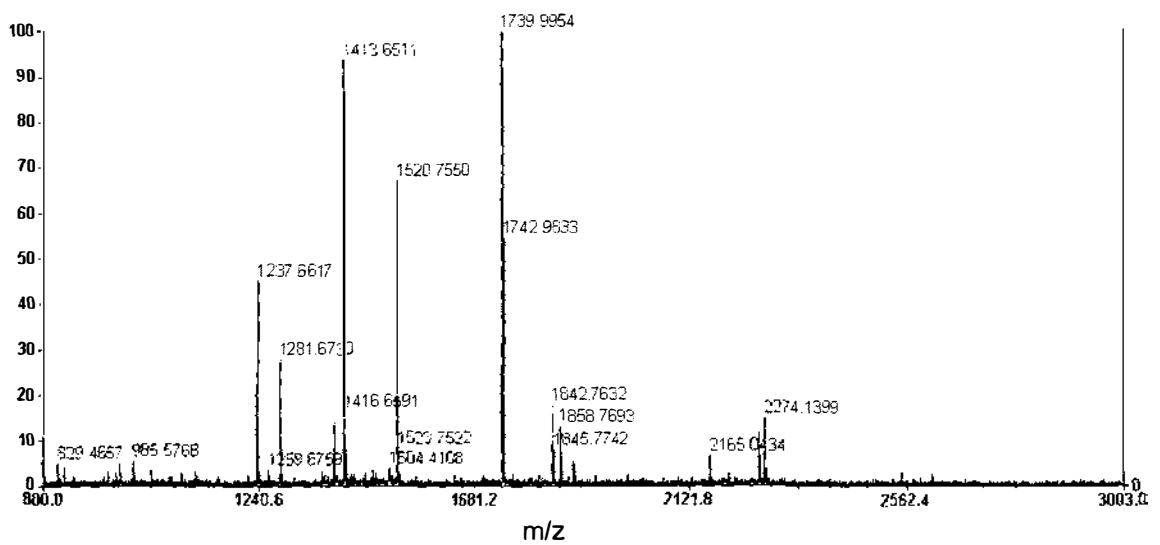

Figure 6.7 MALDI spectrum of 68K tryptic peptides

Table 6.1 68K observed tryptic peptides

Peptide	Observed mass	δ	Sequence
2-16	1739.9954	0.0112	**TQFLPPNLLALFAPR** (N-acetyl)
17-27	1281.6730	-0.0359	**DPIPYLPPLEK**
17-32	1886.0172	-0.0250	**DPIPYLPPLEKLPHEK**
28-46	2273.1490	0.0094	**LPHEKHHNQPYCGIAPYIR**
78-87	1259.6759	0.0169	**RQQEVETELK**
88-103	1842.7632	-0.0232	**MWDPHNDPNAQGDAFK**
122-131	1237.6617	0.0042	**EFEVYGPIKR**
145-155	1413.6511	0.0078	**GYAFIEYEHER**
173-180	985.5768	-0.0021	**RVLVDVER**
174-180	829.4657	-0.0120	**VLVDVER**
219-231	1520.7550	-0.0054	**YDERPGPSPLPHR**

```
          10         20         30         40         50         60
MTQFLPPNLL ALFAPRDPIP YLPPLEKLPH EKHHNQPYCG IAPYIREFED PRDAPPPTRA
          70         80         90        100        110        120
ETREERMERK RREKIERRQQ EVETELKMWD PHNDPNAQGD AFKTLFVARV NYDTTESKLR
         130        140        150        160        170        180
REFEVYGPIK RIHMVYSKRS GKPRGYAFIE YEHERDMHSA YKHADGKKID GRRVLVDVER
         190        200        210        220        230        240
GRTVKGWRPR RLGGGLGGTR RGGADVNIRH SGRDDTSRYD ERPGPSPLPH RDRDRDRERE
         250        260        270        280        290        300
RRERSRERDK ERERRRSRSR DRRRRSRSRD KEERRRSRER SKDKDRDRKR RSSRSRERAR
         310        320        330        340        350        360
RERERKEELR GGGGDMAEPS EAGDAPPDDG PPGELGPDGP DGPEEKGRDR DRERRRSHRS
         370        380        390        400        410        420
ERERRRDRDR DRDRDREHKR GERGSERGRD EARGGGGGQD NGLEGLGNDS RDMYMESEGG
         430
DGYLAPENGY LMEAAPE
```

Figure 6.8 Coverage of tryptic peptides matched to U1 68K

Primary sequence of 68K was taken from SwissProt (Accession # P08621). The peptides covered by mass spectrometry are shown in red. The potential cleavage sites for the truncated 68K are shown at positions 316, 321 and 329.

6.3.4 Effect of RS2 truncation on immunoreactivity

Truncation of bovine 68K appears to include the loss of the RS2 domain. In the recombinant protein (r68K) the RS1 domain was removed because it was found that when present, protein expression was inhibited. The RS2 domain, however, remained intact (Berthold *et al.*, 1992). r68K was digested with chymotrypsin (30 ng, 3 hours, 37 °C) and compared to the chymotryptic digest of bovine 68K by SDS-PAGE (Figure 6.9). Digestion of r68K produced a ladder of fragments ranging from 9 – 25 kDa with the major bands at 14, 18, 21 and 25 kDa.

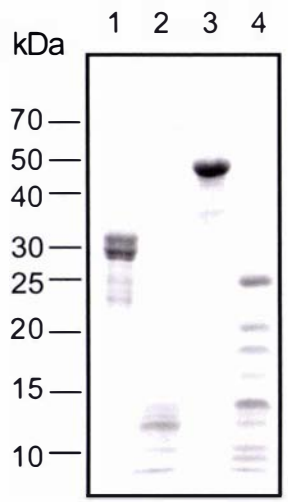

Figure 6.9 Chymotryptic digestion of bovine and recombinant 68K

Bovine and r68K were digested with chymotrypsin for 3 hours at 37 °C. Samples were analysed on SDS-PAGE with Coomassie staining. Lanes: 1, bovine 68K; 2, bovine 68K chymotryptic digest; 3, r68K; 4, r68K chymotryptic digest.

To determine whether the RS1 and RS2 regions contain important autoepitopes, chymotryptic digests of bovine and r68K were western blotted and cut into strips before screening with anti-RNP sera. As shown previously, the RS1 domain 13 kDa chymotryptic fragment of bovine 68K was poorly recognised by anti-RNP sera. In contrast, the r68K fragments were detected by most sera (Figure 6.10).

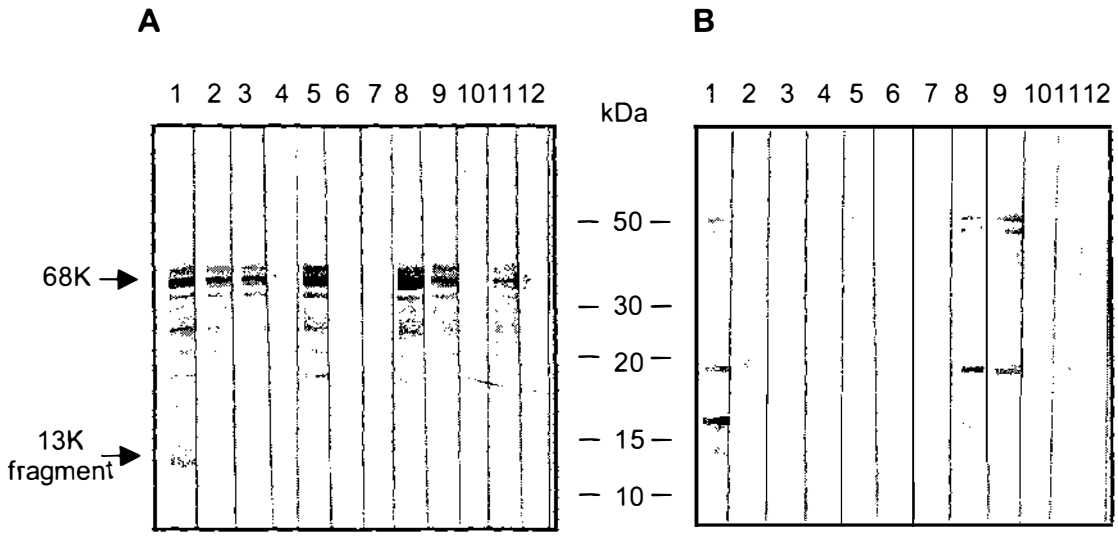

Figure 6.10 Immunoreactivity of 68K chymotryptic fragments

Chymotryptic digests of bovine and r68K were western blotted and cut into strips for immunoprobing with anti-RNP sera. **A**: bovine 68K; **B**: r68K. Each numbered strip represents one anti-RNP serum i.e. A and B strip 1 were immunoprobed with the same serum.

6.3.5 Possible cathepsin L activity in bovine thymus

A number of autoantigens produce consistent fragmentation patterns during necrosis. Topo I is the major autoantigen recognised by sera from scleroderma sufferers, and has distinctive fragmentation patterns for apoptosis and necrosis (Tan *et al.*, 1988; Pacheco *et al.*, 2005). Both cell death pathways produce a 70 kDa degradation fragment of topo I, whereas, necrotic cells have an additional 45 kDa fragment which is a result of cathepsin L activity. Topo I was purified from bovine calf thymus extract by immunoaffinity chromatography and analysed by SDS-PAGE and western blotting (Figure 6.11). The characteristic necrotic topo I 45kDa fragment was clearly observed in bovine purified topo I, which reacts strongly to anti-topo I patient sera.

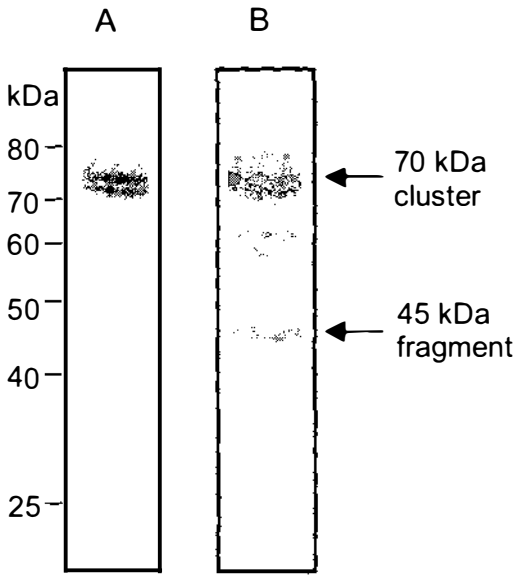

Figure 6.11 Necrotic polypeptide fragment in bovine DNA topoisomerase I

Topo I was purified from bovine thymus extract by immunoaffinity chromatography. Analysis by **A**: SDS-PAGE Coomassie stain and **B**: Western blotting with anti-topo I scleroderma patient sera show the 70 kDa cluster and 45 kDa polypeptide fragment characteristic of necrosis and cathepsin L activity.

6.3.6 Modification of human U1 snRNP with cathepsin L

Cathepsin L was successfully purified from bovine kidney and was concentrated to approximately 1 U/mL, where 1 U is defined as the amount of enzyme required to hydrolyse 1 μmol substrate per hour at 25 °C.

Two mU of cathepsin L were incubated with human U1 snRNP at both pH 6.0 and pH 7.5 at 37 °C for six hours. The digests were analysed by SDS-PAGE and western blotting, and then immunoprobed with anti-RNP sera (Figure 6.12). Samples of U1 snRNP exchanged into both pH 6.0 and 7.5 were retained at 2 – 8 °C as untreated controls. Untreated U1 snRNP component proteins can be clearly observed and are stable at both pH 6.0 and 7.5. However, both U1A and U1C are sensitive to pH at elevated temperature. When incubated at 37 °C, U1A and U1C disappear at pH 6.0, whereas, they remain intact at pH 7.5. U1A and U1C are also sensitive to cathepsin L activity at both pHs, however, 68K is

relatively stable to cathepsin L at pH 7.5 despite being totally digested at pH 6.0.

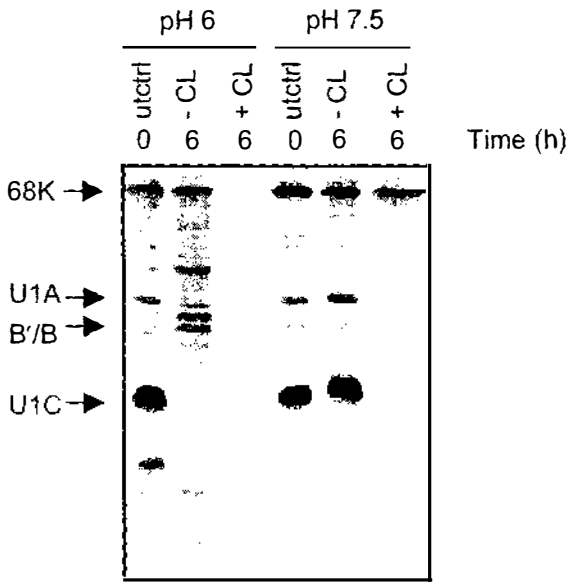

Figure 6.12 The effect of pH and cathepsin L on U1 snRNP composition

Human U1 snRNP, exchanged into pH 6.0 and 7.5 buffer, was incubated with and without 2 mU cathepsin L at 37 °C for six hours and compared to untreated controls (utctrl) for both pHs. Analysis was by western blot immunoprobed with anti-RNP serum.

Multiple specificity of anti-RNP sera complicate the assignment of antigen specificity of hydrolysed U1 snRNP. To determine the fate of 68K, the above experiment was repeated with incubations of one, two and four hours, and the western blot was immunoprobed with immunoaffinity purified anti-68K antibodies. As observed previously, very little proteolysis occured at pH 7.5, whereas, 68K was completely digested after two hours in the presence of cathepsin L at pH 6.0 (Figure 6.13).

Partial digestion after one hour resulted in a faint dimer at approximately 25 kDa. 68K appears to be pH and temperature sensitive. After two hours at 37 °C, intact 68K was diminished and fragments around 38, 32 and 29 kDa began to accumulate.

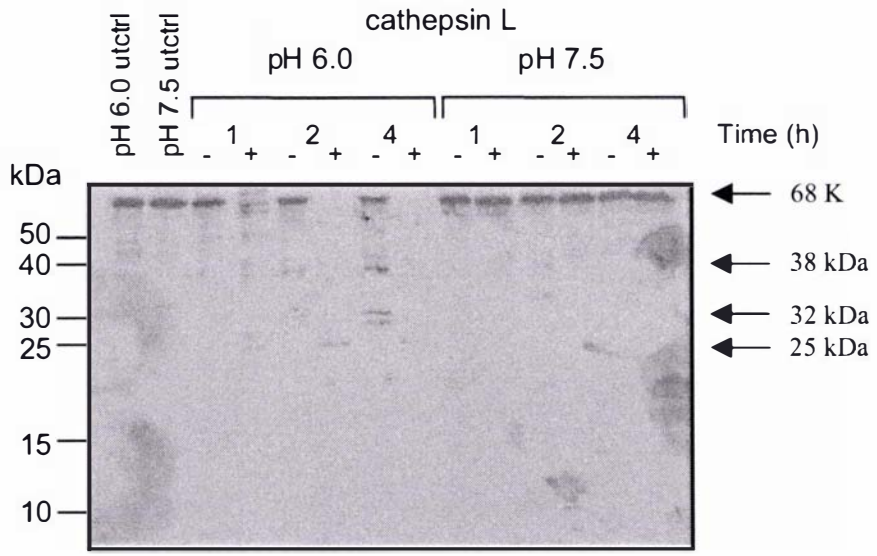

Figure 6.13 Cathepsin L digestion of human U1 snRNP 68K

Human U1 snRNP at pH 6.0 or pH 7.5 was incubated with or without 2 mU cathepsin L for 1, 2 and 4 hours at 37 °C and compared to untreated controls (utctrl). Reactions were stopped by running on SDS-PAGE and western blotted. The blot was immunoprobed with immunoaffinity purified 68K.

U1 snRNP in pH 6.0 buffer was incubated with decreasing amounts of cathepsin L and incubated for one hour at 37 °C to observe the effect of cathepsin L on 68K fragmentation (Figure 6.14). Initially, the predominant cleavage product of 68K increased to 80 kDa in molecular weight before the 25, 38 and 45 kDa fragments accumulated. Fragments 25 and 38 kDa were relatively stable over the range of the cathepsin L activity tested.

Truncation of 68K and the modification of other antigens in bovine U1 snRNP may be a result of cathepsin L activity. To compare protein composition, U1 snRNP pH 6.0 was incubated with and without cathepsin L for one hour at 37 °C and then analysed by western blotting along side purified bovine U1 snRNP.

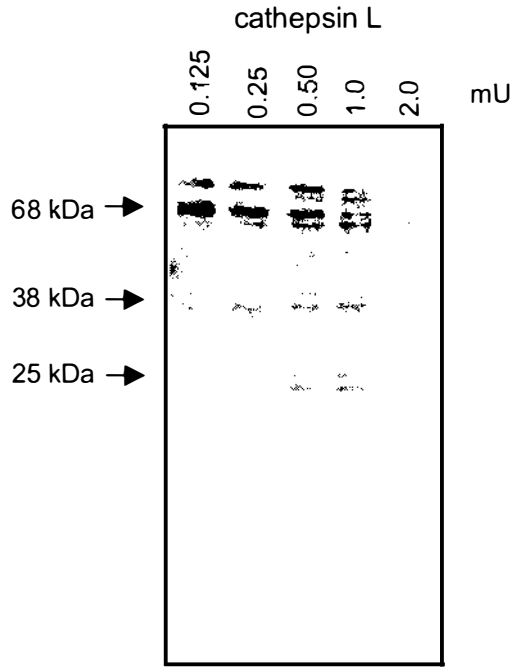

Figure 6.14 Progression of 68K fragment formation by cathepsin L

Human U1 snRNP was incubated with between 0.125 and 2 mU cathepsin L for one hour at 37 °C. Reactions were stopped by analysis on SDS-PAGE and western blotting. 68K fragments were visualised by immunoprobing with anti-68K antibodies.

Nitrocellulose blots were immunoprobed with immunoaffinity purified anti-68K and then re-probed with anti-U1A polyclonal followed by anti-Sm patient sera (Figure 6.15). Human 68K fragments did not correspond to the bovine truncated 68K. Cathepsin L cleavage resulted in peptides migrating both higher (38 kDa) and lower (25 kDa) than the 30 kDa bovine 68K cluster, and U1A appears to be sensitive to incubation at 37°C and pH 6.0, with or without cathepsin L. While some U1A remained intact, a more intense anti-U1A reactive band appeared at approximately 13 kDa during the incubation. This band was diminished after reaction with 1 mU of cathepsin L.

SmB′/B is cathepsin L sensitive but is more resistant to incubation at 37 °C than U1C. As previously shown, U1C is pH and temperature labile, in addition to being very sensitive to cathepsin digestion. SmD proteins do not appear to be affected under any of the conditions used in this experiment.

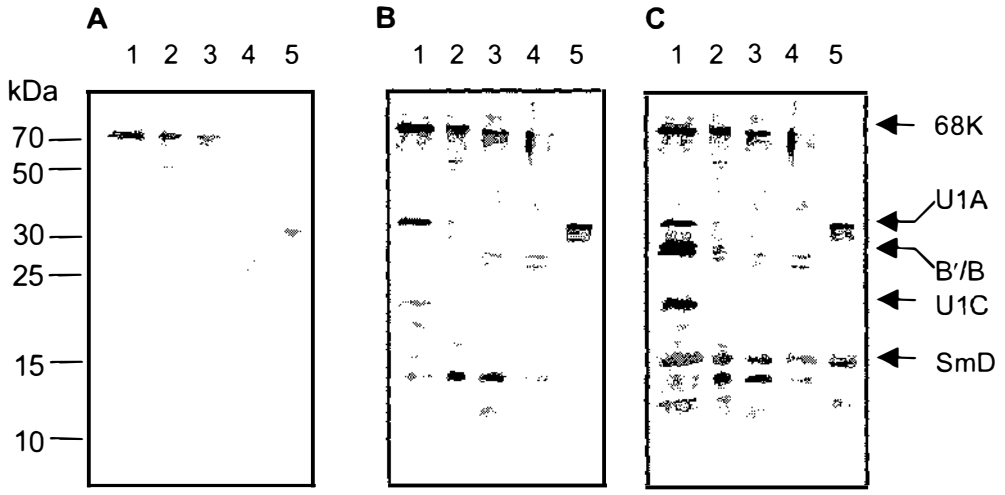

Figure 6.15 Degradation of U1 snRNP proteins by cathepsin L

Human U1 snRNP pH 6.0 was incubated for 1 hour at 37 °C either without protease or with 0.5 or 1 mU cathepsin L. The reactions were stopped and analysed on SDS-PAGE and western blot. The blot was immunoprobed first with **A**: anti-68K antibodies and subsequently re-probed with **B**: anti-U1A polyclonal and **C**: anti-Sm patient sera. Lanes: 1, U1 snRNP untreated control; 2, U1 snRNP 1 hour no cathepsin; 3, U1 snRNP + 0.5 mU cathepsin L; 4, U1 snRNP + 1.0 mU cathepsin L; 5, bovine U1 snRNP.

6.4 Discussion and Future Work

6.4.1 Thymus thawing only partially responsible for changes in U1 snRNP composition

Thawing for an extended period does have an effect on the U1 snRNP purified from calf thymus. The appearance of the 68K polypeptide cluster on SDS-PAGE is slightly altered over the 20 hour period. 68K can be degraded into discrete fragments by several means including metal-induced oxidative cleavage or cell death proteases (Casciola-Rosen *et al.*, 1997; Greidinger e*t al.*, 2000; Hof e*t al.*, 2005). None of the fragmentation patterns described in the literature correspond to the bovine 68K pattern observed.

Caspase-3 cleavage of 68K during apoptosis results in a discrete 40 kDa polypeptide, while digestion with granzyme B produces a 50 kDa polypeptide. Metal-induced oxidative hydrolysis, normally caused by the production of reactive oxygen species during ischemia-reperfusion, produces a peptide cluster between 33-38 kDa (Casciola-Rosen e*t al.*, 1999). Although necrotic tissue is hypoxic, there is no associated reperfusion that could cause oxidative damage. It is proposed, therefore, that the small changes in 68K migration after 20 hours thawing are due to protease action.

The most significant change in U1 snRNP composition occurs during the time between slaughter, thymus excision and freezing. Necrosis, temperature and changes in the cellular environment contribute to the truncation of 68K. To gain a clearer understanding of the events leading to the degradation of 68K, thymus from freshly slaughtered calves would need to be used.

6.4.2 68K is C-terminally truncated during cell death

Intact 68K is known to produce a C-terminal 22 kDa peptide upon chymotryptic digestion (Woppmann e*t al.*, 1993). Limited hydrolysis of 68K with chymotrypsin resulted in a cluster of peptides of approximately 13 kDa, and therefore confirmed that the C-terminal RS2 region of 68K is cleaved during cell death. Potential C-terminal cleavage sites, ^{329}Asp, ^{322}Glu and ^{316}Asp, were also

identified, although these should be confirmed by obtaining an accurate mass using mass spectrometry.

Most of the major peaks in the mass spectrometry of 68K tryptic digest were matched to 68K. The discovery that the N-terminal tryptic peptide is blocked, is consistent with the SwissProt accession. No peptide coverage was detected beyond residue 231. The high concentration of trypsin-cleavable lysine and arginine residues in the RS1 region would result in peptides below 800 Da. These were not examined. Calculated molecular weights of peptides cleaved at the proposed C-terminal sites (38.1 - 39.4 kDa) are larger than the observed peptides (30 – 36 kDa). Given that the N-terminus is likely to be intact, the proposed cleavage sites are probably incorrect. This discrepancy can be best solved using mass spectrometry of truncated 68K and the RS1 domain cleaved by chymotrypsin.

Metal-induced oxidative cleavage occurs within aspartic acid rich regions of the RNA polymerases (I, II and III) (Zaychikov *et al.*, 1996), therefore, a similar mechanism could cause 68K truncation. Indeed, a peptide cluster between 33 – 38 kDa has been shown to result from oxidative cleavage in the presence of Fe^{2+} which would correspond to truncation within the aspartic acid rich domain. Bovine U1 snRNP purified from calf thymus glands is completely truncated, whereas, Casciola-Rosen *et al.* (1997) showed that oxidative cleavage of human U1 68K was very low under the experimental conditions used. Repeating these oxidative cleavage experiments using extended incubation times and mimicking the tissue environment *post-mortem,* may help to clarify whether oxidative cleavage is capable of completely truncating 68K. Topo I is also susceptible to metal-induced oxidative cleavage (Casciola-Rosen *et al.*, 1997). In this study, it was demonstrated that topo I purified from calf thymus was also truncated. There was no evidence of oxidative cleavage, and instead the characteristic 45 kDa proteolytic fragment was present.

6.4.3 U1 snRNP proteins are sensitive to environment pH and temperature

Unexpectedly, U1 snRNP proteins appear to be very sensitive to both pH and temperature. U1C was particularly labile and completely disappeared after one hour incubation at pH 6.0 and 37 °C. U1C remained intact when incubated at pH 7.5, 37 °C or pH 6.0, 2-8 °C. 68K was also susceptible to cleavage when incubated at low pH and elevated temperature. Interestingly, a 32 kDa peptide cluster of 68K, similar to truncated bovine 68K, formed after human U1 snRNP was incubated for 6 hours at pH 6.0, 37 °C. Non-enzyme mediated cleavage of acid-sensitive amide bonds at pH 6.0 is not unprecedented. The secreted mucin (MUC2) is cleaved into two peptides at pH 6.0 and below (Lidell *et al.*, 2003). The susceptible bond, asp-pro, is known to be acid-sensitive although not usually under such mild conditions (Piszkiewicz *et al.*, 1970).

68K contains four N-terminal asp-pro sites, although, cleavage of these bonds would not result in 32 kDa fragments. It is probable that the sequence surrounding the pH labile bond influences its susceptibility to cleavage at low pH. Cleavage under mild acid conditions, therefore, may not be exclusively at asp-pro bonds. Whatever the mechanism, the biological significance of acid labile bonds in 68K, and U1C, is not clear. MUC2 is cleaved at low pH during the golgi secretory pathway and the released C-terminus reacts with other mucins. Opportunities for the exposure of U1 snRNP to low pH are limited. Cell death may provide such an opportunity. The failure of homeostasis mechanisms *post-mortem* cause an initial temperature rise in addition to a drop in pH due to lactic acid accumulation. In muscle tissue the pH can reach as low as 5.5. The pH drop in non-muscle tissue has not been extensively studied. Frozen thymus, thawed and homogenised in high-grade water was pH 6.7 (unreported, this study).

6.4.4 U1 68K is a substrate for cathepsin L

The creation of a low pH environment during necrosis favours the activity of the lysosomal cysteine proteases or cathepsins. The effect of cathepsin L on human U1 snRNP at pH 7.5 and pH 6.0 was examined. U1C was depleted

from U1 snRNP at pH 7.5 in the presence of cathepsin L despite the lower activity of the enzyme under these conditions. 68K remained relatively intact in the presence of cathepsin L at pH 7.5. At pH 6.0, digestion of 68K by cathepsin L produced a 38 kDa fragment and a doublet at 25 kDa. This cleavage pattern is not consistent with bovine 68K truncation. Cathepsin L has a broad cleavage specificity. Attempts to characterise specificity using synthetic peptides has shown a preference for positively charged residues in positions P_5-P_3 and P'_5-P'_3, a hydrophobic residue at P_2, and either phenylalanine or arginine at P_1 (Del Nery e*t al.*, 1997). The intact human U1 snRNP associated 68K is a cathepsin L substrate, however, other factors such as post-translational modifications early in necrosis (dephosphorylation and/or glycosylation) may affect cathepsin L specificity.

Modification can have a profound affect on protease substrate specificity. Myelin basic protein (a major autoantigen in multiple sclerosis), for example, can be modified by citrullination of arginine residues. Citrullination significantly enhances the susceptibility of myelin basic protein to cleavage by cathepsin D. There is a strong link between citrullination, cathepsin D proteolysis and types of multiple sclerosis (Cao *et al.*, 1999).

The observation that topo I extracted from bovine thymus has the characteristic 45 kDa cathepsin L cleavage fragment is circumstantial evidence to the activity of cathepsin L in thymus tissue during cell death. Activities of cathepsin L and other cathepsins in thymus tissue should be confirmed using specific fluorogenic substrates.

This study aimed to characterise how bovine U1 snRNP specific 68K protein extracted from thymus glands becomes truncated into a 32 kDa peptide cluster. Through the use of mass spectrometry and chymotrypsin cleavage fragment analysis, 68K was shown to have completely lost the RS2 domain. The precise cleavage position was not determined.

Truncation occurs *post-mortem* between gland excision and freezing. Processing the thymus for purification of U1 snRNP had little effect on the 68K profile. The necrotic protease, cathepsin L, was examined as the possible cause of the 68K truncation pattern. Although intact human 68K protein is a substrate for cathepsin L, the truncation pattern observed in bovine 68K could not be replicated under the conditions used. Interestingly, both 68K and U1C were found to be pH and temperature sensitive. Incubating 68K at 37 °C, pH 6.0 resulted in 32 kDa fragments, similar to truncated 68K. This raises the possibility that autocatalytic cleavage of 68K is a physiologically significant process that occurs during hypoxic necrosis.

Chapter Seven

Antigenicity of Human SmB′/B in Western Blot

7.1 Introduction

Autoantibodies to the Sm core proteins of U snRNPs are highly concordant with the diagnosis of SLE, whereas, a high titre of autoantibodies reacting with U1 snRNP specific proteins is more likely to indicate MCTD (Benito-Garcia *et al.*, 2004).

The majority of Sm reactive sera recognise both SmD and SmB proteins, although the usefulness of SmB as a diagnostic marker is debated (*Luyckx et al.*, 2005). Ambiguity arises from the sDMA and polyproline multiple cross-reactive autoepitopes within SmB. U1 snRNP specific proteins U1A and U1C both contain polyproline sequences similar to the immunodominant SmB′/B epitope, and this is considered the reason for the reaction of many anti-RNP sera with SmB′/B in western blot.

Alternative explanations have been proposed to reconcile this finding. Perhaps the most plausible, described by Ohosone *et al.* (1992), suggests that SmB contains epitopes accessible only on native U1 snRNP and this epitope was mapped to be within SmB residues 25-103. Earlier in this study (Chapter 4), bovine SmB protein was found to be truncated to a 12 kDa peptide comprising of the N-terminal domain including the epitope determined by Ohosone. The reactivity of some anti-RNP sera with SmB′/B in western blot remains contentious.

The aim of this chapter was to further examine the interaction of some anti-RNP sera with SmB′/B from human U1 snRNP. The reaction of anti-Sm and anti-RNP sera with both purified SmB′/B and human U1 snRNP was tested. In addition an immunoaffinity method, coupled with mass spectrometry, was developed to identify the anti-RNP specific antigen.

7.2 Experimental Procedures

7.2.1 Separation of human U1 snRNP by reverse phase HPLC

U1 snRNP components were purified according to Williams *et al.* (1988). Briefly, human U1 snRNP purified from HeLa cell nuclei was made 8 M in urea and 0.1 M in DTT. The denatured antigen was loaded onto a reverse-phase (RP) C-18 nucleosil 300A high performance liquid chromatography (HPLC) column (Phenomenex, Auckland, NZ) equilibrated in 0.1 % v/v trifluoroacetic acid (TFA) and flowed at 1 mL/min with a Biologic Duoflow system (Bio-Rad Laboratories, Hercules, USA). After washing with equilibration solvent, the column was eluted with a gradient (0-50 %) of Unichrom grade isopropanol (Ajax fine chemicals, Auckland, NZ). The column eluate was monitored at 214 nm using Biologic Quadtec detection. Collected fractions were analysed by SDS-PAGE and western blotting.

7.2.2 Immunoaffinity isolation of peptide epitopes

Anti-SmB′/B or anti-U1A antibodies were immunoaffinity purified from western blot strips as described in section 3.2.10 using human U1 snRNP separated by SDS-PAGE as the antigen source. Antibodies eluted from the nitrocellulose strips were then prepared for immunoprecipitation by coupling to protein A agarose beads as described in section 3.2.8.

Human U1 snRNP was separated by SDS-PAGE and Coomassie stained SmB′/B and U1A bands were excised and the gel pieces digested with trypsin according to section 3.2.17. The tryptic peptides were extracted, dried then resuspended in PBS before being incubated with mixing for 2 hours at ambient temperature with either anti-SmB′/B protein A matrix or anti-U1A protein A matrix. The matrix was washed in PBS and the bound peptides eluted with 20 μL of 2.5 % v/v formic acid. Peptides were further purified using ZipTips (Millipore, Bedford, USA) according to the manufacturers instructions before being analysed by mass spectrometry as in section 3.2.18.

7.3 Results

7.3.1 Reactivity of anti-RNP serum with U1 snRNP in western blot

Human U1 snRNP contains multiple antigens and therefore western blotting was used to examine the fine specificities of anti-RNP sera. Forty anti-RNP sera were tested using western blot strips (see supplement 1), and the majority were found to react with SmB′/B, but without any reaction to SmD (Figure 7.1).

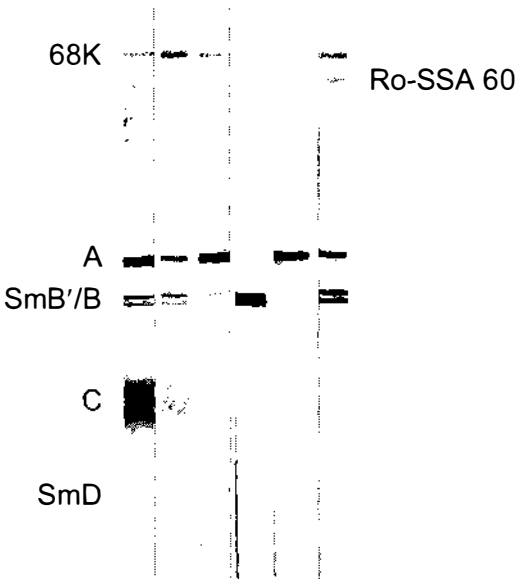

Figure 7.1 Reactivity of some anti-RNP sera with U1 snRNP western strips

Western blot nitrocellulose strips consisting of five ENA antigens including human U1 snRNP were prepared as described in Supplement 1. Strips were immunoprobed with sera designated anti-RNP.

To examine the possibility that the apparent reactivity of anti-RNP sera with SmB′/B was related to the purity of the U1 snRNP antigen preparation, the antigen was further characterised using 2D-gel electrophoresis.

7.3.2 2D-gel electrophoresis of human U1 snRNP

Human U1 snRNP purified from HeLa cell nuclei was made 8 M in urea, 1 % w/v in triton x100 and 10 mM in DTT before it was mixed with an equal volume of 1:1 TRIzol®/chloroform. The aqueous phase containing RNA was removed

and the phase interface, containing precipitated U1 snRNP proteins, was harvested. The protein pellet was washed with 10 volumes of ice-cold acetone and then resuspended in 8 M urea, 2.5 % w/v CHAPS, 10 mM DTT and 2 % v/v pH 3-10 ampholyte. 2D-gel electrophoresis was performed according to sections 3.2.13 and 3.2.14, and the gel was silver stained (Blomberg *et al.*, 1995).

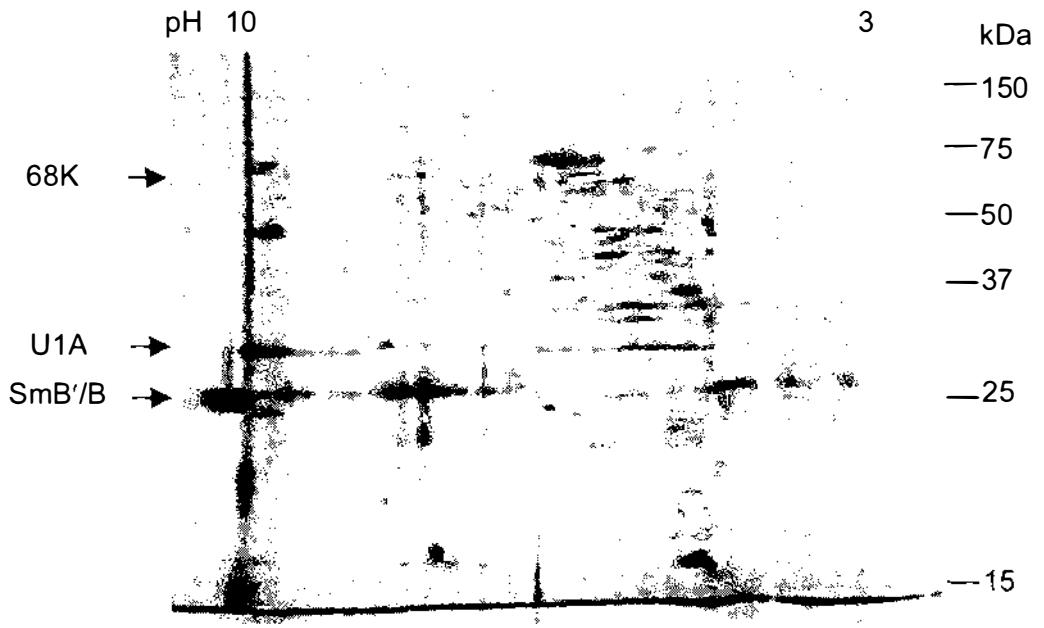

Figure 7.2 2D-gel electrophoresis of human U1 snRNP

RNA was removed from U1 snRNP and the proteins were separated by 2D-gel electrophoresis on a 7 cm pH 3-10 IPG strip followed by SDS-PAGE. The gel was silver stained. The positions of the SmB′/B, U1A and 68K proteins are annotated.

Purified human U1 snRNP, when analysed by 2D-gel electrophoresis, consisted of many more proteins than observed by 1D SDS-PAGE (Figure 7.2). Spots observed in 2D could consist of protein isoforms, but some will be contaminant proteins co-purifying with U1 snRNP. A large number of proteins were clustered between 37-90 kDa at approximate pI 7.5-5.0. More interestingly, however, are the number of proteins that appear in the 25-30 kDa region, which incidentally includes the SmB′/B protein.

7.3.3 Separation of U1 snRNP proteins on RP-HPLC

Non-U1 snRNP proteins co-migrating with SmB′/B on western blot, could be responsible for the incongruous reactivity observed with some anti-RNP sera. U1 snRNP was separated, and the SmB′/B protein purified by RP-HPLC. Fractions were analysed by SDS-PAGE and western blot. Proteins were detected using silver staining and immunoprobing respectively.

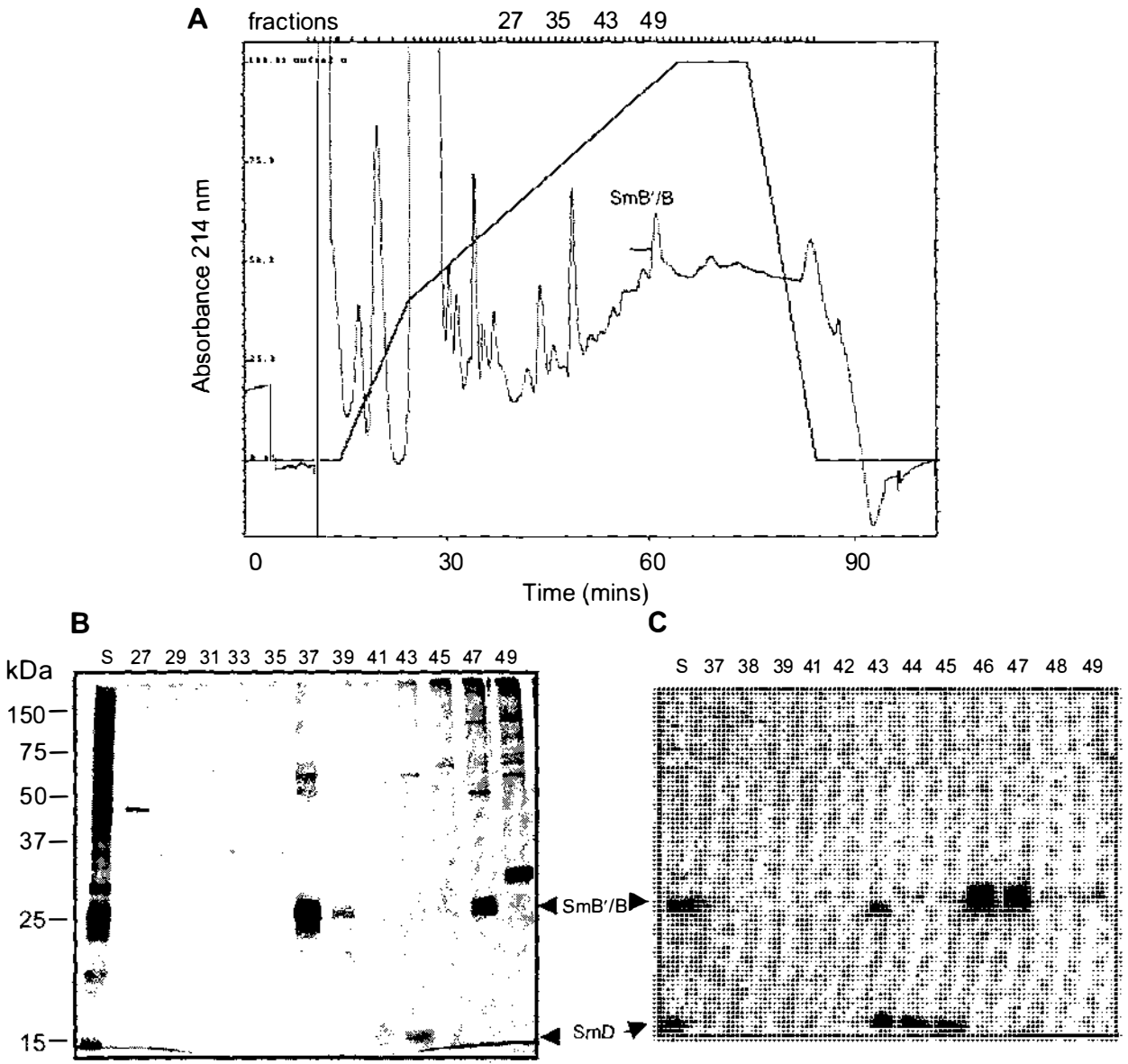

Figure 7.3 SmB′/B purification by RP-HPLC

Human U1 snRNP was denatured in 8 M urea, 100 mM DTT and the protein components separated using C_{18} RP-HPLC with a 0-50 % isopropanol, 0.01% TFA linear gradient. Collected fractions were analysed by SDS-PAGE and western blot. **A**:UV (214 nm) absorption profile of the HPLC eluates. The analysed fraction range and the eluted peak corresponding to SmB′/B are annotated. **B**: SDS-PAGE analysis with silver stain detection of alternate fractions 27-49. S refers to the loaded sample. **C**: Immunoblot analysis of the Sm containing fractions using anti-Sm serum.

A good fractionation was achieved using RP-HPLC. The SmB′/B protein was separated from the other U1 snRNP component proteins at approximately 40-45 % isopropanol, appearing mostly in fractions 46 and 47 (Figure 7.3). The U1A protein eluted later in fraction 49, whereas, the SmD proteins eluted earlier than SmB′/B being collected in fractions 41-45. Western blotting showed that only the 16 kDa protein in fractions 43-45 is reactive with anti-Sm serum. In addition to SmD, anti-Sm serum recognised a protein in fraction 43 which migrated slightly below SmB′/B on western blot (as indicated by the arrow Figure 7.3). Interestingly, fraction 37 contained a protein with a similar molecular weight to SmB′/B on SDS-PAGE that was not reactive with anti-Sm serum. This protein co-eluted with some higher molecular weight proteins and so could be part of a larger complex.

The reactivity of the purified SmB′/B with anti-RNP serum was tested on western blot (Figure 7.4)

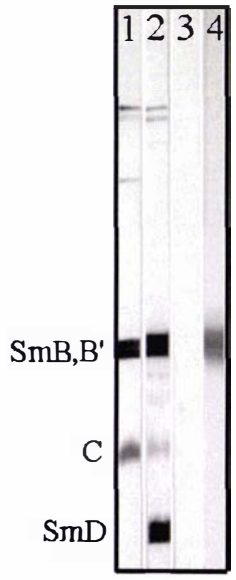

Figure 7.4 Reactivity of anti-RNP serum with purified human SmB′/B
The reactivity of anti-RNP and anti-Sm sera with intact human U1 snRNP and the RP-HPLC purified SmB′/B was tested on western blot. Lanes: **1**, human U1 snRNP probed with anti-RNP serum; **2**, U1 snRNP probed with anti-Sm serum; **3**, RP-HPLC purified SmB′/B probed with anti-RNP serum; **4**, RP-HPLC purified SmB′/B probed with anti-Sm serum.

The SmB′/B in intact U1 snRNP reacted strongly with anti-RNP serum, whereas RP-HPLC purifed SmB was not recognised by the same serum, in contrast to the anti-Sm serum which reacted with both SmB′/B preparations.

As the SmB′/B-like protein reacting with anti-RNP was not identified amongst the U1 snRNP proteins separated by RP-HPLC, an alternative approach to identify it was made.

7.3.4 Mass spectrometry of affinity purified SmB′/B tryptic peptides

U1A tryptic peptides eluted from the anti-U1A affinity matrix were analysed by mass spectrometry and the identified peptides are shown in Figure 7.5.

```
1   MAVPETRPNH TIYINNLNEK IKKDELKKSL YAIFSQFGQI LDILVSRSLK
51  MRGQAFVIFK EVSSATNALR SMQGFPFYDK PMRIQYAKTD SDIIAKMKGT
101 FVERDRKREK RKPKSQETPA TKKAVQGGGA TPVVGAVQGP VPGMPPMTQA
151 PRIMHHMPGQ PPYMPPPGMI PPPGLAPGQI PPGAMPPQQL MPGQMPPAQP
201 LSENPPNHIL FLTNLPEETN ELMLSMLFNQ FPGFKEVRLV PGRHDIAFVE
251 FDNEVQAGAA RDALQGFKIT QNNAMKISFA KK
```

Peptide	Observed mass	delta	Sequence
61 - 70	1047.66	0.12	EVSSATNALR
71 - 83	1603.79	0.05	SMQGFPFYDKPMR
124 - 152	2727.47	0.07	AVQGGGATPVVGAVQGPVPGMPPMTQAPR
239 - 261	2511.53	0.26	LVPGRHDIAFVEFDNEVQAGAAR
244 - 261	1989.00	0.06	HDIAFVEFDNEVQAGAAR

Figure 7.5 U1A tryptic peptides identified in anti-U1A affinity elution
Mass spectroscopic analysis of immunoaffinity purified tryptic peptides of U1A. The identified peptides are highlighted in red.

These peptides were obviously derived from U1A with a 26 % coverage and a match score of 75.

In an attempt to identify the seemingly different autoantigen, in human U1 snRNP, that reacted with anti-RNP serum, an anti-RNP matrix was used to isolate specific tryptic peptides derived from the proteins migrating in the SmB region on SDS-PAGE. Peptides isolated using this method were analysed by MALDI mass spectrometry, and the peptides were mapped by MASCOT. Intriguingly, they matched to the 28 kDa human replication element protein

(HREP) (Figure 7.6). The peptide coverage was low at only 16 % and the match score was 37.

```
1   MDLCKNRLVS GGRDCQVKVW DVDTGKCLKT FRHKDPILAT RINDTYIVSS
51  CERGLVKVWH IAMAQLVKTL SGHEGAVKCL FFDQWHLLSG STDGLVMAWS
101 MVGKYERCLM AFKHPKEVLD VSLLFLRVIS ACADGKIRIY NFFNGNCMKV
151 IKANGRGDPV LSFFIQGNRI SVCHISTFAK RINVGWNGIE PSATAQGGNA
201 SLTECAHMRL HIVGHLPASR LPVAAVQPMT GGMAPTTAPT HVLAMLILFS
251 GV
```

Peptide	Observed mass	delta	Sequence
19 - 29	1320.6640	0.0024	VWDVDTGKCLK
58 - 68	1296.6860	0.9568	VWHIAMAQLVK
117 - 127	1303.8190	0.0570	EVLDVSLLFLR

Figure 7.6 Identifying anti-RNP serum autoantigen in human U1 snRNP
Mass spectroscopic analysis of immunoaffinity purified tryptic peptides of the SmB′/B region of U1 snRNP separated on SDS-PAGE. The identified peptides are highlighted in red.

7.4 Discussion and Future Work

The use of 2D-gel electrophoresis highlighted the presence of many proteins other than the expected U1 snRNP proteins and their isoforms. Rappsilber *et al.* (2002) carried out a comprehensive 2D-gel electrophoresis and mass spectrometric study on the spliceosome and identified 311 proteins that co-purify with splicing complexes. The proteins observed in this study could in fact be involved in the splicing process despite not being directly associated with the U1 snRNP complex but it would need a large time commitment to confirm this, which was not possible within the scope of the present study. A large number of proteins shared the same molecular weight as SmB′/B, even in the purified U1 snRNP. Most immunoblotting systems, described in the literature for the detection of anti-RNP sera specificities, use unfractionated HeLa cell nuclear extracts as their antigen source (Verheijen *et al.*, 1993). These results show that it is possible, indeed even probable that an incorrect antibody specificity could be assigned, which is the most plausable explanation for anti-RNP sera reacting with SmB′/B in western blot. Testing the reactivity of purified SmB′/B with anti-RNP sera was attempted to clarify this issue.

SmB′/B was separated from other contaminating proteins using RP-HPLC, and its elution profile, together with that of U1A and the SmD proteins, was consistent with the findings of Williams *et al.* (1988). SmD proteins may have been fractionated into SmD1, D2 and D3 subunits. As only 17 % of anti-Sm sera contain antibodies to SmD2, it is likely that the Sm-like protein eluted in fraction 41 (which was not detected by western blot) could be SmD2 (Figure 7.3B). Purified SmB′/B reacted well with anti-Sm serum but was not detected with anti-RNP serum. This serum, however, did not detect any other protein in the 28 kDa molecular weight range, for example, fraction 37. A more extensive analysis of both the 2D-gel and RP-HPLC separated proteins using immunochemical and/or mass spectrometry should result in the identification of the anti-RNP reactive antigen.

Immunoaffinity purification of trypsin digested antigen successfully identified the U1A protein, although the epitopes matched were not the sequences most commonly identified as epitopes in mapping studies (James and Harley, 1996; Barakat *et al.*, 1991). In part, this finding can be explained by the use of trypsin which cleaves on the C-terminal side or lysine and arginine residues. Many of the immunodominant epitopes in U1A are within lysine rich sequences and hence would be destroyed by trypsin.

This method is dependent, therefore, on the epitopes not containing critical lysine or arginine residues which limits the number of peptides detected. The preliminary identification of the HREP needs to be confirmed because of the low overall match of peptides. It is interesting, although perhaps coincidental, that HREP (Swiss Prot accession number O43848) has a calculated molecular weight of approximately 28 kDa and that the protein exists as two variants each with slightly different molecular weights. The HREP human specific gene was first identified as being involved in a group of hereditary chronic motor and sensory disorders known as the Charcot-Marie-Tooth neuropathies (Kennerson *et al.*, 1995). The genetic causes of these diseases include point mutations to complete gene deletion.

Intriguingly, the deletion of one of the duplicated SMN genes, which are involved in U snRNP biogenesis, is the cause of another motor neuropathy, spinal muscular atrophy (Selenko *et al.*, 2001). The function of HREP is not clear although it does belong to the WD repeat protein family and therefore may have a role in mediating protein:protein, protein:nucleic acid interaction (Neer *et al.*, 1994). There is no evidence that connects this protein to a splicing or RNA processing function, although a number of WD proteins are associated with messenger (Lauber *et al.*, 1997) and ribosomal RNA splicing (Dragon *et al.*, 2002). It should be reiterated that the identification of HREP is preliminary and requires thorough verification using a combination of proteomic approaches.

This study aimed to clarify the interaction of some anti-RNP sera with SmB′/B in western blot. Purification of SmB′/B by RP-HPLC demonstrated that the

representative anti-RNP serum used, reacted with intact U1 snRNP but failed to identify pure SmB′/B on western blot. The HREP protein, has been tentatively proposed as a candidate antigen which co-migrates with SmB′/B on SDS-PAGE.

Chapter Eight

Overall Summary and Future Work

This thesis compares the composition of the spliceosomal U1 snRNP complex derived from bovine and human sources with the overall aim of authenticating the use of bovine U1 snRNP and constituent proteins as legitimate antigens in autoimmune disease diagnostics. Several techniques were used to achieve this goal.

U1 snRNP was purified from bovine calf thymus using a combination of ion exchange and immunoaffinity methods (Chapter 4). Using antibodies immuno-affinity purified against individual human U1 snRNP component proteins, the composition of bovine U1 snRNP was determined. SDS-PAGE analysis showed that bovine U1A and SmD proteins shared the same molecular weight as their human counterparts, whereas the U1C antigen could not be identified in the bovine complex. Secondly, the bovine 68K antigen appeared as a truncated polypeptide cluster that migrated between 30-36 kDa on SDS-PAGE.

Further characterisation of the 68K antigen derived cluster revealed that the bovine 68K protein, compared to the human protein, was dephosphorylated, and that it was glycosylated. SSB/La, a protein responsible for RNA polymerase III transcript termination, and an autoantigen in SLE and Sjögren's syndrome, has been shown to undergo apoptosis induced proteolysis, and dephosphorylation by protein phosphatase 2A (Rutjes *et al.*, 1999). It is proposed that the 68K antigen is similarly modified during cell death. Several residues within the 68K protein have the potential to be reversibly modified by both phosphorylation and O-glycosylation. It is therefore possible that the dephosphorylated sites may in fact be alternately modified by O-GlcNAc. Dephosphorylation and/or glycosylation may be critical modifications in the creation of a neoepitope thought to increase the antigenicity of the 68K apoptotic fragment (Greidinger *et al.*, 2002). Further work is required to identify these potential glycosylation sites and to confirm the identity of the glycan structure using the BEMAD method devised by Wells *et al*. (2002b). The impact of these modifications on the antigenicity of the 68K protein apoptotic fragment may provide some insight into how the autoimmune response is initiated.

Mass spectrometry was used to identify the presence of a truncated form of SmB in bovine U1 and non-U1 snRNP. The matching of the tryptic peptides to both human and bovine sequences showed complete homology of SmB from bovine and human sources. The 12 kDa peptide consisted of the N-terminal region with the immunodominant polyproline and sDMA sequences removed. Despite the truncation, SmB remains associated with the other Sm proteins and RNA to form a 125 kDa complex, inferring that its RNA binding domain and Sm motifs are intact.

The antigenicity of the SmB fragment is somewhat different to the intact human SmB′/B due to the loss of immunodominant epitopes. Interestingly, some anti-Sm sera remained reactive to the SmB fragment but non of the anti-RNP sera tested were reactive in western blot. Ohosone *et al.* (1992) proposed that an anti-RNP specific epitope was located in the SmB N-terminal domain, however, this finding could not be confirmed in this study. The diagnostic significance of antibodies against the truncated SmB should therefore be examined in more detail.

Antigen selection is critical to the diagnostic and prognostic performance of an assay. For example, a high titre of antibodies against the 68K protein is considered to be a key criterion in the diagnosis of MCTD, and the titre is indicative of a greater risk of pulmonary complication (Greidinger e*t al.*, 2006). However, using the U1 snRNP complex as the antigen limits the ability of the assay to make this important differentiation. In order to address this perceived need for assays to use individual U1 snRNP component antigens, a method for the purification of commercially viable quantities of 68K antigen from bovine U1 snRNP was developed (Chapter 5). U1 snRNP associated proteins were shown to have different affinities for the U1 snRNA moeities, with U1A being the first to be dissociated. Intriguingly, the U1A protein removed during the first CHT step, remained associated with one of two populations of RNA, one that associated mostly with U1A, and the other that associated mostly with SmD proteins. The significance of this finding is not clear although it may reflect the presence of U1 snRNP complexes with different compositions due to the lack of synchrony of

either snRNP biogenesis or cell death. U1A is also known to exist in a snRNP-free complex (SF-A) where it adopts a role in controlling polyadenylation reactions (O'Connor *et al.*, 1997). Specific autoantibodies to this form of U1A have been reported (Faig and Lutz, 2003) and sera which react with purified U1A, but not the intact U1 snRNP complex, have been identified in our laboratory.

The SmD proteins were separated from the U1 snRNP complex into two fractions, SmD1 and SmD2/D3. The use of these proteins, for the differentiation of anti-Sm patient sera specificity, was hindered by contamination with the U1 snRNP specific protein. Further purification is required before the diagnostic potential of the individual SmD proteins can be assessed. Fortunately, SmD proteins could be exchanged into a non-denaturing buffer and hence could refold correctly, enabling the detection of SmD conformational epitopes (James *et al.*, 1994a).

Bovine 68K antigen was purified free from Sm and U1A protein, and U1 snRNA contamination. It was successfully used to differentiate between sera containing antibodies to the 68K and other snRNP component proteins. This purified antigen was shown to be superior to recombinant 68K in its diagnostic performance. Authentic post-translational modification of the purified 68K antigen could be the source of this superiority, although r68K's lack of a RS1 domain could equally influence its antigenicity. Pelsue and Agris (1994) showed that structure dependent epitopes exist within the RS1 domain. Attempts were made to examine the influence of the conformation of the 68K protein on anti-RNP antibody detection, but the 68K protein was not stable in non-denaturing buffer. There are a number of reasons why denatured proteins precipitate when exchanged into a non-denaturing buffer. In this study it was suggested that as refolding occurs, the interaction of coiled-coil domains within the protein are responsible for its instability. It was also proposed that the coiled-coil structure within the RS1 domain, mediates the interaction of 68K with a number of splicing factors. This structural motif may also contain conformation dependent autoepitopes.

It cannot be assumed that U1 snRNA is a passive component within the U1 snRNP autoimmune complex, as anti-U1 snRNA autoantibodies are present in some patient sera. Bovine U1 snRNA was found to be truncated compared to its intact human equivalent, but the impact of this truncation on U1 snRNP antigenicity was not determined. As an extension to this study on purified snRNP components, it would be interesting to reconstitute U1 snRNA with 68K, then to test whether such a complex produces an improved antigen. It is speculated that by mixing U1 snRNA with denatured 68K, before buffer exchange, may stabilise the 68K protein, allowing it refold in a non-denaturing environment.

The overall aim of chapter 4 and 5 in this study, was to characterise the bovine U1 snRNP antigens both biochemically and immunologically. Particular emphasis was given to verifying bovine U1 snRNP, and its constituent proteins, as legitimate antigens for use in autoimmune disease diagnosis. This work showed that despite the differences between human and bovine U1 snRNP composition, their diagnostic performance was identical. In other words, neither the truncation of either 68K or SmB, nor the loss of U1C protein, affected the detection of anti-RNP or anti-Sm antibodies in patient sera. Furthermore, purified bovine 68K antigen was a superior antigen to its recombinant equivalent, demonstrating that factors other than primary sequence appear to influence autoantigenicity. Although the aim of this part of the research project was achieved, sera from patients who have had a thorough clinical evaluation and have undergone the appropriate follow-up should be tested against these bovine antigens. This would ensure that the relationship between antibodies to truncated SmB or the other snRNP components, and a particular clinical finding or disease prognosis, could be characterised.

The factors contributing to the truncation of the bovine 68K were further investigated, not only to determine the biochemistry of the antigen cleavage but also with respect to control of the thymus extraction process (Chapter 6). The influence of thymus processing on U1 snRNP and non-U1 snRNP purification was examined, and was found to have little impact on the final product unless the thymus was allowed to thaw for at least 20 hours. The truncation of the 68K

antigen was, therefore, considered to occur during the events between *post-mortem*, thymus excision and freezing.

Cleavage of the 68K protein was analysed using mass spectrometry of 68K tryptic peptides, and using chymotryptic fragment analysis (Woppmann *et al.*, 1993), which showed that the protein was cleaved only in the C-terminal region, with the N-terminus, including the predicted N-terminal acetylated residue, remaining intact. Intriguingly, analysis of the chymotryptic digestion pattern on SDS-PAGE suggested that it was the C-terminal RS2 domain that had been cleaved. Using the molecular weights of the chymotryptic fragments from SDS-PAGE, the estimated cleavage sites were at the N-terminal side of residues 316, 321 and 329, equating to calculated molecular weights of 38, 38.5 and 39.2 kDa respectively, all of which were higher than the 30-36 kDa range observed in SDS-PAGE. The precise sites of truncation, should in future, be determined unambiguously using mass spectrometry.

The cause of the 68K protein truncation is not clear. During apoptotic cell death, 68K undergoes caspase-3 cleavage, N-terminal of residue 342, to produce a single 40 kDa polypeptide. This protease may contribute to, but can not be entirely responsible for the 68K cleavage pattern observed in this study. Pacheco *et al.* (2005) investigated the effect of necrotic cell death on autoantigen proteolysis and showed that cathepsin L cleaved topo 1 to form 70 and 45 kDa fragments. Similar fragments were observed in topo 1 purified from bovine thymus during this study. In order to investigate mechanisms for 68K protein truncation, therefore, intact human U1 snRNP was exposed to a number of conditions known to occur during necrotic cell death, including cathepsin L. Cathepsin L was shown to cleave the 68K antigen, although the fragments produced did not correlate with the cluster observed in the bovine antigen. Exposure of the 68K antigen to pH 6.5 and 37 °C, in the absence of protease, resulted in a fragmentation pattern which more closely resembled that of the bovine antigen. These results infer the existence of an alternative, non-enzymatic mechanism being responsible for this 68K truncation. Two mechanisms are proposed for 68K truncation. The first is metal-induced

oxidative cleavage which occurs because of hypoxia followed by an influx of oxygen, which has been experimentally shown to occur (Casciola-Rosen *et al.*, 1997). A second mechanism was suggested by the results from this work, whereby, exposure of U1 snRNP to a necrotic tissue environment, of low pH and elevated temperature, induced autocatalytic truncation of 68K within susceptible acid-sensitive amide bonds. Clearly, further work is necessary to determine the exact cleavage sites of bovine 68K and whether this is consistent with autocatalysis.

The objective of chapter 6, in this study, was to investigate the impact of thymus processing on the appearance of bovine U1 snRNP antigen and to determine a probable cause of the 68K protein truncation. Bovine U1 snRNP purified from thymus tissue was shown to have a stable profile and the affects on the antigen complex occur prior to the purification process. Enzymic and environmental factors, during necrotic cell death, are proposed to cause the observed truncation pattern. The scope of the present study concentrated on the use of frozen bovine thymus, in future work, fresh bovine tissue should be used to determine the composition of intact bovine U1 snRNP, and to examine the events leading to antigen truncation.

Considerable debate surrounds the reactivity of both anti-Sm and anti-RNP sera with human SmB′/B in western blot. This section of study extends from the finding that anti-RNP sera do not react with truncated bovine SmB despite the presence of a proposed anti-RNP specific epitope. This work aimed to establish the SmB epitopes recognised by anti-RNP sera (Chapter 7). 2D-gel electrophoresis of human U1 snRNP showed a number of proteins which share the molecular weight with SmB′/B and hence would co-migrate on SDS-PAGE. Further purification of the U1 snRNP complex, by RP-HPLC, revealed that anti-RNP serum did not detect purified SmB′/B, despite reacting in western blot with unpurified U1 snRNP. In order to determine what may be reacting with anti-RNP antibodies, an immunoaffinity technique, coupled with mass spectrometry, was developed. Unexpectedly a WD40 motif protein, HREP, was tentatively identified rather than SmB. This finding represents the first suggestion that anti-

RNP sera may not be reacting with SmB′/B. Further work, using this proteomic approach, is required to verify this result and to establish whether this is a common specificity amongst anti-RNP sera.

Supplementary work in this thesis showed how U1 snRNP and other antigens purified from bovine thymus were used to develop two immunodiagnostic techniques for the analysis of multiple autoantigen specificities in patient sera. Both techniques proved highly sensitive and specific, and were used extensively to characterise many of the sera used during the course of this study.

This body of work has demonstrated that the specificity of autoantibodies for spliceosomal U1 snRNP components is complex. The 68K protein is highly prone to modification as a consequence of *post-mortem* cell death. Its inactivation by truncation, via various means, dephosphorylation and possibly glycosylation, confirm its pivotal role in the initiation of splicing events and the cessation of mRNA production. These modifications appear to enhance 68K's performance as a diagnostic reagent, and thus highlight its potential role in the breaking of immune tolerance during the initiation of an autoimmune response. The recognition of SmB′/B by anti-RNP sera in western blot remains contentious but some of the findings in this study may help to clarify the controversy. One thing is clear, however, that inspite of the many differences in the bovine U1 snRNP purified from thymus, compared to the human equivalent, these studies have shown that bovine U1 snRNP can be legitimately used as a source of antigen in human autoimmune disease diagnostic procedures.

Supplement 1

Development of a Western Blot-Based Autoimmune Diagnostic

S1.1 Introduction

Western blotting is recognised as a useful immunodiagnostic technique. Complex autoantigens such as U snRNPs can be separated allowing the individual specificities to be detected (Habets *et al.*, 1990). The sensitivity and specificity of Western blotting for the detection of SSB/La, Scl-70 (topo I) and Jo-1 can be superior to other solid phase immobilisation diagnostics (Bizarro *et al.*, 1998; Bizarro *et al.*, 2000).

Current commercially available western blot strips rely on the separation of complex protein mixtures such as a HeLa cell extract. In these cases, interpretation of specificity is difficult because of the relative abundance of antigens and the many proteins present. In addition, ENA detection using western blotting is limited due to the loss of antigen conformation on the nitrocellulose strips. Anti-Ro-SSA antibodies are relatively common and many of these antibodies exclusively recognise conformational epitopes, and therefore, are not detected by western blot (Itoh *et al.*, 1992).

The aim of this supplementary study was to design a western blot strip for the specific and sensitive detection of the major ENA. Immunoblot method parameters were systematically altered to optimise the detection of anti-Ro-SSA conformational epitopes, and optimum conditions for the separation, electro-transfer and detection of purified ENA antigens were determined.

S1.2 Experimental Procedures

S1.2.1 Conformation dependence of Ro-SSA antigen epitopes

Conformational dependence of epitopes of Ro-SSA antigen (AroTec Diagnostics Limited, NZ) was examined by denaturation of the antigen by SDS-PAGE and immobilisation of the individual proteins onto nitrocellulose membrane by western blotting. The nitrocellulose was cut into 3 mm strips as described in Chapter 3. Native Ro-SSA antigen was also coated on microtitre ELISA plates at 0.1 μg per well. Both immunoassay formats were probed with a number of anti-Ro-SSA patient sera, followed by an alkaline phosphatase conjugated secondary antibody (Jackson Immunoresearch Inc., West Grove, USA) diluted 1/4000. Western blots were developed using NBT/BCIP reagent, whilst the ELISA plates were developed with 1 mg/mL *para*-nitrophenol phosphate and the rate of absorbance change at 405 nm was measured. Western blot strips were digitised using a gel documentation instrument (Alphaimager, Alpha Innotec, San Diego, USA) and the intensity of NBT staining was analysed using Alphaease v. 4 densitometric software.

The same experiment was carried out using Scl-70 (topo I) antigen, which is not known to have conformational dependent epitopes, in place of Ro-SSA.

S1.2.2 Optimising protein separation on SDS-PAGE

Three 40 % w/v acrylamide monomer stock solutions were prepared containing 2.6, 3.3 and 4.0 % w/w bisacrylamide cross-linker. Using these solutions 10, 11.5 and 13 % acrylamide resolving gels were prepared and overlaid with 4 % acrylamide stacking gels. Five antigens, Scl-70, human U1 snRNP, Jo-1, Ro-SSA and SSB/La were prepared and separated by SDS-PAGE and then western blotted. Proteins were visualised by immunoprobing with antigen specific sera, and the relative migration of each antigen was calculated.

S1.3 Results

S1.3.1 Correlation between ELISA and western blot methods

ELISA absorbance data, expressed as the rate of optical density change per minute at 405 nm (mOD/min), was plotted against the western blot data for the detection of anti-Ro-SSA (Figure S1.1A) and anti-Scl-70 (Figure S1.1B) to determine how well these methods correlate.

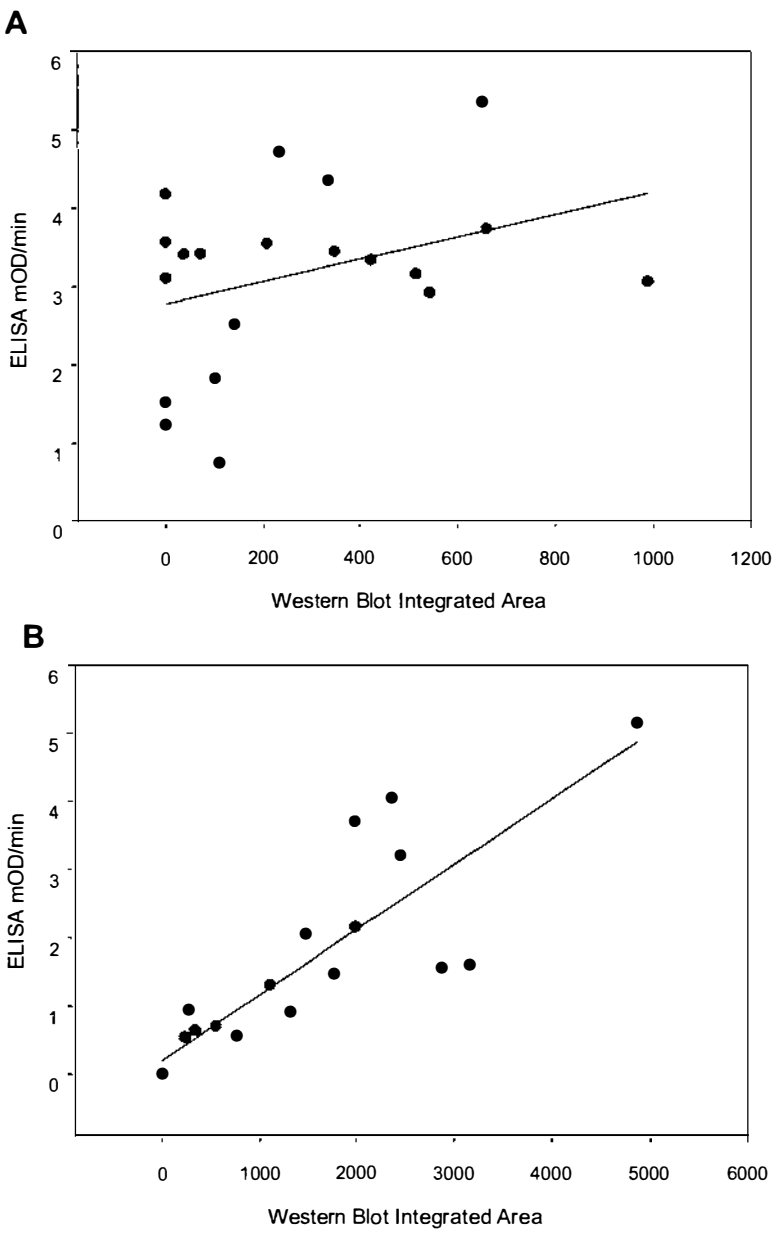

Figure S1.1 Autoantibody detection using ELISA and western blot

Detection of autoantibodies in cohorts of patient sera (n=20) against antigen immobilised either on polystyrene microtitre ELISA plates or on nitrocellulose membrane (western blot) was compared for two autoantigens: **A**. Ro-SSA; **B**. Scl-70.

These two techniques for the detection of anti-Ro-SSA antibodies correlate very poorly. Little or no anti-Ro-SSA response was observed in western blot for greater than 50 % of the sera tested, despite a strong response in ELISA. Sera not responding in western blot are hence referred to as non-blotting sera. Anti-Scl-70 detection by western blot and ELISA correlate well.

The response of anti-Ro-SSA sera to western blotted Ro-SSA antigen was examined further. A non-blotting anti-Ro-SSA patient serum was incubated with western blotted Ro-SSA for between 2 and 24 hours. A time course of anti-Ro-SSA response was plotted (Figure S1.2). Increased incubation time enhances the recognition of Ro-SSA in western blot, although this response reaches a plateau after 24 hours.

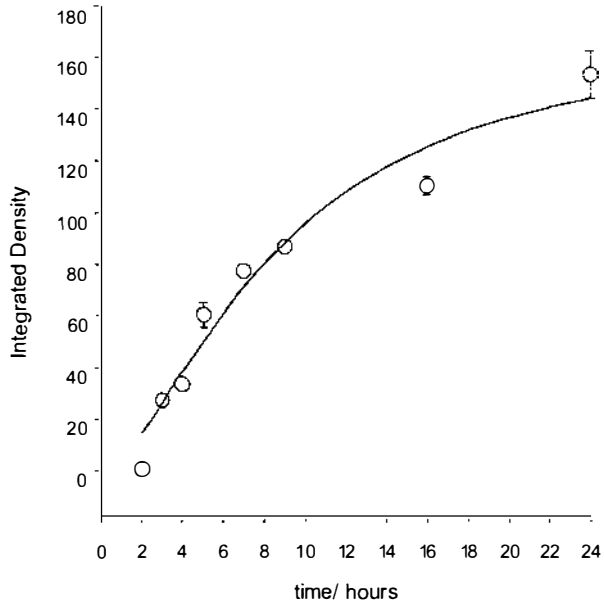

Figure S1.2 Time-dependent response of anti-Ro-SSA to denatured Ro-SSA

A non-blotting anti-Ro-SSA serum was incubated for various times with western blotted Ro-SSA, in triplicate.

The influence of the amount of Ro-SSA antigen applied to SDS-PAGE and western blots on anti-Ro-SSA detection was also examined (Figure S1.3). The response of the good-blotter anti-Ro-SSA patient serum reached plateau with approximately 1 μg Ro-SSA, whereas, the non-blotter serum response remained linear with respect to Ro-SSA amount.

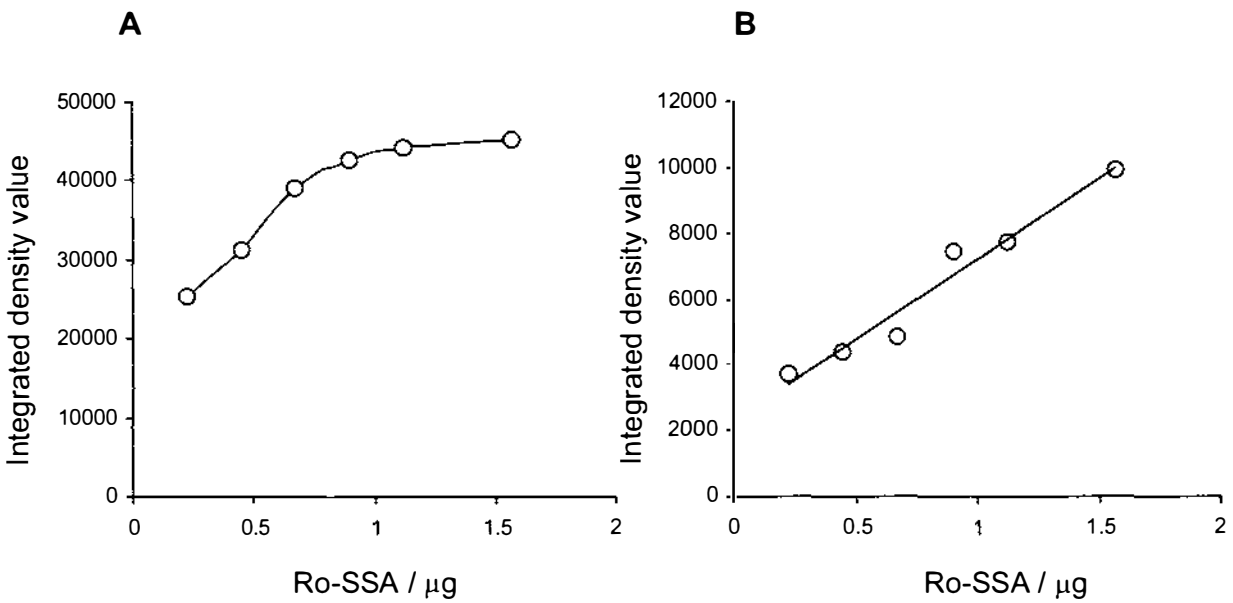

Figure S1.3 Influence of Ro-SSA amount on detection by western blot

Incremental amounts of Ro-SSA antigen were loaded on SDS-PAGE and western blot. Blots were incubated with anti-Ro-SSA patient sera for 16 hours. **A.** Good-blotter anti-Ro-SSA serum; **B.** Non-blotter anti-Ro-SSA serum.

Increased amounts of Ro-SSA together with an increase in the incubation time with patient sera were used in the western blot detection of anti-Ro-SSA antibodies in patient sera. This enhanced detection protocol was compared directly with the standard protocol (Figure S1.4), and showed that the detection rate of anti-Ro-SSA sera was significantly increased, without false-positive detection due to non-specific binding (results not shown).

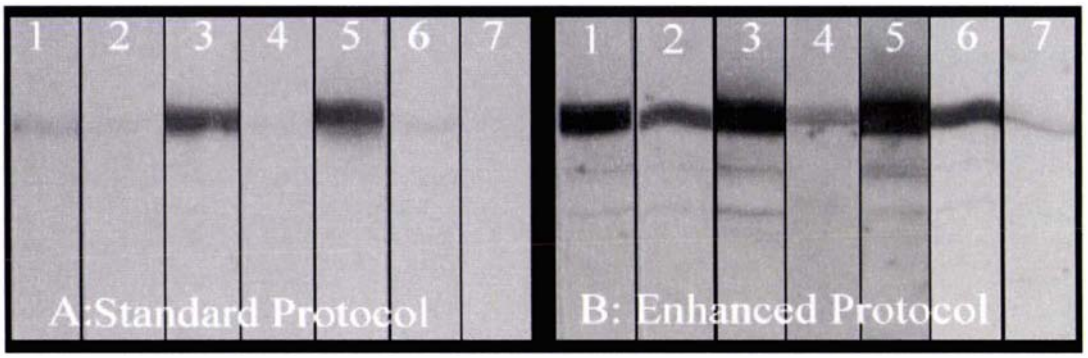

Figure S1.4 Detection of anti-Ro-SSA on western blot

Anti-Ro-SSA patient sera were incubated with Ro-SSA antigen, western blotted onto nitrocellulose and cut into strips. **A**. Sera incubated for 2 hours with nitrocellulose strips blotted with 0.1 μg Ro-SSA/mm membrane; **B**. Sera incubated for 16 hours with nitrocellulose blotted with 0.22 μg Ro-SSA/mm.

S1.3.2 Optimised separation of 12 autoantigens in western blot

Protein separation is critical to the successful application of Western blotting as a multiplexing platform for the detection of multiple antigen specificities. To determine the effect of resolving gel acrylamide concentration on antigen separation, the calculated relative migration data was plotted (Figure S1.5). Resolution of individual antigens and the spread of these bands along the blot length are the main criteria for an effective separation. A 10 % total (T) acrylamide resolving gel consistently separated all the component antigens, although the low molecular weight proteins migrated very close to, and in some instances beyond, the dye front. This caused the SmD protein to appear diffuse and also introduced the risk of SmD migrating off the gel. The cross-linker (C) (bis-acrylamide) concentration had a significant effect on the resolving capacity of both 11.5 and 13 % acrylamide gels. The best separation was achieved with 11.5 %T, 4 %C. All proteins were well resolved and the relative migration ranged from 0.14 – 0.96 which demonstrated high usage of the available gel length.

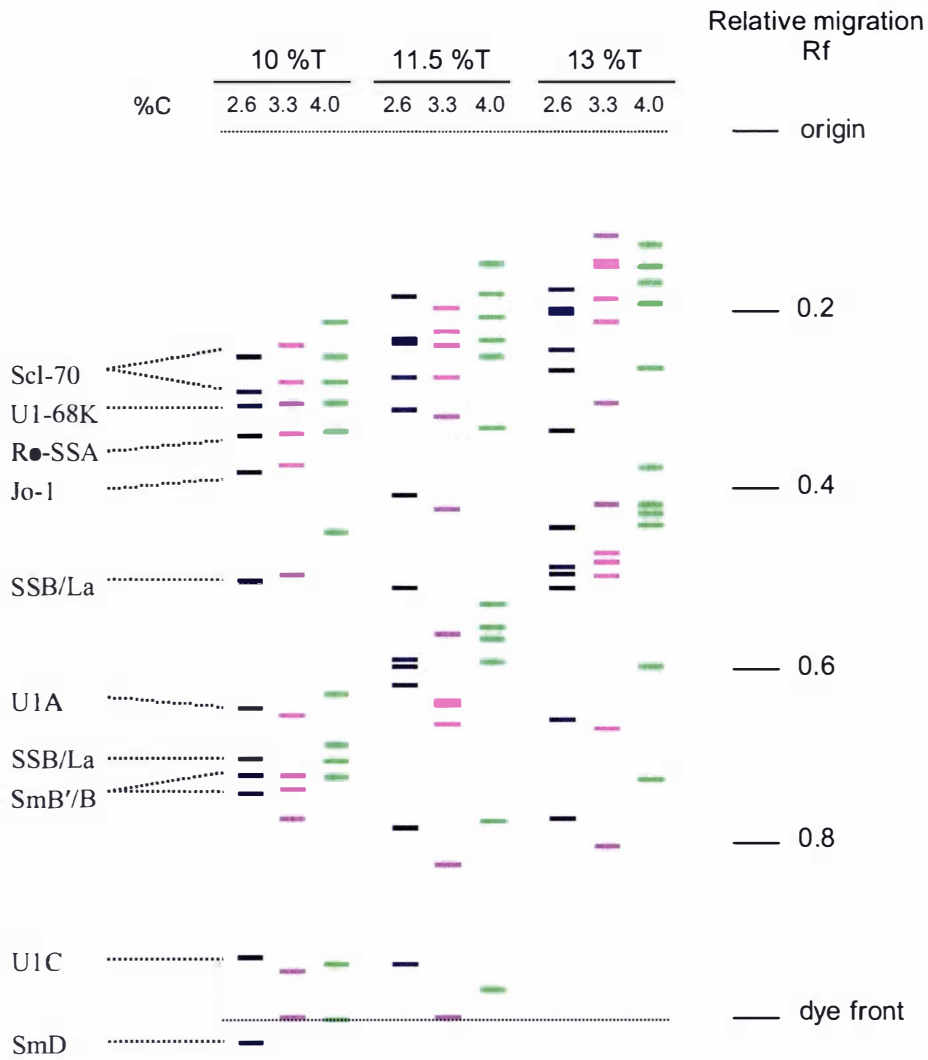

Figure S1.5 Influence of total acrylamide and cross-linker concentration on antigen separation

Twelve protein antigens (annotated in the far left column) were separated on SDS-PAGE and western blot with 10 %, 11.5 % and 13 % total acrylamide concentration resolving gels containing combinations of 2.6 % (blue), 3.3 % (pink) and 4 % (green) cross-linker. The relative migration values for each antigen are plotted. %T = total acrylamide monomer, %C = cross-linker concentration.

The amount of each antigen required for loading on SDS-PAGE was determined using the procedure described for Ro-SSA (Figure S1.3). The optimised loading amounts for each antigen is given in Table S1.1. In order to accommodate scaling up from a mini (Hoefer, SE250) to a large scale (Hoefer, SE600) electrophoresis format, antigen loading was expressed as amount per mm width of the acrylamide gel.

Table S1.1 Antigen loading for SDS-PAGE

Antigen	Scl-70	U1 snRNP	Ro-SSA	Jo-1	SSB/La
Quantity (μg/mm)	0.07	0.17	0.22	0.0055	0.0063

Antigens were mixed in the desired quantities and prepared for SDS-PAGE. Fluorescein labelled phosphorylase b and insulin B chain (Sigma Chemical Co., St Louis, USA) were added to track protein transfer onto the nitrocellulose and to act as markers to ensure antigen alignment when cutting the nitrocellulose into strips. Separated antigens were western blotted onto nitrocellulose as already described. After blocking, the nitrocellulose was cut into 3 mm strips as described in section 3.2.11, and the strips were incubated with autoimmune sera (Figure S1.6). Using this method, all twelve specificities of the five antigens used were identified.

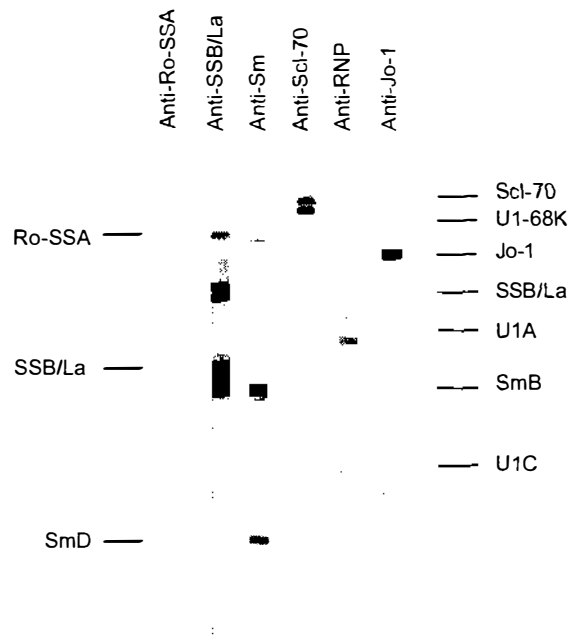

Figure S1.6 Multiple antibody specificity detection on western blot strips

Five antigens containing twelve specificities were western blotted and immunoprobed with autoimmune patient sera.

S1.3.3 Anti-RNP sera fine specificities

Human U1 snRNP contains multiple antigens and western blotting is the ideal diagnostic method to examine the fine specificities of both anti-RNP and anti-

Sm patient sera. Forty anti-RNP sera were tested using the western blot strips. A reaction with at least one U1 snRNP antigen was observed with 39 out of 40 sera. Interestingly, 30 of the 40 sera tested (80 %) reacted with SmB′/B, but without any reaction to SmD (Figure S1.7).

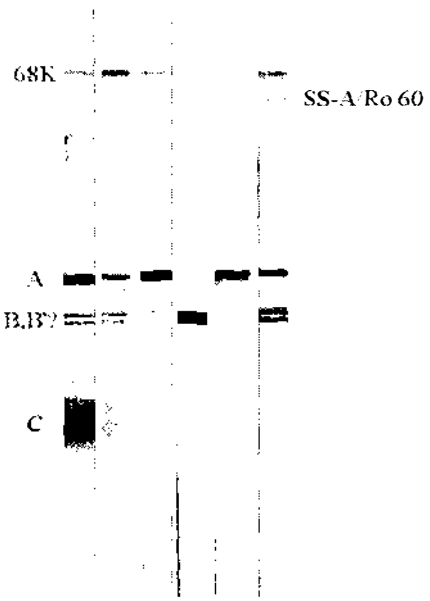

Figure S1.7 Reactivity of some anti-RNP sera with ENA western strips

Western blot nitrocellulose strips consisting of five ENA antigens were prepared as described in the text. Strips were immunoprobed with sera designated anti-RNP.

S1.4 Discussion

The conformational dependence of some anti-Ro-SSA autoantibodies has been well characterised (Boire *et al.*, 1991). Results obtained during this work by correlating data from ELISA (native) and western blot (denatured) assays demonstrate that the majority of anti-Ro-SSA sera contain at least some conformation dependent antibodies. In some cases antigens immobilised on the membrane surface can be re-natured by altering the conditions sufficiently to permit re-folding. Applying this process to Ro-SSA antigen has been of limited success (Zampieri *et al.*, 2000). In this study detection of anti-Ro-SSA antibodies using western blot has been improved by increasing both the Ro-SSA concentration and the incubation time of the patient serum on the blot. Increased detection could be explained by the induced fit phenomenon, whereby, the antibody assists the partial refolding of denatured antigen immobilised on the nitrocellulose surface (Berger *et al.*, 1999). The relatively weak response may be due to only a small proportion of denatured antigen being able to adopt the correct conformation, or perhaps a lower affinity of the antibodies for the refolded conformation.

The western blot technique developed here was used to characterise the fine specificity of a cohort of anti-RNP patient sera. These results strongly influenced the scope of research undertaken during this doctoral work.

A high proportion of anti-RNP patient sera reacted with SmB′/B in western blot, which is consistent with published findings (Habets *et al.*, 1985a; Pettersson *et al.*, 1986; de Rooij *et al.*, 1988; Combe *et al.*, 1989; Ghirardello *et al.*, 1996). The significance of anti- SmB′/B autoantibodies in anti-RNP sera, and the various theories as to why this is the case, have been thoroughly discussed in other sections of this thesis (Chapter 2, Chapter 4 and Chapter 7).

This supplementary study aimed to design and develop a western blot technique for the characterisation of rheumatological autoimmune sera. Poor anti-Ro-SSA sensitivity and interpretation difficulties associated with commercially available western blot strips, were addressed.

Five ENA antigens were selected and the amount of each antigen to be western blotted was optimised to give the required assay sensitivity. With Ro-SSA antigen, optimised antigen quantity and serum incubation time, significantly improved the detection sensitivity of the conformation dependent anti-Ro-SSA antibodies. Acrylamide separation medium pore size was systematically altered to produce the best antigen resolution.

Prototype western blot strips were prepared and successfully detected a range of ENA specificities in autoimmune patient sera. Sera previously identified as Ro-SSA non-blotters were detected using this enhanced technique. Of particular interest was the ability to determine the fine specificity of anti-RNP sera using this method.

By defining and characterising critical process control points such as the antigen quantity, separation and antigen detection parameters, a highly specific, sensitive and reproducible immunodiagnostic procedure has been developed for the detection of serum autoantibodies.

Supplement 2

Development of a Line Blot Membrane-Based Autoimmune Diagnostic

S2.1 Introduction

Indirect immunofluorescence (IIF) using a Hep-2 cell substrate is widely used as a screening method for ANA detection. Staining patterns can be difficult to interpret and often need very skilled microscopists for accurate assignment of sera specificity (Tan *et al.*, 1999). Reporting of ANA by IIF can be variable and often requires follow-up anti-ENA analysis (Damoiseaux and Tervaert, 2006). Enzyme-linked immunoassays (EIA) have become a useful addition to screening and determination of sera specificities (James *et al.*, 2000). This method is less dependent on skilled interpretation and is less labour intensive. Microtitre 96 well plates are the most commonly used EIA format in diagnostic laboratories due to their relatively high throughput capabilitity and ease of automation. Line-blot assays are an alternative EIA format (Paxton *et al.*, 1990). This technique, which allows simultaneous detection of multiple autoantibody specificities, is gaining in popularity for anti-ENA determination (Lopez-Longo *et al.*, 2002; Eissfeller *et al.*, 2005).

The objective for all diagnostic assays is to detect all true-positive sera that contain anti-antigen antibodies (100 % sensitivity) and to not respond to true-negative sera, which do not contain target anti-antigen (100 % specificity). A typical response distribution of true-positive and true-negative sera in a diagnostic test is illustrated in Figure S2.1.

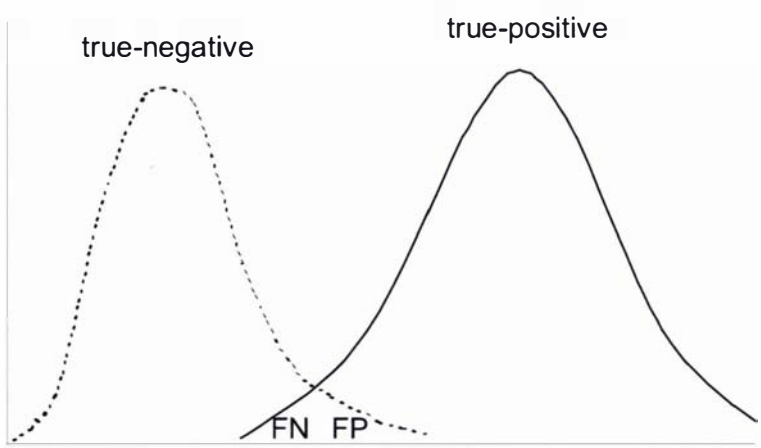

Figure S2.1 Distribution of true-negative and true-positive responses

Arbritary response values for sera containing antibodies against a particular antigen (true-positive) compared to the responses of normal donor sera (true-negative) in a typical diagnostic test. The overlap region contains false-positive (FP) and false-negative (FN) values.

The overlap region determines the sensitivity and specificity characteristics for the assay. Reducing the number of false-negative (FN) results increases the assay sensitivity at the expense of assay specificity, that is, greater numbers of false-positives (FP). The aim is to develop an assay, which maximises the difference between the peak true-negative and true-positive responses and minimises the overlap region.

The aim of this second supplementary study was to design a line-blot immunodiagnostic test using a vacuum-assisted blotting technique. Antigen coating quantity, membrane blocking and washing protocols, blot development and interpretation of results were established for nine autoantigens. The prototype line-blot strips were validated against both patient sera with a variety of anti-ENA specificities, and healthy donor sera. Performance characteristics for the detection of antinuclear antibodies were examined using a consensus panel of ANA positive sera established by the ANA subcommittee of the International Union of Immunological Societies standardisation committee (Smolen *et al.*, 1997; Tan *et al.*, 1999).

S2.2 Experimental Procedures

S2.2.1 Vacuum-assisted blotting

A slot blotting manifold (Immunetics, USA) consisting of 10 slots was assembled according to the manufacturer's instructions. Blotting papers and nitrocellulose membrane were pre-wetted in PBS. Human IgG positive control, negative control, coloured orientation marker or antigen was loaded into the slots. Gentle vacuum (5 mmHg) was applied until the liquid was sucked through the membrane. The membrane was washed *in situ* with PBS and then blocked in 1 % w/v BSA PBST. After drying, the membrane was cut into 3 mm strips.

Strips were incubated with antibody diluted with buffer containing 10 mM phosphate pH 7.4, 0.25 M NaCl, 0.1 % v/v Tween 20, 1 % w/v casein, 5 % v/v normal goat serum (South Pacific Sera, Timaru, NZ), and incubated for 1 hour. The strips were washed 3 times with wash buffer containing 10 mM phosphate pH 7.5, 0.25 M NaCl, 0.2 % v/v Tween 20. Secondary anti-human IgG alkaline phosphatase conjugate was diluted in antibody dilution buffer and incubated with the strips for 30 minutes. The strips were washed and developed with a ready-to-use solution of 0.22 mM NBT/ 1.2 mM BCIP formulated in 0.1 M 2-amino-2-methylpropanol (2A2MP), 5 mM $MgCl_2$ pH 9.5 for 10 minutes, and the reaction was stopped by washing the strips with water.

S2.3 Results

S2.3.1 Non-specific interaction

The background response of an assay is often attributable to non-specific interaction of Ig with the solid phase support. If this background is too high, the increase in FP detection will reduce assay specificity. Line-blot strips were prepared with a serial dilution of Ro-SSA antigen and incubated with anti-Ro-SSA positive serum and normal donor serum to determine the FP distribution using the western blot incubation, washing and development protocol. It was discovered that the donor serum reacted non-specifically with the line-blot strip even in the negative (no antigen) control line (Figure S2.2).

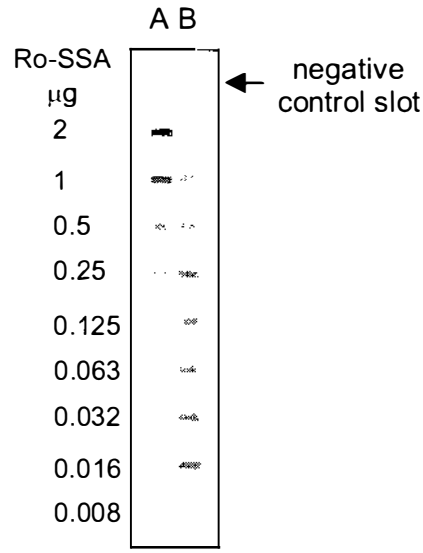

Figure S2.2 Non-specific interaction of normal donor serum with line-blot

Line-blot strips coated with Ro-SSA (2 µg-0.008 µg) were incubated with **A**: anti-Ro-SSA patient serum; **B**: normal donor serum.

One strategy to overcome the non-specific binding problem was to optimise the antibody dilution buffer composition. Phosphate buffer and casein concentrations were kept constant, whilst NaCl and Tween 20 compositions were varied. In addition, the effect of goat normal serum concentration on non-specific binding was determined. Thirteen buffers were prepared and their compositions are described in Table S2.1. ENA antigen strips consisting of Jo-1, Scl-70, CENP-B, Ro-SSA, Ro52, SSB/La, U1 snRNP and SmD were prepared and challenged with anti-Ro-SSA patient serum and normal donor

serum diluted 1/100 in various antibody dilution buffers. Standard PBST wash buffer was used and anti-human IgG conjugate was diluted 1/8000 in various antibody dilution buffers. Strips were developed for 10 minutes in western blot NBT/BCIP substrate. The order in which the buffers were used was randomised to reduce experimental bias. The mid-point buffer was repeated to determine reproducibility.

Table S2.1 Buffer composition of antibody dilution buffer

Buffer	NaCl mM	Tween 20 % v/v	Goat serum % v/v	Random Order
1	150	0.02	1.5	7
2	500	0.02	1.5	6
3	150	0.2	1.5	16
4	500	0.2	1.5	3
5	150	0.1	0	9
6	500	0.1	0	13
7	150	0.1	3.0	15
8	500	0.1	3.0	11
9	250	0.02	0	8
10	250	0.2	0	14
11	250	0.02	3.0	5
12	250	0.2	3.0	4
13	250	0.1	1.5	12
14	250	0.1	1.5	1
15	250	0.1	1.5	2
16	250	0.1	1.5	10
17	250	0.1	1.5	17

Developed strips were air dried and then compared for non-specific responses (Figure S2.3). Goat serum had the most significant effect on non-specific binding reduction. All strips incubated with buffer without goat serum had non-specific responses. Increasing NaCl concentration had a greater effect than Tween 20 on non-specific interactions. Goat serum and NaCl had a compound

effect, that is, by increasing the concentrations of both components the non-specific interaction was reduced by the sum of the effects.

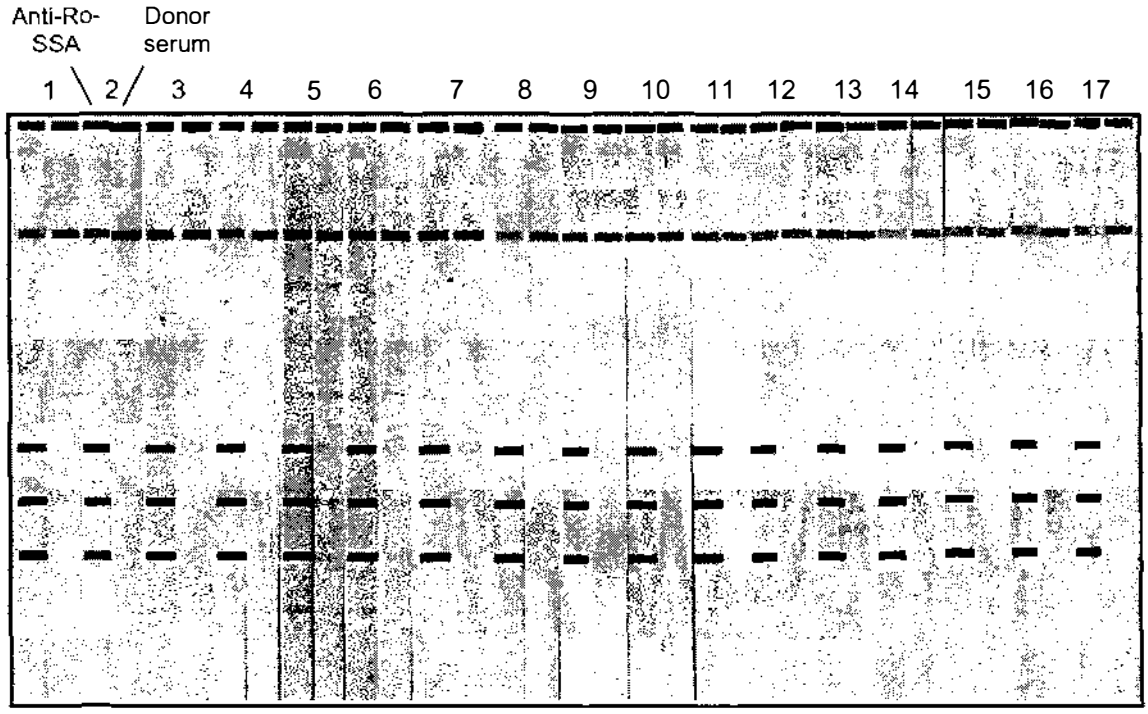

Figure S2.3 Effect of antibody dilution buffer on non-specific binding

Line-blot strips were immunoprobed with either anti-Ro-SSA serum or a donor serum diluted in one of the buffer compositions. Each pair of strips is numbered according to the buffer described in Table S2.1. Responses are assessed by visual interpretation and by densitometry.

Table S2.2 Wash buffer composition

Buffer	Tween 20 % v/v	NaCl mM	Butanol % v/v	Random Order
1	0.2	250	1.0	8
2	0.2	150	1.0	6
3	0.2	250	0	4
4	0.02	150	1.0	5
5	0.02	250	1.0	7
6	0.02	150	0	1
7	0.02	250	0	3
8	0.2	150	0	2

Reduction of non-specific binding by modifying the wash buffer composition was also examined. Three buffer components, Tween 20, NaCl and butan-1-ol were systematically varied and tested with line-blot strips (Table S2.2). Strips were probed with anti-Ro-SSA and normal donor sera and the washing steps were carried out using the appropriate wash buffer.

Strips were developed and then dried before scanning to determine the response level. The Tween 20 content of the wash buffer had the greatest effect on reducing non-specific interactions (Figure S2.4). Butanol and NaCl concentrations both contributed slightly to non-specific signal reduction.

A combination of optimised antibody dilution buffer and wash buffer was used to eliminate non-specific interaction in the line-blot assay.

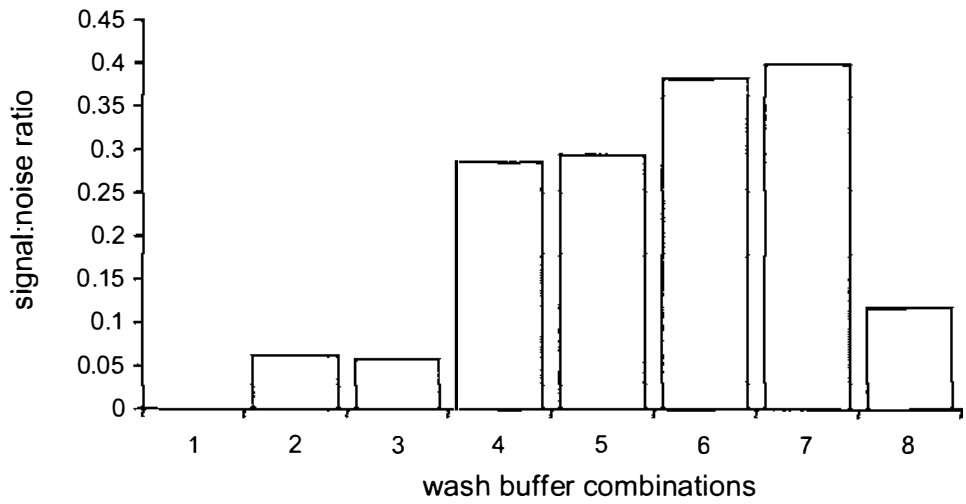

Figure S2.4 Effect of wash buffer composition on non-specific binding

Eight wash buffers, described in Table S2.2, containing different Tween 20, NaCl and butanol combinations were used with line-blot strips immunoprobed with patient serum and normal donor serum. The signal:noise ratios for each buffer was calculated.

S2.3.2 Primary and secondary antibody incubation optimisation

A number of factors affect the detection limit of an immunoassay, one factor is the contact time between antibody and target antigen. The objective is to achieve the maximum response in a time frame that is practical for the analyst, without affecting the signal:noise ratio. Primary anti-serum was incubated with

line-blot strips at 1/100 dilution in antibody dilution buffer for 0, 15, 30, 60, 120 and 420 minutes. All strips were incubated with 1/8000 secondary antibody conjugate for 1 hour and then developed using the western blot protocol (Figure S2.5).

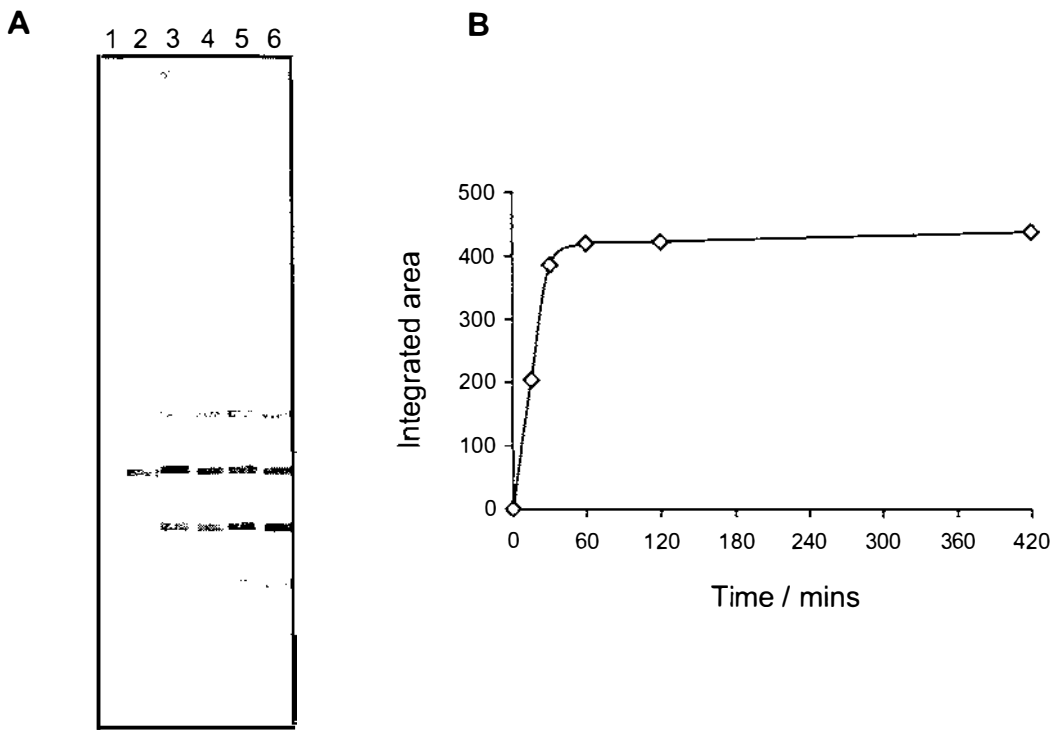

Figure S2.5 Serum incubation time

Patient serum was incubated with line-blot strips over a seven hour time course.
A: Line-blot strips incubated for **1**, 0 ; **2**, 15; **3**, 30; **4**, 60; **5**, 120; **6**, 420 minutes.
B: Slot intensities were integrated and plotted against incubation time.

Primary antibody incubation time reaches its maximum affect on blot staining intensity between 30 and 60 minutes. No increase in non-specific binding was observed over a longer incubation period.

Secondary conjugate concentration and incubation time influence the response outcome. Line-blot strips were immunoprobed with a weak anti-RNP patient serum. After washing, the strips were incubated with secondary conjugate at three concentrations (1/12000, 1/10000, 1/8000) for 15, 30, 45 and 60 minutes. All strips were developed according to the western blot protocol (Figure S2.6). Anti-RNP response was greatest with 1/8000 secondary antibody dilution and a

weak anti-Ro-SSA was detected. Greater than 30 minute incubation was required for adequate detection.

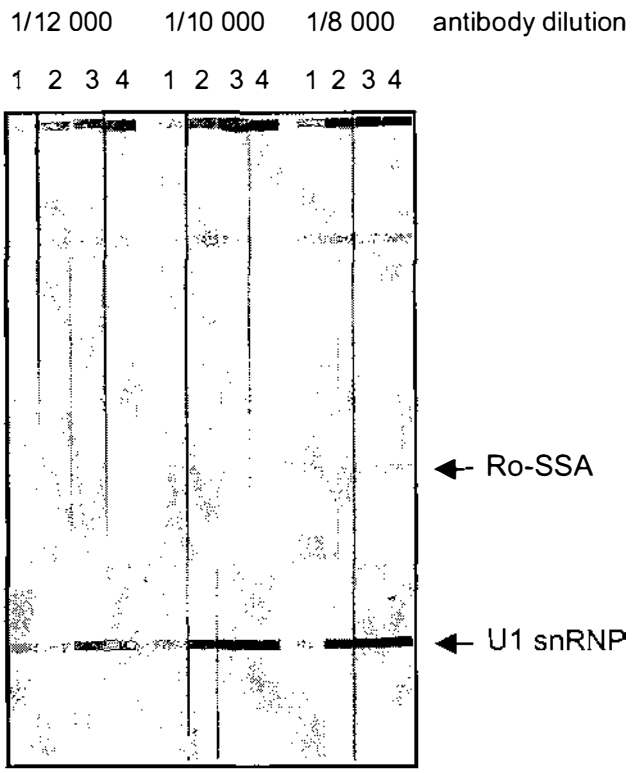

Figure S2.6 Secondary antibody concentration and incubation time

Line-assay strips were incubated with three secondary antibody conjugate concentrations for **1**, 15; **2**, 30; **3**, 45; **4**, 60 minutes.

S2.3.3 The influence of NBT/BCIP substrate

The substrate NBT/BCIP reacts with alkaline phosphatase conjugate to form a black precipitate. Changing the amount and/or ratio of substrate components may influence assay sensitivity. Line-blot strips were incubated with anti-RNP serum, 1/8000 secondary antibody as described in the previous section, and then developed with 0.22 mM NBT/ 0.23 mM BCIP or 0.22 mM NBT/ 1.2 mM BCIP in 50 mM Tris-HCl pH 9.5, 5 mM $MgCl_2$, 150 mM NaCl (Figure S2.7). Increasing the BCIP concentration had a significant effect on the response, particularly to the low antibody titre anti-Ro-SSA specificity. Increasing the substrate concentration did not affect the non-specific noise.

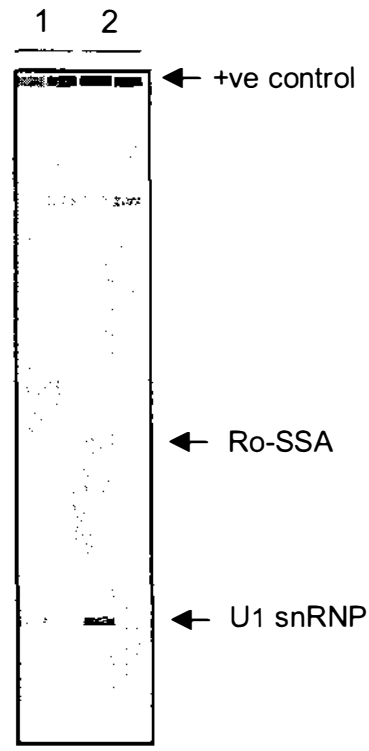

Figure S2.7 Effect of NBT/BCIP substrate on ENA detection

Line-blot strips were immunoprobed with anti-RNP and normal donor serum and then developed with either **1**, 0.2 mM NBT/ 0.23 mM BCIP or **2**, 0.2 mM NBT/ 1.2 mM BCIP.

Substrate can be prepared as a 100 x stock solution that can be diluted into development buffer before use. For convenience and reproducibility, many testing laboratories use ready-to-use substrate. Substrate stability in a ready-to-use solution is critical to assay reproducibility. Line-blot strips were prepared and stored in an airtight container containing dry silica gel. These line-blot strips were used to test the stability of ready-to-use NBT/BCIP formulations stored protected from light at 2-8 °C, room temperature and 37 °C over a two-month period. The responses were measured by densitometry and compared to a zero time point (Figure S2.8). Substrate formulated in 50 mM Tris-HCl pH 9.5, 5 mM $MgCl_2$, 150 mM NaCl buffer was abandoned after three weeks due to the diminished response and the formation of a white precipitate. Other high pH buffering solutions were tried such as ethanolamine, borate and carbonate, however, the best performing buffer was 2A2MP pH 9.5 (Figure S2.8). Performance of substrate formulated in 50 mM 2A2MP pH 9.5, 5 mM $MgCl_2$, 150 mM NaCl was not diminished after two months at any temperature.

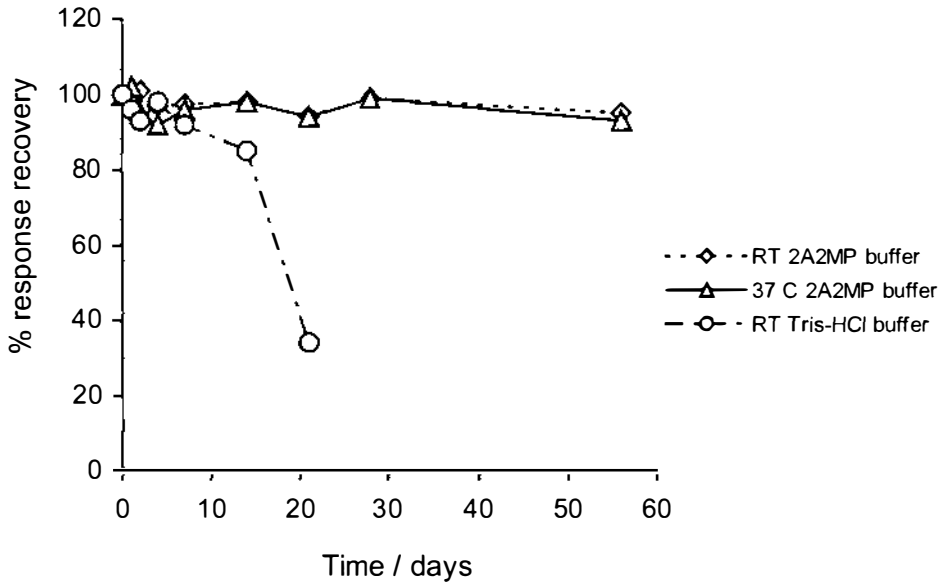

Figure S2.8 Stability testing of NBT/BCIP ready-to-use formulations

NBT/BCIP was formulated as a ready-to-use substrate in either Tris-HCl pH 9.5 buffer or 2-amino-2-methylpropanol pH 9.5 buffer (2A2MP) and incubated at 2-8 °C (results not shown), ambient room temperature (RT) and 37 °C. Substrate stability was tested over a two month period using line-blot strips.

S2.3.4 Antigen coating concentration

Using the revised protocol, a selection of antigens were titrated to determine their optimal coating concentration. Each antigen was diluted in PBS and coated onto nitrocellulose as described in section S2.2. Antigen line-blots were immunoprobed with specific sera and the responses were measured by densitometry. Titration curves were plotted for each ENA (Figure S2.9). Optimum coating quantities were determined as the amount of antigen required to give approximately 85-95 % maximum response (Table S2.3).

Table S2.3 Optimum amount of antigen to coat nitrocellulose

Antigen	Jo-1	Scl-70	CENP-B	SS-A/60	SS-A/52	SS-B/La	U1 RNP	Sm	*Ribo P
Load/ug in 2ml	0.75	1.0	1.0	2.25	1.5	1.0	1.5	2.0	2.0

* Ribosomal P antigen coating optimised but not shown in Figure S2.9

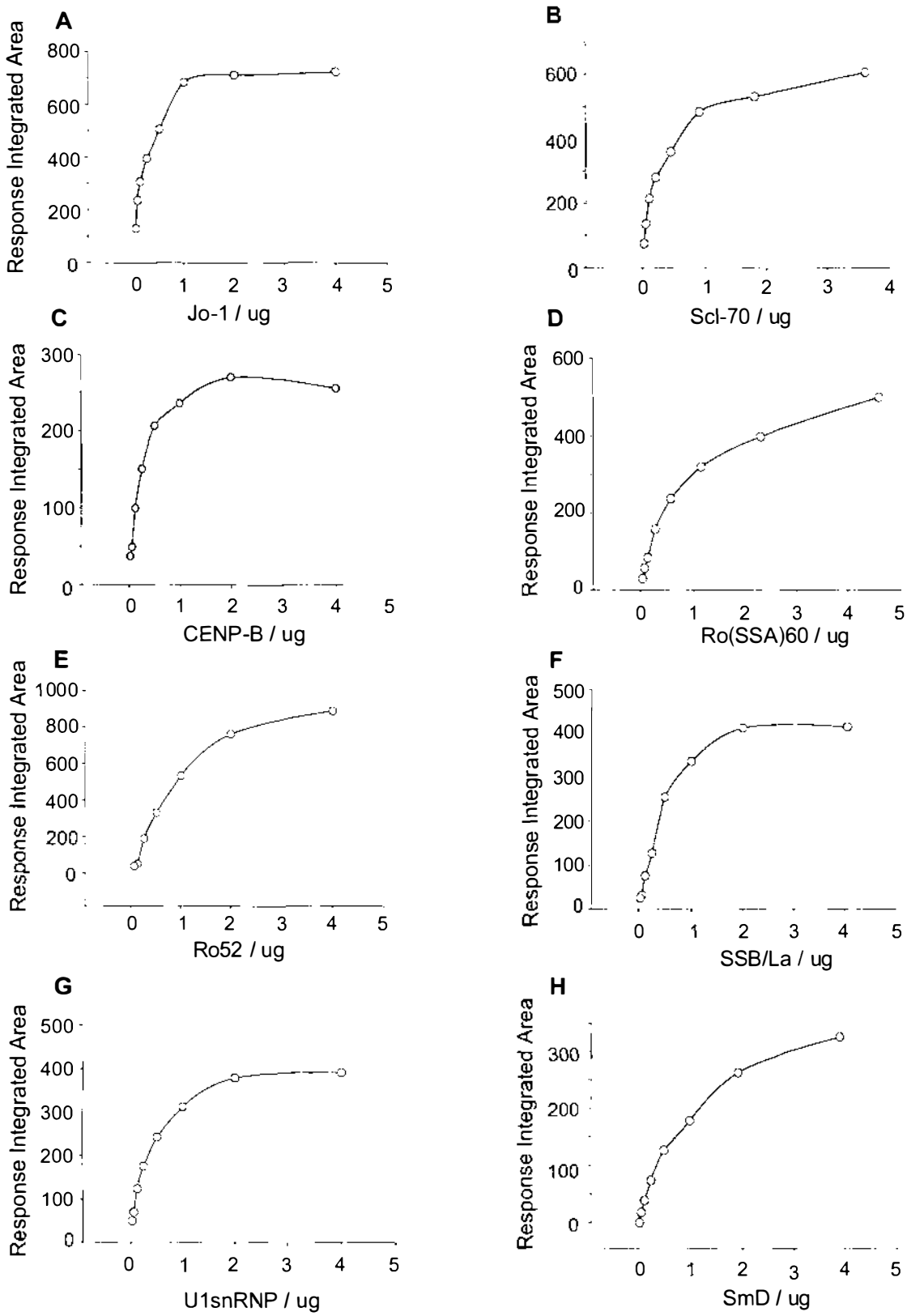

Figure S2.9 Determining optimum antigen coating amount

Antigens were serially diluted 1:1 in 2 mL PBS. Each dilution was coated onto nitrocellulose using the line-blot technique. Line-blot strips of antigen titrations were immunoprobed with antigen specific sera and the resultant responses were plotted as titration curves A-H.

S2.3.5 Line-blot assay performance characteristics

Line-blot assay strips were tested for intra-assay (strips from the same lot) and inter-assay (strips from different lots) reproducibility and repeatability. Responses were measured from six strips of three different lots tested either on the same day or on a consecutive day. Inter-assay reproducibility was determined by ANOVA and the coefficient of variance was calculated for intra-assay repeatability using the measured integrated area responses (Table S2.4). Student's *t*-test was used to analyse the repeatability of each lot.

Table S2.4 Line-blot reproducibility and repeatability

	Lot 1 integrated areas		**Lot 2** integrated areas		**Lot 3** integrated areas	
Day 1	473	558	435	461	454	523
	497	439	452	441	495	417
	487	492	420	467	486	484
% CV	**7.9**		**3.9**		**7.7**	
Day 2	440	497	396	432	497	430
	461	428	352	337	400	473
	441	497	472	404	457	473
% CV	**7.9**		**12.5**		**7.6**	
*Prob (p)	0.162		0.054		0.322	

*Probability (p) < 0.05 indicates significant difference between data

Variability between lots was not significant by ANOVA (F ratio = 3.007 and probability (p) assuming null hypothesis (no significant lot variation) = 0.08). In general, there was no significant difference between the performance of lots used on consecutive days.

Diagnostic performance of an assay must be determined through the analysis of large numbers of patient sera and healthy donor controls. Line-blot strips were tested with a 150 patient sera cohort and 80 normal donor sera. Typical line-blot specificities are shown in Figure S2.10.

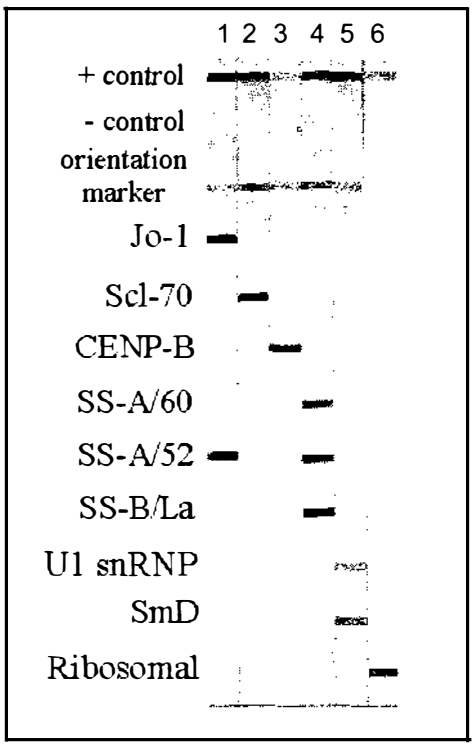

Figure S2.10 Line-blot strips probed with anti-ENA patient sera

Line-blot strips were immunoprobed with a variety of diagnostically significant anti-ENA patient sera. Strips: **1**, polymyositis (Jo-1 +ve); **2**, scleroderma (Scl-70 +ve); **3**, CREST (calcinosis, Raynaud's, eosophogeal dysmotility, sclerodactyly, tangelactasia); **4**, Sjögren's syndrome (SS-A, SS-B +ve); **5** and **6**, systemic lupus erythematosus.

All strips were analysed by densitometry. Responses for each specificity were plotted (Figure S2.11).

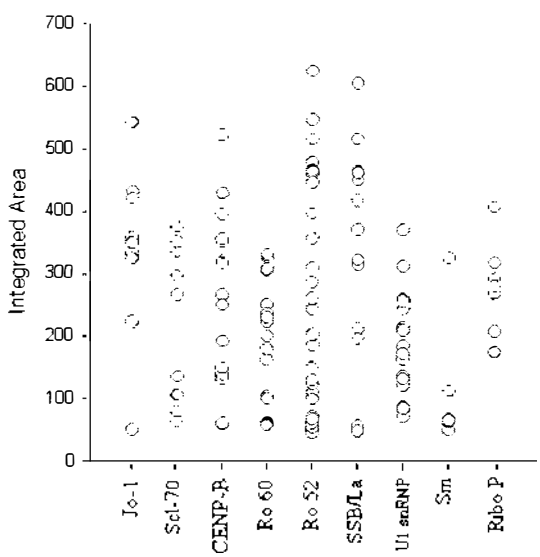

Figure S2.11 Line-blot assay anti-ENA response

Line-blot strips were immunoprobed with a patient sera cohort (n=150) and normal donor sera (n = 80). Responses were determined by densitometry and plotted against ENA specificity.

Results from a small number of Ro-SSA positive sera (n=12) were plotted and compared to normal donor sera (Figure S2.12).

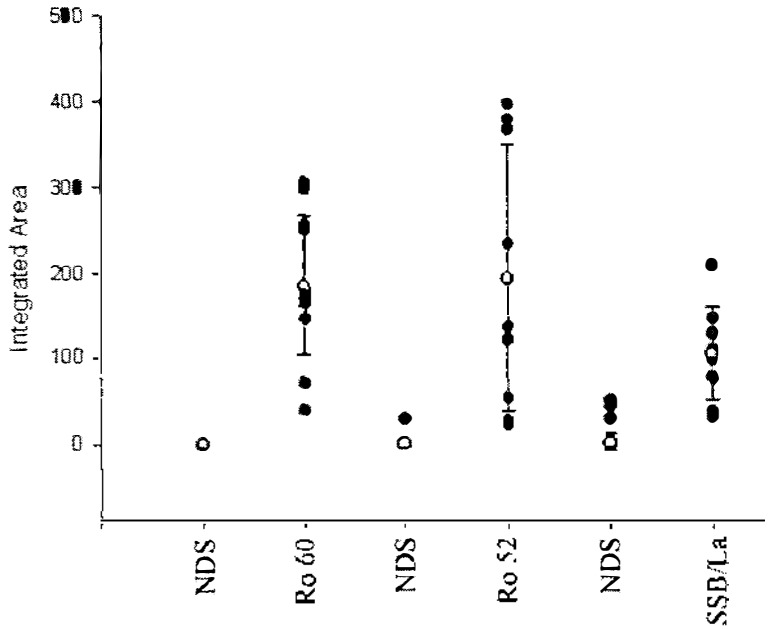

Figure S2.12 Anti-Ro-SSA 60 patient sera compared to donor sera

Ro-SSA +ve patient sera (n=12) were tested on the line-blot assay and compared to results from normal donor sera (NDS) n=80. Response of tested sera to other specificties Ro 52 and SSB/La were also plotted. The error bars show the mean response values for each specificity.

None of the eighty donor sera tested reacted with Ro-SSA 60, whereas, one patient sera was slightly Ro 52 reactive and three responded to SSB/La. These donor sera were not reactive with other specificities.

S2.3.6 Line-blot reactivity with ANA consensus panel sera

Verification of assay performance is best achieved with well-characterised sera. A panel of standardised or consensus sera are available from the Centre for Disease Control (CDC), Atlanta, USA. These sera were used according to the test procedure devised by Tan *et al.* (1999). Various proportions of the CDC sera were mixed and then their specificities were determined using the line-blot assay procedure (Table S2.5).

Table S2.5 Mixing protocol for the CDC consensus sera

	CDC1 dsDNA	CDC2 SSB/La	CDC4 U1 RNP	CDC5 Sm	CDC7 SSA/Ro	CDC9 Scl-70	CDC3 Speck[a]	CDC6 nucleol[b]	CDC8 c'mere[c]	CDC10 Jo-1
A	4	2	1							
B	2			1	4					
C	1		4		2					
D		4	2	1						
E		2		4	1					
F	2	1			4					
G		1	4	2						
H			1	4	2					
I	1		2	4						
J		2		1	4					
K						4	1	2		
L						2	1	4		
						1	4	2		
M										
N							4	1	2	
O						1		2	4	
P						2	1		4	
Q										7

Each test serum labelled A,B,C etc. contains different proportions of CDC sera i.e. sample E contains 2 parts CDC2, 4 parts CDC5, 1 part CDC7.
[a] speckled pattern, [b] nucleolar pattern, [c] centromere pattern by immunofluorescence microscopy.

Line-blot strips were scanned and the responses were quantified by densitometry. Both specificity and sensitivity were 100 % for line-blot strips probed with the test sera (Table S2.6).

Table S2.6 Line-blot response and specificity to consensus sera

Specificity	A	B	C	D	E	F	G	H	I	J	K	L	M	N	O	P	Q
Jo-1																	✓
Scl-70											✓	✓	✓		✓	✓	
CPB														✓	✓	✓	
Ro-SSA	✓	✓	✓	✓	✓	✓	✓	✓		✓	✓	✓	✓	✓		✓	
Ro 52	✓			✓	✓	✓				✓							✓
SSB/La	✓			✓	✓	✓	✓			✓	✓	✓	✓	✓		✓	
U1 RNP	✓	✓	✓	✓	✓		✓	✓	✓	✓	✓	✓	✓	✓		✓	
Sm		✓		✓	✓		✓	✓	✓	✓							

✓ High response (200 +), ✓ good response (150-200), ✓ medium response (100-150), ✓ low response (50-100), ✓ poor response (<50).

Ro-SSA specificity appears in almost all test sera despite CDC7 anti-Ro-SSA not being added to some of the sera mixtures. CDC2 (anti-SSB/La) and CDC3 (speckled) contain low levels of anti-Ro-SSA which accounts for the apparent disparity. Anti-Ro 52 was detected poorly in the CDC2/CDC7 sera, however, a very strong response was obtained with CDC10 (anti-Jo-1).

S2.4 Discussion and Future Work

All assays need to strike a balance between the detection of FPs (specificity) and FNs (sensitivity). This is most often achieved by establishing a cut-off value above the assay background noise. Noise is mostly attributable to non-specific interaction of Igs with the solid phase support. Non-specific interaction with some normal donor sera was initially very high in the line-blot assay. This phenomenon related to the use of a vacuum-assisted coating technique, which somehow modified the nitrocellulose making it more prone to non-specific antibody binding. Cryoprecipitates in sera have been shown to increase non-specific background (Tan *et al.*, 1999), and this may explain why not all donor sera result in such high backgrounds. Introducing an excess of serum proteins and Igs (donor goat serum) to the antibody dilution buffer used in the line-blot assay, had the most significant influence on reducing non-specific binding. This practice, together with increasing the Tween 20 concentration in the wash buffer, reduced non-specific binding to practically zero.

Reduction of background may result in loss in sensitivity, however, tests conducted using an internationally characterised consensus sera panel showed that the line-blot assay was 100 % sensitive and 100 % specific. Some antigens, particularly CENPB, Scl-70 and Ro-SSA gave lower responses than expected, reflecting perhaps the coating conditions used. Coating buffer composition has been shown to profoundly affect the performance of the antigen (Jones, 1999). Changing the pH and ionic strength, and adding methanol or isopropanol to the coating buffer, have been shown to affect protein binding to a membrane solid phase (Schneider, 1980).

Despite the low background, some donor sera reacted with line-blot strips, however, the interaction appeared specific, rather than non-specific, for SSB/La and Ro52 (Figure S2.12). Low levels of specific autoantibodies in the sera of the general donor population complicate the interpretation of assay results. They either represent a FP (background) because the donor does not have an autoimmune disease, or a true positive due to a pre-clinical autoimmune

condition (Lyons *et al.*, 2005). The positive predictive value of an antigen specificity being associated with a disease, together with the likelihood ratio of a positive result being of diagnostic significance within a certain population, are the most important determinants for a successful diagnosis (Phan *et al.*, 2002). The significance of detecting antigen specific autoantibodies present in marginal levels, therefore, may be questionable (Lock and Unsworth, 2001). As assays become more sensitive, clinicians and those developing assays need to define where the compromise should lie. The ability to determine multiple specificities in one assay (multiplexing) may meet clinical diagnostic and prognostic demands through the addition of the positive predictive values for individual antigen responses.

As part of this supplementary work, an immunodiagnostic procedure has been developed using a vacuum-assisted blotting technique to directly immobilise native antigens onto nitrocellulose membrane. This assay was able to detect nine ENA specificities because of the robust, reproducible, highly sensitive and specific format. Non-specific background exhibited with some donor sera was overcome by the addition of donor animal serum and detergent to the assay buffers, resulting in negligible background noise.

References

Achsel, T., Brahms, H., Kastner, B., Bachi, A., Wilm, M. and Lührmann, R. (1999) A doughnut-shaped heteromer of human Sm-like proteins binds to the 3′ -end of U6 snRNA, thereby facilitating U4/U6 duplex formation *in vitro*. *EMBO J*. **18**, 5789-5802.

Algiman, M., Dietrich, G., Nydegger, U.E., Boieldieu, D., Sultan, Y. and Kazatchkine, M.D. (1992) Antibodies to Factor VIII (anti-haemophilic factor) in healthy individuals. *Proc. Natl. Acad. Sci. USA* **89**, 3795-3799.

Amagai, M., Tsunoda, K., Suzuki, H., Nishifuji., Koyasu, S. and Nishikawa, T. (2000) Use of auto-antigen knockout mice in developing an active autoimmune disease model for pemphigus. *J. Clin. Invest*. **105,** 625-631.

Anon. (1992) Diagnosis of Sjogren's Syndrome. *Lancet* **340**, 150-151.

Appelboom, T., Kahn, M.F. and Mairesse, N. (1995) Antibodies to small ribonucleoprotein and to 73-kD heat shock protein: two distinct markers of mixed connective tissue disease. *Clin. Exp. Immunol.* **100**, 486-488.

Asakura, K., Miller, D.J., Pease, L.R. and Rodriguez, M. (1998) Targeting of IgMkappa antibodies to oligodendrocytes promotes CNS remyelination. *J. Neurosci.* **18**, 7700-7708.

Awasthi, S. and Alwine, J.C. (2003) Association of polyadenylation cleavage factor I with U1 snRNP. *RNA* **9**, 1400-1409.

Bach, M., Krol, A. and Lührmann, R. (1990) Structure-probing of U1 snRNPs gradually depleted of the U1-specific proteins A, C and 70K. Evidence that A interacts differentially with developmentally regulated mouse U1 snRNA variants. *Nucleic Acids Res.* **18**, 449-457.

Balczon, R. (1993) Autoantibodies as probes in cell and molecular biology. *Proc. Exp. Biol. Med*. **204**, 138-154.

Barakat, S., Briand, J-P., Weber, J-C., van Regenmortel, M.H.V. and Muller, S. (1990) Recognition of synthetic peptides of Sm-D autoantigen by lupus sera. *Clin. Exp. Immunol*. **81**, 256-262.

Barakat, S., Briand, J-P., Abuaf, N., van Regenmortel, M.H.V. and Muller, S. (1991) Mapping epitopes on U1 snRNP polypeptide A with synthetic peptides and autoimmune sera. *Clin. Exp. Immunol*. **86**, 71-78.

Bedford, M.T., Reed, R. and Leder, P. (1998) WW domain-mediated interactions reveal a spliceosome associated protein that binds a third class of proline–rich motif: the proline glycine and methionine rich motif. *Proc. Natl. Acad. Sci., USA* **95**, 10602-10607.

Beer, R.G., Rischmueller, M., Coates, T., Purcell, A.W., Keech, C.L., McCluskey, J. and Gordon, T.P. (1996) Non-precipitating anti-La(SSB) autoantibodies in primary Sjogren's syndrome. *Clin. Immunol. Immunopath.* **79**, 314-318.

Benito-Garcia, E., Schur, P.H. and Lahita, R. (2004) Guidelines for immunologic laboratory testing in the rheumatic diseases: anti-Sm and anti-RNP antibody tests. *Arthritis Rheum.* **51**, 1030-1044.

Benoist, C. and Mathis, D. (2001) Autoimmunity provoked by infection: how good is the case for T cell epitope mimicry. *Nature Immunol.* **2**, 797-801.

Berger, C., Weber-Bornhauser, S., Eggenberger, J., Hanes, J., Pluckthun, A. and Bosshard, H.R. (1999) Antigen recognition by conformational selection. *FEBS Lett.* **450,** 149-153.

Bernardi, G. (1971) Chromatography of nucleic acids on hydroxylapatite columns. *Methods Enzymol.* **21**, 95-139.

Berthold, H., Scanarini, M., Abney, C.C., Frorath, B. and Northemann, W. (1992) Purification of recombinant antigenic epitopes of the human 68-kDa (U1) ribonucleoprotein antigen using the expression system pH6EX3 followed by metal chelating affinity chromatography. *Protein Expr. Purif.* **3**, 50-56.

Bizzaro, N., Tozzoli, R., Tonutti, E., Piazza, A., Manoni, F., Ghirardello, A., Bassetti, D., Villalta, D., Pradella, M. and Rizzotti, P. (1998). Variability between methods to determine ANA, anti-dsDNA and anti-ENA autoantibodies: a collaborative study with the biomedical industry. *J. Immunol. Methods* **219**, 99-107.

Bizzaro, N., Tonutti, E., Villalta, D., Bassetti, D., Tozzoli, R., Manoni, F., Pirrone, S., Piazza, A., Rizzotti, P. and Pradella, M. (2000) Sensitivity and specificity of immunological methods for the detection of anti-topoisomerase I (Scl70) autoantibodies: results of a multicenter study. *Clin. Chem.* **46**, 1681-1685.

Blomberg, A., Blomberg, L., Fey, S.J., Larsen, P.M., Roepstorff, P., Degand, P., Boutry, M., Posch, A. and Gorg, A. (1995) Interlaboratory reproducibility of yeast

protein patterns analysed by immobilised pH gradient two dimensional gel electrophoresis. *Electrophoresis* **16**, 1935-1945.

Blomberg, S., Ronnblom, L., Wallgren, A.C., Nilsson, B. and Karlsson-Parra, A. (2000) Anti-SSA/Ro antibody determination by enzyme linked immunosorbent assay as a supplement to standard immunofluoresence in antinuclear antibody screening. *Scand. J. Immunol*. **51**, 612-617.

Boak, A.M., Kincaid, L.A., Treadwell, E.L., McDonald, P., Ellis, G.C., Sharp, G.C. and Agris, P.F. (1984) Comparison of various preparations of nuclear antigens by hemagglutination immunisation. *Immunol. Commun.* **13**, 127-136.

Boelens, W.C., Jansen, E.J.R., van Venrooij, W.J., Stripecke, R., Mattaj, I.W. and Gunderson, S.I. (1993) The human U1 snRNP specific U1A protein inhibits polyadenylation of its own pre-mRNA. *Cell* **72**, 881-892.

Boire, G., Lopez-Longo, F.J., Lapointe, S. and Menard, H.A. (1991) Sera from patients with autoimmune disease recognise conformational determinants on the 60kD Ro/SSA protein. *Arthritis Rheum.* **34**, 722-730.

Bondanza, A., Zimmermann, V.S., Dell'Antonio, G., Cin, E.D., Balestrieri, G. and Tincani, A. (2004) Requirement of dying cells and environmental adjuvants for the induction of autoimmunity. *Arthritis Rheum.* **50**, 1549-1560.

Borsi, I., Castellani, P., Balza, E., Siri, A., Pellecchia, C., de Scalzi, F. and Zardi, L. (1986) Large-scale procedure for the purification of fibronectin domains. *Anal. Biochem.* **15**, 335-345.

Boukis, L.A., Liu, N., Furuyama, S. and Bruzik, J.P. (2004) Ser-Arg-rich protein-mediated communication between U1 and U2 small nuclear ribonucleoprotein particles. *J. Biol. Chem.* **279**, 29647-29653.

Bradford, M.M. (1976) A rapid and sensitive assay for the quantitation of microgram quantitites of protein utilizing the principle of protein-dye binding. *Anal. Biochem.* **72**, 248-254.

Brahms, H., Raymackers, J., Union, A., de Keyser, F., Meheus, L. and Lührmann, R. (2000) The C-terminal RG dipeptide repeats of the splicesomal Sm proteins D1 and D3 contain symmetrical dimethylarginines which form a major B cell epitope for anti-Sm autoantibodies. *J. Biol. Chem.* **275**, 17122-17129.

Brahms, H., Meheus, L., de Brabandere, V., Fischer, U. and Lührmann, R. (2001) Symmetrical dimethylation of arginine residues in splicesomal Sm protein B′/B and the Sm-like protein LSm4, and their interaction with the SMN protein. *RNA* **7**, 1531-1542.

Bretscher, P.A. and Cohn, M. (1970) A theory of self-nonself discrimination. *Science* **169,** 1042-1049.

Bridges, A.J., Lorden, T.E. and Havighurst, T.C. (1997) Autoantibody testing for connective tissue diseases. Comparison of immunodiffusion, immunoblot, and enzyme immunoassay. *Am. J. Clin. Pathol*. **108**, 406-410.

Bunn, C.C., Gharavi, A.E. and Hughes, G.R.V. (1982) Antibodies to extractable nuclear antigens in 173 patients with DNA binding positive SLE: an association between antibodies to ribonucleoprotein and Sm antigens observed by counterimmunoelectrophoresis. *J. Clin. Lab. Immunol*. **8**, 13-17.

Bunn, C. and Kveder, T. (1993) Counterimmunoelectrophoresis and immunodiffusion for the detection of antibodies to soluble cellular antigens. In: van Venrooij WJ, Maini RN eds. *Manual of Biological Markers of Disease*. Dordrecht, The Netherlands: Kluwer Academic Publishers. **A3**: 1-12.

Burlinghame, R. (2005) personal communication.

Buyon, J.P., Winchester, R.J., Slade, S.G., Arnett, F., Copel, J., Friedman, D. and Lockshin, M.D. (1993) Identification of mothers at risk for congenital heart block and other neonatal lupus syndromes in their children. Comparison of enzyme-linked immunosorbent assay and immunoblot for measurement of anti-SS-A/Ro and anti-SS-B/La antibodies. *Arthritis Rheum*. **36**, 1263-1273.

Cao, W., Jamison, S.F. and Garcia-Blanco, M.A. (1997) Both phosphorylation and dephosphorylation of ASF/SF2 are required for pre-mRNA spicing *in vitro*. *RNA* **3**, 1456-1467.

Cao, W. and Garcia-Blanco, M.A. (1998) A serine/arginine-rich domain in the human U1 70K protein is necessary and sufficient for ASF/SF2 binding. *J. Biol. Chem.* **273**, 20629-20635.

Cao, L., Goodin, R., Wood, D., Moscarello, M.A. and Whitaker, J.N. (1999) Rapid release and unusual stability of immunodominant peptide 45-89 from citrullinated myelin basic protein. *Biochemistry* **38**, 6157-6163.

Casali, P. and Notkins, A.L. (1989) CD5+ B lymphocytes, polyreactive antibodies and the human B-cell repertoire. *Immunol. Today* **10**, 364-368.

Casciola-Rosen, L., Miller, D.K., Anhalt, G.J. and Rosen, A. (1994) Specific cleavage of the 70-kDa protein component of the U1 small nuclear ribonucleoprotein is a characteristic feature of apoptotic cell death. *J. Biol. Chem.* **269**, 30757-30760.

Casciola-Rosen, L., Nicholson, D.W., Chong, T., Rowan, K.R., Thornberry, N.A., Miller, D.K. and Rosen, A. (1996) Apopain/CPP32 cleaves proteins that are essential for cellular repair: A fundamental principle of apoptotic death. *J. Exp. Med.* **183**, 1957-1964.

Casciola-Rosen, L., Wigley, F. and Rosen, A. (1997) Scleroderma autoantigens are uniquely fragmented by metal-catalysed oxidation reactions: Implications for pathogenesis. *J. Exp. Med.* **185**, 71-79.

Casciola-Rosen, L., Andrade, F., Ulanet, D., Wong, W.B. and Rosen, A. (1999) Cleavage by Granzyme B is stongly predictive of autoantigen status: implications for initiation of autoimmunity. *J. Exp. Med.* **190**, 815-825.

Casiano, C.A., Ochs, R.L. and Tan, E.M. (1998) Distinct cleavage products of nuclear proteins in apoptosis and necrosis revealed by autoantibody probes. *Cell Death Differ.* **5**, 183-190.

Chen, J. and Agris, P.F. (1992) Small nuclear ribonucleoprotein particles contain glycoproteins recognised by rheumatic disease associated autoantibodies. *Lupus* **1**, 119-124.

Chu, J.L. and Elkon, K.B. (1991). The small nuclear ribonucleoproteins, SmB and B′ are products of a single gene. *Gene* **97**, 311-312.

Cloos, P.A.C. and Christgau, S. (2004) Post-translational modifications of proteins: implications for aging, antigen recognition and autoimmunity. *Biogerontology* **5**, 139-158.

Collins, R.J., Neil, J.C., Druery, L.N. and Wilson, R.J. (1989) Detection of antibodies to extractable nuclear antigens using calf thymus and rabbit thymus. A comparative study of 1000 consecutive anti-nuclear antibody positive patients. *J. Immunol. Methods* **116**, 53-57.

Combe, B., Rucheton, M., Graafland, H., Lussiez, V., Brunel, C. and Sany, J. (1989) Clinical significance of anti-RNP and anti-Sm autoantibodies as determined by immunoblotting and immunoprecipitation in sera from patients with connective tissue diseases. *Clin. Exp. Immunol.* **75**, 18-24.

Comer, F.I. and Hart, G.W. (2000) O-glycosylation of nuclear and cytosolic proteins. *J. Biol. Chem.* **275**, 29179-29182.

Comer, F.I. and Hart, G.W. (2001) Reciprocity between O-GlcNAc and O-phosphate on the carboxyl terminal domain of RNA polymerase II. *Biochemistry* **40**, 7845-7852.

Condemi, J.J. (1992) The autoimmune diseases. *JAMA* **268**, 2882-2892.

Cooke, C. and Alwine, J.C. (2002) Characterisation of specific protein-RNA complexes associated with the coupling of polyadenylation and last intron removal. *Mol. Cell Biol.* **22**, 4579-4586.

Cooper, M., Johnston, L.H. and Beggs, J.D. (1995) Identification and characterisation of Uss1p (Sdb23p): a novel U6 snRNA-associated protein with significant similarity to core proteins of small nuclear ribonucleoproteins. *EMBO J.* **14**, 2066-2075.

Coutinho, A., Kazatchkine, M.D. and Avrameas, S. (1995) Natural autoantibodies. *Current Opinion Immunol.* **7**, 812-818.

Cutolo, M., Sulli, A., Capellino, S., Villaggio, B., Montagna, P., Seriolo, B. and Straub, R.H. (2004) Sex hormones influence on the immune system: basic and clinical aspects in autoimmunity. *Lupus* **13**, 635-638.

Dagher, S.F., Wang, J.L. and Patterson, R.J. (1995) Identification of galectin-3 as a factor in pre-mRNA splicing. *Proc. Natl. Acad. Sci. USA* **92**, 1213-1217.

Damoiseaux, J.G.M.C. and Tervaert, J.W.C. (2006) From ANA to ENA: how to proceed? *Autoimmunity Reviews* **5**, 10-17.

de Keyser, F., Hoch, S.O., Takei, M., Dang, H., de Keyser, H., Rokeach, L.A. and Talal, N. (1992) Cross-reactivity of the B′/B subunit of Sm ribonucleoprotein autoantigen with proline rich polypeptides. *Clin. Immunol. Immunopathol.* **62**, 285-290.

de Rooij, D.J., van de Putte, L.B., Habets, W.J., Verbeek, A.L. and van Venrooij, W.J. (1988) The use of immunoblotting to detect antibodies to nuclear and cytoplasmic antigens. *Scand. J. Rheumatology* **17**, 353-364.

Degen, W.G.J., Pieffers, M., Welin-Henriksson, E., van den Hoogen, F.H.J., van Venrooij, W.J. and Raats, J.M.H. (2000a) Characterisation of recombinant human autoantibody fragments directed towards the autoantigenic U1-70K protein. *Eur. J. Immunol.* **30**, 3029-3038.

Degen, W.G.J., van Aarssen.Y., Pruijn, G.J.M., Utz, P.J. and van Venrooij, W.J. (2000b) The fate of U1 snRNP during anti-Fas induced apoptosis: specific cleavage of the U1 snRNA molecule. *Cell Death Differ.* **7**, 70-79.

Del Nery, E., Juliano, M.A., Meldal, M., Svendsen, I., Scharfstein, J., Walmsley, A. and Juliano, L. (1997) Characterisation of the substrate specificity of the major cysteine protease (cruzipain) from *Trypanosoma cruzi* using a portion-mixing combinatorial library and fluorogenic peptides. *Biochem. J.* **323**, 427-433.

Dighiero, G. and Rose, N.R. (1999) Critical self-epitopes are key to the understanding of self-tolerance and autoimmunity. *Immunol. Today* **20**, 423-428.

Dorner, T., Trebeljahr, G., Goldner, B., Yamamoto, K., Apostoloff, E. and Hiepe, F. (1994) Detection of autoantibodies to Ro(SS-A), La(SS-B) and U1RNP in different congenital heart rhythm disorders using immunoblot and enzyme immunoassay. *J. Autoimmun.* **7**, 93-106.

Doyle, H.A. and Mamula, M.J. (2001) Post-translational protein modifications in antigen recognition and autoimmunity. *Trends Immunol.* **22**, 443-449.

Dragon, F., Gallagher, J.E., Compagnone-Post, P.A., Mitchell, B.M., Porwancher, K.A., Wehner, K.A., Wormsley, S., Settlage, R.E., Shabanowitz, J., Osheim, Y., Beyer, A.L., Hunt, D.F. and Baserga, S.J. (2002). A large nucleolar U3 ribonucleoprotein required for 18S ribosomal RNA biogenesis. *Nature* **417**, 967-970.

Drappa, J., Vaishaw, A.K., Sullivan, K.E., Chu, J.L. and Elkon, K.B. (1996) Fas gene mutations in the Canale-Smith syndrome: an inherited lymphoproliferative disorder associated with autoimmunity. *N. Eng. J. Med.* **335**, 1643-1649.

Duran, N., Bach, M., Puigdomenech, P. and Palau, J. (1984) Characterisation of antigenic polypeptides of the RNP, Sm and SS-B nuclear antigens from calf thymus. *Mol. Immunol.* **21**, 731-739.

Eddy, S.R. (1999) Noncoding RNA genes. *Current Opinion in Genetics and Development* **9**, 695-699.

Eissfeller, P., Sticherling, M., Scholz, D., Hennig, K., Luttich, T., Motz, M. and Kromminga, A. (2005) Comparison of different test systems for simultaneous autoantibody detection in connective tissue disease. *Ann. N.Y. Acad. Sci.* **1050**, 327-339.

Ekman, P. and Jager, *O.* (1993) Quantification of subnanomolar amounts of phosphate bound to seryl and threonyl residues in phosphoproteins using alkaline hydrolysis and malachite green. *Anal. Biochem.* **214**, 138-141.

Elkon, K.B. and Jankowski, P.W. (1985) Fine specificities of autoantibodies directed against the Ro, La, Sm, RNP and Jo-1 proteins defined by two-dimensional gel electrophoresis and immunoblotting. *J. Immunol.* **134**, 3819-3824.

Elkon, K.B., Hines, J.J., Chu, J-L. and Parnassa, A. (1990) Epitope mapping of recombinant HeLa SmB and SmB′ peptides obtained by the polymerase chain reaction. *J. Immunol.* **145**, 636-643.

Engvall, E. and Perlmann, P. (1972) Enzyme-linked immunosorbent assay, ELISA. III. Quantitation of specific antibodies by enzyme-linked anti-immunoglobulin in antigen coated tubes. *J. Immunol.* **109**, 129-135.

Ermens, A.A., Bayens, A.J., van Gemert, A.C. and van Duijnhoven, J.L. (1997) Simple dot-blot method evaluated for detection of antibodies against extractable nuclear antigens. *Clin. Chem.* **43**, 2420-2422.

Faig, O.Z. and Lutz, C.S. (2003) Novel specificity of anti-U1A autoimmune patient sera. *Scand. J. Immunol.* **57**, 79-84.

Felbor, U., Dreier, L., Bryant, R.A., Ploegh, H.L., Olsen, B.R. and Mothes, W. (2000) Secreted cathepsin L generates endostatin from collagen XVIII. *EMBO J.* **19**, 1187-1194.

Fischer, U., Sumpter, V., Sekine, M., Satoh, T. and Lührmann, R. (1993) Nucleo-cytoplasmic transport of U snRNPs: definition of a nuclear location signal in the Sm core domain that binds a transport receptor independently of the m_3G cap. *EMBO J.* **12**, 573-583.

Friesen, W.J., Paushkin, S., Wyce, A., Massenet, S., Pesiridis, G.S., Van Duyne, G., Rappsilber, J., Mann, M. and Dreyfuss G. (2001) The methylosome, a 20S complex containing JBP1 and pICln, produces dimethylarginine-modified Sm proteins. *Mol. Cell Biol.* **21**, 8289-8300.

Friesen, W.J., Wyce, A., Paushkin, S., Abel, L., Rappsilber, J., Mann, M. and Dreyfuss G. (2002) A novel WD repeat protein component of the methylosome binds Sm proteins. *J. Biol. Chem.* **277**, 8243-8247.

Friou, G.J., Finch, S.C. and Detre, K.D. (1958) Interaction of nuclei and globulin from lupus erythematosus serum demonstrated with fluorescent antibody. *J. Immunol.* **80**, 324-329.

Froelich, C.J., Wallman, J., Skosey, J.L. and Teodorescu, M. (1990) Clinical value of an integrated ELISA system for the detection of 6 autoantibodies (ssDNA, dsDNA, Sm, RNP/Sm, SSA and SSB). *J. Rheumatol.* **17**, 192-200.

Gaither, K.K. and Harley, J.B. (1985) Affinity purification and immunoassay of anti-Ro/SSA. *Protides Biol. Fluids Proc. Colloq.* **33**, 413-416.

Garcia, B.A., Shabanowitz, J. and Hunt, D.F. (2005) Analysis of protein phosphorylation by mass spectrometry. *Methods* **35**, 256-264.

Gaubitz, M., Wegmann, C., Schotte, H., Willeke, P. and Domschke, W. (2002) Differentiation of RNP and Sm antibody subsets in SLE and MCTD patients by a new ELISA using recombinant antigens. *Cell Mol. Biol. (Noisy-le-grand)* **48**, 317-321.

Ghirardello, A., Doria, A., Vesco, P., Vaccaro, E., Bernardi, C., Catani, C., Fafiolo, U. and Gambari, P.F. (1996) Blotting patterns of IgG anti-(U1) RNP antibodies in mixed connective tissue disease. *Rheumatol. Int.* **16**, 145-150.

Gilburd, B., Abu-Shakra, M., Shoenfeld, Y., Giordano, A., Bocci, E.B., delle Monache, F. and Gerli, R. (2004) Autoantibodies profile in the sera of patients with Sjogren's syndrome: the ANA evaluation—a homogeneous, multiplexed system. *Clin. Dev. Immunol.* **11**, 53-56.

Goodnow, C.C., Sprent, J., Fazekas de St Groth, B. and Vinuesa, C.G. (2005) Cellular and genetic mechanisms of self tolerance and autoimmunity. *Nature* **435**, 590-597.

Gorbunoff, M.J. (1984a) The interactions of proteins with hydroxyapatite II. The role of acidic and basic groups. *Anal. Biochem.* **136**, 433-439.

Gorbunoff, M.J. and Timasheff, S.N. (1984b) The interaction of proteins with Hydroxyapatite. *Anal. Biochem.* **136**, 440-445.

Greenwood, D.L., Gitlits, V.M., Alderuccio, F., Sentry, J.W. and Toh, B.H. (2002) Autoantibodies in neuropsychiatric lupus. *Autoimmunity* **35**, 79-86.

Greidinger, E.L., Casciola-Rosen, L., Morris, S.M., Hoffman, R.W. and Rosen, A. (2000) Autoantibody recognition of distinctly modified forms of the U1-70-kd antigen is associated with different clinical disease manifestations. *Arthritis Rheum.* **43**, 881-888.

Greidinger, E.L. and Hoffman, R.W. (2001) The appearance of U1 RNP antibody specificities in sequential autoimmune human anti sera follows a characteristic order that implicates the U1-70 kD and B′/B proteins as the predominant U1 RNP immunogens. *Arthritis Rheum.* **44**, 368-375.

Greidinger, E.L., Foecking, M.F., Ranatunga, S. and Hoffman, R.W. (2002) Apoptotic U1-70 kD is antigenically distinct from the intact form of the U1-70 kD molecule. *Arthritis Rheum.* **46**, 1264-1269.

Greidinger, E.L., Foecking, M.F., Magee, J., Wilson, L., Ranatunga, S., Ortmann, R.A. and Hoffmann, R.W. (2004) A major B cell epitope present on the apoptotic but not the intact form of the U1-70 kD ribonucleoprotein autoantigen. *J. Immunol.* **172**, 709-716.

Greidinger, E.L., Zang, Y., Jaimes, K., Hogenmiller, S., Nassiri, M., Bejarano, P., Barber, G.N. and Hoffman, R.W. (2006) A murine model of mixed connective tissue disease induced with U1 small nuclear RNP autoantigen. *Arthritis Rheum.* **54**, 661-669.

Grigolo, B., Mazzetti, I., Borzi, R.M., Meliconi, R., Origgi, L., Scorza, R. and Facchini, A. (1995) Comparison of different methods for the detection of autoantibodies in autoimmune diseases. *Int. J. Clin. Lab. Res.* **25**, 205-210.

Guan, F., Palacios, D., Hussein, R.I. and Gunderson, S.I. (2003) Determinants within an 18 amino acid U1A autoregulatory domain that uncouple cooperative RNA binding, inhibition of polyadenylation and homodimerisation. *Mol. Cell Biol.* **23**, 3163-3172.

Gubitz, A.K., Feng, W. and Dreyfuss, G. (2004) The SMN complex. *Exp. Cell Res.* **296**, 51-56.

Guldner, H.H., Lakomek, H-J. and Bautz, F.A. (1983) Identification of human Sm and (U1) RNP antigens by immunoblotting. *J. Immunol. Methods* **64**, 45-59.

Guldner, H.H. (1992) Mapping of epitopes recognised by anti-(U1) RNP autoantibodies. *Mol. Biol. Rep.* **16**, 155-164.

Guma, M. and Krakauer, R. (1994) CD4+ lymphocytopenia in systemic lupus erythematosus. *Ann. Intern. Med.* **120**, 168-169.

Gupta, R., Jung, E., Gooley, A.A., Williams, K.L., Brunak, S. and Hansen, J. (1999a) Scanning the available Dictyostelium discoideum proteome for O-linked GlcNAc glycosylation sites using neural networks. *Glycobiology* **9**, 1009-1022.

Gupta, R. and Ahmad, F. (1999b) Protein stability: Functional dependence of denaturational Gibbs energy on urea concentration. *Biochemistry* **38**, 2471-2479.

Gupta, R. and Brunak, S. (2002) Prediction of glycosylation across the human proteome and the correlation to protein function. *Pac. Symp. Biocomput.* 310-322.

Habets, W., de Rooij, D.J., Hoet, M.H., van de Putte, L.B. and van Venrooij, W.J. (1985a) Quantitation of anti-RNP and anti-Sm antibodies in MCTD and SLE patients by immunoblotting. *Clin. Exp. Immunol.* **59**, 457-466.

Habets, W., Hoet, M., Bringmann, P., Lührmann, R. and van Venrooij, W. (1985b) Autoantibodies to ribonucleoprotein particles containing U2 small nuclear RNA. *EMBO J.* **4**, 1545-1550.

Habets, W.J., Hoet, M.H., de Jong, B.A.W., van der Kemp, A. and van Venrooij, W.J. (1989) Mapping of B cell epitopes on small nuclear ribonucleoproteins that react with

human autoantibodies as well as with experimentally induced mouse monoclonal antibodies. *J. Immunol.* **143**, 2560-2566.

Habets, W.J., Hoet, M.H. and van Venrooij, W.J. (1990) Epitope patterns of anti-RNP antibodies in rheumatic diseases. *Arthritis Rheum.* **33**, 834-841.

Halse, A.K., Marthinussen, M.C., Wahren-Herlenius, M. and Jonsson, R. (2000) Isotype distribution of anti-Ro/SS-A and anti-La/SS-B antibodies in plasma and saliva of patients with Sjögren's syndrome. *Scand. J. Rheumatol.* **29**, 13-19.

Hamm, J. and Mattaj, I.W. (1990) Monomethylated cap structures facilitate RNA export from the nucleus. *Cell* **63**, 109-118.

Hanayama, R., Tanaka, M., Miyasaka, K., Aozasa, K., Koike, M., Uchiyama, Y. and Nagata, S. (2004) Autoimmune disease and impaired uptake of apoptotic cells in MFG-E8-deficient mice. *Science* **304**, 1147-1150.

Hansen, J.E., Lund, O., Tolstrup, N., Gooley, A.A., Williams, K.L. and Brunak, S. (1998) NetOGlyc: prediction of mucin type O-glycosylation sites based on sequence context and surface accessibility. *Glycoconjugate J.* **15**, 115-130.

Harley, J.B., Moser, K.L., Gaffney, P.M. and Behrens, T.W. (1998) The genetics of human SLE. *Curr. Opin. Immunol.* **10,** 690-696.

Harlow, E. and Lane, D. (1988) Immunoaffinity purification. In Harlow, E. and Lane, D. eds. *Antibodies: A laboratory manual*. Cold Spring Harbor Laboratory.

Hassfeld, W., Steiner, G., Studnicka-Benke, A., Skriner, K., Graninger, W., Fischer, I. and Smolen, J.S. (1995) Autoimmune response to the spliceosome: an immunologic link between rheumatoid arthritis, mixed connective tissue disease and systemic lupus erythematosus. *Arthritis Rheum.* **38**, 777-785.

Hay, E.M. (1995) Systemic lupus erythematosus. *Baillieres Clin. Rheumatol.* **9**, 437-470.

Haynes, P.A. and Aebersold, R. (2000) Simultaneous detection and identification of O-GlcNAc modified glycoproteins using liquid chromatography-tandem mass spectrometry. *Anal. Chem.* **72**, 5402-5410.

Hermann, H., Fabrizio, P., Raker, V.A., Foulaki, K., Hornig, H., Brahms, H. and Lührmann, R. (1993) snRNP Sm proteins share 2 evolutionarily conserved sequence motifs which are involved in Sm protein-protein interactions. *EMBO J.* **14**, 2076-2088.

Hines, J.J., Danho, W. and Elkon, K.B. (1991) Detection and quantification of human anti-Sm antibodies using synthetic peptide and recombinant Sm B antigens. *Arthritis Rheum.* **34**, 572-579.

Hirakata, M., Craft, J. and Hardin, J.A. (1993) Autoantigenic epitopes of the B and D polypeptides of the U1 snRNP. *J. Immunol.* **150**, 3592-3601.

Hoch, S.O. (1990) Isolation of small nuclear ribonucleoprotein polypeptides. *Methods Enzymol.* **181**, 257-263.

Hochleitner, E.O., Kastner, B., Frohlich, T., Schmidt, A., Lührmann, R., Arnold, G. and Lottspeich, F. (2005) Protein stoichiometry of a multiprotein complex, the human spliceosomal U1 small nuclear ribonucleoprotein. *J. Biol. Chem.* **280**, 2536-2542.

Hoet, R.M.A., Raats, J.M.H., de Wilts, R., Dumortier, H., Muller, S., van den Hoogen, F. and van Venrooij, W.J. (1999) Human monoclonal autoantibody fragments from combinatorial antibody libraries directed to the U1 snRNP associated U1 C protein: epitope mapping, immunolocalisation and V-gene usage. *Mol. Immunol.* **35**, 1045-1055.

Hof, D., Cheung, K., Ram de Rooij, D-J., van den Hoogen, F.H., Pruijn, G.J.M., van Venooij, W.J. and Raats, J.M.H. (2005) Autoantibodies specific for apoptotic U1-70K are superior serological markers for mixed connective tissue disease. *Arthritis Res. Ther.* **7**, 302-309.

Hogg, R.J. and Davidson, G.P. (1982) Improved specificity of ELISA for rotavirus. *Austr. Paediatr. J.* **18**, 184-185.

Holborow, E.J., Weir, D.M. and Johnson, G.G. (1957) A serum factor in lupus erythematosus with affinity for tissue nuclei. *Br. Med. J.* **2**, 732-740.

Horsfall, A.C. (1992) Molecular mimicry and autoantigens in connective tissue diseases. *Mol. Biol. Reps.* **16**, 139-147.

Hughes, P., Bouillet, P. and Strasser, A. (2006) Role of Bim and other Bcl-2 family members in autoimmune and degenerative diseases. *Curr. Dir. Autoimmun.* **9**, 74-94.

Ihn, H., Yamane, K., Yazawa, N., Kubo, M., Fujimoto, M., Sato, S. (1999) Distribution and antigen specificity of anti-U1RNP antibodies in patients with systemic sclerosis. *Clin. Exp. Immunol.* **117**, 383-387.

Inaoki, M., Sato, S., Weintraub, B.C., Goodnow, C.C. and Tedder, T.F. (1997) CD-19 regulated signalling thresholds control peripheral tolerance and autoantibody production in B lymphocytes. *J. Exp. Med.* **186**, 1923-1931.

Itoh, Y., Itoh, K., Frank, M.B. and Reichlin, M. (1992) Autoantibodies to the Ro/SSA autoantigen are conformation dependent. II: Antibodies to the denatured form of 52 kD Ro/SSA are a cross reacting subset of antibodies to the native 60 kD Ro/SSA molecule. *Autoimmunity* **14**, 89-95.

Izaurralde, E., Lewis, J., Gamberi, C., Jarmolowski, A., McGuigan, C. and Mattaj, I.W. (1995) A cap-binding protein complex mediating U snRNA export. *Nature* **376**, 709-712.

James, J.A. and Harley, J.B. (1992) Linear epitope mapping of an Sm B′/B polypeptide. *J. Immunol.* **148**, 2074-2079.

James, J.A., Mamula, M.J. and Harley, J.B. (1994a) Sequential autoantigenic determinants of the small nuclear ribonucleoprotein Sm D shared by human lupus autoantibodies and MRL *lpr/lpr* antibodies. *Clin. Exp. Immunol.* **98**, 419-426.

James, J.A., Scofield, R.H. and Harley, J.B. (1994b) Basic amino acids predominate in the sequential autoantigenic determinants of the small nuclear 70K ribonucleoprotein. *Scand. J. Immunol.* **39**, 557-566.

James, J.A., Gross, T., Scofield, R.H. and Harley, J.B. (1995a) Immunoglobulin epitope spreading and autoimmune disease after peptide immunisation: Sm B′/B – derived PPPGMRPP and PPPGIRGP induced spliceosome autoimmunity. *J. Exp. Med.* **181**, 453-461.

James, J.A. and Harley, J.B. (1995b) Peptide autoantigenicity of the small nuclear ribonucleoprotein C. *Clin. Exp. Rheumatol.* **13**, 299-305.

James, J.A. and Harley, J.B. (1996) Human lupus anti-splicesome A protein autoantibodies bind contiguous surface structures and segregate into two sequential epitope binding patterns. *J. Immunol.* **156**, 4018-4026.

James, K., Carpenter, A.B., Cook, L., Marchand, R. and Nakamura, R.M. (2000) Development of the antinuclear and anticytoplasmic antibody consensus panel by the association of Medical Laboratory Immunologists. *Clin. Diagnostic Lab. Immunol.* **7**, 436-443.

Jaskowski, T.D., Schroder, C., Martins, T.B., Mouritsen, L. and Hill, H.R. (1995) Comparison of three commercially available enzyme immunoassays for screening of autoantibodies to extractable nuclear antigens. *J. Clin. Lab. Anal.* **9**,166-172.

Jeno, P., Mini, T., Moes, S., Hintermann, E. and Horst, M. (1995) Internal sequences from proteins digested in polyacrylamide gels. *Anal. Biochem.* **224**, 75-82.

Jones, K.D. (1999) Trouble-shooting protein binding in nitrocellulose membranes. *IVD Technol.* **5**, 3241D.

Kamachi, M., Le, T.M., Kim, S.J., Geiger, M.E., Anderson, P. and Utz, P.J. (2002) Human autoimmune sera as molecular probes for the identification of an autoantigen kinase signaling pathway. *J. Exp. Med.* **196**, 1213-1225.

Kambach, C., Walke, S., Young, R., Avis, J.M., de la Fortelle, E., Raker, V.A., Lührmann, R., Li, J. and Nagai, K. (1999) Crystal structures of 2 Sm protein complexes and their implications for the assembly of the spliceosomal snRNPs. *Cell* **96**, 375-387.

Kato, K., Umedo, Y., Suzuki, F. and Kosaka, A. (1980) Improved reaction buffers for solid phase enzyme immunoassay without interference by serum factors. *Clin. Chim. Acta* **102**, 261-265.

Kataoka, N., Ohno, M., Moda, I. and Shimura, Y. (1995) Identification of the factors that interact with NCBP, an 80 kDa nuclear cap binding protein. *Nucleic Acids Res.* **23**, 3638-3641.

Katsamba, P., Myszka, D.G. and Laird-Offringa, I.A. (2001) Two functionally distinct steps mediate high affinity binding of U1A protein to U1 hairpin II RNA. *J. Biol. Chem.* **276**, 21476-21481.

Kavanaugh, A. (2001) The utility of immunologic laboratory tests in patients with rheumatic diseases. *Arthritis Rheum.* **44**, 2221-2223.

Kazatchkine, M.D. (1994) Natural IgG autoantibodies in the sera of healthy individuals. *J. Interferon Res.* **14**, 165-168.

Kelly, K.M., Zhuang, H., Nacionales, D.C., Scumpia, P.O., Lyons, R., Akaogi, J., Lee, P., Williams, B., Yamamoto, M., Akira, S., Satoh, M. and Reeves, W.H. (2006) "Endogenous adjuvant" activity of the RNA components of lupus autoantigens Sm/RNP and Ro 60. *Arthritis Rheum.* **54**, 1557-1567.

Kennerson, M.L., Gordon, M.J., Blair, I.P. and Nicholson, G.A. (1995) Single test for two hereditary neuropathies, CMT1A and HNPP. *Clin. Chem.* **41**, 1534-1535.

Khidelkel, N., Ficarro, S.B., Peters, E.C. and Hsieh-Wilson, L.C. (2004) Exploring the O-GlcNAc modified proteins from the brain. *Proc. Natl. Acad. Sci. USA* **101**, 13132-13137.

Klein-Gunnewick, J.M.T., van Aarssen, Y., Wassenaar, R., Legrain, P., van Venrooij, W.J. and Nelissen, R.L.H. (1995) Homodimerization of the human U1 snRNP-specific protein C. *Nucleic Acids Res.* **23**, 4864-4871.

Klein-Gunnewiek, J.M.T., Hussein, R.I., van Aarssen, Y., Palacios, D., de Jong, R., van Venrooij, W.J. and Gunderson, S.I. (2000) Fourteen residues of the U1 snRNP-specific U1A protein are required for homodimerisation, cooperative RNA binding and inhibition of polyadenylation. *Mol. Cell Biol.* **20**, 2209-2217.

Klinman, D. and Steinberg, A.D. (1987) Systemic autoimmune disease arises from polyclonal B cell activation *J. Exp. Med.* **165**, 1755-1760.

Kotzin, B.L. (1996) Systemic lupus erythematosus. *Cell* **85**, 303-306.

Kramer, A. (1990) Purification of small nuclear ribonucleoprotein particles active in RNA processing. *Methods Enzymol.* **181**, 215-232.

Kurata, N. and Tan, E.M. (1976) Identification of antibodies to nuclear acidic antigens by counterimmunoelectrophoresis. *Arthritis Rheum.* **19**, 574-580.

Lafferty, K.J. and Ronald, G.G. (1993) Maintenance of self-tolerance. *Immunol. Cell. Biol.* **71**, 209-221.

Lauber, J., Plessel, G., Prehn, S., Will, C.L., Fabrizio, P., Groning, K., Lane, W.S. and Lührmann, R. (1997) The human U4/U6 snRNP contains 60 and 90kD proteins that are structurally homologous to the yeast splicing factors Prp4p and Prp3p. *RNA* **3**, 926-941.

Lauber, K., Blumenthal, S.G., Waibel, M. and Wesselborg, S. (2004) Clearance of apoptotic cells: getting rid of the corpses. *Mol. Cell* **14**, 277-287.

Law, M.J., Linde, M.E., Chambers, E.J., Oubridge, C., Katsumba, P.S., Nilsson, L., Haworth, I.S. and Laird-Offringa, I.A. (2006) The role of positively charged amino acids and electrostatic interactions in the complex of U1A protein and U1 hairpin II RNA. *Nucleic Acids Res.* **34**, 275-285.

Lazaro, M.A., Maldonado Cocco, J.A., Catoggio, L.J., Babini, S.M., Messina, O.D. and Garcia Morteo, O.G. (1989) Clinical and serologic characteristics of patients with overlap syndrome. *Medicine* **68**, 58-65.

Leadbetter, E.A., Rifkin, I.R., Hohlbaum, A.M., Beaudette, B.C., Shlomchik, M.J. and Marshak-Rothstein, A. (2002) Chromatin-IgG complexes activate B cells by dual engagement of IgM and Toll-like receptors. *Nature* **416**, 603-607.

Laemmli, UK. (1970) Cleavage of structural proteins during the assembly of the head of bacteriophage T4. *Nature* **227**, 680-685.

Lederberg, J. (1959) Genes and Antibodies. *Science* **129**, 1649-1653.

Lefebvre, S., Burlet, P., Liu, Q., Bertrandy, S., Clermont, O., Munnich, A., Dreyfuss, G. and Melki, J. (1997) *Correlation* between severity and SMN protein level in spinal muscular atrophy. *Nat. Gen.* **16**, 265-269.

Leff, R.L., Love, L.A., Miller, F.W., Greenberg, S.J., Klein, E.A., Dalakas, M.C. and Plotz, P.H. (1992) Viruses in idiopathic inflammatory myopathies: absence of candidate viral genomes in muscle. *Lancet* **339**, 1192-1195.

Lehmeier, T., Foulaki, K. and Lührmann, R. (1990) Evidence for 3 distinct D proteins, which react differentially with anti-Sm autoantibodies, in the cores of the major snRNPs U1, U2, U4/U6 and U5. *Nucleic Acids Res.* **18**, 6475-6484.

Leist, M. and Nicotera, P. (1997) The shape of cell death. *Biochem. Biophys. Res. Commun.* **236**, 1-9.

Lerner, M.R. and Steitz, J.A. (1979) Antibodies to small nuclear RNAs complexed with proteins are produced by patients with systemic lupus erythematosus. *Proc. Natl. Acad. Sci. USA* **76**, 5495-5499.

Lerner, E.A., Lerner, M.R., Janeway, C.A. and Steitz, J.A. (1980) Monoclonal antibodies to nucleic acid containing cellular constituents: probes for molecular biology and autoimmune disease. *Proc. Natl. Acad. Sci. USA* **78**, 2737-2741.

Levinson, S.S. (1994) Organ specific autoimmune disease. *J. Clin. Immunoassay* **17**, 92-97.

Liang, S. and Lutz, C.S. (2006) p54nrb is a component of the snRNP-free U1A (SF-A) complex that promotes pre-mRNA cleavage during polyadenylation. *RNA* **12**, 111-121.

Lidell, M.E., Johansson, M.E.V. and Hansson, G.C. (2003) An autocatalytic cleavage in the C-terminus of the human MUC2 mucin occurs at the low pH of the late secretory pathway. *J. Biol. Chem.* **278**, 13944-13951.

Lipsky, P.E. (2001) Systemic lupus erythematosus: an autoimmune disease of B cell hyperactivity. *Nature Immunol.* **2**, 764-766.

Lock, R.J. and Unsworth, D.J. (2001) Antibodies to extractable nuclear antigens. Has technological drift affected clinical interpretation? *J. Clin. Pathol.* **54**, 187-190.

Lopez-Longo, F.J., Rodriguez-Mahou, M., Escalona-Monge, M., Gonzalez, C.M., Monteagudo, I. and Carreno-Perez, L. (2002) Simultaneous identification of various antinuclear antibodies using an automated multiparameter line immunoassay system. *Lupus* **12**, 623-629.

Lührmann, R., Kastner, B. and Bach, M. (1990) Structure of spliceosomal snRNPs and their role in pre-mRNA splicing. *Biochim. Biophys. Acta* **1087**, 265-292.

Luminex technology, www.luminexcorp.com.

Lutz, C.S., Murphy, K.G.K., Schek, N., O'Connor, J.P., Manley, J.L. and Alwine, J.C. (1996) Interaction between the U1snRNP-A protein and the 160 kD subunit of cleavage –polyadenylation specificity factor increases polyadenylation efficiency in vitro. *Genes Dev.* **10**, 325-337.

Lutz, C.S., Cooke, C., O'Connor, J.P., Kobayashi, R. and Alwine, J.C. (1998) The snRNP-free U1A (SF-A) complex(es): identification of the largest subunit as PSF, the polypyrimidine-tract binding protein-associated splicing factor. *RNA* **4**, 1493-1499.

Lutz-Freyermuth, C., Query, C.C. and Keene, J.D. (1990) Quantitative determination that one of two potential RNA-binding domains of the A protein component of the U1 small nuclear ribonucleoprotein complex binds with high affinity to stem-loop II of U1 RNA. *Proc. Natl. Acad. Sci. USA* **87**, 6393-6397.

Luyckx, A., Westhovens, R., Oris, E., Papisch, W. and Bossuyt, X. (2005) Clinical relevance of measurement of antibodies to individual snU1 RNP proteins. *Clin. Chem.* **51**, 1888-1890.

Lyons, R., Narain, S., Nichols, C., Satoh, M. and Reeves, W.H. (2005) Effective use of autoantibody tests in the diagnosis of systemic autoimmune disease. *Ann. N.Y. Acad. Sci.* **1050**, 217-228.

Mackay, F. and Mackay, C.R. (2002) Role of BAFF in B-cell maturation, T-cell activation and autoimmunity. *Trends Immunol.* **23**, 113-115.

MacKenzie, A.E. and Gendron, N.H. (2001) Tudor reign. *Nature Struct. Biol.* **8**, 13-15.

Maddison, P.J., Provost, T.T. and Reichlin, M. (1981) Serological findings in patients with “ANA-negative” systemic lupus erythematosus. *Medicine* **60**, 87-94.

Mahler, M., Fritzler, M.J. and Bluthner, M. (2004) Identification of a Sm D3 epitope with a single symmetrical dimethylation of an arginine residue as a specific target of a subpopulation of anti-Sm antibodies. *Arthritis Res. Ther.* **7**, 19-29.

Mahoney, J.A. and Rosen, A. (2005) Apoptosis and autoimmunity. *Curr. Opin. Immunol.* **17**, 583-588.

Maloy, K.J. and Powrie, F. (2001) Regulatory T cells in the control of immune pathology. *Nature Immunol.* **2**, 816-822.

Mamula, M.J., Gee, R.J., Elliot, J.I., Sette, A., Southwood, S., Jones, P-J. and Blier, P.R. (1999) Isoaspartyl post-translational modification triggers autoimmune responses to self-proteins. *J. Biol. Chem.* **274**, 22321-22327.

Manoussakis, M.N., Kistis, K.G., Liu, X., Aidinis, V., Guialis, A. and Moutsopoulos, H.M. (1993) Detection of anti-Ro(SSA) antibodies in autoimmune diseases: comparison of five methods. *Br. J. Rheumatol.* **32**, 449-455.

Maraia, R.J., Kenan, D.J. and Keene, J.D. (1994) Eukaryotic transcription termination factor La mediates transcript release and facilitates reinitiation by RNA polymerase III. *Mol. Cell. Biol.* **14**, 2147-2158.

Martins, T.B., Burlinghame, R., von Muhlen, C.A., Jaskowski, T.D., Litwin, C.M. and Hill, H.R. (2004) Evaluation of multiplexed fluorescent microsphere immunoassay for detection of autoantibodies to nuclear antigens. *Clin. Diagn. Lab. Immunol.* **11**, 1054-1059.

Martinson, H.G. (1973) The basis of fractionation of single-stranded nucleic acids on hydroxylapatite. *Biochemistry* **12**, 2731-2736.

Massenet, S., Pellizzoni, L., Paushkin, S., Mattaj, I.W. and Dreyfuss, G. (2002) The SMN complex is associated with snRNPs throughout their cytoplasmic assembly pathway. *Mol. Cell Biol.* **22**, 6533-6541.

Mattaj, I.W. (1986) Cap trimethylation of U snRNA is cytoplasmic and dependent on U snRNP protein binding. *Cell* **46**, 905-911.

McClain, M.T., Ramsland, P.A., Kaufman, K.M. and James, J.A. (2002) Anti-Sm autoantibodies in systemic lupus target highly basic surface structures of complexed autoantigens. *J. Immunol.* **168**, 2054-2062.

McClain, M.T., Lutz, C.S., Kaufman, K.M., Faig, O.Z., Gross, T.F. and James, J.A. (2004) Structural availability influences the capacity of autoantigenic epitopes to induce a widespread lupus-like autoimmune response. *Proc. Natl. Acad. Sci. USA* **101**, 3551-3556.

McMurdy, D.K., Bick, M., Gatti, R.A. and Naeim, F. (1992) Autoantibodies in systemic lupus erythematosus. *Disease Markers* **10**, 37-49.

Meheus, L., van Venrooij, W.J., Wiik, A., Charles, P.J., Tzioufas, A.G., Meyer, O., Steiner, G., Gianola, D., Bombardieri, S., Union, A., de Keyser, S., Veys, E. and de Keyser, F. (1999) Multicenter validation of recombinant, natural and synthetic antigens used in a single multiparameter assay for the detection of specific anti-nuclear autoantibodies in connective tissue disorders. *Clin. Exp. Rheumatol.* **17**, 205-214.

Meilof, J.F., Bantjes, I., De Jong, J., Van Dam, A.P. and Smeenk, R.J. (1990) The detection of anti-Ro/SS-A and anti-La/SS-B antibodies. A comparison of

counterimmunoelectrophoresis with immunoblot, ELISA, and RNA-precipitation assays. *J. Immunol. Methods* **133**, 215-226.

Mermoud, J.E., Cohen, P.T.W. and Lamond, A.I. (1994) Regulation of mammalian spliceosome assembly by a protein phosphorylation mechanism. *EMBO J.* **13**, 5679-5688.

Meyer, O., Bourgeois, P., Aeschlimann, A., Haim, T., Mery, J.P. and Kahn, M.F. (1989) Immunoblotting profiles in 55 systemic lupus erythematosus sera lacking precipitating antibodies to extractable nuclear antigens. *Ann. Rheum. Dis.* **48**, 594-599.

Miller, F.W., Twitty, S.A., Biswas, T. and Plotz, P.H. (1990) Origin and regulation of a disease-specific autoantibody response. Antigenic epitopes, spectrotype stability, and isotype restriction of anti-Jo-1 autoantibodies. *J. Clin. Invest.* **85**, 468-475.

Misteli, T. and Spector, D.L. (1997) Protein phosphorylation and the nuclear organisation of pre-mRNA splicing. *Trends Cell Biol.* **7**, 135-138.

Mitchison, N.A. and Wedderburn, L.R. (2000) B cells in autoimmunity. *Proc. Natl. Acad. Sci. USA* **97**, 8750-8751.

Molden, D.P., Suzuki, H. and Nakamura, R.M. (1985) Assays for Sm and RNP antibodies: pitfalls and technical considerations. *Diagn. Immunol.* **3**, 24-28.

Moller, T., Franch, T., Hojrup, P., Keene, D.R., Bachinger, H.P., Brennan, R.G. and Valentin-Hansen, P. (2002) Hfq: A bacterial Sm-like protein that mediates RNA-RNA interaction. *Mol. Cell* **9**, 23-30.

Monneaux, F., Lozano, J.M., Patarroyo, M.E., Briand, J-P. and Muller, S. (2003) T cell recognition and therapeutic effect of a phosphorylated synthetic peptide of the 70K snRNP protein administered in MRL/lpr mice. *Eur. J. Immunol.* **33**, 287-296.

Mukerji, B. and Hardin, J.G. (1993) Undifferentiated, overlapping and mixed connective tissue diseases. *Am. J. Med. Sci.* **305**, 114-119.

Mura, C., Kozhukhovsky, A., Gingery, M., Phillips, M. and Eisenberg, D. (2003) The oligomerisation and ligand-binding properties of Sm-like archael proteins (SmAPs). *Protein Sci.* **12**, 832-847.

Murakami, A., Kojima, K., Ohya, K., Imamura, K. and Takasaki, Y. (2002) A new conformational epitope generated by the binding of recombinant 70-kd protein and U1

RNA to anti-U1 RNP autoantibodies in sera from patients with mixed connective tissue disease. *Arthritis Rheum.* **46**, 3272-3283.

Murray, M.V., Kobayashi, R. and Krainer, A.R. (1999) The type 2C ser/thr phosphatase PP2Cγ is a pre-mRNA splicing factor. *Genes Dev.* **13**, 87-97.

Muto, Y., Pomeranz-Krummel, D., Oubridge, C., Hernandez, H., Robinson, C.V., Neuhaus, D. and Nagai, K. (2004) The structure and biochemical properties of the human spliceosomal protein U1C. *J. Mol. Biol.* **341**, 185-198.

Nagai, K., Oubridge, C., Ito, N., Avis, J. and Evans, P. (1995) The RNP domain: a sequence specific RNA-binding domain involved in processing and transport of RNA. *TIBS* **20**, 235-240.

Nagai, K., Muto, Y., Pomeranz Krummel, D.A., Kambach, C., Ignjatovic, T., Walke, S. and Kuglstatter, A. (2001) Structure and assembly of the spliceosomal snRNPs. *Biochem. Soc. Trans.* **29**, 15-26.

Nagaraju, K., Raben, N., Loeffler, L., Parker, T., Rochon, P.J., Lee, E., Danning, C., Wada, R., Thompson, C., Bahtiyar, G., Craft, J., Hooft van Huijsduijnen, R. and Plotz, P. (2000) Conditional up-regulation of MHC class I in skeletal muscle leads to self-sustaining autoimmune myositis and myositis-specific autoantibodies. *Proc. Natl. Acad. Sci. USA* **97**, 9209-9214.

Nakagawa, T. (1998) Cathepsin L: critical role in Ii degradation and CD4 T cell selection in the thymus. *Science* **280**, 450-453.

Nakamura, M.C. and Nakamura, R.M. (1992) Contemporary concepts of autoimmunity and autoimmune diseases. *J. Clin. Lab. Anal.* **6**, 275-289.

Navarro, E. and Palau, J. (1991) Anti-Sm sera are misdetected by counterimmunoelectrophoresis. A critical analysis of CIE and western blotting on the detection of human antinuclear antibodies. *J. Autoimmun.* **4**, 213-222.

Neer, E.J., Schmidt, C.J., Nambudripad, R. and Smith, T.F. (1994) The ancient regulatory-protein family of WD-repeat proteins. *Nature* **371**, 297-300.

Nelissen, R.L.H., Heinrichs, V., Habets, W.J., Simons, F., Lührmann, R. and van Venrooij, W.J. (1991) Zinc finger-like structure in U1-specific protein C is essential for specific binding to U1 snRNP. *Nucleic Acids Res.* **19**, 449-454.

Nelissen, R.L., Will, C.L., van Venrooij, W.J. and Lührmann, R. (1994) The association of the U1-specific 70K and C proteins with U1snRNPs is mediated in part by common U snRNP proteins. *EMBO J.* **13**, 4113-4125.

Netter, H.J., Guldner, H.H., Szostecki, C. and Will, H. (1990) Major autoantigenic sites of the (U1) small nuclear ribonucleoprotein-specific 68-kDa protein. *Scand. J. Immunol.* **32**, 163-176.

Netter, H.J., Will, H., Szostecki, C. and Guldner, H.H. (1991) Repetitive p68 autoantigen specific epitopes recognised by human anti-(U1) small nuclear ribonucleoprotein autoantibodies. *J. Autoimmunity* **4**, 651-663.

Nishikai, M., Okano, Y., Mukohda, Y., Sato, A. and Ito, M. (1984) Serial estimation of anti-RNP antibody titres in systemic lupus erythematosus, mixed connective tissue disease and rheumatoid arthritis. *J. Clin. Lab. Immunol.* **13**, 15-19.

Northemann, W., Berg, H., Stahnke, G., Walter, M., Hunt, N. and Fenning, S. (1995) Identification of an inhibitory element within the human 68-kDa (U1) ribonucleoprotein antigen. *Prot. Exp. Purif.* **6**, 748-756.

Northway, J.J. and Tan, E.M. (1972) Differentiation of antinuclear antibodies giving speckled patterns in immunofluorescence. *Clin. Immunol. Immunopathol.* **1**, 140-154.

Nyman, U., Lundberg, I., Hedfors, E. and Pettersson, I. (1990) Recombinant 70-kDa protein used for determination of autoantigenic epitopes recognised by anti-RNP sera. *Clin. Exp. Immunol.* **81**, 52-58.

O'Connor, J.P., Alwine, J.C. and Lutz, C.S. (1997) Identification of a novel, non-snRNP protein complex containing U1A protein. *RNA* **3**, 1444-1455.

Ohosone, Y., Mimori, T., Fujii, T., Akizuki, M., Matsuoka, Y., Irimajiri, S., Hardin, J.A., Craft, J. and Homma, M. (1992) Autoantigenic epitopes of the B polypeptide of Sm small nuclear RNP particles. *Arthritis Rheum.* **35**, 960-966.

Okano, Y. and Medsger, T.A. Jr. (1992) Novel human autoantibodies reactive with 5'-terminal trimethylguanosine cap structures of U small nuclear RNA. *J. Immunol.* **149**, 1093-1098.

O'Keefe, T.L., Williams, G.T., Batista, F.D. and Neuberger, M.S. (1999) Deficiency in CD22, a B cell-specific inhibitory receptor, is sufficient to predispose development of high affinity autoantibodies. *J. Exp. Med.* **189**, 1307-1313.

Orton, S.M., Peace-Brewer, A., Schmitz, J.L., Freeman, K., Miller, W.C. and Folds, J.D. (2004) Practical evaluation of methods for detection and specificity of autoantibodies to extractable nuclear antigens. *Clin. Diagn. Lab. Immunol.* **11,** 297-301.

Oubridge, C., Ito, N., Evans, P.R., Teo, CH. and Nagai, K. (1994) Crystal structure at 1.92 A resolution of the RNA-binding domain of the U1A spliceosomal protein complexed with an RNA hairpin. *Nature* **372**, 432-438.

Ozinsky, A., Underhill, D.M., Fontenot, J.D., Hajjar, A.M., Smith, K.D., Wilson, C.B., Schroeder, L. and Aderem, A. (2000) The repertoire for pattern recognition of pathogens by the innate immune system is defined by cooperation between Toll-like receptors. *Proc. Natl. Acad. Sci. USA* **97**, 13766-13771.

Pace, C.N., Shirley, B.A. and Thomson, J.A. (1990) Measuring the conformational stability of a protein. In: Creighton, T.E. ed. *Protein structure: a practical approach.* Oxford, UK: Oxford University Press Publishers. 311-330.

Pacheco, F.J., Servin, J., Dang, D., Kim, J., Molinaro, C., Daniels, T., Brown-Bryan, T.A., Imoto-Egami, M. and Casiano, C.A. (2005) Involvement of lysosomal cathepsins in the cleavage of DNA topoisomerase I during necrotic cell death. *Arthritis Rheum.* **52**, 2133-2145.

Park, J.W., Voss, P.G., Grabski, S., Wang, J.L. and Patterson, R.J. (2001) Association of galectin-1 and galectin-3 with Gemin4 in complexes containing the SMN protein. *Nucleic Acids Res.* **27**, 3595-3602.

Parodi, A., Drosera, M., Barbieri, L. and Rebora, A. (1998) Counterimmuno-electrophoresis, ELISA and immunoblotting detection of anti-Ro/SSA antibodies in subacute cutaneous lupus erythematosus. A comparative study. *Br. J. Dermatol.* **138**, 114-117.

Paxton, H., Bendele, T., O'Connor, L. and Haynes, D.C. (1990) Evaluation of the RheumaStrip ANA profile test: a rapid test strip procedure for simultaneously determining antibodies to autoantigens U1-ribonucleoprotein (U1-RNP), Sm, SS-A/Ro, SS-B/La, and to native DNA. *Clin Chem.* **36**, 792-797.

Pelsue, S., Jung, K.D. and Agris, P.F. (1993) Immunochemical analysis of an arginine-rich systemic lupus erythematosus autoepitope. *Autoimmunity* **15**, 231-236.

Pelsue, S. and Agris, P.F. (1994) Immunoreactivity between a monoclonal lupus autoantibody and the arginine/aspartic acid repeats within the U1-snRNP 70K autoantigen is conformationally restricted. *J. Prot. Chem.* **13**, 401-408.

Perkins, D.N., Pappin, D.J., Creasy, D.M. and Cottrell, J.S. (1999) Probability-based protein identification by searching sequence databases using mass spectrometry data. *Electrophoresis* **20**, 3551-3567.

Pettersson, I., Wang, G., Smith, E.I., Wigzell, H., Hedfors, E., Horn, J. and Sharp, G.C. (1986) The use of immunoblotting and immunoprecipitation of (U) small nuclear ribonucleoproteins in the analysis of sera of patients with mixed connective tissue disease and systemic lupus erythematosus. *Arthritis Rheum.* **29**, 986-996.

Phan, T.G., Wong, R.C.W. and Adelstein, S. (2002) Autoantibodies to extractable nuclear antigens: making detection and interpretation more meaningful. *Clin. Diagn. Lab. Immunol.* **9**, 1-7.

Pickering, M.C. and Walport, M.J. (2000) Links between complement abnormalities and systemic lupus erythematosus. *Rheumatology* **39**, 133-141.

Piirainen, H.I. and Kurki, P.T. (1990) Clinical and serological follow-up of patients with polyarthritis, Raynaud's phenomenon, and circulating RNP antibodies. *Scand. J. Rheumatol.* **19**, 51-56.

Piszkiewicz, D., Landon, M. and Smith, E.L. (1970) Anomalous cleavage of asp-pro peptide bonds during amino acid sequence determination. *Biochem. Biophys. Res. Commun.* **40**, 1173-1178.

Pourmand, N., Blomberg, S., Ronnblom, L., Karlsson-Parra, A., Pettersson, I. and Wahren-Herlenius, M. (2000). Ro 52kD autoantibodies are detected in a subset of ANA-negative sera. *Scand. J. Rheumatol.* **29**, 116-123.

Raker, V., Plessel, G. and Lührmann, R. (1996) The snRNP core assembly pathway: identification of stable core protein heteromeric complexes and an snRNP subcore particle *in vitro*. *EMBO J.* **15**, 2256-2269.

Rappsilber, J., Ryder, U., Lamond, A. and Mann, M. (2002) Large-scale proteomic analysis of the human spliceosome. *Genome Research* **12**, 1231-1245.

Riemekasten, G., Marell, J., Trebeljahr, G., Klein, R., Hausdorf, G., Haupl, T., Schneider-Mergener, J., Burmester, G.R. and Hiepe, F. (1998) A novel epitope on the C-terminus of Sm D1 is recognised by the majority of sera from patients with systemic lupus erythematosus. *J. Clin. Invest.* **102**, 754-763.

Rokeach, L.A., Jannatipour, M. and Hoch, S.O. (1990) Heterologous expression and epitope mapping of a human small nuclear ribonucleoprotein-associated Sm B′/B autoantigen. *J. Immunol.* **144**, 1015-1022.

Rokeach, L.A. and Hoch, S.O. (1992a) B-cell epitopes of Sm autoantigens. *Mol. Biol. Rep.* **16**, 165-174.

Rokeach, L.A., Jannatipour, M., Haselby, J.A. and Hoch, S.O. (1992b) Mapping of the immunoreactive domains of the small nuclear ribonucleoprotein associated Sm D autoantigen. *Clin. Immunol. Immunopathol.* **65**, 315-324.

Rouquette, A.M., Desgruelles, C. and Laroche, P. (2003) Evaluation of the new multiplexed immunoassay, FIDIS, for simultaneous quantitative determination of antinuclear antibodies and comparison with conventional methods. *Am. J. Clin. Pathol.* **120**, 676-681.

Rosen, A. and Casciola-Rosen, L. (1999) Autoantigens as substrates for apoptotic proteases: implications for the pathogenesis of systemic autoimmune disease. *Cell Death Differ.* **6**, 6-12.

Roth, V. (2000) Cathepsin L deficiency as molecular defect of furless: hyperproliferation of keratinocytes and perturbation of their follicle cycling. *FASEB J.* **14**, 2075-2086.

Rupert, P.B., Xiao, H. and Ferre-D'Amare, A.R. (2003) U1A RNA-binding domain at 1.8 A resolution. *Acta Crystallogr. D.* **59**, 1521-1524.

Rutjes, S.A., Utz, P.J., van der Heijden, A., Broekhuis, C., van Venrooij, W.J. and Pruijn, G.J.M. (1999) The La(SSB) autoantigen, a key protein in RNA biogenesis is dephosphorylated and cleaved early during apoptosis. *Cell Death Diff.* **6**, 976-986.

Salgado-Garrido, J., Nilsson-Bragado, E., Kandels-Lewis, S. and Seraphin, B. (1999) Sm and Sm-like proteins assemble in two related complexes of deep evolutionary origin. *EMBO J.* **18**, 3451-3462.

Santoro, M.F., Annand, R.R., Robertson, M.M., Peng, Y.W., Brady, M.J., Mankovich, J.A., Hackett, M.C., Ghayer, T., Walter, G., Wong, W.W. and Giegel, D.A. (1998) Regulation of protein phosphatase 2A activity by caspase-3 during apoptosis. *J. Biol. Chem.* **273,** 13119-13128.

Satoh, J., Prabhakar, B.S., Haspel, M.V., Ginsberg-Fellner, F. and Notkins, A.L. (1983) Human monoclonal autoantibodies that react with multiple endocrine organs. *New Engl. J. Med.* **309**, 217-220.

Satoh, M., Ajmani, A.K., Ogasawara, T., Langdon, J.J., Hirakata, M., Wang, J. and Reeves, W.H. (1994) Autoantibodies to RNA polymerase II are common in systemic lupus erythematosus and overlap syndrome. Specific recognition of the phosphorylated form by a subset of human sera. *J. Clin. Invest.* **94**, 1981-1989.

Satoh, M., Langdon, J.J., Hamilton, K.J., Richards, H.B., Panka, D., Eisenberg, R.A. and Reeves, W.H. (1996) Distinctive immune response patterns of human and murine autoimmune sera to U1 small nuclear ribonucleoprotein C protein. *J. Clin. Invest.* **97**, 2619-2625.

Satoh, M., Richards, H.B., Hamilton, K.J. and Reeves, W.H. (1997) Human anti-nuclear ribonucleoprotein antigen autoimmune sera contain a novel subset of autoantibodies that stabilises the molecular interaction of U1 RNP-C protein with the Sm core proteins. *J. Immunol.* **158**, 5017-5025.

Savill, J. and Fadok, V. (2000) Corpse clearance defines the meaning of cell death. *Nature* **407**, 784-788.

Schmitt, J. and Papisch, W. (2002) Recombinant autoantigens. *Autoimmunity Reviews* **1**, 79-88.

Schneider, Z. (1980) Aliphatic alcohols improve the adsorptive performance of cellulose nitrate membranes – application in chromatography and enzyme assays. *Ann. Biochem.* **108**, 96-103.

Schwartz, M. and Cohen, I.R. (2000) Autoimmunity can benefit self-maintenance. *Immunol. Today* **21**, 265-268

Seelig, H.P., Ehrfeld, H., Schroeter, H., Heim, C. and Renz, M. (1991) A recombinant 70K protein ELISA – screening for antibodies against U1snRNP protein in human sera. *J. Immunol. Methods* **143**, 11-24.

Selenko, P., Sprangers, R., Stier, G., Buhler, D., Fischer, U. and Sattler, M. (2001) SMN tudor domain structure and its interaction with the Sm proteins. *Nature Struct. Biol.* **8**, 27-31.

Sentandreu, M.A., Aubry, L. and Ouali, A. (2004) A rapid purification procedure for cathepsin L from bovine species and production of specific antibodies. *J. Sci. Food Agric.* **84**, 2052-2060.

Shlomchik, M.J., Marshall-Rothstein, A., Wolfowicz, C.B., Rothstein, T.L. and Weigert, M.G. (1987) The role of clonal selection and somatic mutation in autoimmunity. *Nature* **328**, 805-811.

Shoenfeld, Y., Hsu-Lin, S.C., Gabriels, J.E., Silberstein, L.E., Furie, B.C., Furie, B., Stollar, B.D. and Schwartz, R.S. (1982). Production of autoantibodies by human-human hybridomas. *J. Clin. Invest.* **70**, 205-208.

Showalter, S.A. and Hall, K.B. (2003) Altering the RNA-binding mode of the U1A RBD1 protein. *J. Mol. Biol.* **335**, 465-480.

Smeenk, R.J.T. (2000) Antinuclear antibodies: cause of disease or caused by disease? *Rheumatology* **39**, 581-584.

Smolen, J.S., Butcher, B., Fritzler, M.J., Gordon, T., Hardin, J., Kalden, J.R., Lahita, R., Maini, R.N., Reeves, W., Reichlin, M., Rothfield, N., Takasaki, Y., van Venrooij, W.J. and Tan, E.M. (1997). Reference sera for antinuclear antibodies. II. Further definition of antibody specificities in international antinuclear antibody reference sera by immunofluorescence and western blotting. *Arthritis Rheum.* **40**, 413-418.

Smolen, J.S. and Steiner, G. (1998). Mixed connective tissue disease: to be or not to be? *Arthritis Rheum.* **41**, 768-777.

Sompayrac, L.M. (1999) Chapter seven. In: Sompayrac, L.M. ed. *How the Immune system works*. Blackwell Science Publishers.

Sontheimer, E.J. (2001) The spliceosome shows its metal. *Nature Struct. Biol.* **8**, 11-13.

Stark, H., Dube, P., Lührmann, R. and Kastner, B. (2001) Arrangement of RNA and proteins in the spliceosomal U1 small nuclear ribonucleoprotein particle. *Nature* **409**, 539-542.

Stetler, D.A. and Jacob, S.T. (1984) Phosphorylation of RNA polymerase I augments its interaction with autoantibodies of systemic lupus erythematosus patients. *J. Biol. Chem.* **259**, 13629-13632.

Stewart, J.J. (1998) The female X-inactivation mosaic in systemic lupus erythematosus. *Immunol. Today* **19**, 352-357.

Stoll, M.L. and Gavalchin, J. (2000) Systemic lupus erythematosus – messages from experimental models. *Rheumatology* **39**, 18-27.

Sturgess, A. (1992) Recently characterised autoantibodies and their clinical significance. *Austr. NZ. J. Med.* **22**, 279-289.

Sumpter, V., Kahrs, A., Fischer, U., Kornstadt, U. and Lührmann, R. (1992) *In vitro* reconstitution of U1 and U2 snRNPs from isolated proteins and snRNA. *Mol. Biol. Reps.* **16**, 229-240.

Surowy, C.S, van Santen, V.L., Sceib-Wixted, S.M. and Spritz, R.A. (1989) Direct sequence-specific binding of the human U1-70K ribonucleoprotein antigen to loop I of U1 small nuclear RNA. *Mol. Cell Biol.* **9**, 4179-4186.

Takano, M., Golden, S.S., Sarp, G.C. and Agris, P.F. (1981) Molecular relationships between two nuclear antigens, ribonucleoprotein and Sm: purification of active antigens and their biochemical characterisation. *Biochemistry* **20**, 5929-5936.

Takeda, Y., Wang, G.S., Wang, R.J., Anderson, S.K., Pettersson, I., Amaki, S. and Sharp, G. (1989) Enzyme-linked immunosorbent assay using isolated (U) small nuclear ribonucleoprotein polypeptides as antigens to investigate the clinical significance of autoantibodies to these polypeptides. *Clin. Immunol. Immunopathol.* **50**, 213-230.

Talken, B.L., Schafermeyer, K.R., Bailey, C.W., Lee, D.R. and Hoffman, R.W. (2001) T cell epitope mapping of the Smith antigen reveals that highly conserved Smith antigen motifs are the dominant target of T cell immunity in Systemic Lupus Erythematosus. *J. Immunol.* **167**, 562-568.

Tan, E.M., Chan, E.K., Sullivan, K.F. and Rubin, R.L. (1988). Antinuclear antibodies (ANAs): diagnostically specific immune markers and clues toward the understanding of systemic autoimmunity. *Clin. Immunol. Immunopathol.* **47**, 121-141.

Tan, E.M., Feltkamp, T.E.W., Smolen, J.S., Butcher, B., Dawkins, R. and Fritzler, M.J. (1997) Range of antinuclear antibodies in healthy individuals. *Arthritis Rheum.* **40**, 1601-1611.

Tan, E.M., Smolen, J.S., McDougal, J.S., Butcher, B.T., Conn, D., Dawkins, R., Fritzler, M.J., Gordon, T., Hardin, J.A., Kalden, J.R., Lahita, R.G., Maini, R.N., Rothfield, N.F., Smeenk, R., Takasaki, Y., van Venrooij, W.J., Wiik, A., Wilson, M. and Koziol, J.A. (1999). A critical evaluation of enzyme immunoassays for detection of antinuclear autoantibodies of defined specificities. I. Precision, sensitivity, and specificity. *Arthritis Rheum.* **42**, 455-464.

Tazi, J., Kornstadt, U., Rossi, F., Jeanteur, P., Cathala, G., Brunel, C. and Lührmann, R. (1993) Thiophosphorylation of U1 70K protein inhibits pre-mRNA splicing. *Nature* **363**, 283-286.

Tijssen, P. (1993) In Burdon, R.H. and van Knippenberg, P.H. eds. *Practice and theory of enzyme immunoassays: Laboratory Techniques in Biochemistry and Molecular Biology*. Elsevier, Amsterdam.

Tomer, Y., Buskila, D. and Shoenfeld, Y. (1993) Pathogenic significance and diagnostic value of lupus autoantibodies. *Int. Arch. Allergy Immunol.* **100,** 293-306.

Towbin, H., Staehelin, T. and Gordon, J. (1979) Electrophoretic transfer of proteins from polyacrylamide gels to nitrocellulose sheets: procedure and some applications. *Proc. Natl. Acad. Sci. USA* **76**, 4350-4354.

Tsay, G.J., Chan, E.K., Peebles, C.L., Pollard, K.M. and Tan, E.M. (1987) An immunoassay differentiating sera with antibodies to Sm alone, antibodies to Sm/RNP complex, and antibodies to RNP alone. *Arthritis Rheum.* **30,** 389-396.

Turk, B., Turk, D. and Turk, V. (2000) Lysosomal cysteine proteases: more than scavengers. *Biochim. Biophys. Acta.* **1477**, 98-111.

Turk, V., Turk, B. and Turk, D. (2001) Lysosomal cysteine proteases: facts and opportunities. *EMBO J.* **20**, 4629-4633.

Urlaub, H., Hatmuth, K., Kostka, S., Grelle, G. and Lührmann, R. (2000) A general approach for identification of RNA-protein cross-linking sites within native spliceosomal small nuclear ribonucleoproteins (snRNPs). *J. Biol. Chem.* **275**, 41458-41468.

Urlaub, H., Raker, V.A., Kostka, S. and Lührmann, R. (2001) Sm protein-Sm site RNA interactions within the inner ring of the spliceosomal snRNP core structure. *EMBO J.* **20**, 187-196.

Utz, P.J., Gensler, T.J. and Anderson, P. (2000) Death, autoantigen modifications and tolerance. *Arthritis Res.* **2**, 101-114.

van Venrooij, W.J. and Sillekens, P.T.G. (1989) Small nuclear RNA associated proteins: autoantigens in connective tissue diseases. *Clin. Exp. Rheumatol.* **7**, 635-645.

van Venrooij, W.J. and Pruijn, G.J.M. (2000) Citrullination: a small change for a protein with great consequences for rheumatoid arthritis. *Arthritis Res.* **2**, 249-251.

Venables, P.J., Smith, P.R. and Maini, R.N. (1983) Purification and characterisation of the Sjögren's syndrome A and B antigens. *Clin. Exp. Immunol.* **54**, 731-738.

Venables, P.J.W. (1993) Epitope mapping of ribonucleoprotein antigens: answers without questions? *Clin. Exp. Immunol.* **94**, 225-226.

Verheijen, R., Saiden, M. and van Venrooij, W.J. (1993) Protein blotting. In: van Venrooij, W.J., Maini, R.N. eds. *Manual of Biological Markers of Disease*. Dordrecht, the Netherlands: Kluwer Academic Publishers. A4: 1-25.

Vignali, D.A.A. (2000) Multiplexed particle-based flow cytometric assays. *J. Immunol. Methods* **243**, 243-255.

Vlachoyiannopoulos, P.G., Guilis, A., Tzioufas, G. and Moutsopoulos, H.M. (1996) Predominance of IgM anti-U1RNP antibodies in patients with systemic lupus erythematosus. *Br. J. Rheumatol.* **35**, 534-541.

Vorm, O., Roepstorff, P. and Mann, M. (1994) Improved resolution and very high sensitivity in MALDI TOF of matrix surfaces made by fast evaporation. *Anal. Chem.* **66**, 3281-3287.

Wagatsuma, M., Asami, N., Miyachi, J., Uchida. S., Watanabe, H. and Amann, E. (1993) Antibody recognition of the recombinant human nuclear antigens RNP 70kD, SS-A, SS-B, Sm-B and Sm-D by autoimmune sera. *Mol. Immunol.* **30**, 1491-1498.

Wandstrat, A. and Wakeland, E. (2001) The genetics of complex autoimmune diseases: non-MHC susceptibility genes. *Nature Immunol.* **2**, 802-809.

Warburg, O. and Christian, W. (1941) Isolation and crystallisation of the enzyme enolase. *Biochem. Z.* **310**, 384-421.

Watanabe-Fukunaga, R., Brannan, C.I., Copelan, N.G., Jenkins, N.A. and Nagata, S. (1992) Lymphoproliferation disorder in mice explained by defects in Fas antigen that mediates apoptosis. *Nature* **356**, 314-317.

Welin-Henriksson, E., Wahren-Herlenius, M., Lundberg, I., Mellquist, E. and Pettersson, I. (1999) Key residues revealed in a major conformational epitope of the U1-70K protein. *Proc. Natl. Acad. Sci. USA* **96**, 14487-14492.

Wells, L., Vosseller, K. and Hart, G.W. (2001) Glycosylation of nucleocytoplasmic proteins: signal transduction and O-GlcNAc. *Science* **291**, 2376-2378.

Wells, L., Gao, Y., Mahoney, J.A., Vosseller, K., Chen, C., Rosen, A. and Hart, G.W. (2002a) Dynamic O-glycosylation of nuclear and cytosolic proteins. *J. Biol. Chem.* **277**, 1755-1761.

Wells, L., Vosseller, K., Cole, R.N., Cronshaw, J.M., Matunis, M.J. and Hart, G.W. (2002b) Mapping sites of O-GlcNAc modification using affinity tags for serine and threonine post-translational modifications. *Mol. Cell Proteomics* **1**, 791-804.

Whelan, S.A. and Hart, G.W. (2003) Proteomic approaches to analyze the dynamic relationships between nucleocytoplasmic protein glycosylation and phosphorylation. *Circ. Res.* **93**, 1047-1058.

Whitacre, C.C. (2001) Sex differences in autoimmune disease. *Nat. Immunol.* **2**, 777-780.

White, P.J., Gardner, W.D. and Hoch, S.O. (1981) Identification of the immunologically active components of the Sm and RNP antigens. *Proc. Natl. Acad. Sci. USA* **78**, 626-630.

White, P.J., Billings, P.B. and Hoch, S.O. (1982) Assays for the Sm and RNP autoantigens: the requirement for RNA and the influence of tissue source. *J. Immunol.* **128**, 2751-2756.

Will, C.L., Rumpler, S., Klein-Gunnewiek, J., van Venrooij, W.J. and Lührmann, R. (1996) *In vitro* reconstitution of mammalian U1 snRNPs active in splicing: the U1C protein enhances the formation of early (E) spliceosomal complexes. *Nucleic Acids Res.* **24**, 4614-4623.

Will, C.L. and Lührmann, R. (2001) Spliceosomal UsnRNP biogenesis, structure and function. *Curr. Opin. Cell Biol.* **13**, 290-301.

Williams, D.G., Charles, P.J. and Maini, R.N. (1988) Preparative isolation of p67, A, B′, B and D from nRNP/Sm and Sm antigens by reverse-phase chromatography. *J. Immunol. Methods* **113**, 25-35.

Williams, D.G., Sharpe, N.G., Wallace, G. and Latchman, D.S. (1990) A repeated proline rich sequence in Sm B′/B and N is a dominant epitope recognised by human and murine autoantibodies. *J. Autoimmunity* **3,** 715-725.

Williamson, J.R. (2000) Induced fit in RNA-protein recognition. *Nature Struct. Biol.* **7**, 834-837.

Wilm, M. and Mann, M. (1996) Analytical properties of the nanoelectrospray ion source. *Anal. Chem.* **68**, 1-8.

Woppmann, A., Patschinsky, T., Bringmann, P., Godt, F. and Lührmann, R. (1990) Characterisation of human and murine snRNP proteins by two-dimensional gel electrophoresis and phosphopeptide analysis of U1-specific 70K proteins. *Nucleic Acids Res.* **18**, 4427-4438.

Woppmann, A., Will, C.L., Kornstadt, U., Zuo, P., Manley, J.L. and Lührmann, R. (1993) Identification of an snRNP-associated kinase activity that phosphorylates arginine/serine rich domains typical of splicing factors. *Nucleic Acids Res.* **21**, 2815-2822.

Wraith, D.C., Goldman, M. and Lambert, P-H. (2003) Vaccination and autoimmune disease: what is the evidence? *Lancet online*
*http://*image.thelancet.com/extras/02art9340web.pdf

Wu, X., Molinaro, C., Johnson, N. and Casiano, C.A. (2001) Secondary necrosis is a source of proteolytically modified forms of specific intracellular autoantigens. *Arthritis Rheum.* **44**, 2642-2652.

Xiao, S.H. and Manley, J.L. (1997) Phosphorylation of the ASF/SF2 RS domain affects both protein-protein and protein-RNA interactions and is necessary for splicing. *Genes Dev.* **11**, 334-344.

Yago, M., Belmonte, M.A., Olmos, M.J., Beltran, J., Teruel, C. and Segarra, M. (1999) Detecting anti-SSA and anti-SSB antibodies in routine analysis: a comparison between double immunodiffusion and immunoblotting. *Ann. Clin. Biochem.* **36**, 365-371.

Yanagisawa, H., Bundo, M., Miyashita, T., Okamura-Oho, Y., Tadokoro, K., Tokunaga, K. and Yamada, M. (2000) Protein binding of a DRPLA family through arginine-glutamic acid dipeptide repeats is enhanced by extended polyglutamine. *Hum. Mol. Genet.* **9**, 1433-1442.

Yean, S-L., Wuenschell, G., Termini, J. and Lin, R-J. (2000) Metal-ion coordination by U6 snRNA contributes to catalysis in the spliceosome. *Nature* **408**, 881-884.

Yong, J., Golembe, T., Battle, D.J., Pellizzoni, L. and Dreyfuss, G. (2004) snRNAs contain specific SMN binding domains that are essential for snRNP assembly. *Mol. Cell Biol.* **24**, 2747-2756.

Yoshida, S. and Reichlin, M. (1990) A radioimmunoassay for antibodies to the Ro/SSA particle. *J. Immunol. Methods* **131**, 113-118.

Zampieri, S., Ghirardello, A., Doria, A., Tonello, M., Bendo, R., Rossini, K. and Gambari, P.F. (2000) The use of Tween 20 in immunoblotting assays for the detection of autoantibodies in connective tissue diseases. *J. Immunol. Methods* **239**, 1-11.

Zaychikov, E., Martin, E., Denissova, L., Kozlov, M., Markovtsov, V., Kashlev, M., Heumann, H., Nikiforov, V., Goldfarb, A. and Mustaev, A. (1996) Mapping of catalytic residues in the RNA polymerase active center. *Science* **273**, 107-109.

Zieve, G.W. and Khusial, P.R. (2003) The anti-Sm immune response in autoimmunity and cell biology. *Autoimmun. Rev.* **2**, 235-240.

Appendix

Table A.1 A260/280 nucleic acid conversion

A260/280	% nucleic acid
0.57	0.00
0.61	0.25
0.66	0.50
0.71	0.75
0.74	1.00
0.77	1.25
0.80	1.50
0.86	2.00
0.92	2.50
0.97	3.00
1.02	3.50
1.06	4.00
1.15	5.00
1.18	5.50
1.22	6.00
1.25	6.50
1.28	7.00
1.30	7.50
1.33	8.00
1.37	9.00
1.41	10.0
1.49	12.0
1.56	14.0
1.61	17.0
1.67	20.0

Data adapted from Warburg and Christian (1941).
A260/280 for pure RNA = 2.0.